Tumour targeting with indium and silver labelled macrocycles

Craig, Andrew Simon

TUMOUR TARGETING WITH INDIUM AND SILVER LABELLED MACROCYCLES

by

Andrew Simon Craig, B.Sc. (Hons.), Dunelm

(Graduate Society)

University of Durham

A Thesis submitted for the degree of Doctor of Philosophy

September 1989.

DECLARATION

The work described in this thesis was carried out in the Department of Chemistry at the University of Durham between October 1986 and September 1989. All the work is my own unless stated to the contrary and it has not been submitted previously for a degree at this or at any other university.

To my parents

ACKNOWLEDGEMENTS

I would like to thank Dr. David Parker for his enthusiastic guidance during the course of this research project.

I am also indebted to the following people: Professor G. Ferguson, Dr. H. Adams and Dr. N. Bailey for crystal structure determinations; Dr. H-J. Buschmann and Dr. H. Schneider for the determination of stability constants by potentiometric titration; Dr. R. Kataky for the analysis of pH-metric data; Dr. R.S. Matthews and Mr. J. Banks for assistance with NMR studies; Dr. M. Jones and Mr. V.J. McNeilly for running the mass spectra, and all the technical and laboratory staff in the Department of Chemistry, for their assistance over the last three years.

I acknowledge the financial support from SERC and Celltech Ltd. (CASE Award). I would like to express my gratitude to Dr. M.A.W. Eaton, Dr. N.R.A. Beeley, Dr. A. Millican and Mr. K. Millar for their guidance and cooperation and for the warm hospitality extended to me during my visits to Celltech.

Special thanks go to Jean Eccleston for typing this thesis.

Friends and colleagues in the Department of Chemistry at Durham have helped to make the last three years very enjoyable ones and they will be sorely missed.

Finally, I wish to thank my parents and Lissa for their love and support.

ABBREVIATIONS

Mab	Monoclonal Antibody
Lys	Lysine
IgG	Immunoglobulin
$t_{\frac{1}{2}}$	Physical Half Life
β^-	Electron
β^+	Positron
PET	Positron Emission Tomography
EDTA	Ethylenediaminetetraacetic Acid
DTPA	Diethylenetriaminepentaacetic Acid
Cyclam	1,4,8,11-tetraazacyclotetradecane
Py	Pyridine
en	ethylenediamine
TACN	1,4,7-triazacyclononane
[9]-N_3-triacid (TCTA)	1,4,7-triazacyclononane-N,N',N''-triacetate
[10]-N_3-triacid	1,4,8-triazacyclodecane-N,N',N''-triacetate
TMSiI	Trimethylsilyl Iodide
DIPEA	Diisopropylethylamine
TsCl	p-toluenesulphonyl chloride
Pipes	1,4-Piperazinebis(ethane sulphonic acid)
TMS	Tetramethylsilane
THF	Tetrahydrofuran
DMF	Dimethylformamide
HPLC	High Performance Liquid Chromatography
TLC	Thin Layer Chromatography
CI	Chemical Ionisation
DCI	Desorption Chemical Ionisation
FAB	Fast Atom Bombardment
PAC	Perturbed Angular Correlation

ABSTRACT

Monoclonal antibodies which recognise tumour associated antigens provide a means of targeting radionuclides selectively to tumour cells. Work has been directed towards the synthesis of functionalised macrocyclic ligands to bind indium(III) [^{111}In:- γ-emitter] and gallium(III) [^{67}Ga:- γ-emitter] for use in radioimmunoscintigraphy and silver(I) [^{111}Ag:- β-emitter] for use in radioimmunotherapy. Macrocyclic ligands have been selected to bind the respective radionuclides rapidly, under mild conditions, to form complexes which are kinetically inert in vivo.

Four tribasic hexadentate macrocyclic ligands (9, 10, 11 and 12-membered rings) have been synthesised to bind indium and gallium. Comparison of the rate of ^{111}In uptake under mild conditions at low concentration (10-100 μM) revealed that the nine-membered triaza-triacid was the most effective. The X-ray crystal structures of the indium and gallium complexes of the [9]-N_3-triacid have been determined.

A C-functionalised derivative of the [9]-N_3-triacid has been synthesised by two routes, both starting from (2S)-Lysine. The syntheses of two N-functionalised derivatives of the [9]-N_3-triacid are also described. Antibody linkage has been effected (in collaborative work with Celltech Ltd.) by reacting the functionalised macrocycle with a heterobifunctional linker molecule (maleimide ester) followed by incubation with the antibody (previously treated with 2-iminothiolane).

Three new nitrogen and sulphur donor macrocyclic ligands have been synthesised to bind silver(I) and the 1:1 silver complexes have been isolated as crystalline solids and characterised by FAB mass spectrometry and ^{1}H nmr. Silver(I) complexes of two of the ligands have been characterised by X-ray crystallographic analysis. The stability constants (log K_s, MeOH) for the silver(I) complexes of the [18]-membered N_4S_2 and $N_4S_2Me_4$ macrocyclic ligands (14.1 and 14.6 respectively) are the highest recorded for monocyclic ligands.

CONTENTS

PAGE

CHAPTER ONE

INTRODUCTION

1.1. Cancer - The Need for Effective Diagnosis and Therapy

1.1.1. Cancer[1]

At the beginning of this century the Imperial Cancer Research Fund (ICRF) was founded in London, an indication at the time of the growing concern for the mystical disease, cancer. Cancer has been known since the time of the ancient Egyptians, but it is only relatively recently, as life expectancy has increased, that cancer has become a major cause of death. Today, in the developed world, cancer accounts for one death in every five, and one person in three is likely to contract the disease.

1.1.2. Carcinogenesis

Carcinogenesis is a multistage process. Exposure to a carcinogen leads to an "initiation" process, which is widely believed to involve a disruption of certain genes in DNA. "Initiated" cells may exist for a long period of time without transforming to tumour cells. Only when acted upon by a "promoting agent" do the subsequent stages of carcinogenesis occur, resulting in tumour growth. Much is yet to be learnt about the growth control processes of cells, but it is understood that in normal circumstances there are finely balanced stimulating and inhibiting factors. Tumour cells may be defined as being different from normal cells in that they are no longer responsive to normal growth controlling factors, or at least not all of them, so the balance is lost.

1.1.3. Cancer Research - the goals

The primary goal of cancer research is to gain a full understanding of the disease and ultimately to develop the technology to prevent it. In the meantime the objective of much cancer research work is the ability to at least control cancer. This involves devising a reliable

method for the detection of tumours at an early stage followed by administration of an effective therapy treatment.

1.1.4. **Existing Chemotherapy**

Many chemotherapeutic agents have been used in the treatment of cancers and many more are being investigated for antitumour activity. It is possible for chemotherapy to cure some cancers e.g. certain types of leukemia, soft tissue sarcomas and lymphomas. The drugs cisplatin (cis-$(PtCl_2(NH_3)_2)$) and carboplatin (C_3H_6-$C(CO_2)_2$-$Pt(NH_3)_2$) which are known to cross link between adjacent guanine residues in DNA,[2-4] causing distortion of the double helix structure, have been used successfully in the treatment of some cancers. For example, greater than 80% remission has been achieved for testicular and certain types of ovarian cancer. However, this constitutes only a small percentage of the cancers in the world. Some of the most common cancers (e.g. lung, colon/rectum and prostate) are among the least treatable by chemotherapeutic drugs and have the lowest survival rates [Fig. 1.1]. One of the main disadvantages of chemotherapeutic agents is their lack of specificity of action upon tumour cells over normal cells. For this reason high doses have to be administered in order to have any effect upon the tumour cells, but this often has harmful effects on normal tissue and vital organs.

1.1.5. **The aims of this research project**

An obvious solution to the problem of dosage is to use a targeting device in order to direct the cytotoxic agent specifically to the tumour, such that a lethal dose can be delivered to the tumour cells without harming normal cells. This project is dedicated to a method of tumour targeting using monoclonal antibodies (section 1.2.3.) that have been raised against specific tumour associated antigens (section

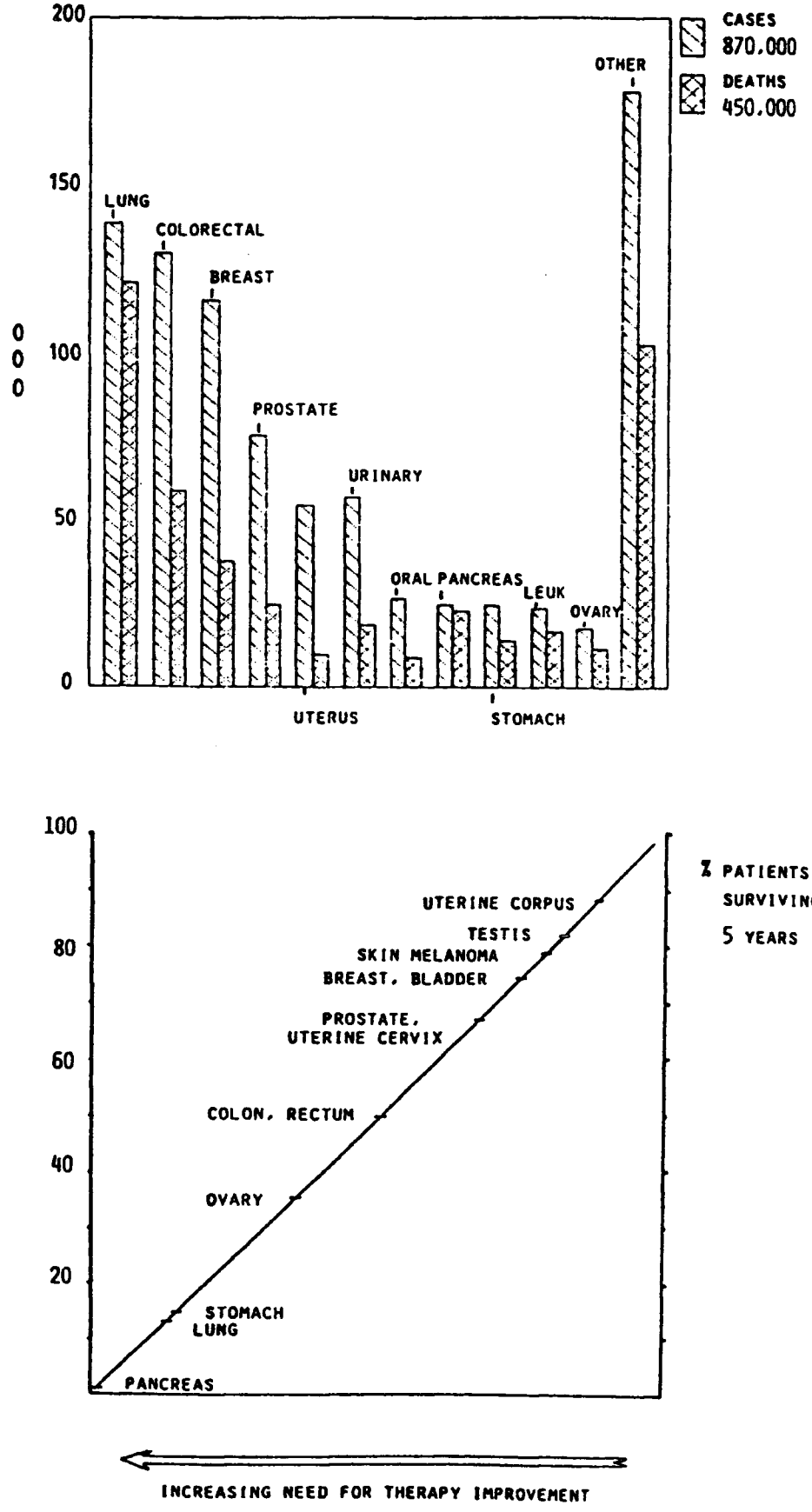

Fig. 1.1. Top: Estimated new cases and deaths in U.S.A. (1984). Bottom: The need for therapy improvement (% patients surviving 5 years).

1.2.2.). It is proposed that by labelling the antibody with selected radioisotopes it will be possible to detect and destroy tumour cells, with minimal effect to normal cells. This method is hoped to be particularly useful in the detection and destruction of small secondary tumours or metastases which are at present very difficult to detect and treat (larger primary tumours can often be removed surgically).

The work described in this project is concerned with the chemistry of binding the radionuclide and attaching it to the monoclonal antibody.

1.2. Antibodies for Tumour Targeting[1,5-12]

1.2.1. Antibodies

Antibodies are proteins (immunoglobulins) made by higher animals when infected with bacteria, viruses or other foreign substances. They are produced by B-Lymphocyte cells (present in the lymph nodes and the spleen) as part of a complex immune response against the foreign substance.

In their simplest form antibodies are made of two pairs of heavy and light polypeptide chains linked by disulphide bonds (Fig. 1.2). The heavy chains consist of one variable region and three or four constant

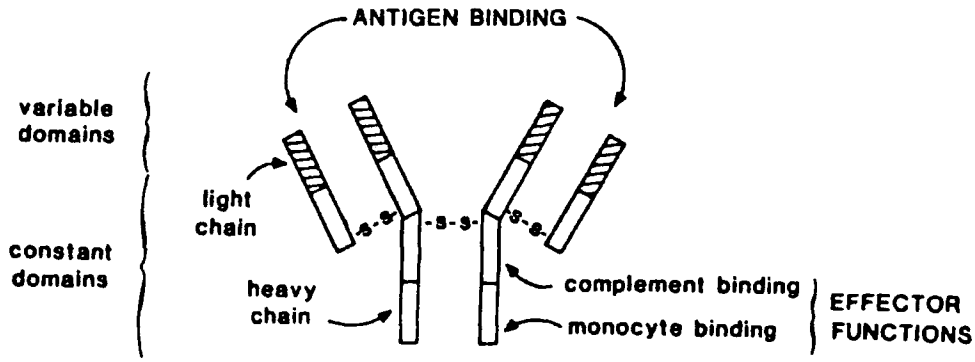

Fig. 1.2. Antibody Structure.

regions. The light chains consist of one variable region and only one constant region. One light chain folds over the first half of one heavy chain forming a "F(ab)" arm with a complex 3-D structure which constitutes the antigen binding site. The complete antibody consists of two F(ab) arms attached through disulphide bridges. The remaining constant regions of the heavy chain, the "Fc" portion, mediates the effector functions of the antibody (complement binding, attachment to and transport across membranes) according to the immunoglobulin class to which it belongs.

1.2.2. **Antigens**

Antigens are the foreign substances which invoke a response from the immune system. Tumour cells usually express antigens which are not produced by normal cells (e.g. altered proteins or carbohydrates). These antigens may be specific to the tumour cell, or at least highly selective to them.

Antibodies which recognise a particular antigen may be raised by injecting that antigen into a mouse and collecting the antibody producing B-Lymphocyte cells from the spleen. In this way antibodies may be raised against specific tumour associated antigens. However, this normal antibody response in the mouse produces a great diversity of antibodies, all of which recognise the tumour associated antigen. These are known as 'polyclonal' antibodies. The use of radiolabelled polyclonal antibodies for radioimmunoimaging and radioimmunotherapy has in the past been shown to be very limited. This is because the polyclonal antibodies are not specific enough in targeting the tumour cells.

1.2.3. **Monoclonal antibodies**

In 1975 Köhler and Milstein[5] developed the so called "Hybridoma"

technique for cloning individual antibody forming cells such that a single type of antibody ('monoclonal') having a specific antigen binding site, could be produced. This was a significant breakthrough in the field of antibody technology and meant that antibodies with sufficiently high specificity for tumour targeting could be produced. This led to a revival of interest in the "magic bullet" approach of targeting cytotoxic agents to tumour cells.

The "hybridoma" technique (Fig. 1.3) involves the fusing of the

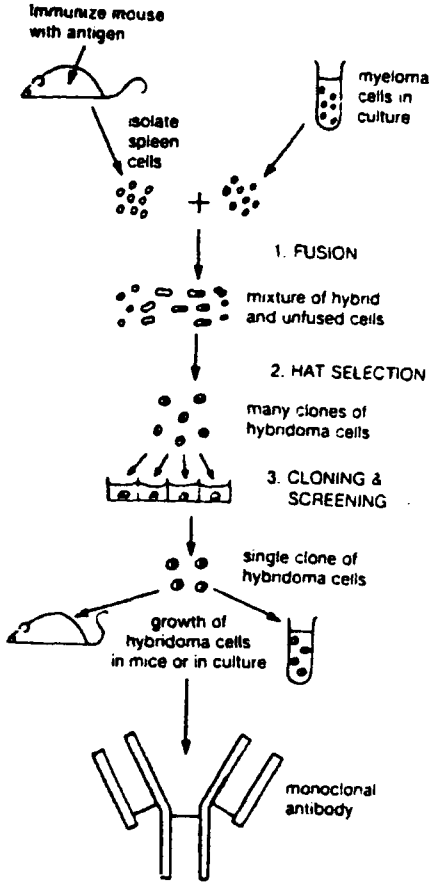

Fig. 1.3. The "hybridoma" technique for the production of monoclonal antibodies.

B-Lymphocyte cells from the spleen of the immunised mouse, with mouse myeloma cells, producing a hybrid cell (Hybridoma). The hybrid cell inherits the capacity of the myeloma cell for continuous proliferation as well as the B-Lymphocyte cell for producing the specific antibody.

The hybrid cells are then separated from unfused myeloma cells by growing the mixture in a culture which encourages hybridoma growth but not myelomal growth. The mixture is then diluted and placed in microtitre wells such that each well contains, on average, less than one cell. The clones are allowed to grow and the contents of each well assayed for the required monoclonal antibody. The antibody used in the studies discussed herein is B72.3[13] which binds selectively to tumour associated glycoprotein (TAG-72) found particularly in human colorectal and breast cancers.

1.2.4. Antibody fragments and chimaeric antibodies[10]

A major problem with the use of mouse monoclonal antibodies for tumour targeting is that they are themselves immunogenic in man. Human antibodies would be less immunogenic because, although the hypervariable region constituting the antigen binding site would inherently be foreign, the remaining constant regions would be consistent with other human immunoglobulins. However, several problems are encountered when using the hybridoma technique with human B-Lymphocyte cells and it has proved difficult to produce human 'monoclonals' with appropriate specificity in sufficient quantities. At present other ways of immortalising human antibody forming cells are being sought.

In an attempt to reduce the immunogenicity the use of antibody 'fragments' has been investigated, where only the antigen binding portion of the antibody is used. The constant "Fc" region is necessary for the normal immune response of antibodies, but is not required for tumour targeting. The intact molecule may be cleaved using the proteolytic enzymes pepsin or papain to give $F(ab')_2$ or Fab fragments respectively (Fig. 1.4).

A further advantage of using antibody fragments is that the small

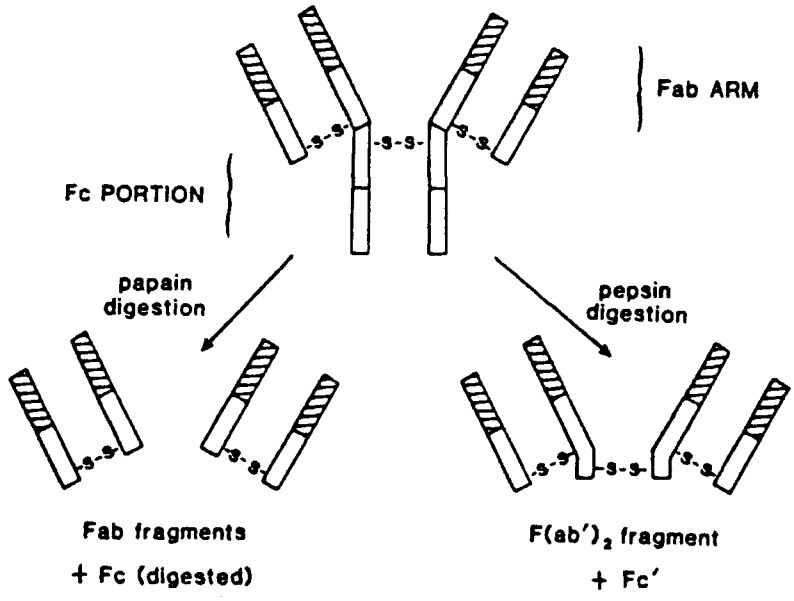

Fig. 1.4. Proteolytic cleavage of the antibody to Fab and $F(ab')_2$ fragments.

protein molecules travel more easily through narrow capillaries and so localise more quickly at the site of a tumour, with a greater chance of penetrating the more hindered sites. The fragment antibodies are also cleared more rapidly from general circulation, improving the tumour to background ratio when radiolabelled. One disadvantage is the high kidney background level observed as a result of the faster and more direct clearance.

An alternative approach to the problem of immunogenicity of mouse monoclonals has been investigated. Using recombinant DNA technology the immunologists have devised a way of making antibodies called "Chimaeric" antibodies which are part human and part mouse. This is done by combining portions of one antibody gene with segments of another. Chimaeric antibodies have been constructed in which the variable regions of the heavy and light chains are encoded by genes of the mouse antibody

secreting cells and the constant regions are encoded by human genes. Hence the antibody has the antigen recognisable variable regions of the mouse antibody and the constant "Fc" region of the human antibody, which is much less likely to produce an immune response in humans.

1.3. Radionuclides For Tumour Imaging[14-20]

1.3.1. Imaging methods[14]

In vivo imaging relies upon a form of electromagnetic radiation which has minimal interaction with the biological tissues of the body, but which can interact efficiently with a detector to produce a signal. Biological tissues absorb radiation in the mid range (10^{10}-10^{18} Hz) leaving the high energy and low energy ends of the spectrum for use in imaging. NMR (radiofrequency) and ultrasound are examples of low energy radiations which may be used for imaging. The use of radionuclides, emitting high energy radiation, is the most common form of imaging to date.

The radionuclides most suitable for imaging are gamma (γ) emitters. There are two different types of γ emitters: single photon emitters, where the γ emission occurs as a direct result of simple nuclear decay; and positron emitters where the isotope emits a positron and leads to the creation of two opposing 511 keV γ-rays, by electron positron annihilation. Two different methods of detection are used for the two types of gamma emission.

Gamma Ray Scintigraphy - single photon emitters

The single photon emitting isotopes require a static Anger camera (Fig. 1.5). A collimator is required due to the random nature of the gamma emission. The gamma rays then strike the NaI(Tl) crystal, producing flashes of light which are amplified by photomultipliers to

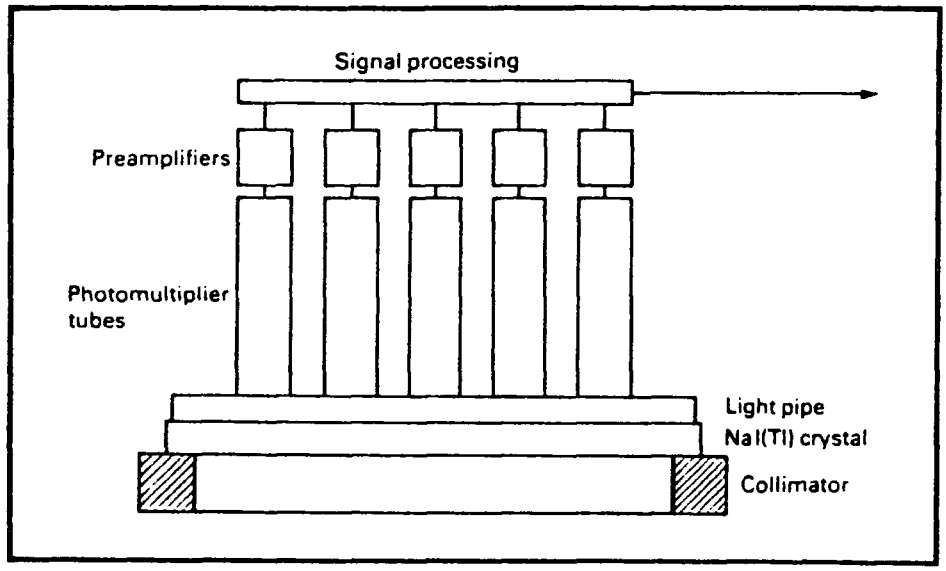

Fig. 1.5. The Anger Camera.

give an electrical signal and the electrical pulses are thereafter counted. As there is a limited number of photomultiplier tubes, the position of the γ ray interaction with the crystal is identified by the light intensity detected by each tube. The resolution obtainable from this system is modest at 1-2 cm.

In order to obtain a more three dimensional image of the tumour (Tomography) the Anger camera may be rotated around the patient, recording the signals at different angles and reconstructing the activity distribution through a back projection process. The procedure is computerised and known as Single Photon Emission Computerised Tomography (SPECT).

Positron Emission Tomography[17]

If a radionuclide emits a positron (β^+) which annihilates with an electron from the surrounding tissue, two photons (511 keV) are produced which travel at 180^o to each other. As a result of the directional

nature of these emissions, tomographical information may be obtained by detecting the two gamma's in coincidence. A line may be drawn between the two points of detection, on which the isotope must lie. The exact position of the source may be determined by the difference in the 'time of flight' measurements, after correcting for an absorbance factor associated with the body tissues. The early PET scanners consisted of two detectors opposite each other which were rotated around the patient, whereas today the designs usually consist of a continuous ring of detectors in which the patient is positioned in the centre. In order to make a more accurate determination of the time of flight, faster scintillators such as CsF or BaF_2 (rather than NaI) are used in the modern instruments. This is important for achieving better resolution which at 3-4 mm is much better than with single photon emitters and the Anger camera. The main disadvantage with PET scanners is the cost of the cameras required. At around one million pounds they are approximately ten times more expensive than the Anger cameras. For this reason it is expected that the latter rather than the former will continue to be used most commonly.

1.3.2. Selection of radionuclides for tumour imaging

In addition to selecting the type of radiation required for tumour imaging, there are several more nuclear properties to consider before selecting the most suitable radionuclides:

Half life

The half life of the radionuclide needs to be long enough to allow transportation to the tumour site and allow complete diagnosis, but short enough to limit the radiation dose required. One must consider the time required for radiolabelling the antibody, or antibody conjugate (see section 1.5.), the time it takes for optimal target to non-target

ratio to be achieved after injection and the time it takes to record an image. The biodistribution characteristics are particularly important. Before binding at the target antigen can occur, the radiolabelled antibody must proceed from the blood stream to the extracellular fluid of the tumour site. This is the rate limiting step, as transport of large lipid-insoluble antibody molecules (molecular weight of an IgG is typically 150,000) through the endothelial pores into the extracellular fluid is relatively slow (e.g. 18-24 hours). Once there, the binding to the surface antigens is expected to be relatively fast. Taking these factors into account a suitable range of half life is considered to be;

$$6 \text{ hours} < t_{\frac{1}{2}} < 8 \text{ days}.$$

Gamma energy

The gamma energies of the single photon emitters must be such that the Anger camera (NaI scintillation) can detect them and such that biological tissues are relatively transparent to them. Suitable photon energies are;

$$80 \text{ keV} < E \text{ photon} < 240 \text{ keV}.$$

Gamma abundance

To minimise the dose required it is desirable to have a high abundance of the single energy gamma radiation used for the detection. Also desirable, is a zero or low abundance of particulate emissions (beta or alpha particles) which may damage surrounding tissue.

Radiochemical properties

The method of production of the radioisotope needs to be relatively straightforward, such that it may be made available to the clinician at a reasonable cost. It is necessary to be able to purify the required isotope from the parent to avoid labelling with 'cold' isotope. Also it is important that the selected isotope does not have hazardous daughter

products (Alpha or Beta emitters).

Chemical properties

The radionuclide must be suitable for attachment to the antibody either directly or, more usefully, by bifunctional complexing agents (sect. 1.5.).

1.3.3. Candidates for imaging

A list of candidates which satisfy some or all of the criteria discussed in section 1.3.2. are listed in Table 1.1.

Of these, Iodine-131, Technetium-99m and Indium-111 are the isotopes which have been most extensively investigated to date.

Table 1.1

List of candidates for tumour imaging

Radionuclide	$t_{\frac{1}{2}}$	E photon (%)
^{123}I	13.2 hr	159(83)
^{125}I	60.0 d	27(138)
		35(7)
^{131}I*	8.05 d	364(82)
^{113m}In	1.68 hr	391(66)
^{111}In	2.83 d	171(88)
		247(94)
^{99m}Tc	6.02 hr	141(89)
^{67}Ga	3.25 d	184(24)
^{82}Rb (PET)	1.4 hr	511
^{64}Cu† (PET)	12.8 hr	511(120)
^{68}Ga (PET)	1.20 hr	511(178)

* ^{131}I has an accompanying β^- emission E_{max} 0.188 MeV

† ^{64}Cu has an accompanying β^- emission E_{max} 0.57 MeV

Iodine-123 has ideal properties, but is very expensive to produce in a carrier free form (generated using a cyclotron). Iodine-131 was used most extensively in the early attempts at imaging,[15] but the gamma energy is too high for efficient detection with an Anger camera and the half life is rather long. Furthermore, Iodine-131 has a cytotoxic beta emission and the radiolabelled antibody tends to deiodinate in vivo. This leads to incorporation of metabolised Iodine-131 in the thyroid and the excretion of Iodine by the stomach and urinary tracts, impairing specific tumour imaging.

Technetium-99m has been favoured for imaging purposes by virtue of its ideal gamma energy (141 keV) of high abundance and its ready availability at a reasonable cost from a Molybdenum-99 generator (obtainable carrier free via Al_2O_3/SiO_2 column chromatography). The major limiting feature however, is the short half life (6.02 h). By the time a high target to non-target ratio has been obtained (e.g. 2 days - see sect. 1.3.2.) most of the gamma activity will have been lost.

Indium-111 has received most attention in recent years as a suitable imaging candidate. It has two high abundance gamma emissions (173 and 247 keV) with no associated particulate radiation and an ideal half life of 2.83 days. The main disadvantage is that it is obtained from a reactor which is more inconvenient and expensive than a generator.

Gallium-67 is beginning to receive some attention as a potential imaging isotope, though the gamma intensity is significantly lower than that of indium-111.

Of the positron emitters listed, only Copper-64 has a suitable half life (12.8 h). However, the cost of production is ten times that of indium-111, so again the high cost disfavours the use of PET.

1.4. Radionuclides For Tumour Therapy[21-26]

1.4.1. Introduction

The use of radionuclides for tumour therapy is based upon their destructive power i.e. the ability of particulate radiation to irreversibly cleave bonds in the DNA of tumour cells and so destroy them. The advantage of using radionuclides, rather than anti-cancer drugs that are covalently linked to monoclonal antibodies, is that the former need not enter the cell to destroy it. Anti-cancer drugs lose their ability to pass readily through cell membranes when attached to large antibody molecules and consequently lose most of their activity.

It should be noted that radioimmunotherapy is a much more 'critical' process than radioimmunoscintigraphy. The latter can tolerate a certain level of background radiation with little ill-effect. The former depends much more heavily on the achievement of a high target to non-target ratio, especially with respect to the radiosensitive organs such as bone marrow, intestinal mucosa, liver and kidneys.

1.4.2. Choice of radiation

Alpha emitters

Alpha emitters on first considerations appear to be ideal candidates for therapy. They have a short range (50-90 μm) and have a high "linear energy transfer" (LET) i.e. they deliver a relatively large amount of energy within a short distance (~ 80 keV/μm). Approximately four hundred times as many beta particles would be required to obtain a similar sort of energy deposition when traversing a cell nucleus (approx. 10 μm). Potential alpha sources are Bismuth-212 and Astatine-211. In general, the problem with alpha sources is that the very large alpha recoil energy (typically several hundred keV) is likely to rupture the antibody radionuclide bond, leaving the daughter product

to diffuse away from the tumour. As alpha emitters are usually the heavier elements (atomic number > 82) which decay to unstable daughter products, this is a major limitation to their use in therapy. There are certain workers[26] who continue to promulgate the case for ^{212}Bi despite its obvious limitations.

Beta emitters

The majority of radionuclides considered for therapy are beta emitters. Despite having a lower LET than alpha particles, beta particles have the advantage of having a much greater variation in range. The radionuclide can be selected according to the range required i.e. tailored to the requirements of a particular type and size of tumour. For example, Gold-199 has a range of 100 μm which is suitable for the treatment of certain types of Leukemia, small metastases and small tumours generally. Yttrium-90, on the other hand, has a mean range of 3.9 mm and is suitable for the treatment of larger tumours. In many tumours there are "cold regions" where there are low levels of the target antigen, so an important factor is the "crossfire" effect associated with long range emitters i.e. the beta radiation traverses many cell diameters, penetrating the cold regions and administering a lethal dose of radiation.

1.4.3. General criteria for the selection of radionuclides for therapy

Half life

The half life required for therapy is generally a little longer than that for imaging. The same principles apply for allowing the required biodistribution to take place (sect. 1.3.2.), but with therapy a continued presence of the radionuclide is required. This is to enable a sterilising dose of radiation (e.g. 6000 rad) to be administered to the tumour cells, perhaps over a period of days. However, experiments

have shown that a radiation dose delivered over a long period of time is less effective than the same dose delivered more rapidly by a shorter lived isotope. Furthermore, the radiation dose must be delivered before the radiolabelled antibody is itself catabolised. A suitable range of half life is considered to be;

$$6 \text{ hr} < t_{\frac{1}{2}} < 4 \text{ weeks}.$$

More specifically, the ideal half life has been suggested to be between three and six days.

Other criteria

The beta emitter should have no gamma emissions (which make virtually no contribution to the sterilising dose) although a limited level could be tolerated and in fact used, for simultaneous imaging purposes.

The radionuclide must be obtained "carrier free" as discussed in section 1.3.2. This is particularly important for therapy, due to the difficulties associated with radiolabelling the antibody with enough activity to result in a sterilising dose of radiation being delivered to the tumour. The problem is merely increased if the antibody is labelled with any "cold" isotope.

Again, the radionuclide must have no hazardous daughter products and its chemistry should be amenable to permit stable attachment to the antibody.

1.4.4. Candidates for therapy

The isotopes which have been seriously considered for use in therapy are listed in Table 1.2.

Although Iodine-131 is the only isotope to have been used so far in the treatment of human cancer, its properties are far from ideal. It has a relatively high intensity gamma component and the iodinated

Table 1.2

Candidates for therapy

Isotope	Half life (hr)	β_{max} (MeV %)	Mean Range (mm)	Gamma (keV %)
^{67}Cu	62	0.40 (45)	0.2	93 (17)
		0.48 (35)		184 (47)
		0.58 (20)		
^{90}Y	64	2.25 (100)	3.9	---
^{111}Ag	179	1.04 (93)	1.1	342 (6)
		0.69 (6)		
^{131}I	193	0.61 (90)	0.4	364 (79)
^{161}Tb	166	0.45	0.3	75
		0.57		57 (21)
		0.58		
^{188}Re	17	1.96	3.3	155
		2.12		
^{199}Au	75	0.25 (22)	0.1	158 (76)
		0.30 (72)		

antibody does not have the required in vivo stability for effective tumour therapy. The remaining isotopes are attached to the antibody by the use of bifunctional complexing agents (section 1.5.).

Terbium-161 has good nuclear properties as a medium range beta emitter but is very difficult to obtain in carrier free form. Rhenium-188 and Gold-199 have potentially useful characteristics, as long range and short range emitters respectively. However, both have somewhat complex aqueous coordination chemistries that do not lend themselves to rapid ($\leq$ 2 hr.) formation of kinetically inert complexes,

though some progress has been made recently with rhenium.[27] The three most promising candidates are Yttrium-90, Silver-111 and Copper-67. ^{90}Y has received the most attention as a therapy candidate. It is a pure beta emitter (long range) with a useful half life (64 hours) and is available "carrier free" from a Strontium-90 generator at a relatively low cost. The decay product Zirconium-90 is stable.

^{111}Ag has a high abundance of a medium range beta emission and a suitable half life (7.4 days). It decays to a stable product, Cadmium-111 and is obtainable from Palladium-111m by a (n,γ) reaction (reactor), though it is relatively expensive.

^{67}Cu has a high abundance of beta particles (E_{max}: 0.40, 0.48, 0.58 MeV) and a moderate abundance of gamma rays which can be used for simultaneous imaging. It has a similar half life to ^{90}Y and decays to stable Zinc-67. However, its production from Zinc-68 (p,2p) using a linear accelerator makes it expensive.

1.5. Bifunctional Complexing Agents

1.5.1. Introduction

For some time it has been recognised that the way forward in radiolabelling antibodies involves the implementation of bifunctional complexing agents.[28] This is because certain ligands can bind metallic radioisotopes much more effectively than an antibody can itself. A bifunctional ligand is one which has the capacity to bind a metal ion by virtue of its donor atoms and also has a functionality that may be used to attach the complex to the antibody. It has been demonstrated that radioactive metal complexes may be covalently attached to the antibody (through the NH_2 of the lysine residue of the antibody) without compromising antigen binding.[29,30]

1.5.2. **Acyclic chelating agents**

Conventionally the acyclic chelators ethylenediaminetetraacetic acid (EDTA) and diethylenetriaminepentaacetic acid (DTPA) have been used to bind the metal radionuclide.[28-31] EDTA is a hexadentate chelate with two nitrogen and four oxygen donor atoms whereas DTPA is octadentate with three nitrogen and five oxygen donor atoms.

These ligands were chosen initially as a result of their remarkable versatility in binding metal ions. For example EDTA and its analogues are known to form stable complexes with about half the known elements.

Examples of bifunctional EDTA and DTPA ligands prepared by Gansow

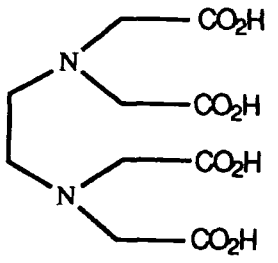

EDTA

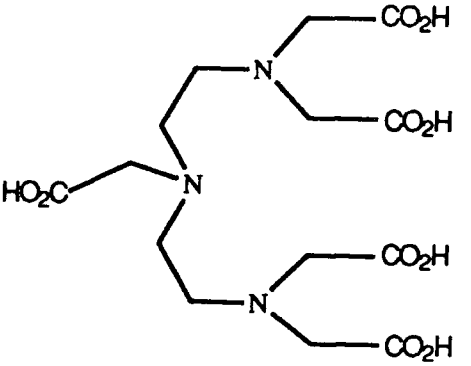

DTPA

et al.[32] are given in Fig. 1.6. Linkage to the antibody is achieved through the C-1 position or with the DTPA dianhydride system, through one of the N-carboxymethyl substituents. Bifunctional DTPA systems have been used to attach Indium-111 and Yttrium-90[33-37] to antibodies. These isotopes are the preferred candidates for radioimmunoimaging and radioimmunotherapy respectively.

1.5.3. **Thermodynamic vs. kinetic stability**

The 1:1 EDTA and DTPA complexes of indium(III) and yttrium(III) possess good thermodynamic stabilities (e.g. log K = 24.9 for In-EDTA

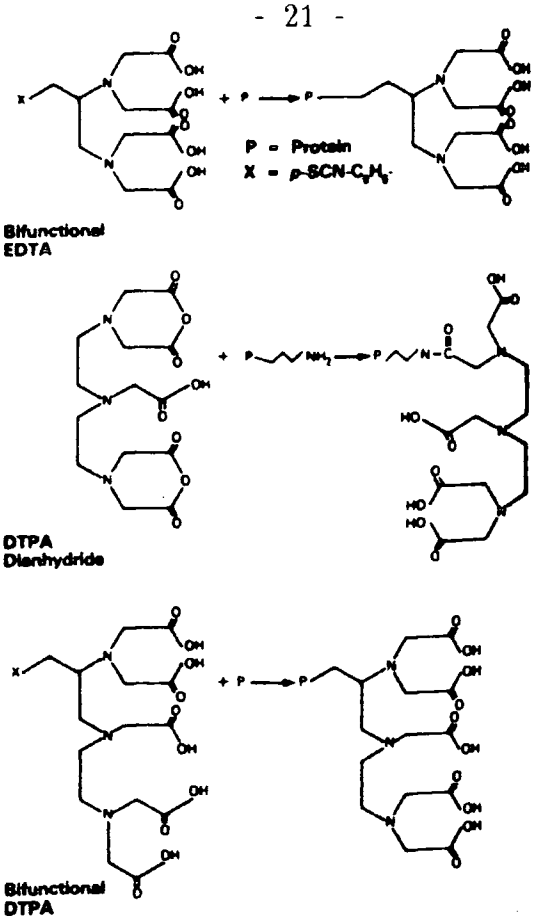

Fig. 1.6. Bifunctional EDTA and DTPA systems.

and log K = 22.1 for Y-DTPA). However, when the goal is an application to a living system, the stability constant merely serves as a useful guide to the suitability of the complex. The more important factor is the kinetic stability of the complex in vivo. The concentration of the complex in the blood is very low and it is subject to competition from metal binding proteins such as transferrin and albumin. Furthermore, there is competition for the ligand from metal ions such as Zn^{2+} (10^{-8} M) and Ca^{2+} (10^{-3} M) present in human serum. (Studies[39] have shown that Ni^{2+} and Cu^{2+} promote metal ion loss from EDTA and DTPA complexes.) Moreover, ligands such as EDTA and DTPA are very susceptible to protonation and the stabilities of their complexes are very much pH dependent[31] [Fig. 1.7].

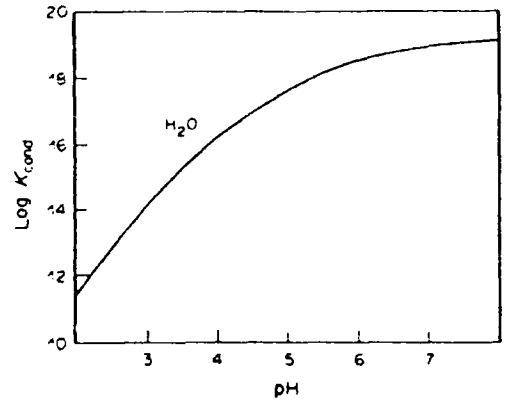

Fig. 1.7. Logarithmic plot of the "conditional" (or apparent) stability constant of the In(III) EDTA complex as a function of pH.

The complex used for radioimmunotargeting must remain kinetically inert over the full physiological pH range. The important factor is the rate of protonation of the ligand-complex. Ideally the rate constants

$$ML \underset{Ka_1}{\overset{k_1}{\rightleftharpoons}} MLH \underset{Ka_2}{\overset{k_2}{\rightleftharpoons}} MLH_2 \underset{Ka_3}{\overset{k_3}{\rightleftharpoons}} MLH_3 \ldots . \text{etc.}$$

k_1, k_2 ... etc. should be small and the pK_a values (protonation constants) low, so that protonation of the complex occurs only at low pH. DTPA forms an anionic complex with indium $[In\text{-}DTPA]^{2-}$ and so attracts protons or other metal ions which encourages dissociation.

Radioimmunoimaging studies using DTPA bound indium have had some success. However, tumours smaller than 1.5 cm in diameter have proved difficult to detect. In all cases the investigators have struggled against relatively high background levels of radiation, especially in the vital organs e.g. liver, kidney and bone marrow.[38] This indicates that the loss of indium from the chelate is still a problem. For

radioimmunotherapy the background level is more critical and high radiation levels in these organs cannot be tolerated.

For the future success of the radioimmunotherapy and imaging, complexes which are less susceptible to acid promoted dissociation and which have greater in vivo stability are required. It is proposed that the use of macrocyclic ligands, which have been 'tailored' to the binding requirements of individual radionuclides, will significantly enhance the in vivo properties of the antibody conjugate.

1.6. Macrocyclic Complexing Agents

1.6.1. Introduction

Since Pedersen[40] reported the synthesis and properties of crown ethers e.g. (1) 18-Crown-6 and (2) tribenzo-18-Crown-6, a vast amount of work has been directed towards the synthesis and complexation properties of macrocyclic ligands.

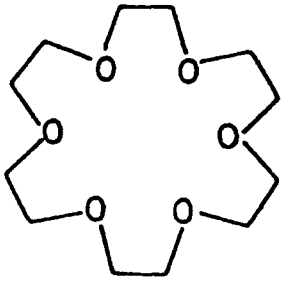

(1) 18-Crown-6

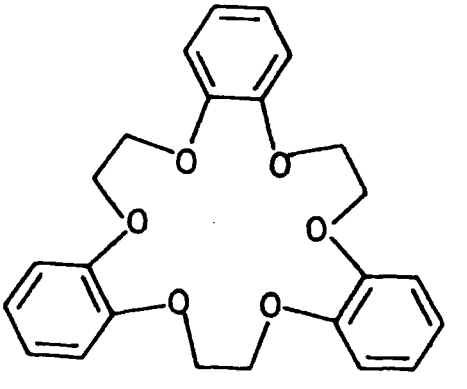

(2) Tribenzo-18-Crown-6

Pedersen's cyclic polyethers were observed to form stable 1:1 complexes with alkali and alkaline earth metal cations. The macrocyclic rings were seen to form molecular cavities, lined with oxygen donor atoms, which were able to bind metal ions through ion-dipole

interactions, forming 'host-guest' complexes. High stability constants were observed when there was a good correlation between the size of the macrocyclic cavity and the size of the cation.

Soon after, the synthesis of macrocyclic diamines was reported[41,42] and since then a great variety of macrocycles of different sizes with different donor atoms (usually O, N or S) have been reported.

1.6.2. Factors affecting the binding properties of macrocycles[43]

The factors which effect the binding properties of macrocycles include;

1) The type of binding site(s) in the ring
2) The number of binding sites in the ring
3) The physical placement of the binding sites
4) The relative sizes of the ion and the macrocyclic cavity
5) Steric hindrance in the ring
6) The solvent and the extent of solvation of the ion and of the ligand
7) The electrical charge of the ion.

With so many variables there is considerable scope to design macrocycles which match the requirements of individual metal ions.

The polycyclic ethers show little tendency to bind transition metal ions. However, when the oxygen atoms are replaced by softer nitrogen or sulphur donor atoms then more stable macrocyclic complexes are observed. The "softer" transition metal cations (with larger and more polarisable valence shells) prefer to interact with "softer" donor atoms forming metal donor bonds which are more covalent in nature than the purely electrostatic interaction of group I and II metal cations with "hard" oxygen donor atoms.

By analogy with known natural products[44] (e.g. the iron and

magnesium porphyrins of haemoglobin and chlorophyll) most of the early macrocycles designed to bind first row transition metals were tetradentate nitrogen donor ligands such as (3) and (4).

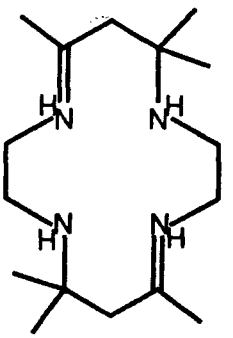

(3)

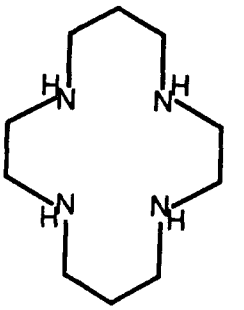

(4) 14N4 "Cyclam"

For a macrocycle of this type to bind a first row transition metal it most often consists of a thirteen to sixteen membered ring[45,46] with spacing between the atoms such that five, six or seven membered chelate rings are formed with the metal ion (five and six membered rings are most common) [Fig. 1.8].

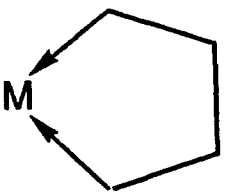

Five membered chelate ring

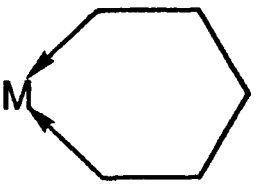

Six membered chelate ring

Fig. 1.8.

A list of the common tetraaza macrocyclic ligands that have been used to bind transition metal ions are given below (5)-(10).

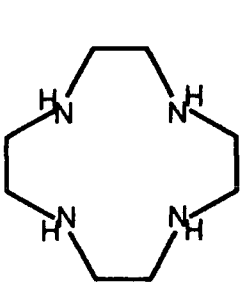

(5) 12N4

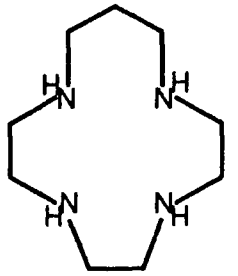

(6) 13N4

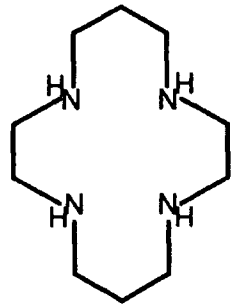

(7)14N4

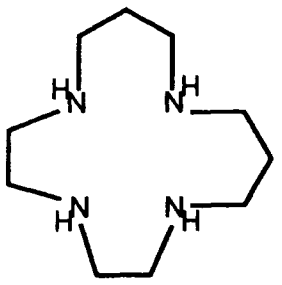

(8) 14N4'

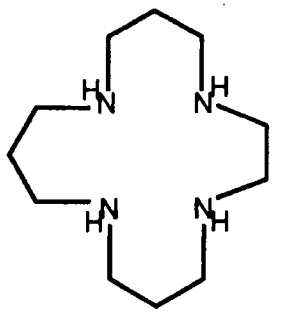

(9) 15N4

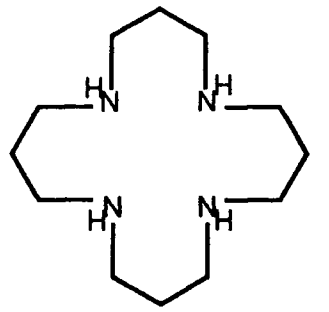

(10) 16N4

Square planar coordination geometries are most often observed, with the cation sitting in the plane of the four nitrogen atoms e.g. Cu(II)-cyclam [Fig. 1.9]. The highest stability constants are generally observed for those transition metal complexes where there is good correlation between the size of the cation and the cavity of the ligand, allowing optimum metal-nitrogen bond lengths. For example, the stability constant of the copper(II) complex of 14N4 ("cyclam") is at a maximum and falls off rapidly with smaller or larger ring sizes.

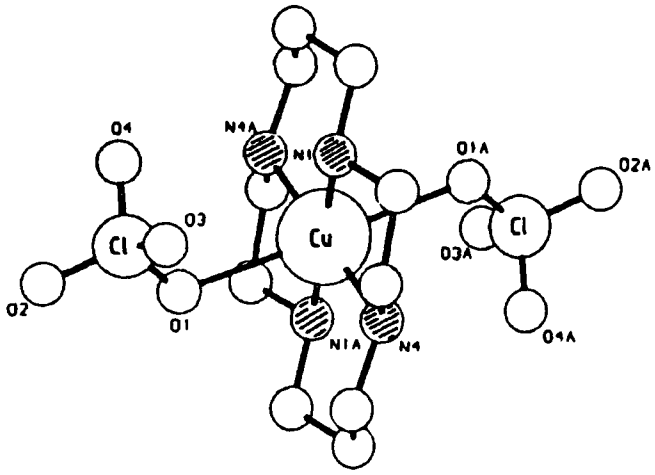

Fig. 1.9. Crystal structure of $[Cu(cyclam)].2ClO_4$.

1.6.3. The macrocyclic effect

Macrocyclic metal ion complexes are almost always found to be considerably more thermodynamically and kinetically stable with respect to dissociation of the cation, than their acyclic counterparts. That is, there is an additional enhancement in stability beyond that expected from the gain in translational entropy when chelates replace coordinated solvent from the metal ions ("chelate effect"). This feature is known as the "macrocyclic effect".

Much calorimetric and spectroscopic work has been done to investigate the thermodynamic parameters involved in the macrocyclic effect. Cabbiness and Margerum[47] reported that the red copper(II) complex of 5,7,7,12,14,14-hexamethyl-1,4,8,11-tetraazacyclotetradecane ["tet-a"] (11) was 10,000 times more stable than the copper(II) complex of the open chain analogue "2,3,2-tet"(12), Table 1.3.

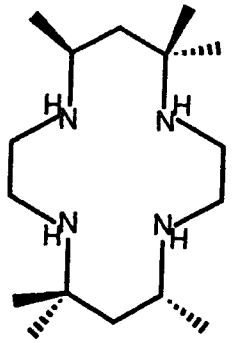

(11) "tet-a"

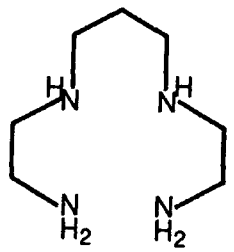

(12) "2,3,2-tet"

Table 1.3

Complex	log K_s
$Cu(2,3,2\text{-tet})^{2+}$	23.9
$Cu(tet\text{-}a)^{2+}$ - red	28

Similarly, there is a 10^6 fold increase in the stability of the nickel(II) complex of cyclam (4) compared to the nickel(II) complex of "2,3,2-tet" (12)[47] (both complexes square planar). Calorimetric studies by Margerum suggested that the effect was enthalpic in origin, Table 1.4. Such a large effect could not be attributed to stronger nickel-

Table 1.4

Complex	log K_s	ΔH/kcal mol^{-1}	ΔS cal K^{-1} mol^{-1}
Ni(2,3,2-tet)$^{2+}$	15.8	-13.0±0.6	7.4
Ni(cyclam)$^{2+}$	22.2	-19.4±0.1	-2

nitrogen bonds in the macrocyclic complex as both formed similar square planar coordination geometries. Margerum[48,49] postulated that the free macrocycle was less solvated in solution than the acyclic counterpart due to greater steric hindrance, hence fewer hydrogen bonds (OH----N) were needed to be broken to form the complex. A small unfavourable entropy effect was suggested as a consequence of less molecules of solvation being released upon complexation, for the macrocycle.

However, two different sets of authors, Fabrizzi, Paoletti[50,51] and Kimura[52] found that there was a large entropic contribution to the macrocyclic effect for transition metal complexes of polyamines. Kimura,[53] for example, reported that the effect for Cu(II)-cyclam arose from both enthalpic (ca. 60%) and entropic (ca. 40%) contributions [Table 1.5].

Table 1.5

Complex	log K_s	-ΔH/kcal mol^{-1}	ΔS/cal K^{-1} mol^{-1}
Cu(cyclam)$^{2+}$	27.2	30.4	22.4
Cu(2,3,2-tet)$^{2+}$	23.9	27.7	16.5

Fabrizzi and Paoletti[54,55] reported a similar ratio of enthalpic and entropic contributions for nickel(II)-cyclam, Table 1.6.

Table 1.6

Complex	log K	-ΔH/kcal mol^{-1}	ΔS/cal K^{-1} mol^{-1}
N_1(cyclam)$^{2+}$	22.2	20.3	33.6
N_1(2,3,2-tet)$^{2+}$	15.8	18.6	10.4

Here, it was suggested that the most significant factor was the preorganisation of the macrocyclic ligand in the required conformation for complexation, unlike the acyclic ligand which has to undergo major conformational changes.

Investigations of different types of macrocyclic systems have given equally variable results; Sokol et al.[56] studying copper(II) complexes of 12-16 membered tetrathiaethers reported that entropic contributions were dominant; Izatt et al.[57] investigating 18-Crown-6 systems with Na^+, K^+ and Ba^{2+} reported favourable entropic contributions and Schwing-Weill et al.[58] with copper(II) mixed O, N, S donor macrocycles, reported both enthalpic and entropic contributions.

More recently a study of the thermodynamic data for a series of polyamine Ni(II) complexes[59] has shown that the weighting of enthalpic and entropic contributions changes through the series.

The only conclusion to draw is that the nature of the macrocyclic effect i.e. the relative importance of the entropy and enthalpy of complexation, varies according to the type of cation and ligand involved. For example, the highly solvated 'hard' alkali metal ions e.g. Li^+ tend to have have dominant entropic contributions associated with the loss of solvation molecules upon complexation, whereas, larger

softer cations tend to have dominant enthalpic contributions associated with metal donor atom bond energies.

Another feature associated with the macrocyclic effect is the kinetic inertness of macrocyclic complexes towards metal ion dissociation. Possibly the most extreme example is provided by the square planar Nickel(II) cyclam complex[60] which under acid conditions (1.0 Molar $HClO_4$, 25^oC) was claimed to have an estimated half life of approximately thirty years.[61]

The kinetics of the acid catalysed dissociation of the copper(II) complex of 15N5 (13) has been investigated.[62,63] The rate of

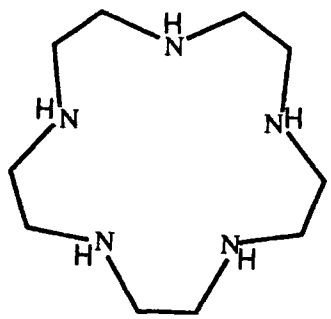

(13)

dissociation was found to be first order in ligand and second order in acid, suggesting the involvement of two protons in the transition state structure. A proposed scheme for the dissociation is given in Fig. 1.10. The stepwise dissociation of the ligand from the coordination sphere of the metal requires distortion of the ligand, in order to minimise electrostatic repulsion between the protonated site and the cation and to allow room for the incoming solvent molecule. The conformational restrictions of the macrocycle can make this energetically unfavourable, resulting in an energy barrier to dissociation. In contrast, acyclic ligands are relatively free to

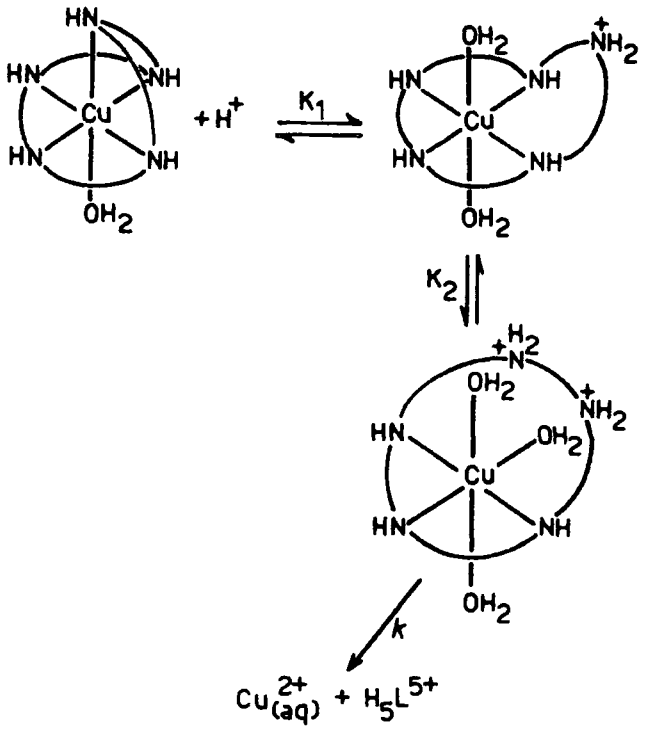

Fig. 1.10. Stepwise dissociation of $(CuL)^{2+}$ in acid.

change their conformation as the donor atoms dissociate from the metal ion. It follows that the more rigid the macrocycle the greater is the energy barrier for dissociation and hence the greater the kinetic stability.

Similar principles apply to the rate of association, in that conformational changes are required in order for complexation to occur, but the effect is less marked.

1.6.4. Cavity size correlations

In previous sections, examples where there has been reasonable correlation between the cavity/cation size and the observed stability constant of the complex have been described. However, this is not always the case. Macrocyclic ligands, especially the larger rings can be flexible and can adapt their conformations to accommodate cations of

different size.

As discussed earlier, the copper(II) complexes of the tetramine series (5)-(10) show good cavity size correlation and a maximum stability is achieved with 14N4 (cyclam). However, studies by Hancock[64] have shown that the large cations Ca^{2+} and Pb^{2+} actually form more thermodynamically stable complexes with the smaller 12N4 ring. This is attributed to the fact that the macrocycles can adopt different conformations, Fig. 1.11.

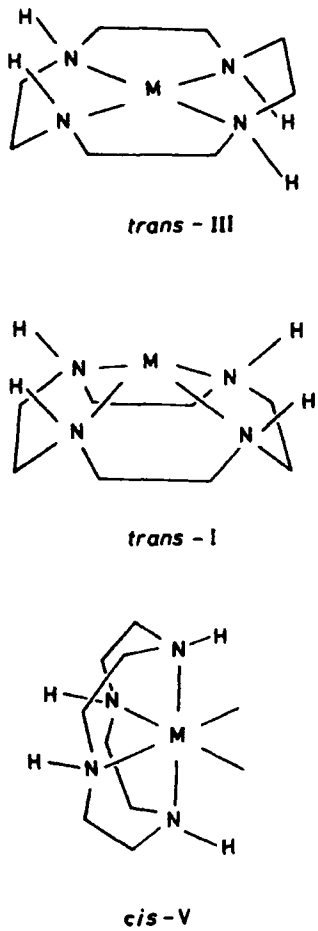

Fig. 1.11. Conformers of the 12N4 macrocycle.

The trans III isomer allows the metal to sit inside the ring with square planar coordination geometry. The 'trans I' isomer allows a slightly larger cation to sit above the plane of the ring and the 'cis

V' isomer allows yet larger cations to coordinate facially (e.g. Cd^{2+} and Pb^{2+}). In this case the overall stability is determined by the relative stabilities of 5 and 6 membered chelate rings formed with the metal. For large cations the 5 membered chelate is preferred,[64] so 12N4 gives the highest stability complex.

Smaller rings e.g. 1,4,7-triazacyclononane (14) and 1,4,7-triazacyclodecane (15) have more rigid structures and the lone pairs are often exposed on one face of the cycle. Consequently, many complexes are observed where the metal ion sits on top of the macrocycle e.g. Cu-$[9]N_2S^{2+}$ [Fig. 1.12] or even sandwiched between two macrocycles e.g. Ni-$([10]N_3)_2^{2+}$ [Fig. 1.13].

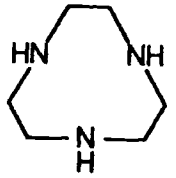

(14)

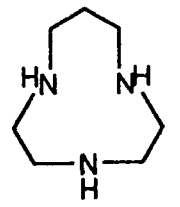

(15)

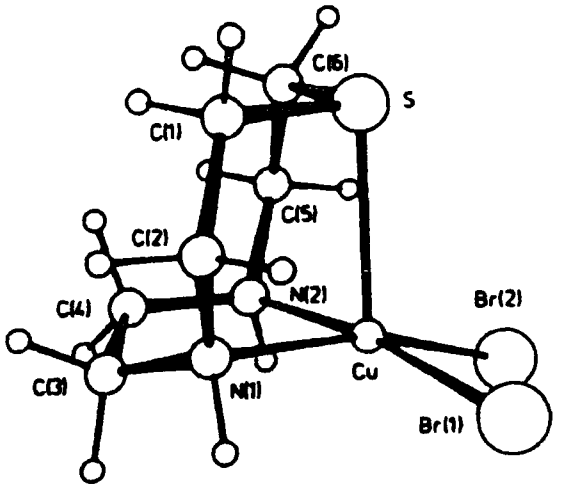

Fig. 1.12. Crystal structure of (Cu-$[9]N_2S$)(Br_2).

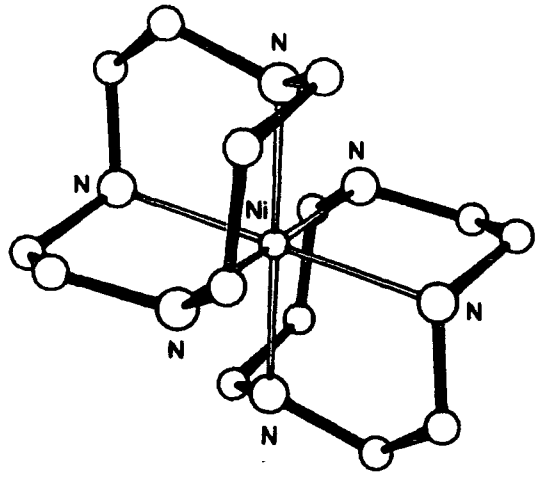

Fig. 1.13. Crystal structure of Ni($[10]N_3)_2^{2+}$.

For nine membered macrocycles the most commonly observed conformation is referred to as the [3.3.3] conformer, according to a scheme devised by Dale.[65,66] The numbers in the bracket refer to the number of bonds between "bends" or "corners" in the ring, starting with the smallest and moving in the direction around the ring so as to minimise the next number. A corner may be defined by particular combinations of torsional angles around the ring [Fig. 1.14]. Positions 1, 2 and 3 with respect to R define torsion angles of 60^{o} (gauche [+]),

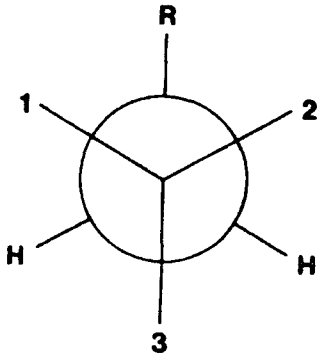

Fig. 1.14. Torsion Angles.

-60^{o} (gauche [-]) and 180^{o} (anti) respectively. More generally a gauche bond may be defined as having a torsion angle $\theta < 90^{o}$.[44] A corner occurs at the junction of two gauche bonds ([+] or [-]) or at the junction of an isolated gauche bond with the adjacent bond of smaller torsion angle.

Most complexes of the cyclononane macrocycles exist in a [3.3.3] conformation e.g. $Ni([9]N_2S)^{2+}$ though some do exist in a [2.3.4] conformation e.g. $Cu([9]N_2S)^{2+}$ [Fig. 1.15].

Molecular mechanics calculations[44] have shown that for all sulphur and nitrogen mixed donor cyclononane macrocycles in the free form the [2.3.4] conformation was more strained than the [3.3.3] conformation. Hence [2.3.4] conformations are usually associated with metal ions which

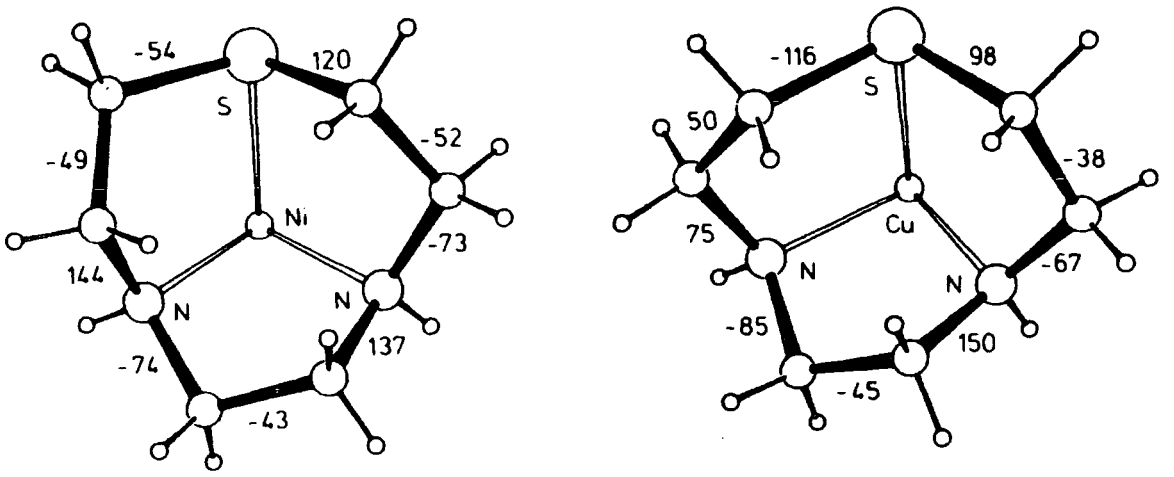

a b

Fig. 1.15. a) [3.3.3] conformation of $Ni([9]N_2S)^{2+}$ and b) the [2.3.4] conformation of $Cu([9]N_2S)^{2+}$

cannot accept symmetrical facial coordination, such as the Jahn-Teller distorted Cu(II) complex [Fig. 1.15].

1.6.5. Cryptands and spherands

In 1968 Lehn[67,68] reported the synthesis of a macrobicyclic ligand (16) which consisted of a 1,10-diaza-18-crown-6 ring bridged between the two nitrogens with another polyether chain, forming a 3-dimensional

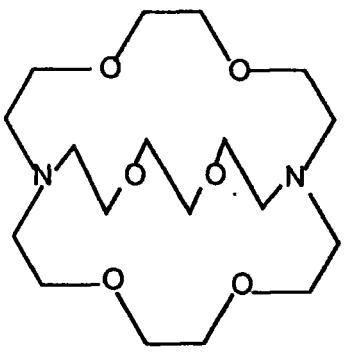

(16)

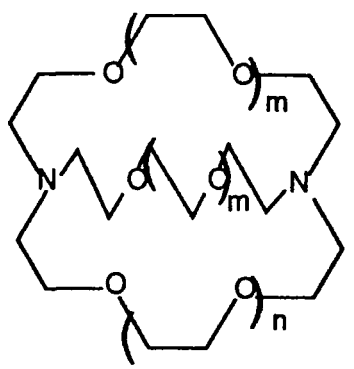

(17)

a) [2.1.1]m=0,n=1
b) [2.2.1]m=1,n=0
c) [2.2.2]m=1,n=1
d) [3.2.2] m=1,n=2
e) [3.3.2] m=2,n=1
f) [3.3.3] m=2,n=2

cavity. A series of ligands with the general structure (17) were synthesised[69-72] and their complexation properties investigated. They

were found to form inclusion complexes with a substrate (usually a cation) sitting inside the cage like cavity (or 'crypt') [Fig. 1.16] relatively shielded from the outside environment. Lehn named such ligands, 'cryptands' and their inclusion complexes 'cryptates'.

Analogous to the "macrocyclic effect" there is a "cryptate effect" for metal ion complexes of cryptands. The bicyclic ligands are more conformationally restricted than their monocyclic counterparts and hence

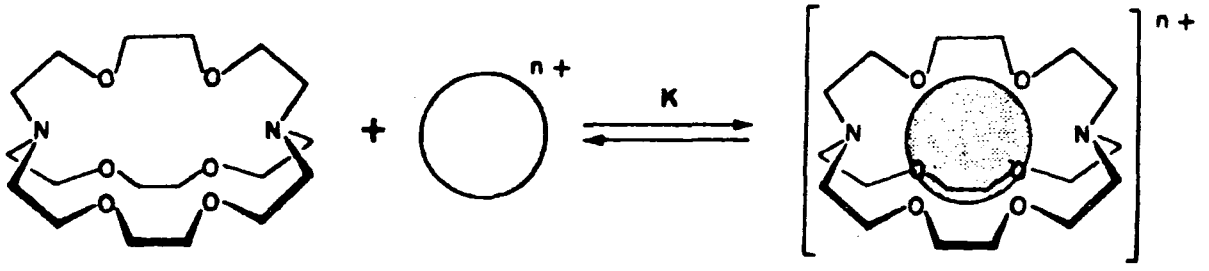

Fig. 1.16. Formation equilibrium of a cryptate inclusion complex between cryptand [2.2.2] and a metal ion.

show a more pronounced thermodynamic and kinetic stability. Thus the K^+ complex of [2.2.2] is 10^5 times more stable than the corresponding monocyclic analogue (diaza-18-crown-6). As a consequence, the stability and selectivity characteristics are usually consistent with the simple cavity/cation 'best fit' idea. The polyether cryptands (17) form stable complexes with alkali and alkaline earth metal ions. Li^+, Na^+ and K^+ are complexed preferentially by cryptands [2.1.1] (17a), [2.2.1] (7b) and [2.2.2] (17c) respectively.

Replacing the oxygen atoms by sulphur or nitrogen donor atoms favours the binding of transition metal ions, as with monocyclic ligands[73] (sect. 1.6.1).

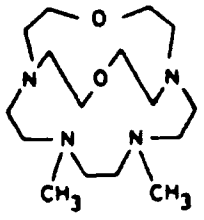

(18)

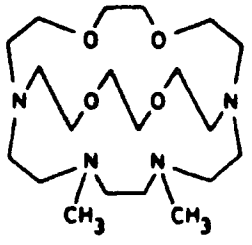

(19)

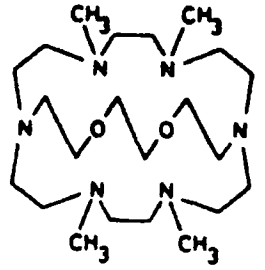

(20)

For example the aza analogue of [2.2.1] (18) forms stable complexes with Co^{2+}, Ni^{2+} and Zn^{2+} and the aza analogues of [2.2.2] form stable complexes with the larger cations Cd^{2+}, Hg^{2+} and Pb^{2+}.

Cryptate (19) shows very high selectivities for Cd^{2+}, Hg^{2+} and Pb^{2+} over the smaller cation Zn^{2+} (10^6, 10^{18} and 10^9 respectively) highlighting the significance of cavity size for the cryptates.

A potentially limiting factor to the use of cryptands for labelling antibodies with radionuclides, is the relatively slow rate of metal ion complexation. This can be attributed to the restricted access for the cation and the limited flexibility of the ligand. Spherands such as (21)[74] exhibit an even greater degree of preorganisation in the ligand. In this example, the six oxygen donor atoms are locked into an octahedral arrangement by the rigidity of the benzene ring backbone (the cavities of the cryptands in the unbound state are partially filled by the methylene groups turned inwards). This results in enhanced selectivity and stability for metal ion complexes of the right size. For example spherand (21) binds Na^+ and Li^+ (log K: 14 and 16 respectively)[75] but does not bind K^+, Rb^{2+}, Cs^{2+}, Mg^{2+} or Ca^{2+}.

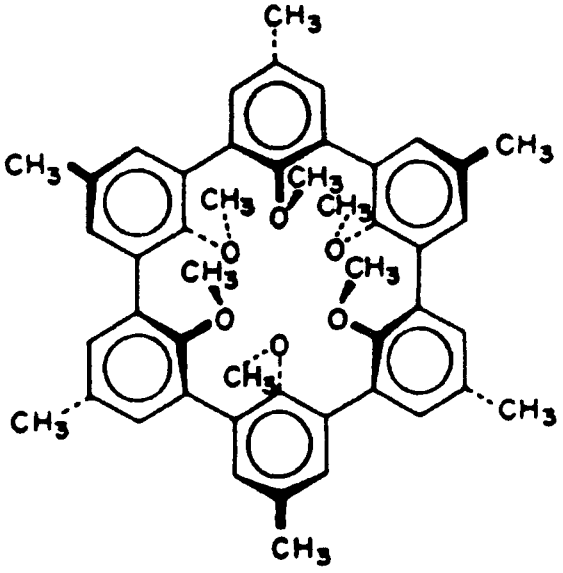

(21)

However the rates of complex formation are characteristically slow.

1.6.6. Conclusion

It is the combined cation complexation characteristics of macrocycles, the high thermodynamic and kinetic stabilities as well as the acceptable rates of association, that make them the first choice for binding radionuclides for tumour targeting.

The specific coordination chemistries of indium(III) and silver(I) are discussed at the beginning of Chapter 2 and Chapter 4 respectively. [^{111}In a candidate for tumour imaging and ^{111}Ag a candidate for tumour therapy.]

1.7. References

1. "Introduction to the Cellular and Molecular Biology of Cancer", L.M. Frank and N. Teich (eds.), Oxf. Science Publ. (1986).

2. C.J. van Garderen, H. van den Elst, J.H. van Boom and J. Reedijk, J. Am. Chem. Soc., 111, 4123 (1989).

3. J.H.J. den Hartog, C. Altona, J.H. van Boom, G.A. van der Marel, C.A.G. Hasnoot and J. Reedijk, J. Am. Chem. Soc., 106, 1528 (1984).

4. P.J. Stone, A.D. Kelman and F.M. Sinex, Nature, 251, 736 (1974).

5. G. Köhler and C. Milstein, Nature, 256, 495 (1975).

6. F.R. Seiler, P. Gronski, R. Kurrle, G. Lüben, H.-P. Harthus, W. Ax, K. Bosslet and H.-G. Schwick, Angew. Chem. Int. Ed. Engl., 24, 139 (1985).

7. N.K. Jerne, Angew. Chem. Int. Ed. Engl., 24, 810 (1985).

8. C. Milstein, Angew. Chem. Int. Ed. Engl., 24, 816 (1985).

9. G. Köhler, Angew. Chem. Int. Ed. Engl., 24, 827 (1985).

10. J.L. Marx, Science, 229, 455 (1985).

11. S.E. Halpern and R.O. Dillman, J. Biol. Response Mod., 6(3), 3, 235 (1987).

12. L. Riechmann, M. Clark, H. Waldmann and G. Winter, Nature, 332, 323 (1988).

13. D. Colcher, A.M. Keenan, J.M. Larson and J. Schlom, Cancer Res., 44(12), 5744 (1984).

14. R.D. Neirinkx, Chem. Br., 22 (no. 4), 335 (1986).

15. W. Wolf and J. Shani, Nucl. Med. Biol. (Int. J. Rad. Appl. Instrum. Part B), 13(4), 319 (1986).

16. B.W. Wessels and R.D. Rogus, Med. Phys., 11(5), 638 (1984).

17. A.D. Guerra, Physica Scripta, T19, 481 (1987).

18. D.A. Scheinberg, M. Strand and O. Gansow, Science, 275, 1511 (1982).

19. D.M. Goldenberg (ed.), Cancer Res., 40(8), part 2 (1980).

20. S.E. Halpern and R.O. Dillman, J. Biol. Response Mod., 6, 235 (1987).

21. J.L. Humm, J. Nucl. Med., 27(9), 1490 (1986).

22. R.P. Spencer, Nucl. Med. Biol., 13(4), 461 (1986).

23. M.J. Myers, A.A. Epenetos and G. Hooker, Nucl. Med. Biol., 13(4), 437 (1986).

24. R.A. Fawwaz, T.S.T. Wang, S.C. Srivastava and M.A. Hardy, Nucl. Med. Biol., 13(4), 429 (1986).

25. E. Deutch, K. Libson, J.-L. Vanderheyden, A.R. Ketring and R. Maxon, Antibody, Immunoconjugates and Radiopharmaceuticals, 1(3) (1988).

26. K. Kumar, M. Magerstädt and O. Gansow, J. Chem. Soc. Chem. Commun., 3, 145 (1989).

27. D. Parker and P.S. Roy, Inorg. Chim. Acta, 148(2), 251 (1988).

28. B.A. Khaw, J.T. Fallon, H.W. Strauss and E. Haber, Science, 209, 295 (1980).

29. D.A. Scheinberg, M. Strand and O. Gansow, Science, 275, 1511 (1984).

30. C.F. Meares and T.G. Wensel, Acc. Chem. Res., 17, 202 (1984).

31. C.F. Meares, Nucl. Med. Biol., 13(4), 311 (1986).

32. M.W. Brechbeiel, O.A. Gansow, R.W. Atcher, J. Schlom and J. Esteban, Inorg. Chem., 25, 2772 (1986).

33. W.T. Anderson-Berg, R.A. Squire and M. Strand, Cancer Res., 47, 1905 (1987).

34. L.C. Washburn, T.T. Hwa Sun, J.E. Crook, B.L. Byrd, J.E. Carlton, Y.-W. Hung and Z.S. Steplewski, Nucl. Med. Biol., 13(4), 453 (1986).

35. S.E. Halpern, R.O. Dillman, K.F. Witztum, J.F. Shega, P.L. Hagan, W.M. Burrows, J.B. Dillman, M.L. Clutter, R.E. Sobol, J.M. Frincke, R.M. Bartholomew, G.S. David, D.J. Carlo, Radiology, 155(2), 493 (1985).

36. R.M. Rainsbury, Br. J. Surg., 71(10), 804 (1984).

37. B.A. Khaw, J.C. Lasher and W.L. McGuire, Eur. J. Nuc. Med., 14, 362 (1988).

38. H. Sands, Antibody, Immunoconjugates and Radiopharmaceuticals, 1(3), 213 (1988).

39. T. Rhyl, Acta Chem. Scand., 26, 3955 (1972).

40. C.J. Pedersen, J. Am. Chem. Soc., 89, 7017 (1967).

41. H.K. Frensdorff, J. Am. Chem. Soc., 93, 600 (1971).

42. (a) D. Dietrich, J.M. Lehn and J.P. Sauvage, Tet. Lett., 2885, 2889 (1969).
(b) C.J. Pedersen, H.K. Frensdorff, Angew. Chem. Int. Ed. Engl., 11, 16 (1972).

43. J.J. Christensen, J. Eatough and R.M. Izatt, Chem. Rev., 74, 351 (1974).

44. J.C.A. Boeyens and S.M. Dobson, Ch. 1 in "Stereochemical and Stereophysical Behaviour of Macrocycles", I. Bernal (ed.) Elsevier, 1987.

45. L.F. Lindoy, Chem. Soc. Review, 4, 421 (1975).

46. (a) L.Y. Martin, L.J. Dettayes, L.J. Zompa and D.H. Busch, J. Am. Chem. Soc., 96, 4046 (1974).
(b) A. Anichini, L. Fabrizzi, P. Paoletti and R.M. Clay, Inorg. Chim. Acta, 22, L25 (1977).

47. (a) D.K. Cabbiness and D.W. Margerum, J. Am. Chem. Soc., 91, 6540 (1969).
(b) D.K. Cabbiness and D.W. Margerum, J. Am. Chem. Soc., 92, 2151 (1970).

48. F.P. Hinz and D.W. Margerum, J. Am. Chem. Soc., 96, 4993 (1974).

49. F.P. Hinz and D.W. Margerum, Inorg. Chem., 13, 2941 (1974).

50. P. Paoletti, L. Fabrizzi and R. Barbucci, Inorg. Chem., 12, 1961 (1973).

51. L. Fabrizzi, P. Paoletti and A.P.B. Lever, Inorg. Chem., 15, 1502 (1976).

52. E. Kimura and M. Kodama, J. Chem. Soc. Chem. Commun., 326 and 891 (1975).

53. E. Kimura and M. Kodama, J. Chem. Soc. Dalton Trans., 1473 (1977).

54. L. Fabrizzi, P. Paoletti and R.M. Clay, Inorg. Chem., 17, 1042 (1978).

55. L. Fabrizzi, M. Micheloni and P. Paoletti, J. Chem. Soc. Dalton Trans., 1581 (1979).

56. L.L. Diaddario, L.L. Zimmer, T.E. Jones, L.S. Sokol, R.B. Cruz, E.L. Yee, L.A. Ochrymowycz and D.B. Rorabacher, J. Am. Chem. Soc., 101, 3511 (1979).

57. B.L. Haymore, J.D. Lamb, R.M. Izatt and J.J. Christensen, Inorg. Chem., 21, 1598 (1982).

58. F. Arnaud-Neu, M.-J. Schwing-Weill, R. Louis and R. Weiss, Inorg. Chem., 18, 2956 (1979).

59. M. Micheloni, P. Paoletti and J. Sabatini, J. Chem. Soc. Dalton Trans., 1189 (1983).

60. D.H. Busch, Acc. Chem. Res., 11, 392 (1978).

61. E.J. Billo, Inorg. Chem., 23(2), 236 (1984).

62. R.W. Hay, R. Bembi, W.T. Moodie and P.R. Norman, J. Chem. Soc. Dalton Trans., 2131 (1982).

63. L.F. Lindoy, "The Chemistry of Macrocyclic Ligand Complexes", (Camb. Univ. Press), 1989.

64. R.D. Hancock and M.P. Ngwenya, J. Chem. Soc. Dalton Trans., 2911 (1987).

65. J. Dale, Acta Chem. Scand., 27, 1115 (1973) and Tetrahedron, 20, 1683 (1974).

66. J. Dale, Israel J. Chem., 20, 3 (1980).

67. B. Dietrich, J.M. Lehn and J.P. Sauvage, Tet. Lett., 2885 (1969).

68. B. Dietrich, J.M. Lehn and J.P. Sauvage, Tet. Lett., 2889 (1969).

69. B. Dietrich, J.M. Lehn and J.P. Sauvage, Tetrahedron, 29, 1629 (1973).

70. B. Dietrich, J.M. Lehn and J.P. Sauvage, Tetrahedron, 29, 1647 (1973).

71. J.M. Lehn, Structure and Bonding, 16, 1 (1973).

72. J.M. Lehn and J.P. Sauvage, J. Am. Chem. Soc., 97, 6700 (1975).

73. J.M. Lehn and F. Montavon, Helv. Chim. Acta, 61, 67 (1978).

74. D.J. Cram, Science, 219, 1177 (1983) and ref. therein.

75. G.M. Lein and D.J. Cram, J. Chem. Soc. Chem. Commun., 301 (1982).

CHAPTER TWO

MACROCYCLES TO BIND INDIUM(III) AND GALLIUM(III)

2.1. Indium Coordination Chemistry

2.1.1. Introduction

Indium is the fourth member of group III in the periodic table, with an electronic configuration of $[Kr]4d^{10}5s^{2}5p$. Indium(III) is the most common oxidation state, but indium(I) and indium(II) complexes are also known.[1,2]

Indium(III) forms neutral, cationic and anionic complexes e.g. $InCl_3(py)_3$, $[In(en)_3][3Cl]$ and $[NH_4][InF_6]$ respectively. The majority of indium(III) complexes are octahedral and many examples[2] are known of neutral complexes with monodentate amine donors of stoichiometry InX_3L_3 (e.g. L = pyridine, α-picoline, aniline and X = Cl, Br, I).

As mentioned in Chapter 1, the modified chelates EDTA and DTPA have been used to bind indium(III) for use in radioimmunoscintigraphy. The nitrogen donor atoms and the negatively charged oxygen donor groups of these ligands are well suited to the binding of indium(III) as they form relatively strong covalent In-N and In-O bonds. However, EDTA with an $N_2O_4^{4-}$ donor set and DTPA with an $N_3O_5^{5-}$ donor set produce anionic complexes when bound to indium(III) ($[In\text{-}EDTA]^-$ and $[In\text{-}DTPA]^{2-}$). These complexes are stable at pH 7 but they protonate at lower pH (e.g. liver, stomach for <u>in vivo</u> application). These protonated complexes may be more susceptible to dissociation (either acid or metal catalysed) compared to a neutral complex. The X-ray crystal structure of $Na_2In(DTPA).7H_2O$ has recently (July 1989) been reported.[3] The indium ion is bound by the three amino groups and all five of the deprotonated carboxylate groups in a complex which adopts a slightly distorted Archimedian antiprismatic configuration [Fig. 2.1].

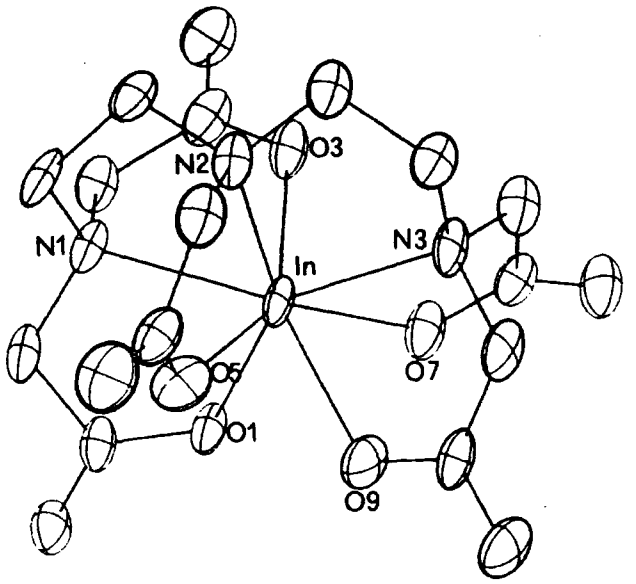

Fig. 2.1. ORTEP view of $Na_2In(DTPA).7H_2O$.

2.1.2. **Indium(III) macrocyclic complexes**

Little work has been reported on the complexation of indium(III) with macrocyclic ligands, although indium(III) porphyrin complexes of the type InX-L (L = porphyrin X = Cl^-, OAc^- or PhO^-)[4-6] have been known for some time. In 1981 Tuck[7] reported the formation of indium(III) halide complexes of dibenzo-18C6 (22) and cyclam (4) during the course of studies directed towards the use of macrocycles to stabilise the

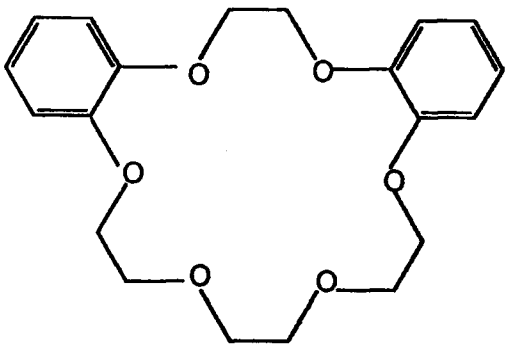

(22) Dibenzo-18C6

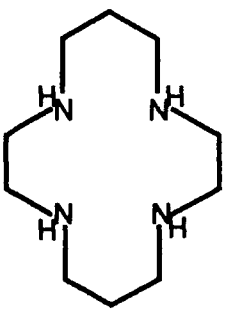

(4) "Cyclam"

indium(I) oxidation state.

Wieghardt[8] has reported that the tridentate macrocycles 1,4,7-triazacyclononane (14) and N,N',N"-trimethyl-1,4,7-triazacyclononane (23) form 1:1 complexes with indium(III), of the type $LInX_3$ (X =

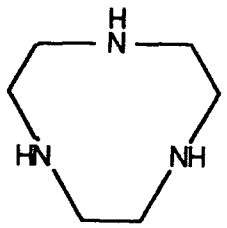

(14)

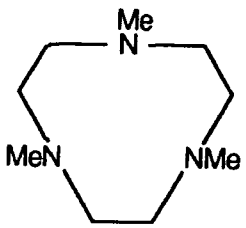

(23)

Cl, Br, I), with facial coordination of the nine-membered ring. Also, ligand (14) forms the octahedral bis-macrocyclic complex with indium(III). These triaza macrocycles show a strong "macrocyclic effect" with transition metal ions (e.g. Cu(II), Zn(II) and Ni(II)[9]) but no thermodynamic or kinetic data has been reported for the indium(III) complexes.

X-ray crystal structures have been reported for the related oxo and hydroxo bridged indium(III) complexes of ligand (14). In the hydroxy bridged tetrameric cation $[L_4In_4(\mu\text{-}OH)_6]^{6+}$ (Fig. 2.2) each indium cation

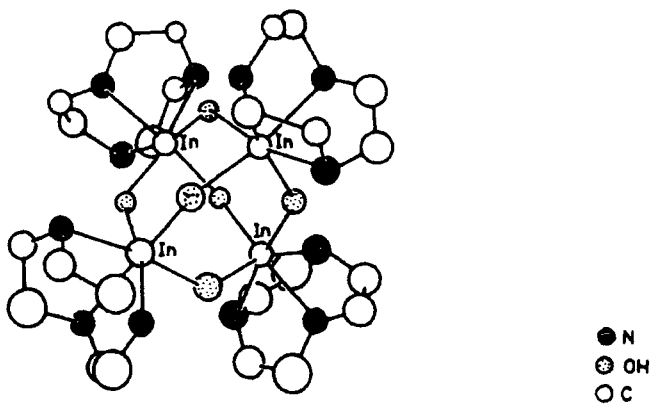

Fig. 2.2. The structure of $[L_4In_4(\mu\text{-}OH)_6](S_2O_6)_3 \cdot 4H_2O$.

binds to three bridging hydroxy groups forming a $[In_4(\mu\text{-}OH)_6]^{6+}$ core, with an adamantane-like structure. In addition, each indium cation is bound facially by the triaza macrocycle, resulting in a slightly distorted octahedral coordination sphere with an N_3O_3 donor set.

Similarly, in the binuclear oxo bridged structure $[L_2In_2(CH_3CO_2)_4(\mu\text{-}O)]$ (Fig. 2.3) the indium is bound facially by the macrocycle and is also bound by three negatively charged oxygen donor atoms (two acetate ions and one bridging oxygen) forming a neutral complex. The 1:1 complexes $LInX_3$ (L = (14), (23) X = Cl, Br) are useful starting materials for the synthesis of indium hydroxy and oxy bridged species, as no appreciable dissociation occurs when they are treated

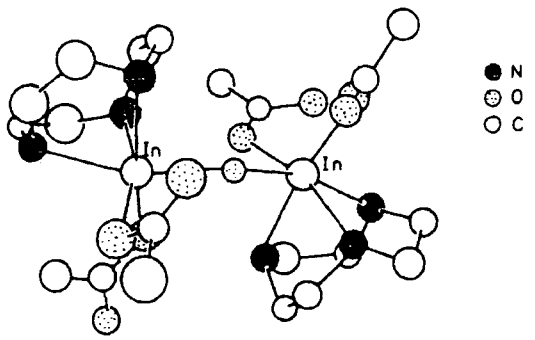

Fig. 2.3. The structure of $[L_2In_2(CH_3CO_2)_4(\mu\text{-}O)].2NaClO_4$.

with aqueous alkaline solution: hence no precipitation of $In(OH)_3$ is observed.

2.1.3. <u>The selection of new macrocycles to bind indium(III)</u>

In order to bind indium(III) effectively for use in radioimmunoscintigraphy, a hexacoordinating ligand which could adopt octahedral geometry was required. In addition, a ligand with three ionisable groups was sought, in order to reduce the effective nuclear

charge at the metal centre. The overall complex would then be electrically neutral and thereby much less sensitive to acid catalysed dissociation.

The triaza macrocycle (14) has been shown to form stable complexes with indium(III) as discussed in the previous section. When the macrocycle is N-functionalised with three carboxymethyl groups the donor set is expanded from three (N_3) to six (N_3O_3). Furthermore, with the negatively charged oxygen donor groups the overall complex is neutral. The four N-functionalised triaza macrocycles (24) to (27), with ring sizes varying from nine to twelve, were selected for synthesis and investigation of their indium(III) complexation chemistry.

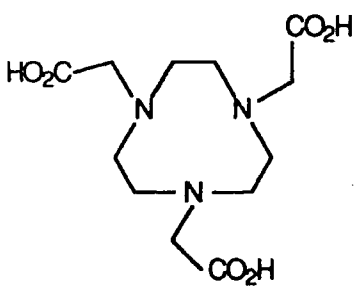

(24)

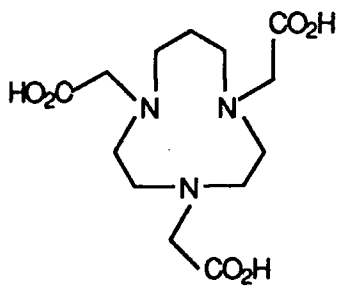

(25)

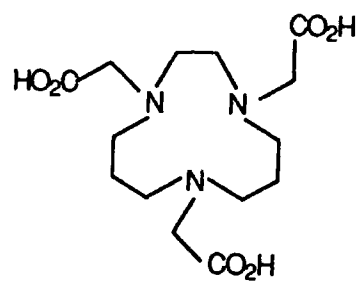

(26)

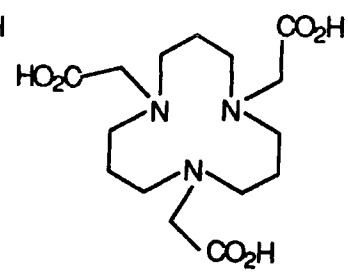

(27)

(24) 9N3-triacetate (TCTA) (25) 10N3-triacetate (26) 11N3-triacetate (27) 12N3-triacetate

The synthesis of the ligand (24) was first reported in 1973[10] and the formation of neutral Fe(III), Cr(III) and Co(III) complexes of ligands (24) and (25) reported in 1977.[11] Hancock prepared the nickel(II) complex of ligand (24) $H_3O[Ni(TCTA)]$[12] and found that on standing in acid solution it converted to the neutral nickel(III) complex Ni(TCTA)[13] [Fig. 2.4]. Wieghardt[14] has reported the syntheses and spectral properties (UV-visible, Infra-red) of several transition

metal complexes of TCTA and has reported the preparation of the group III metal complex Al-TCTA.

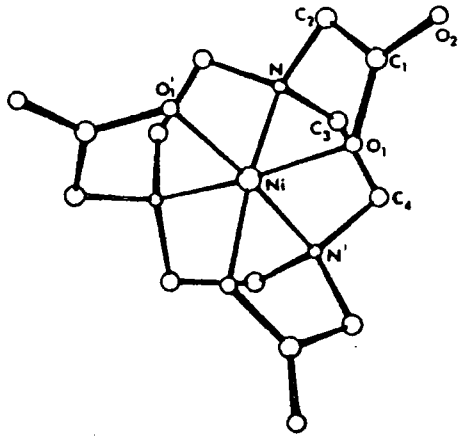

Fig. 2.4. X-ray crystal structure of Ni(TCTA).

In recent years the synthesis of several other N-functionalised derivatives of triaza macrocycles have been reported,[15] of which some examples are listed in Table 2.1.[9,15-22] A potentially useful

Table 2.1

N-functionalised derivatives of TACN (14)

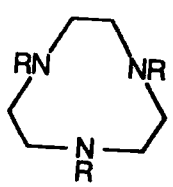

R	Abbreviation
$-CH_2CO_2(C_2H_5)$	TCTAE
$-CH_2CH_2-SO_3H$	TES
$-CH_2CH_2OH$	THETAC
$-CH_2CH(OH)CH_3$	-
$-CH_2PO_3H_2$	-
$-CH_2P(O)(Ph)_2$	TPA
$-CH_2CH_2NH_2$	TAETACN
$-CH_2-(2)pyr$	TPTCN

alternative to the carboxylate functionality of the pendant arm is the phosphinic acid group ($-CH_2P(R)O_2H$, R = H, alkyl) which also provides a singly charged oxygen donor atom for binding to the metal ion. In theory, the lower pK_a of the phosphinic acid group would reduce the susceptibility of the metal complex to protonation and hence acid catalysed dissociation. For similar reasons the sulphonic acid group ($R-SO_3H$) would appear to be a favourable candidate for pendant arm functionality. However, in aqueous solution the amino(methylsulphonato) functionality undergoes hydrolysis;[23]

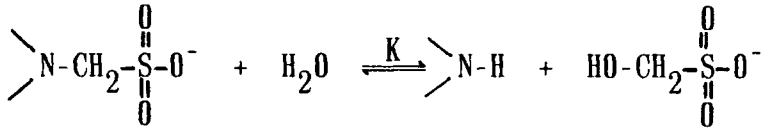

The species exists in equilibrium with the free secondary amine with K (equilibrium constant) = 1.2×10^{-4}.

The carboxylate functionality was chosen in the first instance for the relative ease of synthesis. The synthesis of triaza macrocycles bearing pendant arms with phosphinic acid functionality is currently underway in our laboratories at Durham.

In mid-1989, Kaden[24] reported the syntheses and X-ray crystal structures of the indium(III) complexes of two N,N',N''-triscarboxymethyl tetraaza macrocycles (28) and (29). In both cases the indium is hepta-

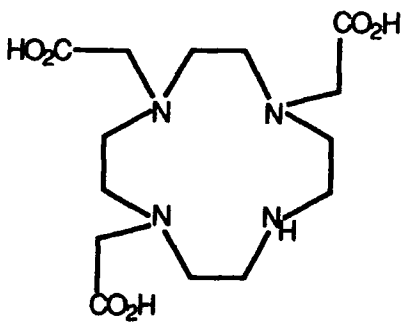

(28)

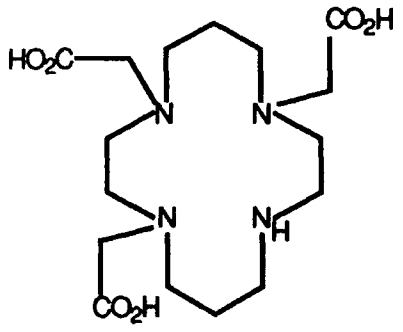

(29)

coordinate, binding to four nitrogens and three carboxylates and both complexes adopt a capped trigonal prismatic geometry [Fig. 2.5].

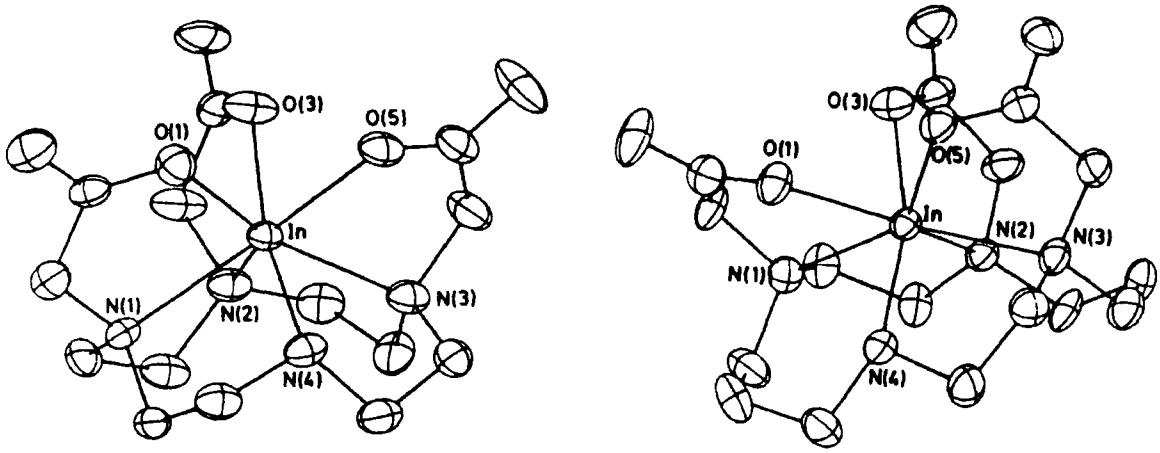

Fig. 2.5. a) X-ray crystal structure of the In(III) complex of ligand (28).

b) X-ray crystal structure of the In(III) complex of ligand (29).

The smaller ligand (28) is seen to fulfil the geometrical requirements of In^{3+} better than (29) with more uniform bond lengths and angles resulting in a more compact and symmetrical structure.

2.1.4. <u>Synthesis of four tribasic hexacoordinating macrocyclic ligands</u>

With the exception of the nine-membered ring, 1,4,7-triaza-cyclononane (14) which is available from Aldrich, the triaza macrocycles (33) to (35) [Table 2.2] were synthesised according to the method outlined in Scheme 2.1. The acyclic tosylates and tosylamides were prepared from the parent amines and alcohols according to literature procedures,[25-27] using p-toluensulphonyl chloride and pyridine. Cyclisation reactions to form small triamine ring systems have been reported previously.[28-30] The method used here was a modification of the ditosylamide method of Richman and Atkins,[29] using caesium carbonate in DMF, as reported by Kellogg.[31] The ditosylate in DMF was added

Table 2.2

	n=2, m=2	n=2, m=3	n=3, m=2	n=3, m=3
	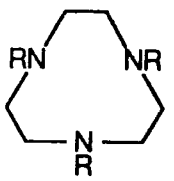	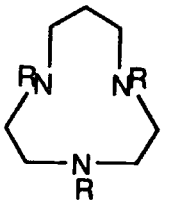	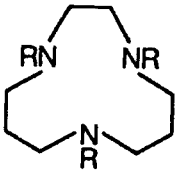	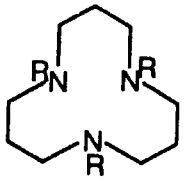
R=Ts	-	(30)	(31)	(32)
R=H	(14)	(33)	(34)	(35)
R=-CH_2CO_2H	(24)	(25)	(26)	(27)

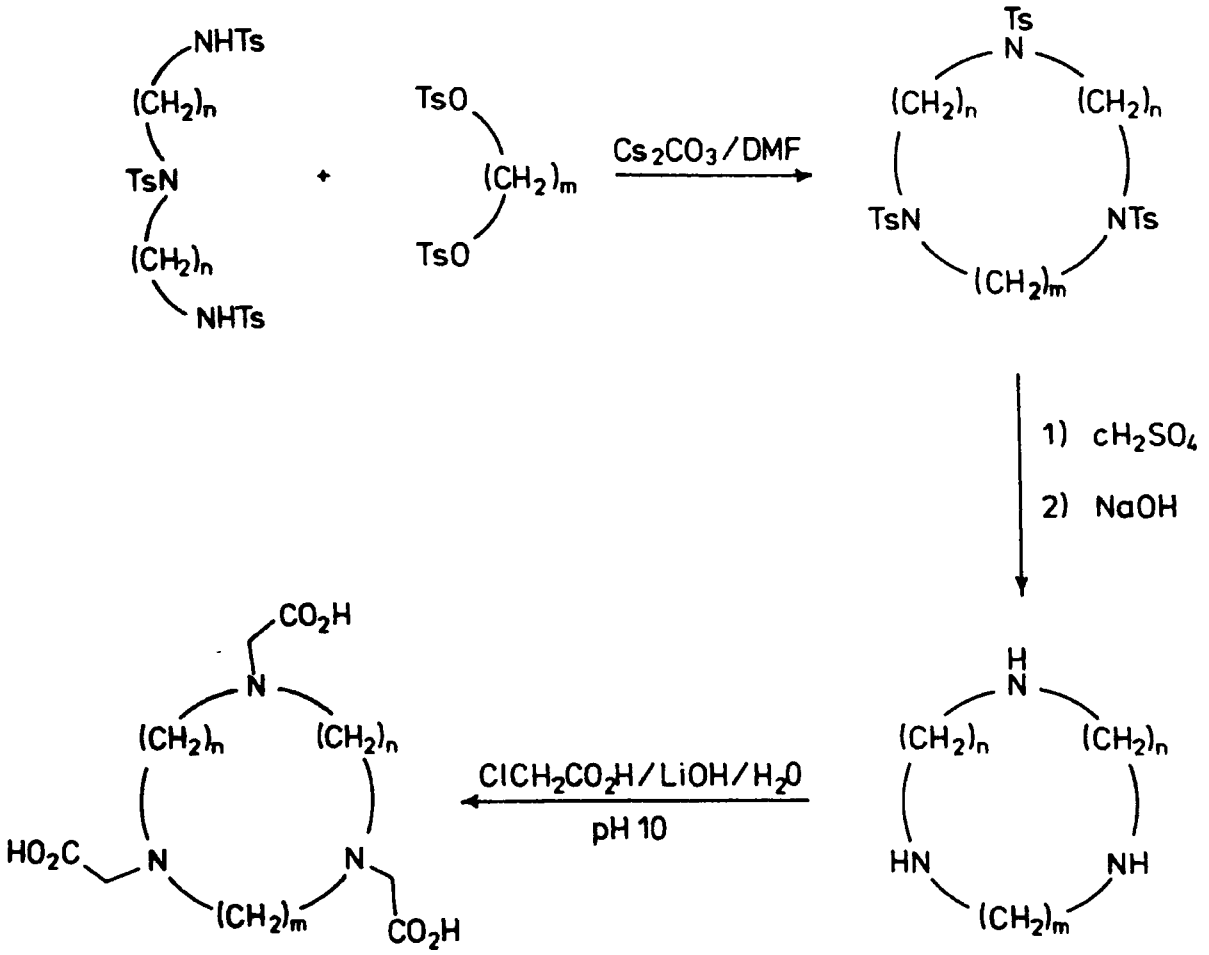

Scheme 2.1. The synthesis of N,N',N"-triacetate-triaza macrocycles.

slowly to a well stirred suspension of caesium carbonate in a solution of the ditosylamide in DMF, under anhydrous conditions. The tritosylamide cycles were obtained in good yield (60-80%) after purification by recrystallisation (EtOH-CH_2Cl_2) for (30) and silica gel chromatography, eluting with dichloromethane-methanol, for (31) and (32).
Detosylation was effected using concentrated sulphuric acid at 120°C followed by basification with sodium hydroxide solution and extraction into chloroform.[32] The nine, ten and eleven membered cycles were N-alkylated with chloroacetic acid in aqueous solution at pH 10 (LiOH) according to the method of Takamoto.[33] The N,N',N''-triacetates were purified by recrystallisation from an acidic aqueous (HCl)-ethanol system with slow diffusion of the ethanol into the aqueous layer, yielding colourless crystals. Microanalysis revealed that the nine-membered N-alkylated cycle was isolated as the dihydrochloride salt whereas the ten and eleven-membered analogues were obtained as the free amines. In order to obtain the former chloride free, the alkylation reaction was repeated using bromoacetic acid and acidification was effected with nitric acid, rather than hydrochloric acid, in the work up. Recrystallisation from the aqueous-ethanol system proved to be more difficult, but did in fact yield the chloride free product as a fine white solid.

The twelve-membered triaza ring (prepared by Dr. I.M. Helps) was N-alkylated using ethylbromoacetate with caesium carbonate in ethanol. The triester was purified by alumina chromatography eluting with dichloromethane-methanol and then hydrolysed to the triacid with hydrochloric acid.

2.1.5. **Indium complexation at low concentration**

An important feature of any complexing agent for application in

radioimmunotargeting is the ability to bind the radioisotope rapidly at low concentration and moderate temperature and pH. Once the macrocycle has been linked to the antibody it is necessarily present in low concentration (typically 10-40 μM) in aqueous solution. The temperature and pH must not exceed that of normal physiological conditions (pH 4-9; $T \leq 37^{o}C$) in order not to denature the immunoglobin. This method of radiolabelling the antibody-macrocycle conjugate is known as "post-labelling". The alternative procedure of "pre-labelling" involves radiolabelling the macrocycle prior to antibody linkage, and allows greater freedom in the complexation step. However, this method is severely limited by the time required to covalently link the radiolabelled macrocycle to the antibody and purify the conjugate. In addition to the practical problems of the chemistry using a 'hot' radioisotope, much of the activity would be lost before the radiolabelled antibody was injected into the patient.

Hence, the four triaza-triacid macrocycles (24)-(27) were screened for their ability to bind indium-III rapidly ($\leq$ 1 hr) under mild conditions ($20^{o}C$, pH 5) at low concentration, yet still form a kinetically inert complex <u>in vivo</u>. The ligands were investigated at concentrations of 10-100 μMolar in aqueous solution buffered at pH 5 with 0.1M NaOAc, at $20^{o}C$. The forward rate of association with ^{111}In was monitored by HPLC (reverse phase-polymer, 150 x 4.6 mm) with radiometric detection. Elution times for the indium complexes, eluting with H_2O (89%), 1.0M NH_4OAc (10%) and MeCN (1%) with flow rate 1.0 ml/min., were between 2.5 and 4.0 minutes. The results are summarised in Table 2.3.[34]

At 100 μM (ligand concentration) the extent of indium uptake after 30 minutes was;

$$(24) > (25) >> (27) > (26).$$

Table 2.3

Relative rates of ^{111}In association of ligands (24) to (27) at low concentration (not optimised)

Ligand	Concentration	time/min.	% ^{111}In uptake
(24)	1 mM	10	72
	100 μM	20	75
	10 μM	30	74
(25)	1 mM	30	32
	100 μM	40	19
	10 μM	20	0
(26)	1 mM	20	0
	100 μM	30	0
	10 μM	40	0
(27)	1 mM	30	15
	100 μM	40	8
	10 μM	60	0

At 10 μM, only the nine-membered triacid showed effective radiolabelling, with a yield of 74% after 30 minutes. In subsequent studies an improved radiolabelling yield of 96% was determined (30 min., pH 5, 20^{o}C). When the ^{111}In complex of (24) was injected into normal mice, all radioactivity was cleared from the tissue in a few hours. This indicated that the isotope was staying bound to the macrocycle *in vivo*, which, as a foreign body, is excreted by the mouse.

Hence the nine-membered triaza-triacid was selected for further investigation.

2.1.6. Synthesis and characterisation of indium(III) complexes

The complexation of In(III) by ligand (24) was observed by ^1H nmr in D_2O. An equimolar quantity of indium trichloride was added to the ligand (25 mMolar) in D_2O, buffered at pD 5 with deuteroacetate/ deuteroacetic acid (I = 0.1, pD = 5.0). The diastereotopic ring protons of the complex resonated as an AA'BB' system with multiplets centred at 3.28 and 3.12 ppm and the methylene 'CH_2CO' protons gave a single resonance at 3.75 ppm (Fig. 2.6). In the free ligand the ring protons

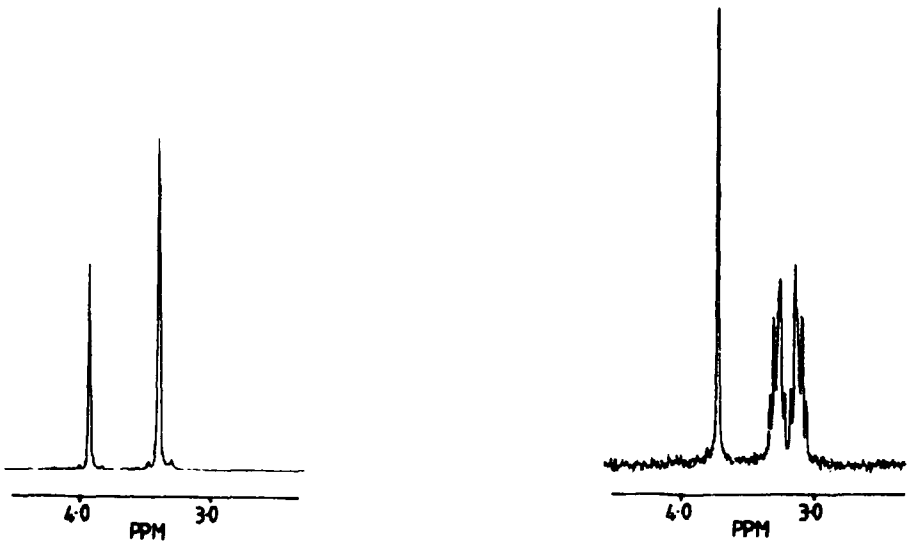

a) Ligand b) In(III) complex

Fig. 2.6. ^1H nmr of a) the ligand (24) and b) its indium(III) complex in D_2O.

resonated as a singlet at 3.42 ppm and the methylene protons 'CH_2CO' gave a singlet at 3.96 ppm.

Two forms of the indium complex of (24) were isolated as crystalline solids, the simple 1:1 complex In-L (36) and the hydrated chloroindium complex [(In-L).HCl.H_2O] (37). The former was prepared by

reacting equimolar quantities of indium nitrate and ligand (24) (prepared chloride free - section 2.1.4.) in aqueous nitric acid (0.04M) at room temperature for several hours (acidic conditions stabilises the $In(NO_3)_3$ with respect to hydrolysis to the insoluble hydroxide $In(OH)_3$). The complex was precipitated by the addition of acetone and recrystallised from water-acetone (1:4). Microanalysis and DCI mass spectrometry (m/e: 416 $[M^+ +1]$) results were consistent with the formation of a neutral 1:1 hexacoordinate complex. The hydrated chloroindium complex (37) was prepared by reacting equimolar quantities of indium trichloride with the ligand [dihydrochloride] in hydrochloric acid (initially 0.04 Molar). Slow evaporation of solvent over several days yielded colourless crystals of the $[(InL)HCl.H_2O]$ complex. The two complexes gave the same proton nmr in D_2O (at similar pD) indicating that the solution state structures were the same.

Crystals suitable for X-ray diffraction were obtained by the slow evaporation method for the hydrated chloroindium complex. The solid-state structure (Fig. 2.7) was determined independently at two centres.

The molecule comprises an indium(III) ion in a pentagonal bipyramidal coordination environment in which the axial sites are occupied by a chloro ligand and one tertiary amine (In-N(3) 2.288(5)Å) of the triaza macrocycle. The two remaining nitrogens occupy positions in the equatorial plane (In-N(1) 2.332(5), In-N(2) 2.331(5) and N(1)-In-N(2) 75.3°). The remaining three equatorial sites are filled by an oxygen atom from each of the three carboxymethyl groups, one of which is protonated (In-O 2.284, 2.424, 2.116Å). These and other selected bond lengths and angles are given in Table 2.4.

The indium-nitrogen and indium-oxygen bond lengths compare

InCl-LH , L =

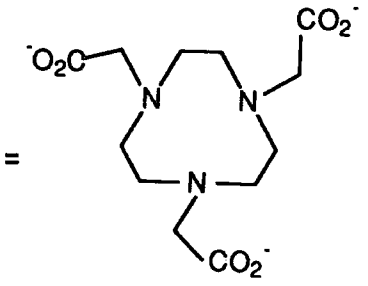

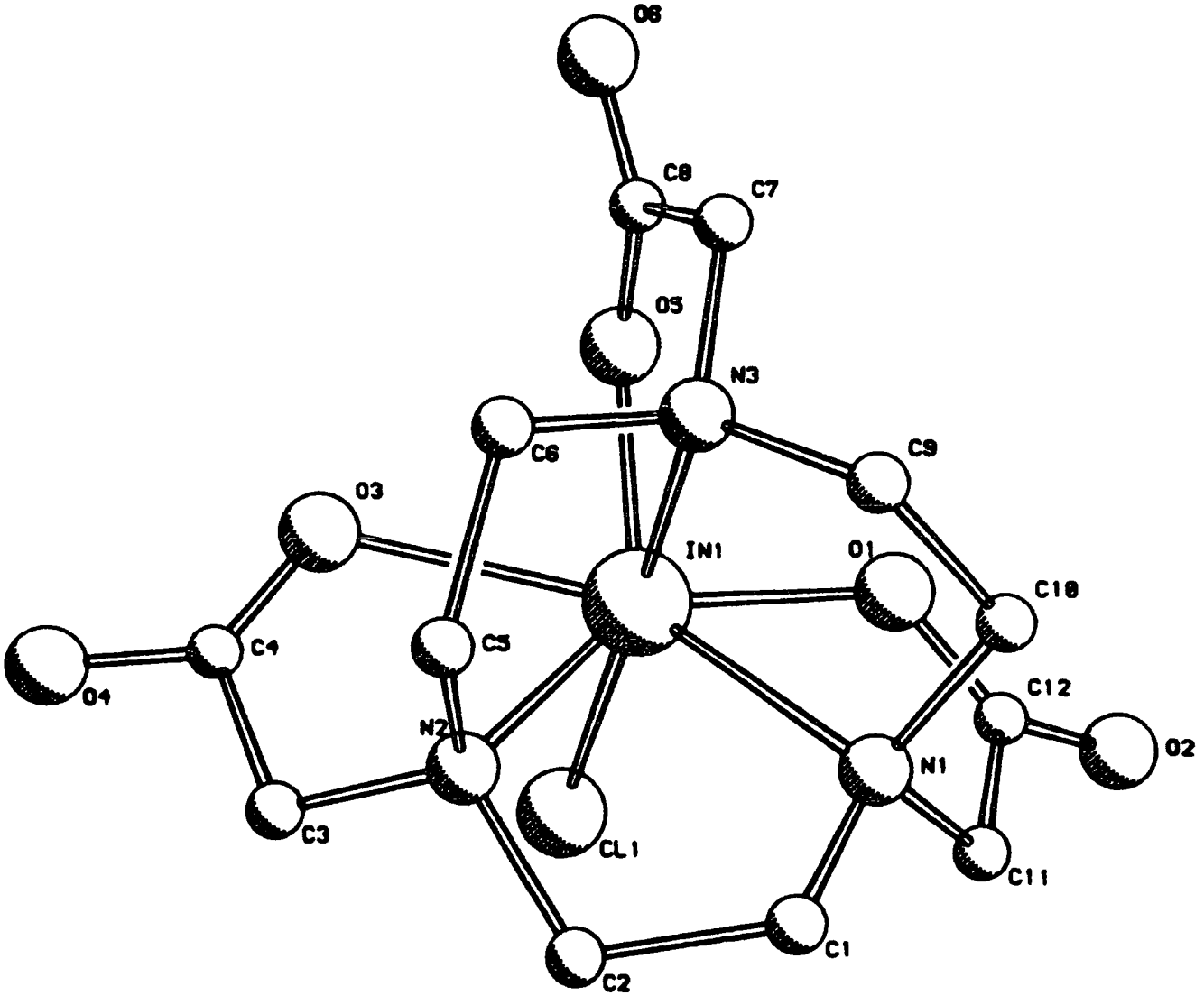

Fig. 2.7. X-ray crystal structure of (In-L).HCl.H_2O, L = (24).

Table 2.4

Selected bond lengths (Å) and bond angles (deg) for (In-L).HCl.H_2O

In-Cl	2.399(2)	In-O(1)	2.284(4)
In-O(3)	2.424(4)	In-O(5)	2.116(5)
In-N(1)	2.332(5)	In-N(2)	2.331(5)
In-N(3)	2.288(5)		
Cl-In-O(1)	83.1(1)	Cl-In-O(3)	83.0(1)
O(1)-In-O(3)	143.2(1)	Cl-In-O(5)	112.0(1)
O(1)-In-O(5)	80.3(1)	O(3)-In-O(5)	73.8(1)
Cl-In-N(1)	99.6(1)	O(1)-In-N(1)	71.3(2)
O(3)-In-N(1)	144.8(2)	O(5)-In-N(1)	134.2(2)
Cl-In-N(2)	91.0(1)	O(1)-In-N(2)	144.5(2)
O(3)-In-N(2)	69.5(2)	O(5)-In-N(2)	133.5(2)
N(1)-In-N(2)	75.3(2)	Cl-In-N(3)	168.3(2)
O(1)-In-N(3)	104.8(2)	O(3)-In-N(3)	94.9(1)
O(5)-In-N(3)	78.1(2)	N(1)-In-N(3)	75.4(2)
N(2)-In-N(3)	77.6(2)		

favourably with those reported for other indium complexes, with the exception of the one long In-O bond. For example, the hydroxy bridged indium tetrameric cation of the triamine (14) [Fig. 2.2, section 2.1.2.] has In-N bonds ranging from 2.29-2.35Å and the oxo bridged binuclear tetraaceto species of the same ligand [Fig. 2.3] gives In-N bonds 2.27-2.32Å and In-O (aceto) bonds of 2.14 and 2.87Å. Hepta-coordination in indium complexes is unusual, as 5 or 6-coordinate complexes are usually observed. However, Kaden has recently reported[24] two more heptacoordinate indium complexes of the tetraaza-tricarboxymethyl

macrocyles (28) and (29) [Fig. 2.5, section 2.1.2.] as mentioned earlier. In these complexes, the In-N bonds are generally longer than for the smaller macrocyclic ligand reported here, with In-N bonds ranging from 2.31-2.39Å for (28) and 2.26-2.47Å for (29). In-O bonds are reported as 2.16-2.32Å. Furthermore, the indium complex reported here has shorter In-N bond lengths than observed in the In-DTPA complex [In-N, 2.388(8) to 2.414(8)Å][3].

The indium complex of the ten-membered triaza-triacid (25) [In-L] was prepared in a similar manner to that used for the nine-membered analogue (Indium trinitrate method). Microanalysis and mass spectrometry confirmed that a 1:1 neutral complex had formed, with no chloride or water of hydration. The ^{1}H nmr in D_2O was very complex, consistent with the lower symmetry of the complex. The indium complexes of the eleven and twelve-membered analogues, (26) and (27), were not isolated as crystalline solids, but their complexation was observed by ^{1}H nmr (again rather complex ^{1}H nmr spectra were observed).

2.2. Dissociation Kinetics of In-[9]-N_3 triacid

2.2.1. Introduction

Of primary importance for radiopharmaceutical application is the kinetic stability of the indium-macrocycle complex in vivo. In particular, the kinetic stability at low pH is of interest since dissociation is acid catalysed. In some parts of the human body acidic conditions as low as pH 2 may be encountered (e.g. liver and stomach). Therefore, ideally no appreciable dissociation of the macrocycle indium complex should occur at that pH.

2.2.2. ^{13}C nmr studies

The kinetics of dissociation, under acidic conditions, were investigated for the indium complex of the [9]-N_3 triacid (24), using ^{13}C nmr. The ^{13}C aceto carbonyl enriched ligand (39) was synthesised [Scheme 2.2] using ^{13}C aceto carbonyl enriched bromoacetic acid [Aldrich, 99%], using the same procedure as for the non-labelled analogue. The indium complex In-L was prepared using indium trinitrate

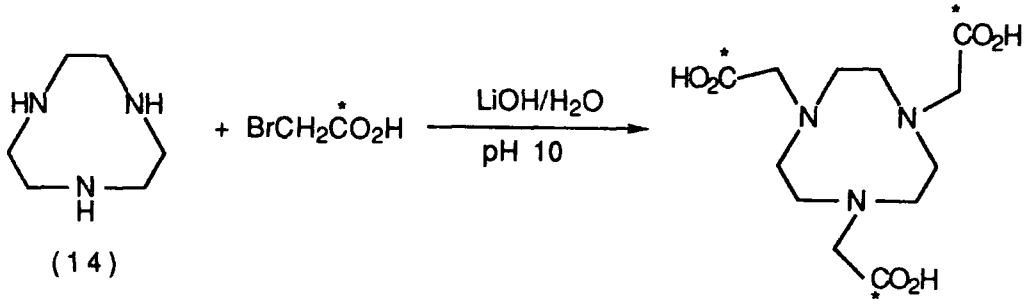

(14) (39)

* = ^{13}C enriched

Scheme 2.2. Synthesis of ^{13}C labelled [9]-N_3-triacid (39).

in nitric acid (0.04 Molar) to give the neutral complex [In-L].

The ^{13}C nmr (D_2O, pD 2-3) of the complex gave a sharp singlet at 175.4 ppm. A separate sharp singlet was observed at 172.1 ppm for the free ligand, hence the dissociation of the indium complex of the [9]-N_3 triacid could be monitored by ^{13}C nmr. The ^{13}C nmr spectra were recorded at 60.896 MHz on a Bruker AC 250 spectrometer. Typically 75-100 scans with a relaxation delay of 1 second were required to obtain spectra in which the signals could be integrated to give the relative ratio of complexed to dissociated ligand. Longer relaxation delays of 2 and 3 seconds resulted in no change in the signal intensities. Representative spectra are shown in Fig. 2.8.

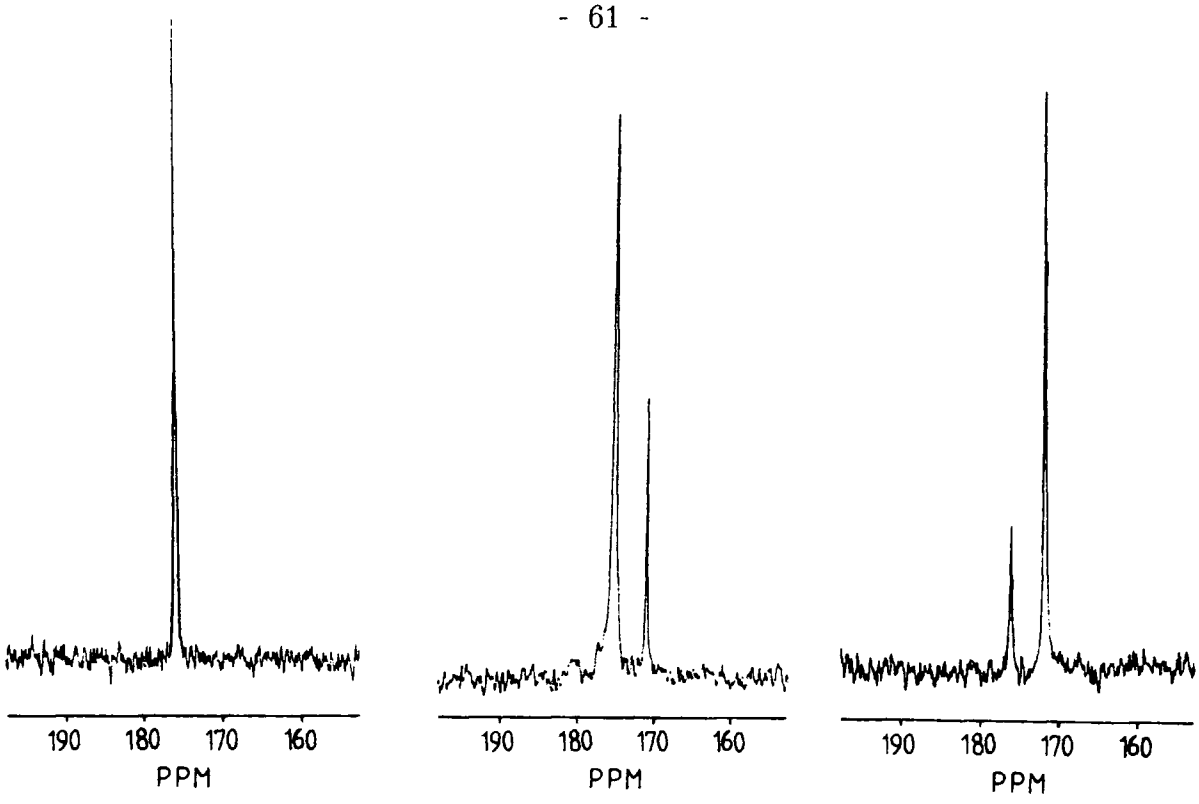

A) 100% In-L

(B) 80% In-L
20% LH_3

C) 18% In-L
82% LH_3

Fig. 2.8. ^{13}C nmr spectra showing the dissociation of the In-L complex in D_2O

Dissociation of the indium complex (0.01 mol dm^{-3}, D_2O) was monitored at pD 1, pD 0, pD -0.4 and pD -0.6 (acidified with concentrated nitric acid) at 23°C. In an early experiment it was discovered that the sample was being heated in the nmr probe, hence an early run was observed at 39°C. This was attributed to the local heating of the sample caused by the proton decoupler, which was running continuously. In a second experiment the temperature of the sample was reduced to 31.5°C by blowing air over the probe. The problem was solved by using a gated-decoupling technique, combined with maintaining a constant stream of air over the probe, which resulted in no heating of the D_2O solution. Thereafter, all further experiments were conducted at a constant 23°C.

At pD 2 the complex was observed to be stable in D_2O. Addition of indium trinitrate to a solution of the free ligand (equimolar quantities) revealed that complex formation occurred at this pD and was seen to be complete within 25 minutes. At pD 1 the dissociation of the complex was seen to reach an equilibrium. Approximately 20% dissociation was observed over a period of several hours, but no further dissociation was observed over several weeks. When indium trinitrate was added to a solution of the ligand in more strongly acidic conditions (pD = 0) no complex formation was observed over a period of 200 hours i.e. association was too slow to observe at this pD. Hence the dissociation of the preformed complex at pD $\leq$ 0 is essentially irreversible. The dissociation of the complex at pD 0 occurred over 3-4 hours. The results of this run and experiments conducted at pD = -0.4 and pD = -0.6 are presented as plots of $-\log[C]_t/[C]_0$ vs. time (sec) [Fig. 2.9] where $[C]_t$ = concentration of the complex at time 't' and $[C]_0$ = initial concentration of the complex.

These plots gave straight lines indicating that the dissociation reaction was pseudo-first order [in fact the kinetics of the dissociation was second order; first order dependence on complex concentration and first order acid dependence]. The rate expression is;

$$\text{Rate} = k[C][H^+]^n \qquad k = \text{rate constant}$$

When the acid is in large excess, as in the experiments described here, we can make the approximation that its concentration does not alter significantly during the reaction. Hence, the concentration of the acid can be incorporated into a new rate constant "k_{obs}", the pseudo-first order rate constant;

$$\text{Rate} = k_{obs}[C] \qquad \text{where } k_{obs} = k[H^+]^n$$

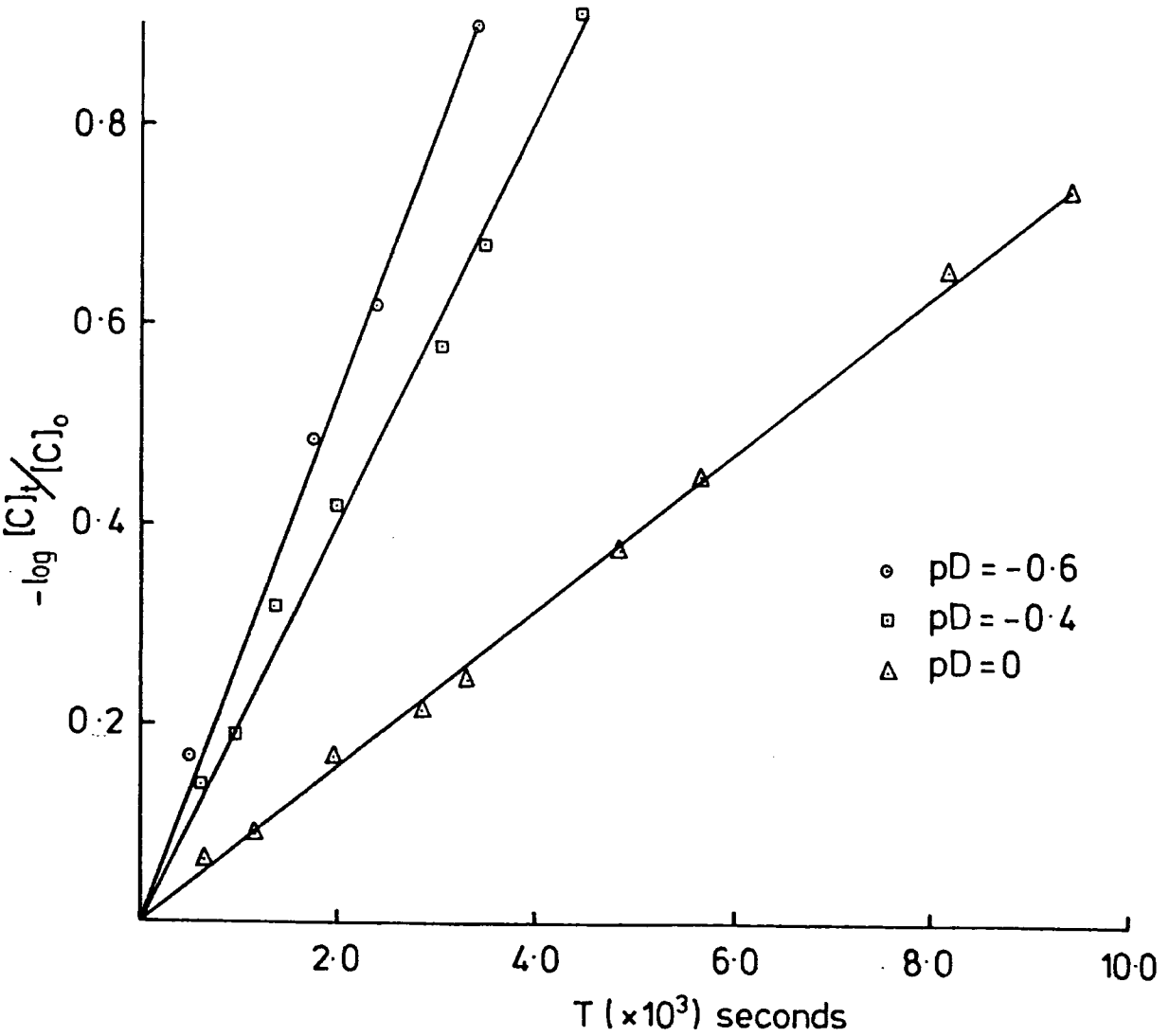

Fig. 2.9. Plot of $-\log[C]_t/[C]_o$ vs. t/sec for the dissociation of In-[9]N_3-triacid at pD = 0, -0.4 and -0.6 (23^oC).

and;

$$\frac{-d[C]}{dt} = k_{obs}[C]$$

integrates;

$$\ln \frac{[C]_t}{[C]_o} = -k_{obs}t$$

By measuring the "k_{obs}" values (determined from the slopes of the plots, Fig. 2.9, where lnX = 2.3026 log X) at different acid concentrations, we were able to deduce that the dissociation process was first order in acid concentration:

$$k_{obs} = k[H^+]$$

The rate constants are listed in Table 2.5.

Table 2.5

Results of the kinetic experiments on In-[9]N_3-triacid complex

Run	Temp/^oC	$[D^+]$ (pD)	$k_{obs}(x10^{-4})s^{-1a}$	$k(x10^{-4})/mol^{-1}dm^3s^{-1}$
(1)	39.0	0.98 (0)	9.34 ± 0.24	9.53 ± 0.24
(2)	31.5	0.98 (0)	4.04 ± 0.32	4.12 ± 0.33
(3)	23.0	0.98 (0)	1.81 ± 0.06	1.85 ± 0.06
(4)	23.0	2.36 (-0.4)	4.81 ± 0.20	2.04 ± 0.09
(5)	23.0	4.08 (-0.6)	6.56 ± 0.21	1.61 ± 0.05

a) errors are reported as the estimated deviation of the slope from the line of best fit.

Hence it was concluded that the dissociation of the indium complex [In-L] was overall second order;

$$\text{Rate} = k[C][H^+]$$

and the value of the second order rate constant was;

$$k = 1.8 \pm 0.3\ (x10^{-4})\ mol^{-1}dm^3s^{-1}$$

The "k_{obs}" values obtained for the dissociations observed at the three

different temperatures (23.0, 31.5 and 39.0^{o}C) at the same pD (0) gave reasonable agreement with the Arrhenius relationship;

$$k = Ae^{-Ea/RT}$$

$$\ln k = \ln A - Ea/RT$$

i.e. a plot of lnk vs. $^{1}/T$ gave a straight line (as far as could be determined with just three points) with a slope = 9.40 x 10^{3} s. Using the Arrhenius plot to estimate the errors associated with temperature fluctuation, it was found that a deviation of ± 1.0^{o}C in the temperature led to a deviation of ±0.23 x $10^{-4}s^{-1}$ in the value of the rate constant. This is similar to the error actually observed in the experiments described. It is most likely, therefore, that temperature fluctuations were the major source of error in these experiments.

The results reported here do not lead to a precise value of the second order rate constant 'k' and require more experiments to be performed to enable a satisfactory assessment of the errors involved. However, our immediate goals were achieved in that we were able to determine an approximate value of the rate constant and deduce that the dissociation was first order with respect to the acid concentration at low pH ($\leq$ 0).

Further information with respect to the acid catalysed dissociation pathway was available from the relative ^{13}C nmr shifts of the indium complex at different pD (Table 2.6). The ^{13}C nmr shift of the complex remained unchanged between pD 4.5 and 1.0, but was shifted by +0.78 ppm at pD 0. This suggests that at pD < 1.0 the complex may have protonated and thus the ^{13}C nmr signal observed at pD $\leq$ 0 (176.17) was in fact that of the monoprotonated species In-LH. Furthermore, the line broadening observed at pD 1 suggests that the pK_{a1} value for the complex may be close to one. By comparison, a shift of 0.68 ppm was observed for the

Table 2.6

^{13}C nmr shifts ($-CO_2-$) and linewidths '$\omega_{\frac{1}{2}}$' of the indium complex of (24) at different pD

pD	^{13}C nmr shift/ppm[a]	$\omega_{\frac{1}{2}}$/Hz[b]
4.5	175.40	19
2.0	175.39	21
1.0	175.41	59
$\leq$ 0	176.17	24

[a] ^{13}C shifts typically ±0.02 ppm.
[b] linewidths typically ±2.0 Hz.

free ligand between pD 3.5 (172.78 ppm) and pD 2.0 (172.14 ppm) and a further shift of 0.98 ppm between pD 2.0 and pD 1.0 (171.16). This is consistent with the reported pK_a values[35] for the ligand (pK_{a3} = 3.163 for LH_3 and pK_{a4} = 1.955 for LH_4^+). If the indium complex observed at pD < 1 was in fact the monoprotonated species In-LH, then a second protonation would then result in rapid dissociation of the complex. The acid catalysed dissociation pathway may then be represented as;

$$A + H^+ \underset{}{\overset{K_{a1}}{\rightleftharpoons}} B + H^+ \overset{K_{a2}}{\rightleftharpoons} C \xrightarrow{k}$$

where A = In-L, B = In-LH, C = $InLH_2$ and K_{a1}, K_{a2} are the acid dissociation constants where;

$$K_{a1} = \frac{[H^+][A]}{[B]} \quad \text{and} \quad K_{a2} = \frac{[H^+][B]}{[C]}$$

The rate of dissociation is;

$$\text{Rate} = k[C] = \frac{k[H^+][B]}{K_{a2}}$$

where [B] is related to the total substrate concentration [S] - 10^{-2} mol dm^{-3} in the ^{13}C nmr experiments - where [A] + [B] = [S], so;

$$[S] = [B] + \frac{K_{a1}[B]}{[H^+]} \quad \text{hence} \quad [B] = \frac{[S][H^+]}{([H^+] + K_{a1})}$$

Therefore

$$\underline{\underline{\text{Rate} = k.\frac{[S]}{K_{a2}} \frac{[H^+]^2}{([H^+] + K_{a1})}}}$$

In the limiting cases of a) low acid concentration ($K_{a1} > [H^+]$) then the rate expression approximates to;

$$\text{Rate} = \frac{k[S]}{K_{a2}.K_{a1}} [H^+]^2$$

hence dissociation of the complex is second order with respect to $[H^+]$ whereas b) high acid concentration ($[H^+] > K_{a1}$) then the rate expression approximates to;

$$\text{Rate} = \frac{k[S]}{K_{a2}} [H^+]$$

hence dissociation is first order with respect to acid concentration. It is proposed that this may have been the case for the dissociation of the indium complex at pD $\leq$ 0, i.e.;

$$\underline{k_{obs} = \frac{k}{K_{a2}} [H^+]}$$

2.2.3. <u>Conclusions</u>

Both solid state studies (X-ray diffraction) and solution studies (^1H and ^{13}C nmr) have shown that In(III) is bound effectively by the [9]-N_3-triacid ligand (24). Furthermore, the ^{13}C nmr studies have provided a useful indication of the kinetic stability of the indium complex towards acid catalysed dissociation. A desirable extension of this work would be to perform similar studies on the In-DTPA complex, which, we believe, would dissociate more readily at considerably higher pH values. The stability of In-DTPA (or other indium complexes for use in radioimmunoimaging) at low pH has not been reported. Traditionally

the kinetic stability of relevant indium complexes has been determined in serum in the presence of transferrin,[24,36] in an attempt to reproduce in vivo conditions. However, at pH 7.4, these studies are unlikely to provide an accurate measure of the kinetic stabilities of the complexes in vivo.

Perturbed angular correlation (PAC) spectroscopic measurements for the ^{111}In-[9]-N_3-triacetate complex revealed a quadrupole frequency (78K), w_q of 60 MHz. This compares favourably with the values for ^{111}In-transferrin (14 MHz) and ^{111}In-DTPA (9.8 MHz) and is consistent with a high complex stability in solution.[37]

2.3. Gallium(III) Coordination Chemistry

2.3.1. Introduction

Gallium (67) has attractive features as a γ-emitting isotope for use in radioimmunoscintigraphy. It has a half life of 78.1 hours, a single energy γ-emission (184 keV) and the isotope is obtainable 'carrier-free' from ^{67}Zn (p,n). A second isotope, gallium (68) also has considerable radiopharmaceutical application as a positron emitter for use in positron emission tomography (PET). Although the half life is rather short (68 min.) for monoclonal antibody related tumour imaging, it does have potential use in brain/renal scanning[38,39] and evaluation of myocardial blood flow.[40] A major advantage of gallium (68) over other positron emitting isotopes is that it is available relatively easily and cheaply from a germanium (68) generator.[39]

The coordination requirements of both types of gallium radiopharmaceutical are the same. The metal ion must be bound by a ligand such that it is rendered kinetically inert towards (i) exchange with the plasma protein, transferrin (Ga-Transferrin log K_s = 20.3[40]),

(ii) metal or acid catalysed dissociation and (iii) hydrolysis to the insoluble $Ga(OH)_3$. Hence it was considered suitable to assess the complexation properties of gallium(III) with the $[9]N_3$-triacid (24). As for its neighbouring group (III) element, indium, the $N_3O_3^{3-}$ donor set of this ligand provides a potentially octahedral coordination of the gallium ion, forming an overall neutral complex. This may be particularly useful for the use of ^{68}Ga in brain scanning, as the increased lipophilicity of a neutral complex enhances its ability to cross the blood-brain barrier. More hydrophilic complexes such as the anionic EDTA complex ($[Ga\text{-}EDTA]^-$) are known to be unable to cross the blood-brain barrier.[41]

In order to form neutral more lipophilic complexes of gallium(III) (and indium(III)) new acyclic ligands such as HBED (40) and PLED (41) have been synthesised recently.[42,43] However, as with the analogous

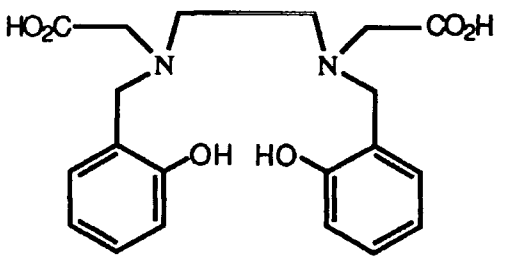

(40) HBED

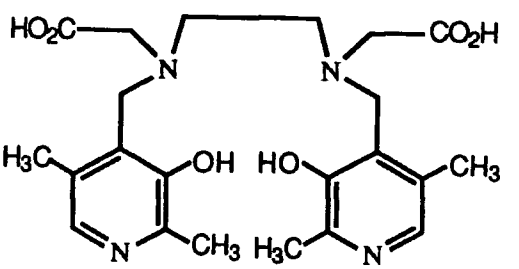

(41) PLED

EDTA ligand they possess an $N_2O_4^{4-}$ donor set and their gallium or indium complexes are unlikely to have any greater stability towards acid catalysed dissociation. Although the non-protonated complexes Ga-L and In-L (L = (40) and (41)) have high thermodynamic stability constants (e.g. log K_s for Ga-HBED = 39.57 and for In-HBED = 39.66) these are not

the major species in aqueous solution at pH $\leq$ 7 (the complexes exist as equilibrium mixtures of various protonated species).

The ^{13}C nmr of the $[Ga\text{-}DTPA]^{2-}$ complex in D_2O has been reported recently[3] and reveals that two of the carboxylate groups do not bind the metal ion, highlighting the unsuitability of this complex for in vivo radiopharmaceutical application.

2.3.2. **Macrocyclic complexes of gallium(III)**

Very little work has been reported on the macrocyclic coordination chemistry of gallium. Wieghardt[9,44] has investigated the complexation of gallium trihalides with 1,4,7-triazacyclonane (14) and reported the formation of complexes of the type $LGaX_3$ (X = Cl, Br, I), as with indium trihalides. Also μ-hydroxy bridged gallium complexes of this ligand have been prepared,[44] for example, the binuclear species $[L_2Ga_2(\mu\text{-}OH)_2(\mu\text{-}CH_3CO_2)]I_3.H_2O$ (Fig. 2.10).

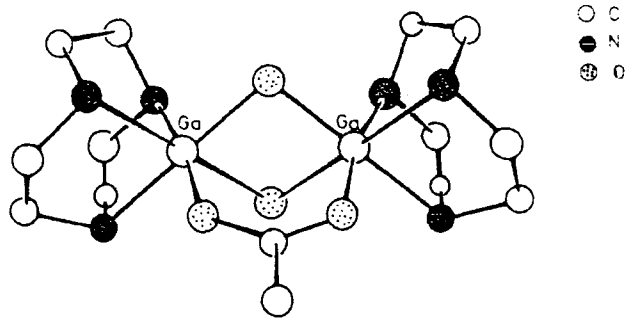

Fig. 2.10. Crystal structure of the $[L_2Ga_2(\mu\text{-}OH)_2(\mu\text{-}CH_3CO_2)]I_3.H_2O$ complex.

The complex adopts an approximately octahedral geometry with three nitrogens from the macrocycle coordinating facially and three oxygen donor atoms (two hydroxy and one aceto).

In recent months (1989) Moore[45] has reported the synthesis and gallium(III) complexation of a new [9]-N_3 N-functionalised hexacoordinate ligand (42). The X-ray structure is reported for the 1:1

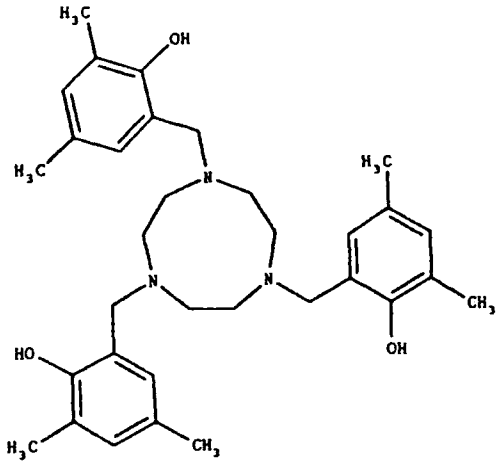

(42) TX-TACN

complex in a monoprotonated form, with one molecule of solvation (MeOH) $[Ga(TX\text{-}TACN)H]^+[ClO_4]^-.CH_3OH$ (Fig. 2.11). The interaction of the methanol with the complex (hydrogen bonds with the O donor atoms) results in a slightly distorted octahedral coordination geometry.

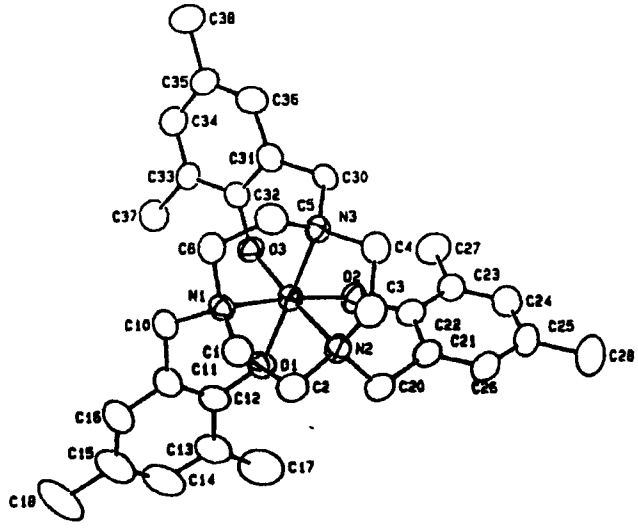

Fig. 2.11. ORTEP drawing of $[Ga(TX\text{-}TACN)]H^+$.

2.3.3. Synthesis of gallium(III) complexes

The 1:1 gallium(III) complexes of the nine and ten-membered triaza-triacids (24) and (25) were prepared. The neutral complexes were isolated as colourless crystalline solids using a method similar to that for the preparation of the indium(III) complexes. Equimolar amounts of gallium trinitrate and ligand were reacted in nitric acid (0.04 mol dm^{-3}) at room temperature for 12 hours. The complexes were precipitated by the addition of acetone and recrystallised from water.

The proton nmr of the [9]-N_3 triacid gallium complex in D_2O [Fig. 2.12] gave a similar spectrum to the indium complex. The methylene protons (CH_2CO) resonated as a singlet at 3.88 ppm and the diastereotopic ring protons gave multiplets centred at 3.51 and 3.23 ppm.

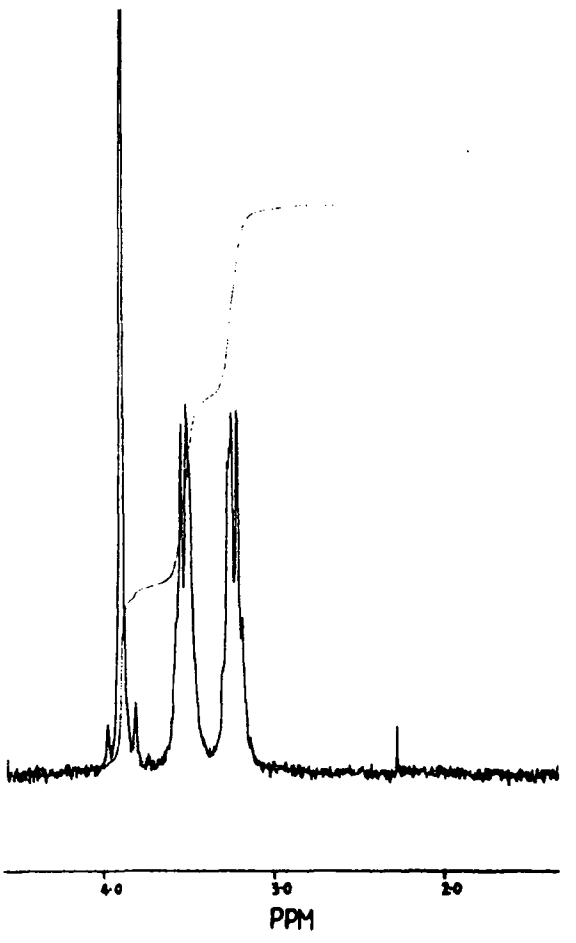

Fig. 2.12. ^1H nmr of the Ga(III) complex of (24).

The gallium complex of the [10]-N_3 triacid (25) gave a well defined proton nmr [Fig. 2.13] in contrast to the indium complex. The "CH_2CO" protons resonated as one singlet (2H) at 3.81 ppm and an AB doublet of

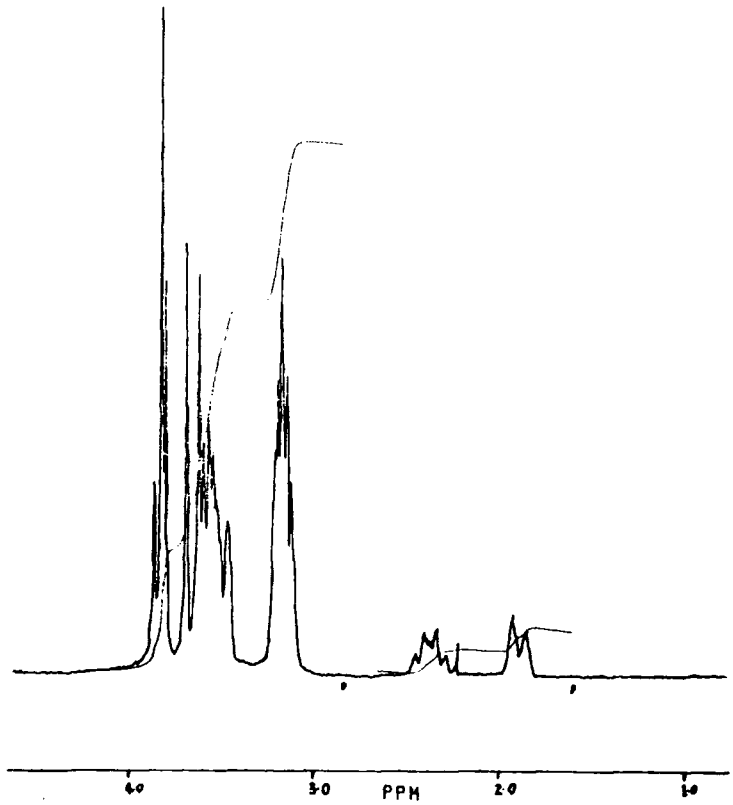

Fig. 2.13. ^1H nmr of the [10]-N_3 triacid-gallium(III) complex.

doublets centred at 3.73 ppm. This is seen more clearly in the proton decoupled (3.16 ppm) spectrum (Fig. 2.14) and is consistent with a plane of symmetry in the complex. The diastereotopic ring protons resonate as two AA'BB' systems with multiplets centred at 3.56, 3.16 ppm (12H, CH_2N) and 2.37, 1.88 ppm (2H, CH_2-C). Slow recrystallisation of the gallium-[9]N_3-triacid complex from D_2O gave crystals of suitable quality for X-ray diffraction. The X-ray crystal structure is illustrated in Fig. 2.15 and selected bond lengths and angles, with estimated standard deviations, are given in Table 2.6. The coordination of the gallium atom is approximately octahedral with the three nitrogens

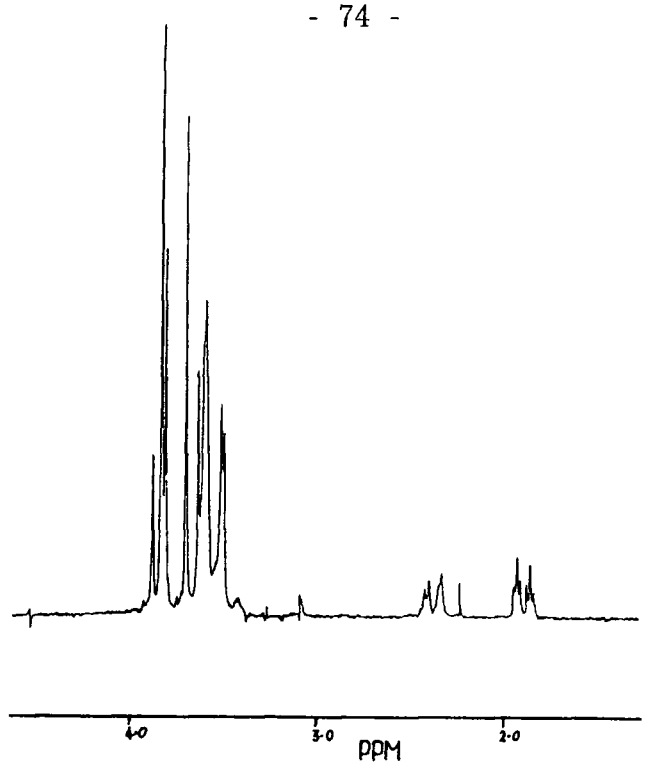

Fig. 2.14. ^{1}H nmr, decoupled (3.16 ppm), of [10]-N_3-triacid-Ga(III) complex.

of the macrocycle occupying a facial set of sites and the pendant carboxylates occupying the opposite face. All three trans N-Ga-O angles are approximately 167^{o} corresponding to the limited 5-ring chelate "bite" of the pendant arms. This has resulted in a relative twist of the O_3 and N_3 planes of donor atoms by 13^{o} away from a symmetrically staggered conformation (i.e. perfect octahedron). The O_3 atoms are 'twisted' clockwise relative to the N_3 atoms (when viewed from above, on the side of the O atoms) and so constitute a "type I" structure, according to the classification of Boeyens and Hancock.[12,13] "Type I" structures were observed for Ni(II), Ni(III) and Cr(III) complexes[9,14] of TCTA (24), whereas "type II" structures (anticlockwise twist) were observed for the Cu(II) and Fe(II) complexes. Twist angles are listed in Table 2.7. The gallium-TCTA structure most closely resembles those of the Ni(II) and Cr(III) complexes.

Ga-L , L =

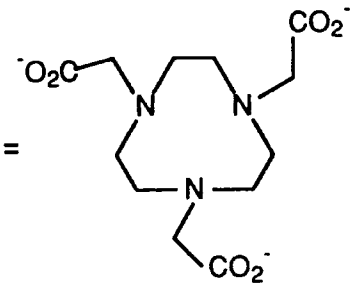

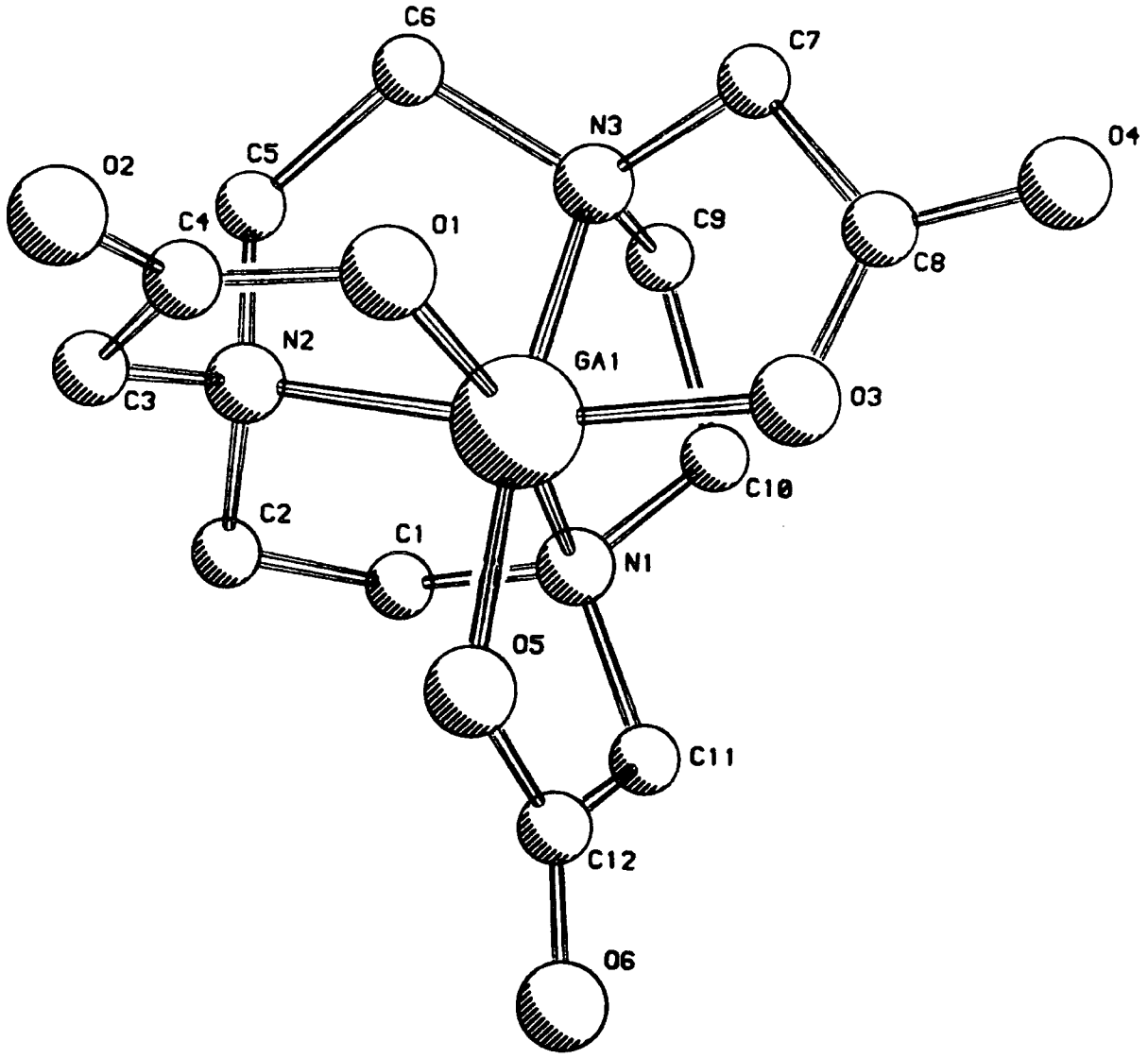

Fig. 2.15. X-ray crystal structure of the Ga(III) complex of (24).

Table 2.6

Selected bond lengths (Å) and bond angles (deg) for the Ga(III) complex of (24)

Ga-O(1)	1.948(5)	Ga-O(3)	1.933(6)
Ga-O(5)	1.940(5)	Ga-N(1)	2.104(6)
Ga-N(2)	2.102(6)	Ga-N(3)	2.110(6)
O(1)-Ga-O(3)	95.6(2)	O(1)-Ga-O(5)	94.2(2)
O(3)-Ga-O(5)	95.0(2)	O(1)-Ga-N(1)	167.1(2)
O(3)-Ga-N(1)	97.2(2)	O(5)-Ga-N(1)	83.6(2)
O(1)-Ga-N(2)	83.5(2)	O(3)-Ga-N(2)	167.7(2)
O(5)-Ga-N(2)	97.3(2)	N(1)-Ga-N(2)	84.2(2)
O(1)-Ga-N(3)	98.8(2)	O(3)-Ga-N(3)	83.8(2)
O(5)-Ga-N(3)	167.0(2)	N(1)-Ga-N(3)	83.7(2)
N(2)-Ga-N(3)	84.3(2)		

Table 2.7

Twist angles and structure type for M-TCTA complexes

Complex	Twist angle 'θ'[a]	Type
Ni[TCTA]	6.9	I
Ni[TCTA]$^-$	12.0	I
Cr[TCTA]	11.0	I
Ga[TCTA]	13.0	I
Fe[TCTA]	35.0	II
Cu[TCTA]$^-$	33.4	II

a) $\theta = 0^o$ (octahedral) and $\theta = 60^o$ (trigonal prismatic).

The two symmetrically occupied faces are parallel (0.6^{o}) but the O_3 set is enlarged, hence the O-Ga-O angles average 95^{o} whereas the N-Ga-N angles average 84^{o}. The whole molecule has approximate, but not crystallographically imposed, C_3 symmetry. There is little variation in the individual Ga-N and Ga-O bond lengths and the average bond lengths [Ga-N 2.105Å and Ga-O 1.940Å] are just marginally shorter than those reported for the complex $[Ga(TX\text{-}TACN)H]^{+}$ [42] [Ga-N 2.109Å and Ga-O 1.944Å, see section 2.3.2.]. Similar Ga-N (2.107Å) and Ga-O (1.941Å) bond lengths were reported for the C_3 symmetric complex of the hexadentate ligand (43).[46]

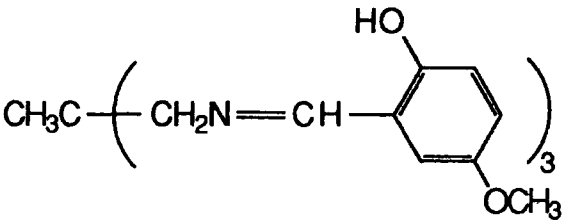

(43) $H_3[(5\text{-MeOsal})_3TAME]$

2.4. Gallium NMR Studies

2.4.1. Introduction[47,48]

Gallium occurs naturally as a mixture of two isotopes, ^{69}Ga (60.4%) and ^{71}Ga (39.6%) both possessing spin, I = $^{3}/_{2}$. The nuclear characteristics are summarised in Table 2.8.

The ^{71}Ga isotope is preferred for nmr work, despite having the lower abundance, as it has a higher receptivity and a slightly less efficient quadrupolar relaxation and hence narrower line widths. It may be noted that 99.8% enriched ^{71}Ga is available from Oakridge (U.S.A.) at a cost of £1.50 per mg.

The use of ^{71}Ga nmr for *in vivo* imaging has so far proved to be impossible, as the resonances of all the complexes investigated e.g.

Table 2.8

Nuclear properties of ^{69}Ga and ^{71}Ga

	^{69}Ga	^{71}Ga
Spin	$^3/_2$	$^3/_2$
Nat. Abundance	60.4	39.6
Receptivity/^{13}C	237	319
Gyromagnetic ratio	6.420	8.158
Quad. moment	0.178	0.112

citrate, lactate and EDTA have proved to be too broad to observe.

Gallium shifts are quoted relative to the $Ga(D_2O)_6^{3+}$ signal which is reported to have a minimum line width of 140 Hz [Lit: 200 Hz[47]]. Although the gallium signals tend to be relatively broad, this is compensated by the large chemical shift range of approximately 1400 ppm [Fig. 2.16].

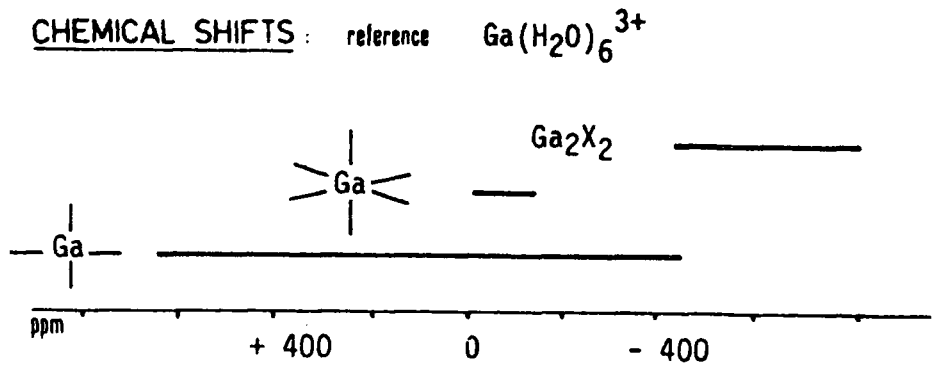

Fig. 2.16. ^{71}Ga shifts.

The majority of gallium shifts reported are for the gallium tetrahalo species, which generally give relatively sharp signals in aqueous or non aqueous solvent, with shifts ranging from -500 ppm

(GaI_4^-/MeCN) to +250 ppm ($GaCl_4^-$/MeCN). Octahedral species which have been observed by gallium nmr include the cations, $Ga(DMF)_6^{3+}$, $Ga(MeCN)_6^{3+}$ and $Ga(T.M.P.)_6^{3+}$ [T.M.P. = trimethylphosphate] with shifts between 0 and -100 ppm.

2.4.2. **^{71}Ga NMR of Ga-[9]-N_3-triacid**

The ^{71}Ga nmr of the gallium complex of [9]-N_3-triacid (24) was recorded in D_2O (0.03 mol dm^{-3}). Referenced to $Ga(D_2O)_6^{3+}$ ($Ga(NO_3)_3$, 0.1 mol dm^{-3} in D_2O) at 0 ppm the complex gave a sharp signal ($\omega\frac{1}{2}$ = 210 Hz) at +170.2 ppm. A second reference peak for $Ga(OD)_4^-$ was observed at 222.6 ppm ($\omega\frac{1}{2}$ 220 Hz) in D_2O (pD 12). The resonance of the gallium complex is shown relative to the two reference signals in Fig. 2.17. No shift of the signal was observed in the pD range 0 to 12.

The narrow line width of the ^{71}Ga-[9]N_3-triacid signal is consistent with the formation of a complex of relatively high symmetry in which the metal ion is tightly bound. Intrinsic line broadening in the spectra of quadrupolar nuclei is caused by the interaction of the nuclear quadrupole moment with the electric field gradient (efg) at the nucleus. Since quadrupolar transitions change the electromagnetic environment, the magnetic dipole and electric dipole are strongly coupled, hence relaxation of the nuclear electric quadrupole with changes in the local efg (due to molecular motions, in the liquid phase) also relaxes the nuclear spin ("Quadrupolar relaxation"). For an octahedral complex with a pair of facial N_3 and O_3 donors the meridional gradient (i.e. in the 'x-y' plane) tends to zero and the resultant field gradient at the nucleus is highly anisotropic (i.e. only in the 'z' axis). This results in a minimal degree of line broadening. The gallium complex of the [10]-N_3 triacid (25) gave a very broad signal at 132.5 ppm ($\omega\frac{1}{2}$ = 2000 Hz) which was only just discernable against a

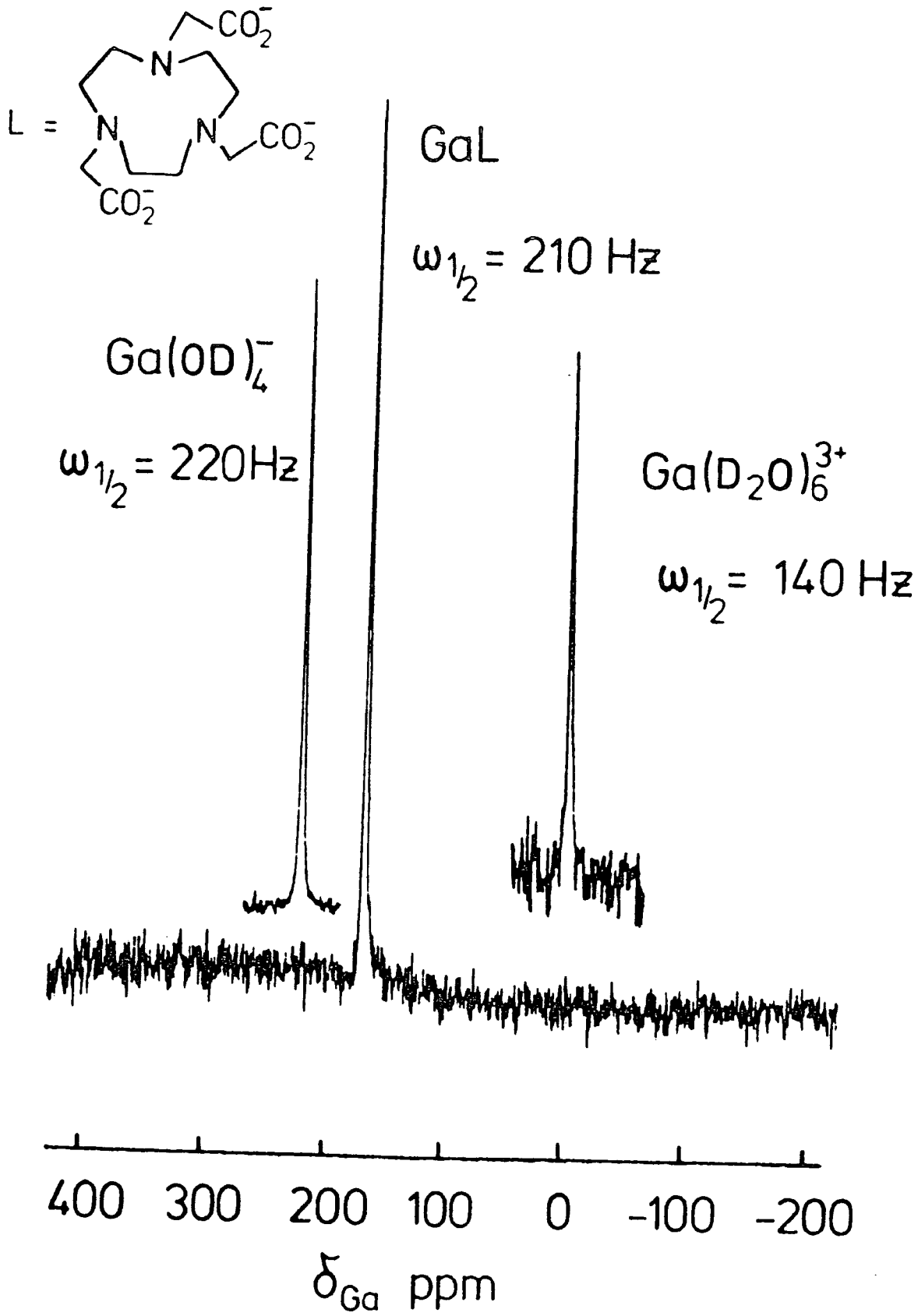

Fig. 2.17 ^{71}Ga NMR (298K, D_2O)

non-linear baseline. No ^{71}Ga resonance was observed for the [11]-N_3 triacid complex. The enhanced line broadening is consistent with the lower symmetry of these complexes, with strong interaction between the enhanced electric field gradient and the quadrupole moment.

The kinetic stability of the Ga(III)-[9]N_3-triacid complex was investigated at low pH, using ^{71}Ga nmr. The complex was found to be remarkably stable with respect to acid catalysed dissociation, with the signal at 170.2 ppm being observed with the sample in 6 molar nitric acid. No sign of dissociation of the complex to give free gallium(III) (i.e. $Ga(H_2O)_6^{3+}$ at 0 ppm) was observed at this pH, over a period of several weeks. The complex was also stable towards dissociation in basic media up to pH 13.5, at least.

2.4.3. **In vivo ^{71}Ga nmr imaging**

Recent studies at the Medical Research Council Radiobiology Unit have shown encouraging results with respect to the use of the ^{71}Ga-[9]N_3-triacid complex in NMR imaging. A sample of the complex (0.012 mol dm^{-3} in H_2O, phosphate buffer) was injected intravenously into a mouse and the ^{71}Ga-[9]N_3-triacid signal observed 20 minutes later, in the liver, using an external 3 cm surface coil as a probe. The spectrum obtained is presented along with that observed for the gallium complex in aqueous solution using the same probe [Fig. 2.18].

Further work is in progress to evaluate the utility of ^{71}Ga nmr *in vivo*.

2.4.4. **Conclusion**

The very high kinetic and thermodynamic stability of the gallium-[9]N_3-triacid complex in aqueous solution at both low and high pH, makes this an ideal candidate for *in vivo* radiopharmaceutical

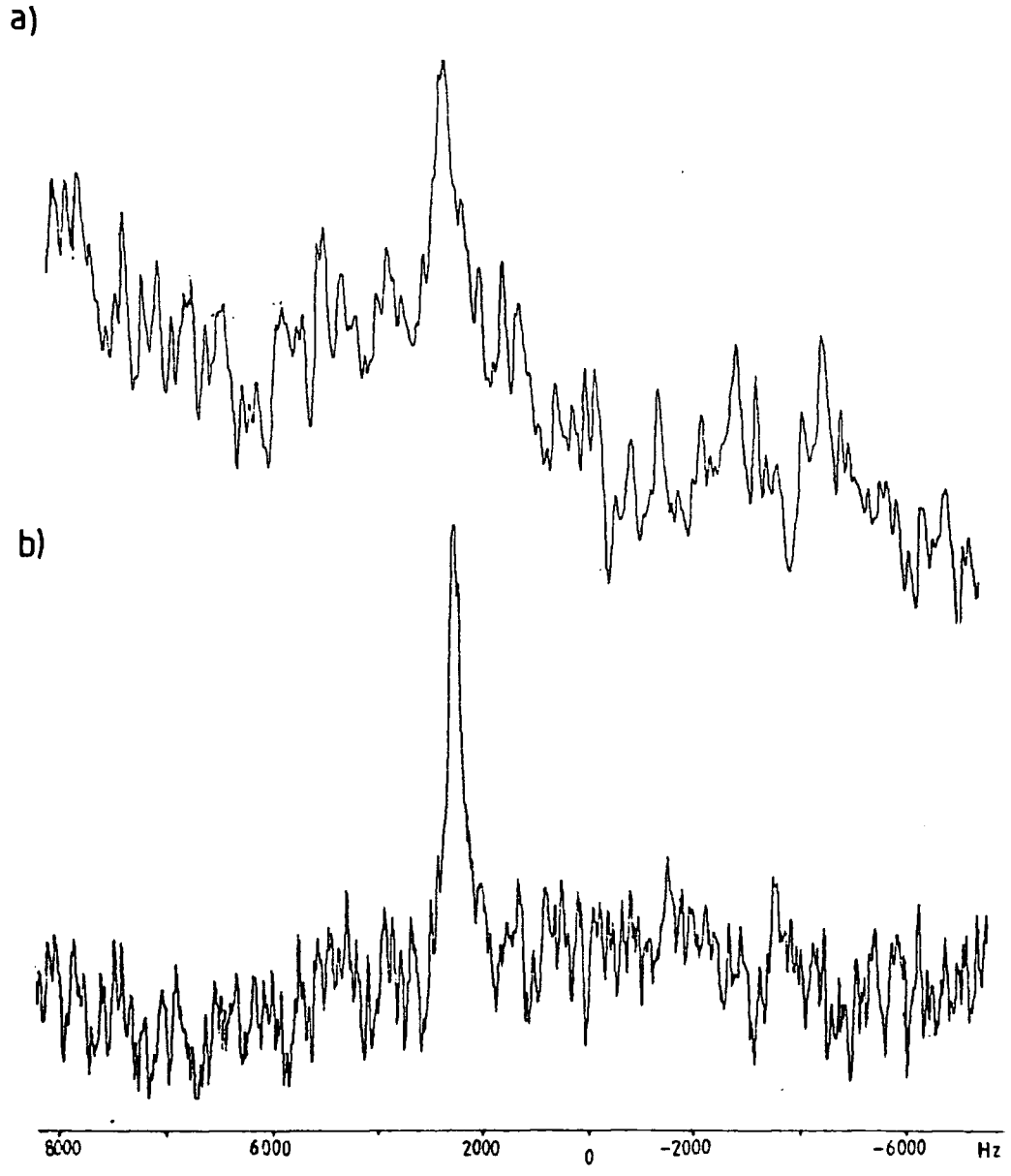

Fig. 2.18. ^{71}Ga nmr spectra of the Ga-[9]N_3-triacid complex observed in a) the liver region of the mouse (20 min.) and b) in aqueous solution.

application. In addition to the potential use in radioimmuno-scintigraphy (^{67}Ga) and PET (^{68}Ga), is the possibility of its use in <u>in vivo</u> NMR imaging by direct observation of the ^{71}Ga nucleus.

2.5. References

1. F.A. Cotton and G. Wilkinson, "Advanced Inorganic Chemistry", 5th ed., Wiley Interscience, New York (1988).

2. a) A.J. Carty and D.G. Tuck, "Coordination Chemistry of Indium", Prog. Inorg. Chem., 19, 243 (1975).
b) D.C. Bradley, Prog. Stereochem., 3, 1 (1962).

3. H.R. Maecke, A. Riesen and W. Ritter, J. Nucl. Med., 30, 1235 (1989).

4. J.W. Buehler, G. Eikelman, L. Puppe, K. Rohbock, H.H. Schneehage and D. Weck, Justuis. Liebigs. Ann. Chem., 745, 135 (1971).

5. C. Colaitis, Bull. Soc. Chim. Fr., 23 (1962).

6. M. Bhatti, W. Bhatti and G. Mast, Inorg. Nucl. Chem. Lett., 8, 133 (1972).

7. M.J. Taylor, D.G. Tuck and L. Victoriano, J. Chem. Soc. Dalton Trans., 928 (1981).

8. a) K. Wieghardt, M. Kleine-Boymann, B. Nuber and J. Weiss, Inorg. Chem., 25, 1654 (1986).
b) K. Wieghardt, M. Kleine-Boyman, B. Nuber and J. Weiss, Z. Anorg. Allg. Chem., 536, 179 (1986).

9. P. Chaudhuri and K. Wieghardt, Prog. Inorg. Chem., 35, 329 (1987).

10. T. Arishima, K. Hamada and S. Takamoto, Nippon. Kagaku. Kaishi, 1119 (1973).

11. M. Takahashi and S. Takamoto, Bull. Chem. Soc. Jap., 50, 3413 (1977).

12. M.J. Van der Merwe, J.C.A. Boeyens and R.D. Hancock, Inorg. Chem., 24, 1208 (1985).

13. M.J. Van der Merwe, J.C.A. Boeyens and R.D. Hancock, Inorg. Chem., 22, 3489 (1983).

14. K. Wieghardt, U. Bossek, P. Chaudhuri, W. Herrmann, B.C. Menke and J. Weiss, Inorg. Chem., 21, 4308 (1982).

15. T.A. Kaden, Topics Curr. Chem., 121, 157 (1984), F. Vögtle and E. Weber (eds.), Springer Verlag, Heidelberg, 1984.

16. B.A. Sayer, J.P. Michael and R.D. Hancock, Inorg. Chim. Acta, 77, L63 (1983).

17. M.I. Kabachnik, T. Ya Medved, Yu. M. Polikarpou, B.K. Shcherbakov, F.I. Bel'skii, E.I. Matrosov and M.P. Pasechnick, Izv. Akad. Nauk. SSSR Ser. Khim., 835 (1984).

18. A. Hammershoi and A.M. Sargeson, Inorg. Chem., 22, 3554 (1983).

19. G.W. Bushnell, D.G. Fortier and A. McAuley, Inorg. Chem., 27, 15 (1988).

20. L. Christiansen, D.N. Hendrickson, H. Toflund, S.R. Wilson and C.L. Xie, Inorg. Chem., 25, 2813 (1986).

21. K. Wieghardt, E. Schöffmann, B. Nuber and J. Weiss, Inorg. Chem., 25, 4877 (1986).

22. A.A. Belal, L.J. Farrugia, R.D. Peacock and J. Robb, J. Chem. Soc. Dalton Trans., 931 (1989).

23. J.F. King and S. Skonieczny, Phospherous and Sulphur, 25(1), 11-20 (1985).

24. A. Riesan, T.A. Kaden, W. Ritter and H.R. Macke, J. Chem. Soc. Chem. Commun., 460 (1989).

25. T.M. Laakso and D.D. Reynolds, J. Am. Chem. Soc., 73, 3518 (1951).

26. R. Gerdill, Helv. Chim. Acta, 56, 1859 (1973).

27. H. Koyama and T. Yoshino, Bull. Chem. Soc. Jpn., 45, 481 (1972).

28. H. Stetter and E.E. Roos, Chem. Ber., 87, 566 (1954).

29. J.F. Richman and T.J. Atkins, J. Am. Chem. Soc., 96(7), 2269 (1974).

30. H. Koyama and T. Yoshino, Bull. Chem. Soc. Jpn., 45, 481 (1972).

31. B.K. Vriesema, J. Buter and R.M. Kellogg, J. Org. Chem., 49, 110 (1984).

32. M. Briellmann, S. Kaderli, C.J. Meyer and A.D. Zuberbuhler, Helv. Chim. Acta, 70, 680 (1987).

33. M. Takahashi and S. Takamoto, Bull. Chem. Soc. Japan, 50(12), 3413 (1977).

34. A. Harrison, A. Millican and K. Jankowski, unpublished results.

35. A. Bevilacqua, R.I. Gelb, W.B. Hebard and L.J. Zompa, Inorg. Chem., 26, 2699 (1987).

36. C.F. Meares and T.G. Wensel, Acc. Chem. Res., 17, 202 (1984).

37. For details of PAC spectroscopy see: a) D.J. Lurie, F.H. Smith and A. Shukri, Int. J. Appl. Radiat. Isot., 36, 57 (1985); b) F.A. Smith, D.J. Lurie, F. Brady, H.J. Danpure, M.J. Kensett, S. Osman, D.J. Silvester and S.L. Waters, Int. J. Appl. Radiat. Isot., 35, 501 (1984).

38. H.O. Anger and A. Gottschalk, J. Nucl. Med., 4, 326 (1963).

39. M.J. Welch and S. Moerlein, A.C.S. Symp. Ser., Inorg. Chem. Biol. Med., 140, 121 (1980).

40. M.A. Green, M.J. Welch, C.J. Mathias, K.A.A. Fox, R.M. Knabb and J.C. Huffman, J. Nucl. Med., 26, 170 (1985).

41. C.J. Mathias, Y. Sun, M.J. Welch, M.A. Green, J.A. Thomas, K.R. Wade and A.E. Martell, Nucl. Med. Biol., 15(1), 69 (1988).

42. C.H. Taliaferro, R.J. Motekaitis and A.E. Martell, Inorg. Chem., 23, 1188 (1984).

43. M.A. Green, M.J. Welch, C.J. Mathias, P. Taylor and A.E. Martell, Int. J. Nucl. Med. Biol., 12(5), 381 (1985).

44. K. Wieghardt, M. Kleine Boymann, B. Nuber and J. Weiss, Z. Anorg. Allg. Chem., 536, 179 (1986).

45. D.A. Moore, P.E. Fanwick and M.J. Welch, Inorg. Chem., 28, 1504 (1989).

46. M.A. Green and M.J. Welch, J. Am. Chem. Soc., 106, 3689 (1984).

47. R.K. Harris and B.E. Mann, "NMR and the Periodic Table", Academic, N. York (1978).

48. J. Mason (ed.), "Multinuclear NMR", Plenum Press, New York (1987).

CHAPTER THREE

SYNTHESIS OF FUNCTIONALISED MACROCYCLES TO BIND INDIUM(III) AND GALLIUM(III)

3.1. Introduction

Having selected the [9]-N_3-triacid (24) as the preferred macrocycle for binding indium and gallium, the synthesis of a functionalised analogue permitting attachment of the ligand to the antibody was required.

A number of different methods for ligand-antibody conjugation have been reported. The majority of these involve the reaction of an electrophilic group on a side chain of the ligand with the lysine ϵ-amino group of the antibody.

DTPA has been conjugated to antibodies using a route based on the cyclic dianhydride (CA-DTPA)[1-3] [Fig. 3.1]. The anhydride reacts with a lysine ϵ-amino group forming an amide link with the antibody. However, in the case of the indium complex it is known that the loss of one of

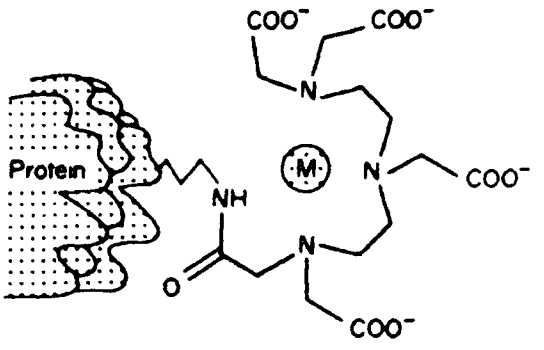

Fig. 3.1. Conjugation of DTPA dianhydride (CA-DTPA) to the lysine NH_2 group of the antibody.

the carboxylate binding sites reduces the kinetic stability of the complex *in vivo*.

A series of reagents derived from aromatic amines[3-5] [Fig. 3.2]

have been used for the linkage of EDTA, DTPA and the macrocyclic ligand TETA [Fig. 3.3] to an antibody. The early azobenzyl-EDTA system was

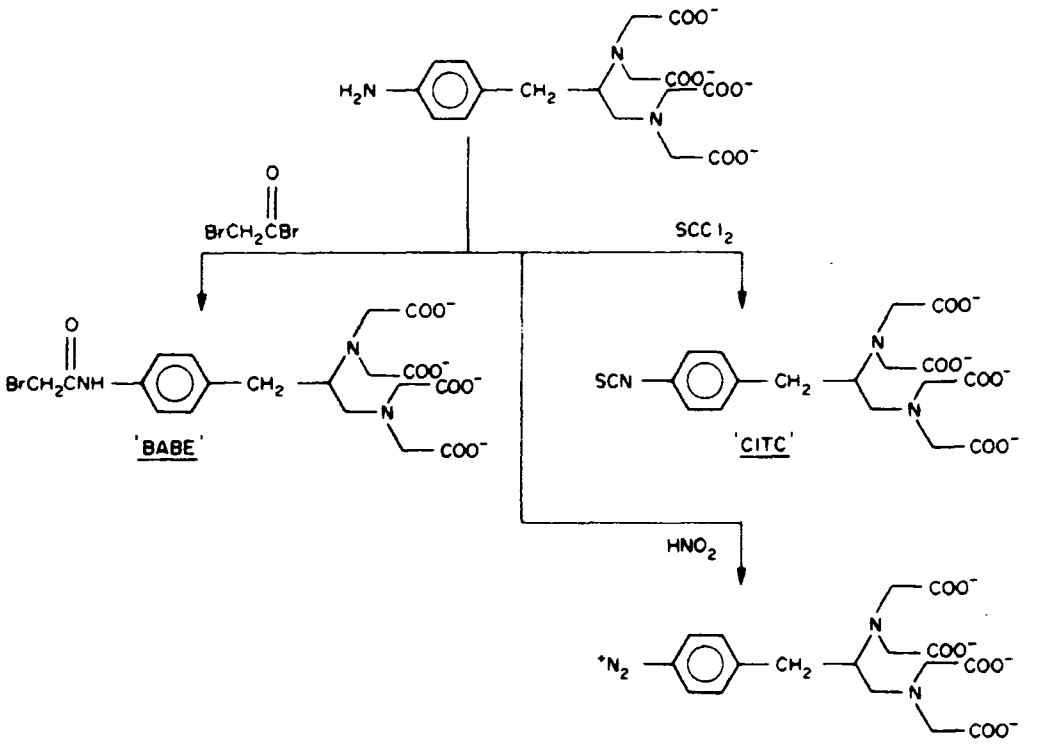

Fig. 3.2. Synthesis of functionalised EDTA derivatives ('BABE', 'CITC' and 'azobenzyl-').

found to react with several different amino acid residues of the antibody (e.g. tyrosine (OH) and histidine (NH)[7]). The p-isothiocyanatobenzyl-EDTA ('CITC') and p-(α-bromoacetamidobenzyl)-EDTA ('BABE') systems were found to react more specifically with the lysine ϵ-amino group. The α-bromoacetamido reagents also react with free thiol groups as shown for the 'TETA' system in Fig. 3.3. In this case the antibody was treated with 2-iminothiolane ("Trauts reagent") which reacts with the lysine ϵ-amino group forming a C_4S "spacer" group, in addition to

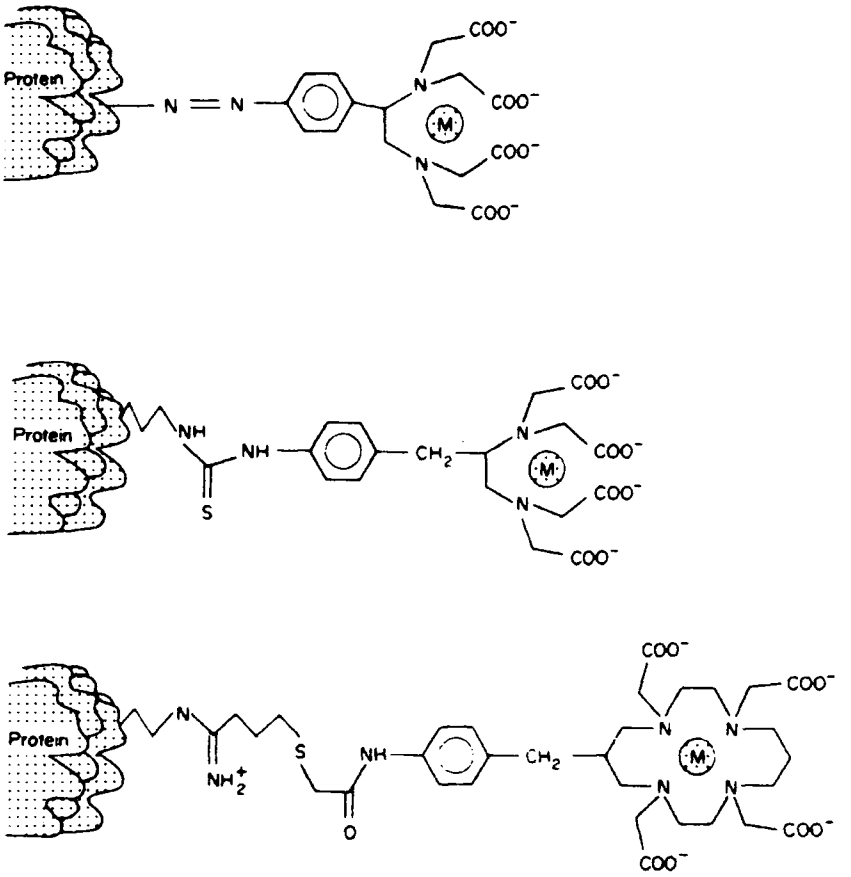

Fig. 3.3. Antibody conjugates of top: azobenzyl-EDTA, middle: 'CITC' and bottom: α-bromoacetamidobenzyl-TETA (via 2-iminothiolane spacer).

generating a free thiol. Meares reported[5] that the labelling of the TETA-antibody conjugate with ^{67}Cu, was only effective when the side chain had first been extended in this way.

For the $[9]N_3$-triacid system, the synthesis of a C-functionalised derivative with a simple aliphatic primary amine side arm (52) is reported.

The linkage of the macrocycle, with a nucleophilic amino group, to a nucleophilic residue on the antibody, requires the use of a hetero-bifunctional cross linker molecule. The linker molecule must contain two distinct groups, one of which will react specifically towards the

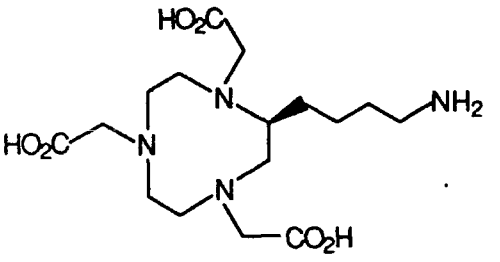

(52)

amine of the macrocycle and the other towards the antibody residue (i.e. a thiol group - when treated with "Trauts" reagent). Two such heterobifunctional linker molecules, (a 2-vinyl pyridine ester system and a maleimide ester system) are discussed later (sect. 3.4.).

Arano et al.[8] and Meares et al.[9] have reported that the radiolabelling of antibody-ligand conjugates is affected by the length and lipophilicity of the chain separating the two. If the chain was too short or too lipophilic then the ligand was "buried" within the antibody and unavailable for radiolabelling. It was postulated that the use of "Trauted" antibodies and cross linker molecules would minimise any radiolabelling problems associated with the restricted access to the ligand, in the conjugate.

3.2. Synthesis of the C-Functionalised [9]-N_3-triacid

The C-functionalised macrocycle (52) has been synthesised by two routes, starting from the commercially available (2S)-lysine monohydrochloride.

3.2.1. Route A

The first route is outlined in Scheme 3.1. The (2S)-lysine was converted to the methyl ester (43) by boiling under reflux in methanol with 1% acetyl chloride. Treatment of the methyl ester (43) in methanol

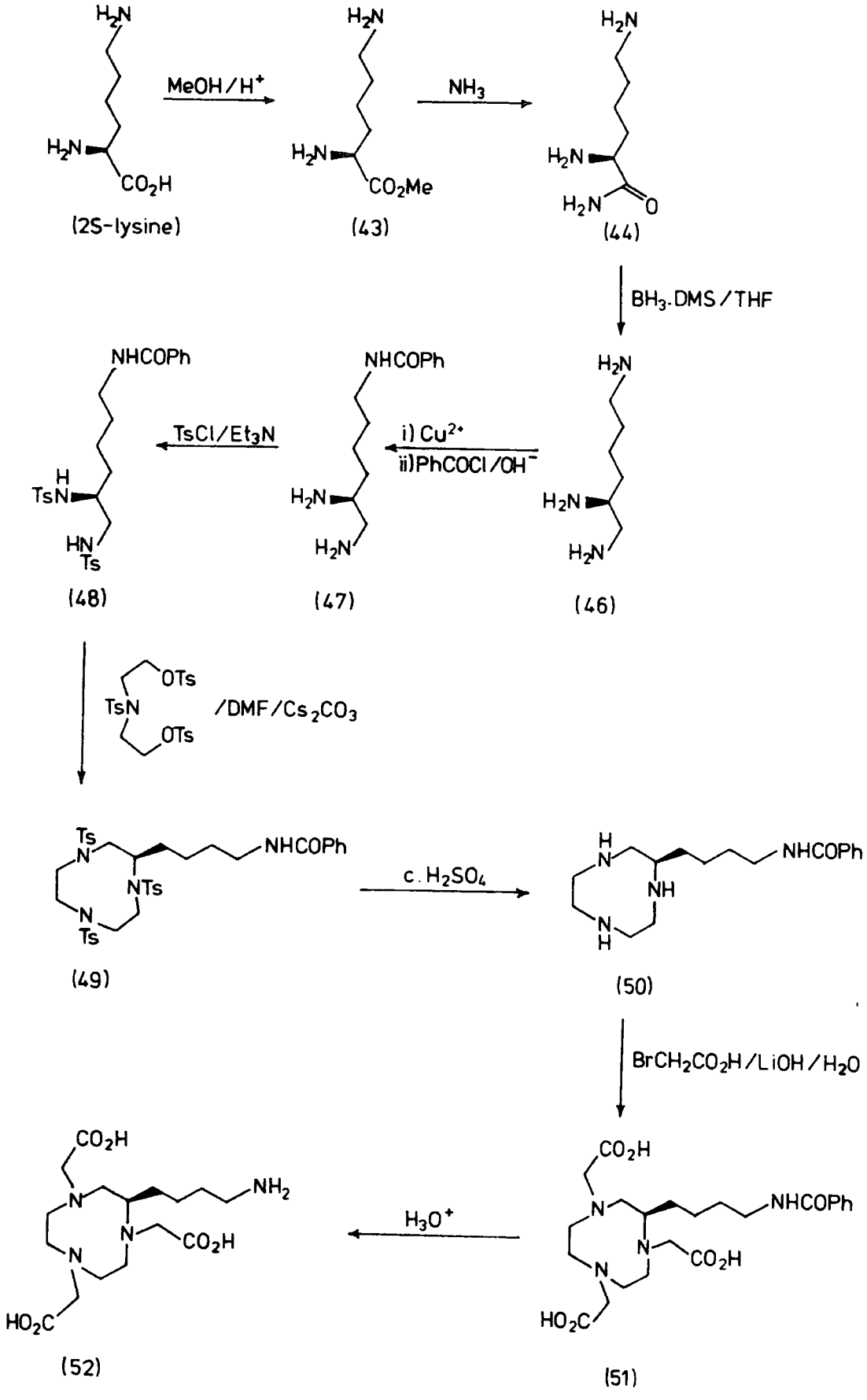

Scheme 3.1. Synthesis of a C-functionalised [9]N_3-triacid (Route A).

with liquid ammonia at -77°C resulted in only partial conversion to the amide (44). It was found that by treatment with liquid ammonia alone at -77°C for several hours, all of the ester was consumed to give a mixture of the required product and one minor impurity. Mass spectrometry data and ^{13}C nmr revealed that this was the lactam (45), the product from a competing intramolecular cyclisation reaction. Partial purification was

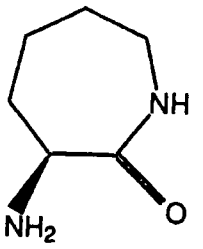

(45)

achieved by taking up the mixture in methanol and removing the insoluble white solid by filtration. The product was sufficiently pure (approx. 90%) to continue with the next steps of the synthesis, with purification at the tosylamide stage. However, in subsequent syntheses the commercially available, but expensive, (2S)-lysine amide dihydrochloride was used. The amide (44) proved to be very insoluble in THF, resulting in a very slow reduction, using a large excess of borane.DMS in THF, with heating under reflux (2 weeks). (Both $LiAlH_4$ in THF and $NaAlH_2(OCH_2CH_2OCH_3)_2$ [REDAL] in toluene (3.4M) failed to reduce the amide.) The crude triamine (46) was obtained in quantitative yield by extraction into chloroform from basic aqueous solution and used without further purification. In order to tosylate the amines in the 1- and 2-positions, it was necessary to protect the primary amine at the 6-position. The ethylenediamine sub-unit of (46) was protected by complexation with copper(II) (using $CuCO_3.Cu(OH)_2$) in aqueous solution,

thereby permitting selective acylation of the remote primary amine group, with benzoyl chloride ($0^{o}C$, pH $\geq$ 9). Treatment with hydrogen sulphide afforded the benzamide (47) in 49% yield after exhaustive extraction into chloroform from basic aqueous solution. The ditosylamide (48) was prepared by reaction of the benzamide (47) with tosyl chloride in dichloromethane in the presence of triethylamine. Purification was effected by 'flash' silica gel chromatography with a low polarity gradient elution (MeOH-CH_2Cl_2). Two 'column' purifications were required in order to obtain an analytically pure sample (43%). Condensation of (48) with the relevant 1,5-ditosylate, using caesium carbonate in DMF (18 hr.)[10] afforded the cyclic tritosylamide (49). As with the acyclic ditosylamide (48), purification required careful 'flash' silica column chromatography with slow movement of the product down the column, to give analytically pure material (35%). Detosylation was effected by heating (49) in concentrated sulphuric acid ($115^{o}C$, 18 hr.), leaving the benzoyl group intact. The triamine (50) was obtained in 41% yield after extraction into dichloromethane from basic aqueous solution. The product gave a single peak by cation exchange HPLC [Fig. 3.4]. The triacetate (51) was prepared by treatment of the triamine

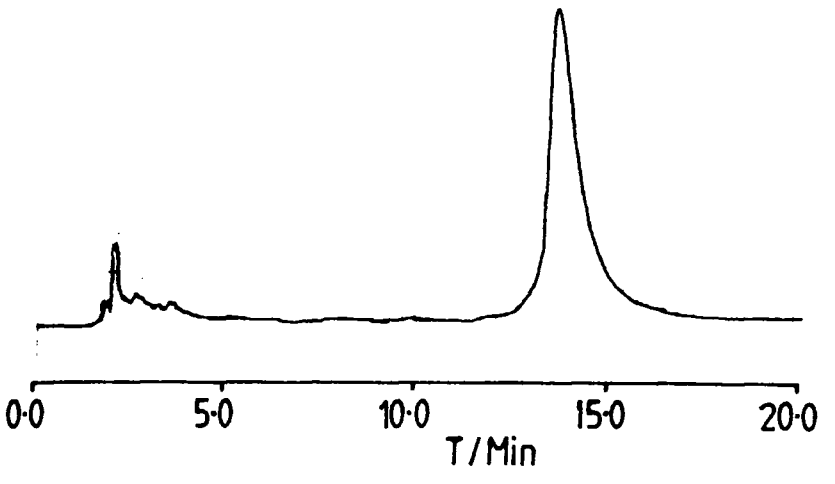

Fig. 3.4. HPLC trace of (50).

(50) with a large excess of bromoacetic acid in water (65°C) with addition of LiOH to maintain the solution at pH 10. The reaction was monitored by reverse phase HPLC ("Spherisorb" S5ODS) . After the addition of several portions of bromoacetic acid over a period of 46 hours, no further change was observed in the HPLC trace and a major peak had emerged at 12.0 minutes (see Ch. 6 for HPLC conditions). The triacetate was purified by ion exchange chromatography (sepharose, DEAE-cation exchange: gradient elution with NH_4OAC) followed by reverse phase column chromatography, to remove excess NH_4OAc. For the ion exchange chromatography, the starting mixture had to be diluted (500 ml, H_2O) in order to reduce its ionic strength to that of the starting eluant. The ^1H nmr (D_2O) and the anion exchange HPLC trace of the product, which was obtained in 79% yield, are given in Fig. 3.5. In the ^1H nmr characteristic resonances were observed for the benzoyl group (7.5-7.8 ppm) and the alkyl chain (6H, 1.4-1.7 ppm). The methylene 'CH_2CO' groups resonated between 3.5 and 4.1 ppm and the remaining 'CH_2N' protons gave a complex set of multiplets between 2.9 and 3.5 ppm.

The benzoyl group was readily cleaved by reflux in hydrochloric acid (6M, 12 hr.) to yield the amino-functionalised triacid (52) in quantitative yield.

3.2.2. **Route B**

The second route to the synthesis of the amino-functionalised [9]N_3-triacid [Scheme 3.2] was similar in strategy to that of the first. The major difference was that 'route B' involved the synthesis of a tritosylamide acyclic precursor for condensation with a 1,3-ditosylate, to form the nine-membered ring. Alternative methods for detosylation and N-alkylation are also described. Reaction of the methyl ester of (2S)-lysine (43) with neat ethylenediamine (reflux, 16 hr.)[11] afforded

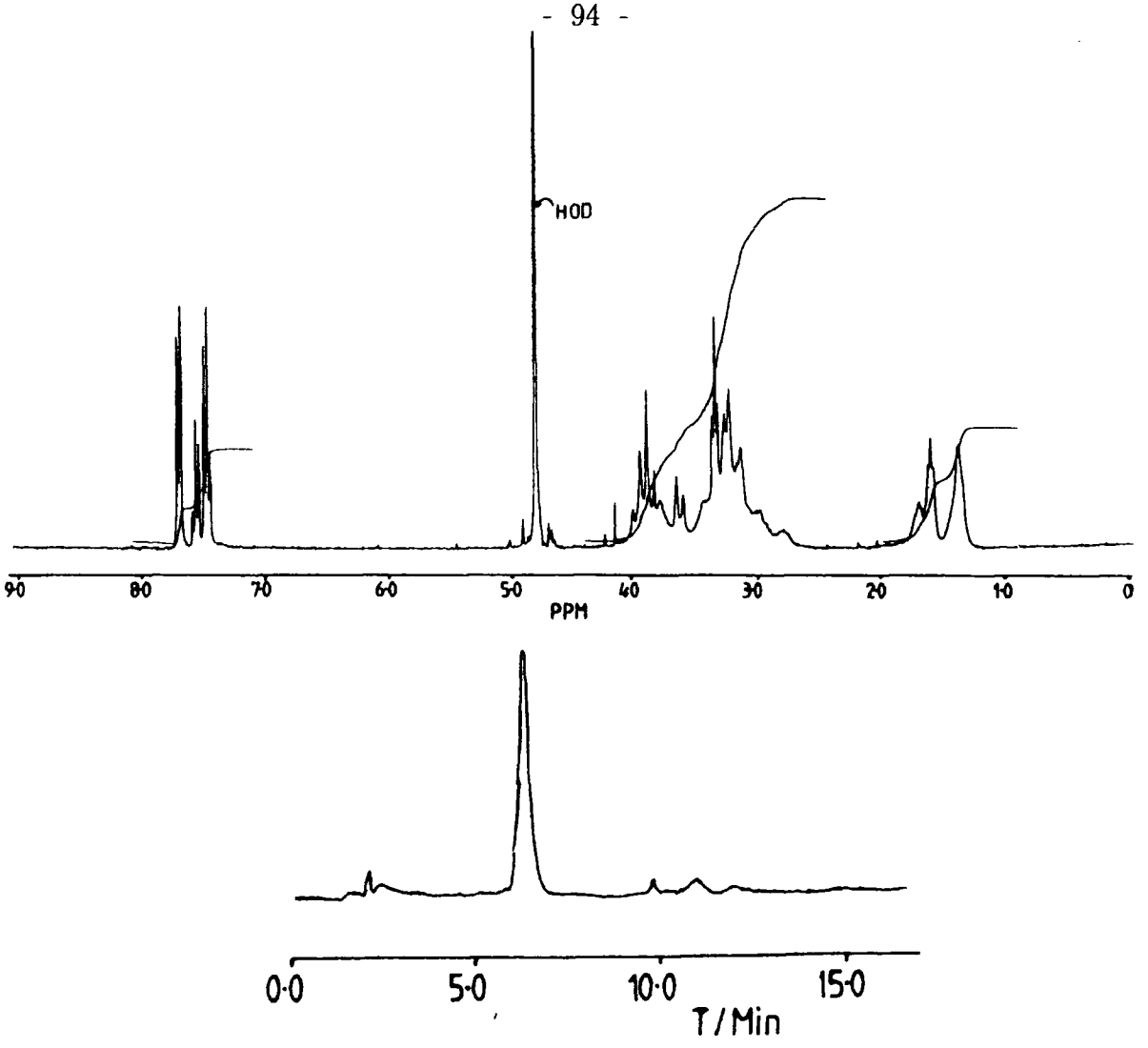

Fig. 3.5. ^{1}H nmr and cation exchange HPLC trace of (51).

the amide (53) in 96% yield (excess ethylenediamine was removed by distillation under reduced pressure). Reduction of the amide (53) was effected using borane.THF in THF, heating under reflux for 21 hours. The tetraamine (54) was obtained in 75% yield after exhaustive extraction from basic aqueous solution. Alternatively the product could be obtained, for use in the next step, as the hydrochloride salt. The diethylenetriamine sub-unit was protected by forming the copper(II) complex in aqueous solution, allowing acylation of the remote primary amine with benzoyl chloride (as in 'route A'). The copper was removed by treatment with H_2S followed by exhaustive extraction with

dichloromethane from basic aqueous solution, to yield the benzamide (55) in 58% yield. (Further extraction into chloroform gave a mixture of benzoylated and non-benzoylated products.) The tritosylamide (56) was

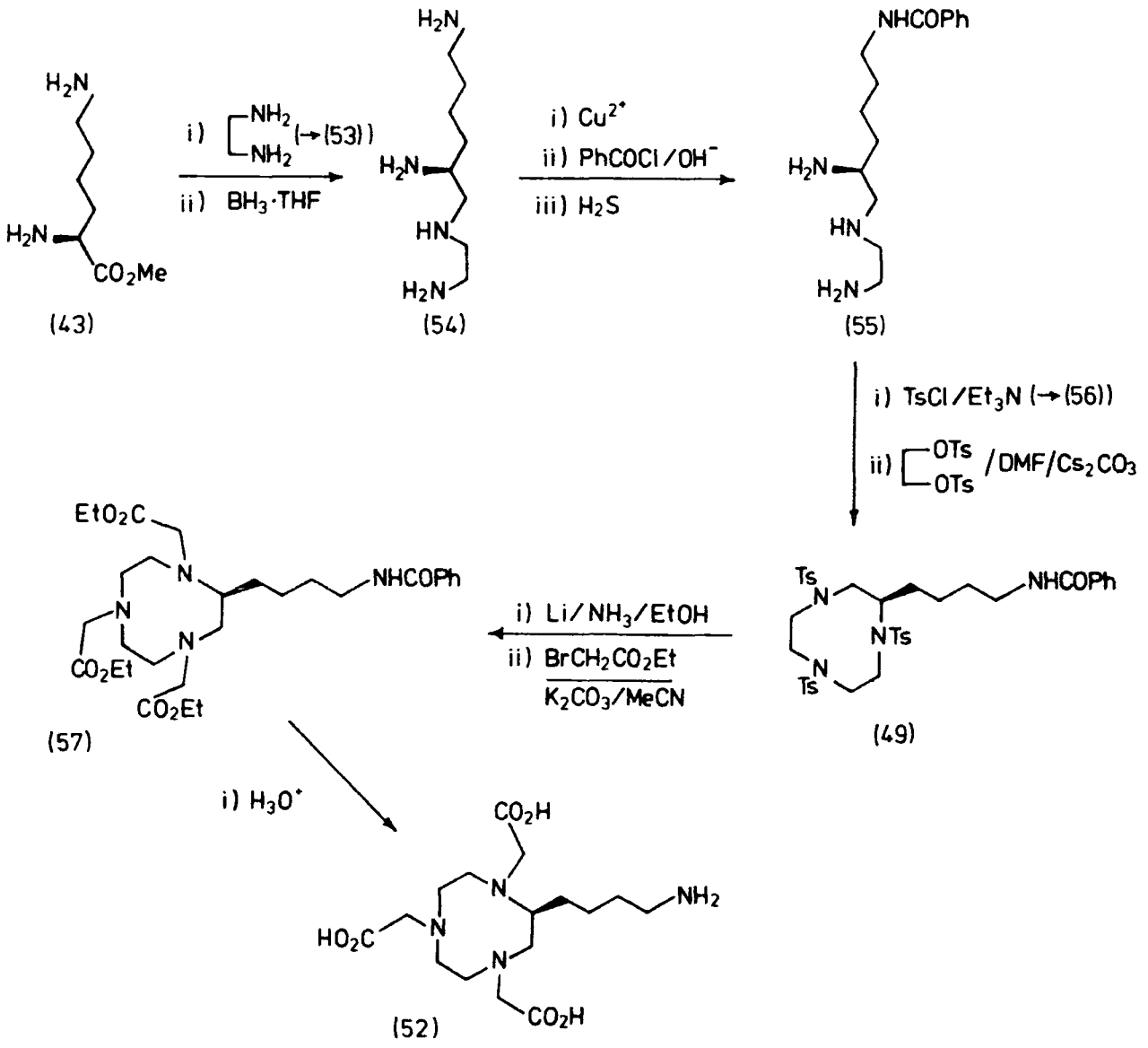

Scheme 3.2. Synthesis of C-functionalised [9]-N_3-triacid: 'Route B'.

prepared by the reaction of (55) with tosylchloride in dichloromethane in the presence of triethylamine. The product was found to precipitate from dichloromethane and was obtained in 68% yield. Co-condensation of (56) with ethyleneglycol ditosylate (Cs_2CO_3/DMF/65°C/18 h.) afforded the cyclic tritosylamide (49) in 71% yield. An alternative method of detosylation was attempted using Li/NH_3/MeOH/THF. The ^1H nmr of the crude product revealed that the cycle had fully detosylated, but also some cleavage of the benzoyl group had occurred (ca. 30%). Furthermore, the appearance of a benzylic signal at 3.75 ppm indicated that some reduction of the benzamide to the benzylamine had also occurred. Previous studies[12] had shown that the benzylamine functionality was unsuitable as a protecting group, as all standard methods failed to cleave the benzyl-amine bond.

The triester (57) was prepared by the reaction of (50) with ethylbromoacetate and caesium carbonate in ethanol (70°C, 16 hr.) followed by purification by alumina column chromatography (77%). Treatment of (57) with hydrochloric acid (6M, 18 hr. reflux) effected hydrolysis of the ester groups and benzamide group to give the amino functionalised triacid in quantitative yield.

3.2.3. Conclusion

The most efficient synthesis of the amino functionalised [9]N_3-triacid is achieved with a combination of the two synthetic routes. Route 'B' is preferred up to the synthesis of the cyclic tritosylamide (49) as a result of the higher yields (19% overall from the amide c.f. 6% for route 'A') and more straightforward purification procedures. Concentrated sulphuric acid is the preferred reagent for detosylation, giving a clean product, leaving the benzamide group intact. The N-alkylated product can be prepared equally well with

either bromoacetic acid or ethylbromoacetate.

The optical rotation results $[\alpha]_D^{20}$ of the intermediate products (49) to (51) [Table 3.1] are consistent with a lack of racemisation. Although the $[\alpha]_D^{20}$ values are not conclusive evidence of 100% enantiomeric purity, it is most probable that racemisation has not occurred, as the chiral centre is not involved directly (i.e. as a reaction centre) in any of the conversions.

Table 3.1

$[\alpha]_D^{20}$ values for (49), (50) and (51)

Product	$[\alpha]_D^{20}$ (c 1.0 g/100 ml)
(49)	+9.2 (CH_2Cl_2)
(50)	+4.1 (CH_2Cl_2)
(51)	+7.5 (H_2O)

3.2.4. Synthesis of C-functionalised DTPA

In order to run a direct comparison of the indium-[9]N_3-triacid system with an analogous indium-DTPA system (in animal biodistribution studies) the ligand (60) was prepared.

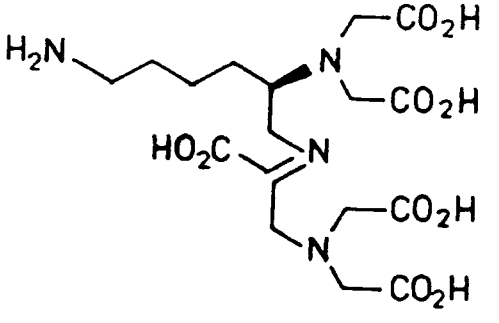

(60)

This ligand contains the same lysine-derived aminoalkyl

functionality, at the C-1 position, as the $[9]N_3$-triacid system described in the last section. As a suitable precursor had already been prepared (Intermediate (55) - Scheme 3.2), the synthesis of the DTPA analogue (requiring N-alkylation of (55)) appeared to be relatively straightforward. However, several attempts at the synthesis of the DTPA analogue failed;

(i) ($BrCH_2CO_2H/LiOH/H_2O/80^oC$) - reaction gave a mixture of products (no major component) which could not be separated by column chromatography, or 'semi-preparative' HPLC.

(ii) $ClCH_2CO_2H/LiOH/H_2O/80^oC$) - no reaction observed.

(iii) ($BrCH_2CO_2Me/K_2CO_3/DMF/90^oC$) - no reaction observed.

(iv) ($BrCH_2CO_2Et)/Cs_2CO_3/EtOH/70^oC$) - a mixture of several products by alumina t.l.c.

The DTPA analogue was eventually prepared using a method reported by Gansow et al.[3] [Scheme 3.3]. The triamine (55) was treated with a

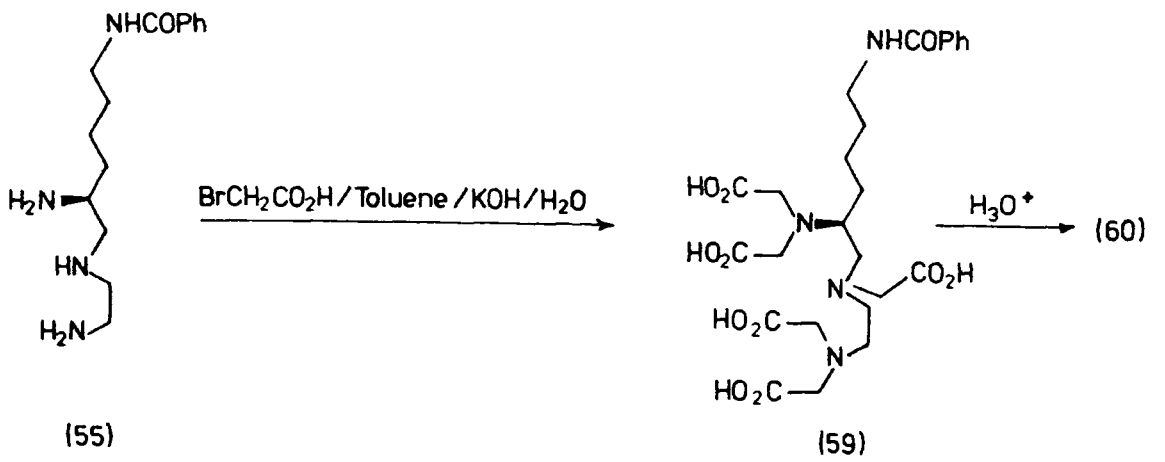

Scheme 3.3. Synthesis of C-functionalised DTPA.

solution of bromoacetic acid in toluene and aqueous KOH solution, at $0^{o}C$, with vigorous stirring. After 24 hours a mixture of products was observed by anion exchange HPLC, so further quantities of reagent ($BrCH_2CO_2H$/KOH, 3 eq.) were added. After a further 24 hours a major component had emerged, with a relatively long retention time by anion exchange HPLC (R_t = 18 min. - consistent with a doubly or triply negatively charged species). The crude mixture was acidified and passed down a cation exchange column, eluting initially with water, to remove salts and hydrolysis products and later with aqueous ammonia solution, to bring off the product. The ^{1}H nmr of (59) [Fig. 3.6(a)] was similar

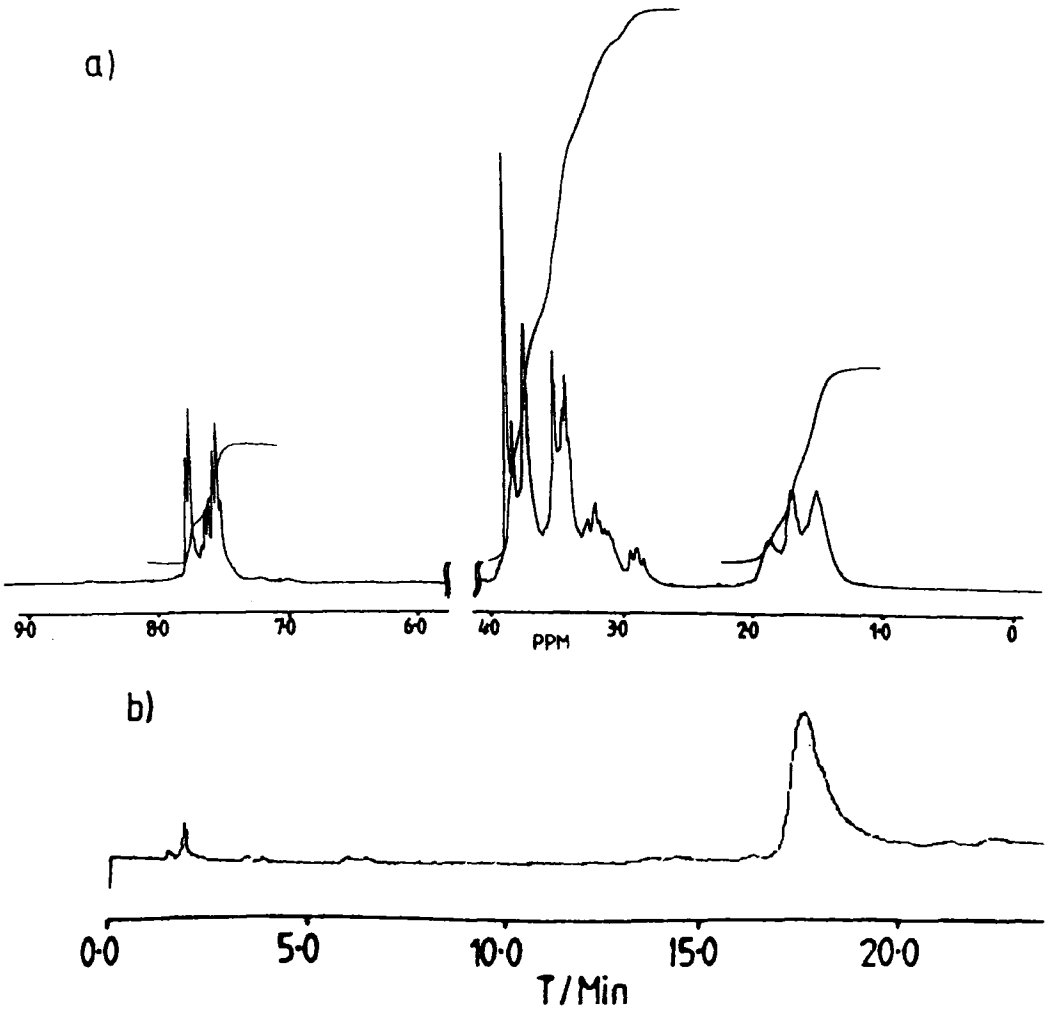

Fig. 3.6. a) ^{1}H nmr and b) anion exchange HPLC trace of (59).

to that observed for the analogous [9]-N_3 system and the anion exchange HPLC trace [Fig. 3.6(b)] of the purified product gave a single peak at 18 min. Hydrolysis to the amine (60) was effected by heating under reflux in hydrochloric acid (6M, 12 hr.).

3.3. Synthesis of N-Functionalised [9]N_3-triacids

The preparation of an N-functionalised derivative of the [9]N_3-triacid was sought, in order to investigate the effect that the position of functionality had on the <u>in vivo</u> stability of the indium complex. A shorter synthetic route to a functionalised system was also sought. Furthermore, the synthetic strategy proposed for N-functionalisation enabled the synthesis of a ligand with two aminoalkyl side arms to be prepared. This was considered to be of potential use with respect to new methods of linkage to the antibody, as being investigated by our industrial collaborators at Celltech Ltd. (see section 3.4.).

2-Bromo-N-benzoyl-6-aminohexylethanoate (63) was synthesised in two steps from the commercially available N-benzoyl-6-aminohexanoic acid (61) [Scheme 3.4].[13] Treatment of (61) with red phospherous and bromine

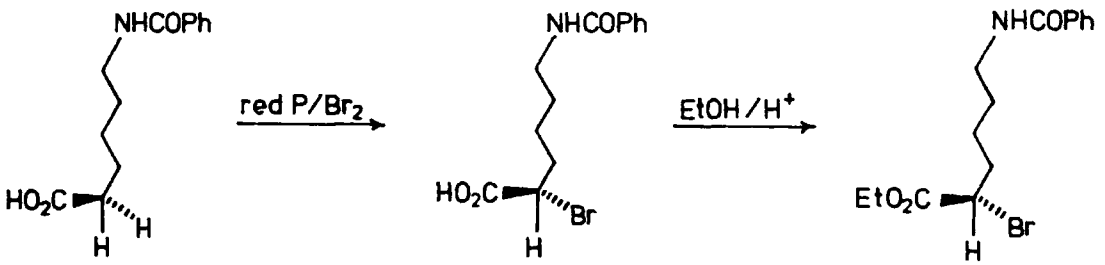

(61) (62) (63)

Scheme 3.4.

according to the method of Eck et al.[14] gave the α-bromoacid (62). This

was converted to the α-bromoester (63) by boiling under reflux in ethanol and 5% acetyl chloride, with purification by 'flash' silica gel chromatography.

The α-bromo ester (63) can be considered as an ethylbromoacetate derivative, with a protected alkylamine functionality at the 2-position.

The initial strategy was to prepare the N,N'-bis(ethoxycarbonylmethyl) derivative of $[9]N_3$, as reported by Wieghardt[15] ($BrCH_2CO_2Et$/NaOEt/EtOH), followed by alkylation with the α-bromo ester (63) to give the N-functionalised product (67) (Scheme 3.5).

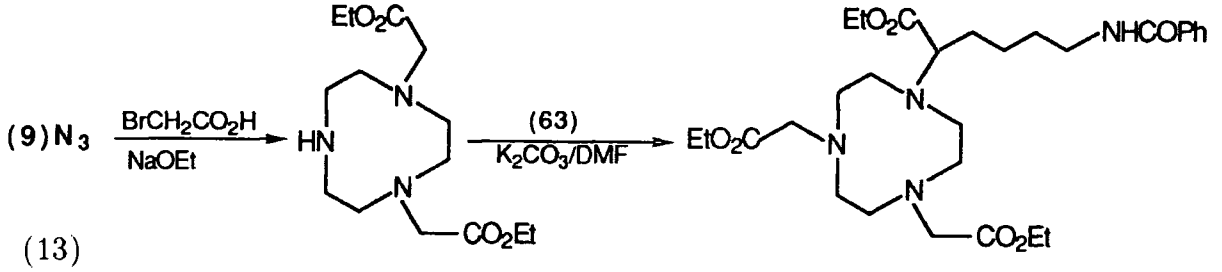

(13) (64) (67)

Scheme 3.5.

However, the diester (64) failed to react with the α-bromoester (63) under several different reaction conditions ((i) K_2CO_3/DMF (ii) K_2CO_3/CH_3CN (iii) Cs_2CO_3/EtOH or (iv) NaOEt/EtOH). It was postulated that the steric hindrance to the last secondary nitrogen may have been a significant factor with the relatively bulky α-bromoester. In previous reactions where the N-alkylation was monitored by HPLC, it was noted that the final alkylation took significantly longer than the first two. Hence the order of the synthesis was reversed, such that alkylation of the third amine would be with the less sterically hindered ethylbromoacetate (Scheme 3.6).

Reaction of equimolar quantities of 1,4,7-triazacyclononane with

the α-bromoester (63) and potassium carbonate in DMF ($60^{o}C$) gave a mixture of the "mono" and "di-" alkylated products (65) and (66) in a 1:2 ratio (unreacted $[9]N_3$ must have been present in the crude product also). These were separated on a relatively small scale ($\leq$ 100 mg) by 'semi-preparative' cation exchange HPLC (monitored at λ = 282 nm). The

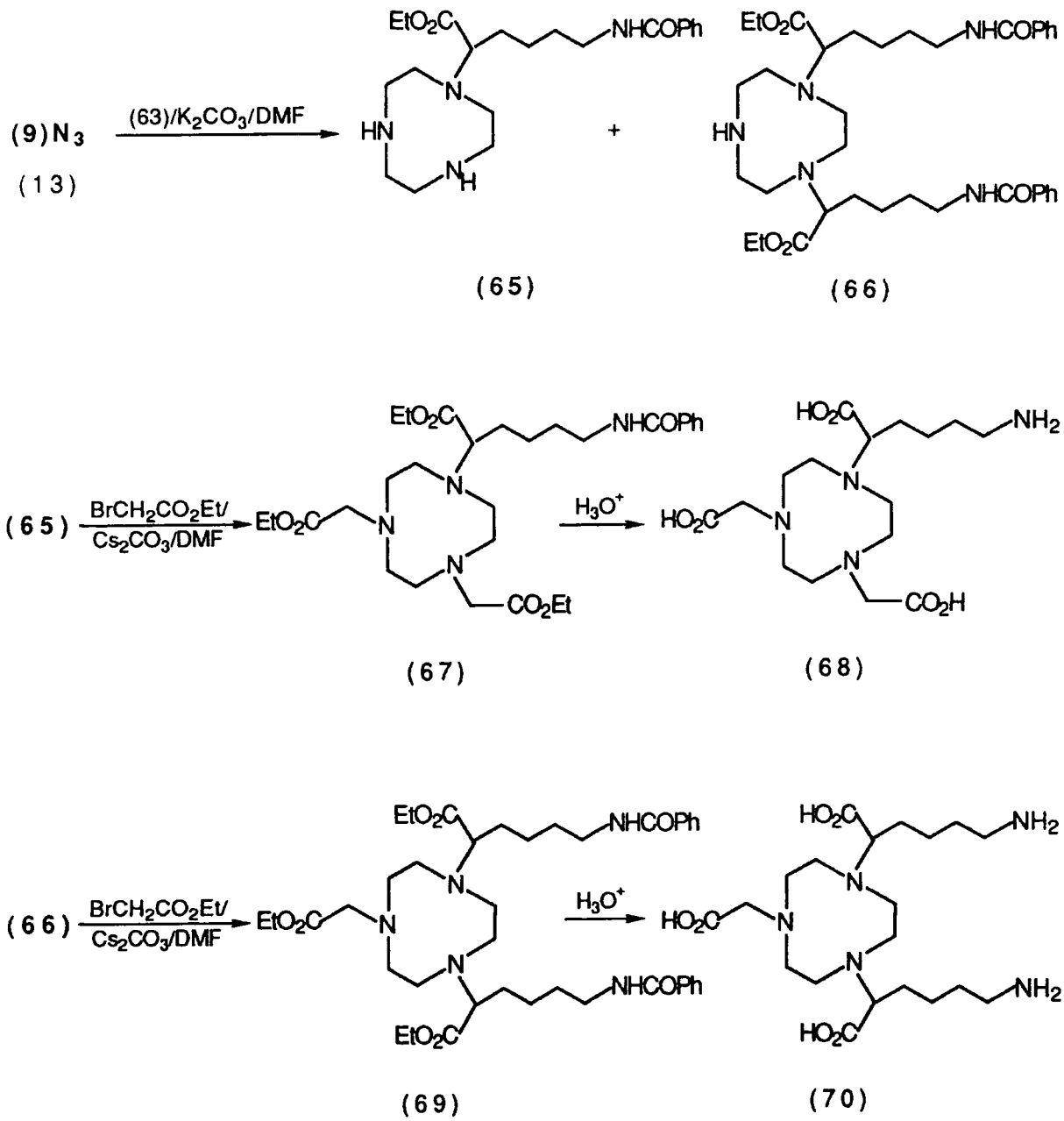

Scheme 3.6. Synthesis of "mono-" and "di-" N-functionalised $[9]$-N_3 triacid.

ratio of the products (65) and (66) were reversed (3:1) by increasing the ratio of the triamine to α-bromoester, to 2:1, with slow dropwise addition of the latter. The crude product was used without purification in the next step. Treatment with ethylbromoacetate and caesium carbonate in DMF ($60^{o}C$, 20 hours) yielded a mixture, with two major components, (67) and (69). Initially, investigation of the crude product proved to be confusing, as both products had the same R_F by alumina t.l.c. and the same retention time on cation exchange HPLC. However, very careful gravity alumina column chromatography did afford the separation of quantities of each component (though many middle fractions contained a mixture). Alternatively, the synthesis of the "mono-" and "di-" functionalised systems were effected separately on a small scale, using the material purified by HPLC in the previous step. These products (67) and (69) were also purified by cation exchange HPLC. Hydrolysis of (67) and (69) with hydrochloric acid (6M, 6 hr.) afforded the "mono-" and "di-" N-aminofunctionalised triacids (68) and (70).

3.4. Bifunctional Linker Molecules

3.4.1. Vinylpyridine linker molecules

A bifunctional linker molecule was sought which could be attached selectively to the exocyclic primary amino group of the macrocycle, at one terminal position and which was reactive selectively towards an antibody thiol residue at the other terminal position.

In an attempt to improve the thiol specificity and reactivity of known bifunctional linker systems (e.g. maleimides)[16,17] the p-nitrophenyl ester of 2-vinyl-6-(4'-carboxy-3'-oxabutyl)pyridine (71) was synthesised[3] (Durham/Celltech collaborative work). It has been reported that the thiol group of a cysteine derivative, 5-β-(4-pyridyl-

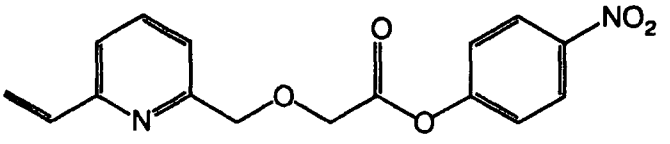

(71)

ethyl)-L-cysteine, is 300 times more reactive towards 4-vinylpyridine than its amino group.[18,19] The thiol reacts at the electrophilic terminal site of the vinylpyridine group [Fig. 3.7]. The 4-vinyl-pyridine system is more reactive towards thiols than the 2-vinylpyridine

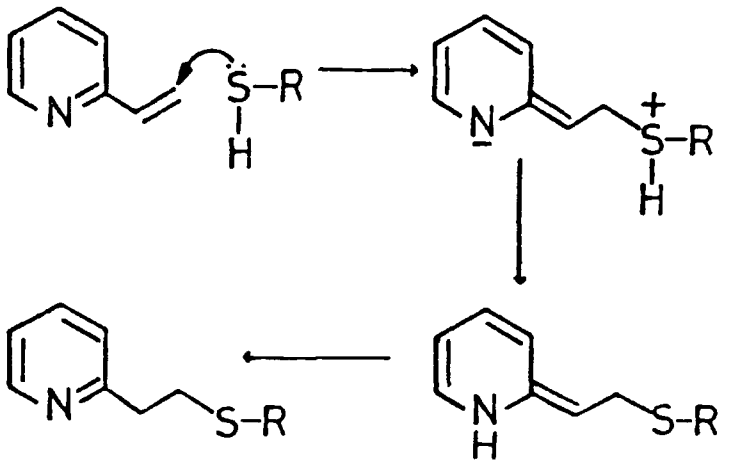

Fig. 3.7. Reaction of a thiol with 2-vinylpyridine.

(though both are specific to thiols over primary amines) due to the greater degree of conjugation with the electron deficient pyridine ring, with the former, leading to a more electrophilic terminal site.

However, for the ease of synthesis from commercially available starting materials, the 2-vinyl-pyridine ester (71) was preferred initially.

The exocyclic primary amino group of the macrocycle is thus unreactive towards the vinylpyridine group and reacts selectively with the ester group, forming an amide link.

3.4.2. Synthesis of macrocycle-vinylpyridine conjugates

Condensation of the macrocyclic primary amine with the p-nitrophenol ester (71) to afford the macrocycle-linker conjugate (72) was effected in two different ways [Scheme 3.7].

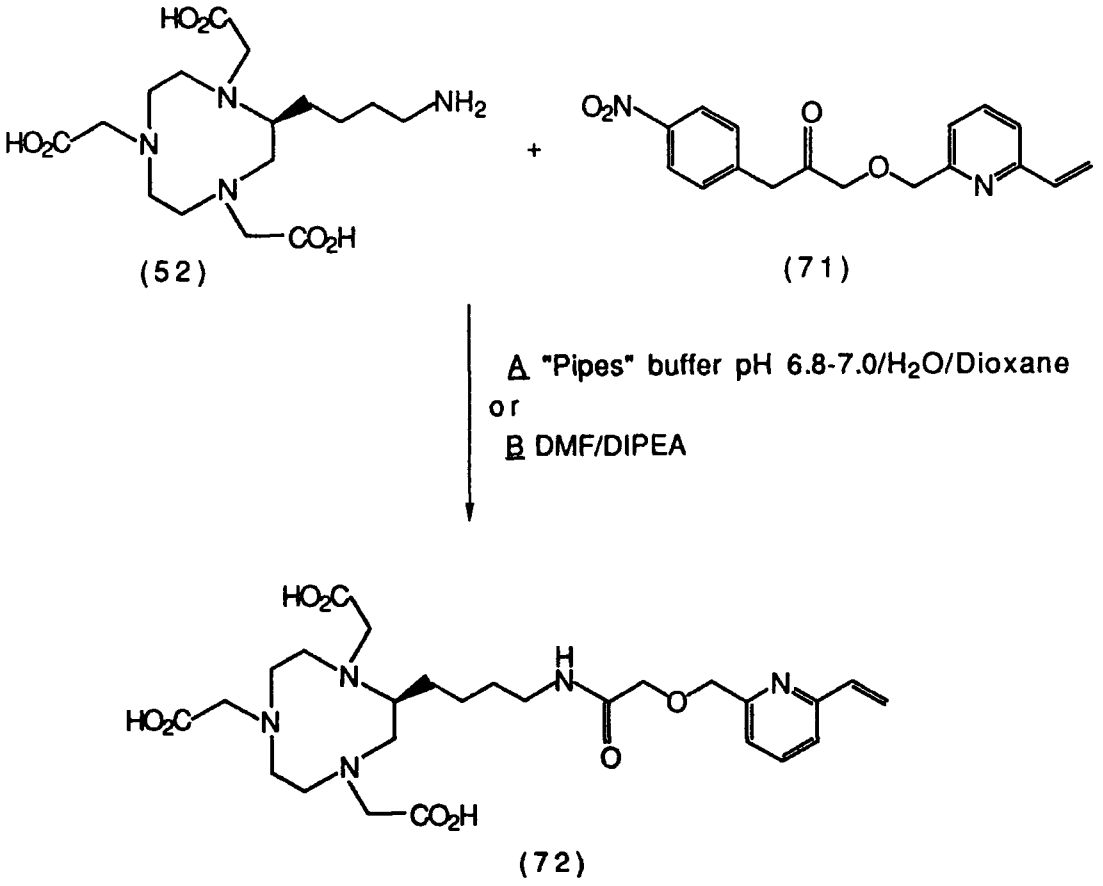

Scheme 3.7. Synthesis of the C-functionalised-vinylpyridine conjugate of the [9]-N_3 triacid.

The conjugate was synthesised by the addition of a solution of the ester (1.5 eq) in dioxane to an equal volume of an aqueous solution of the amine, buffered at pH 6.8-7.0 with "pipes" buffer (0.5M). Reaction proceeded to completion over a period of 12 hours at $40^{o}C$. Alternatively, the reaction was carried out at room temperature, in DMF, by mixing the same reagents in the presence of diisopropylethylamine. The majority of starting material was consumed after 3-4 hours, although the reaction was usually left for 12 hours to ensure completion. In both cases the reaction was monitored by reverse phase HPLC and the product (72) was separated from starting materials and hydrolysis products by the same technique. The macrocycle vinylpyridine conjugate had a retention time of 12 minutes [Fig. 3.8(a)] when run with a gradient elution of MeCN(0.1% TFA)-H_2O(0.1% TFA) [5:95] to [95:5] over 20 minutes. The smaller peak observed at 10 minutes was discovered to be the copper(II) complex of (72), due to metal ion contamination in the HPLC guard column. The ^{1}H nmr of the product [Fig. 3.8(b)] revealed the characteristic resonances of the vinylpyridine group (5.8 to 8.3 ppm) and two diagnostic methylene (CH_2O) resonances at 4.15 and 4.88 ppm.

Attempts to synthesise the analogous vinylpyridine conjugate of the DTPA C-functionalised ligand (60) were initially unsuccessful using both methods outlined previously. Only after further purification of the starting material (66) by reverse phase HPLC did the reaction proceed in DMF in the presence of DIPEA.

3.4.3. Maleimide linker molecules

The use of N-maleimidobenzoyl-N-hydroxysuccinimide ester (MBS) (73) as a coupling reagent for proteins was first reported by Kitagawa[16] in 1976. Primary amines react readily with the ester group to form an amide link, leaving the maleimide group at the other terminal position,

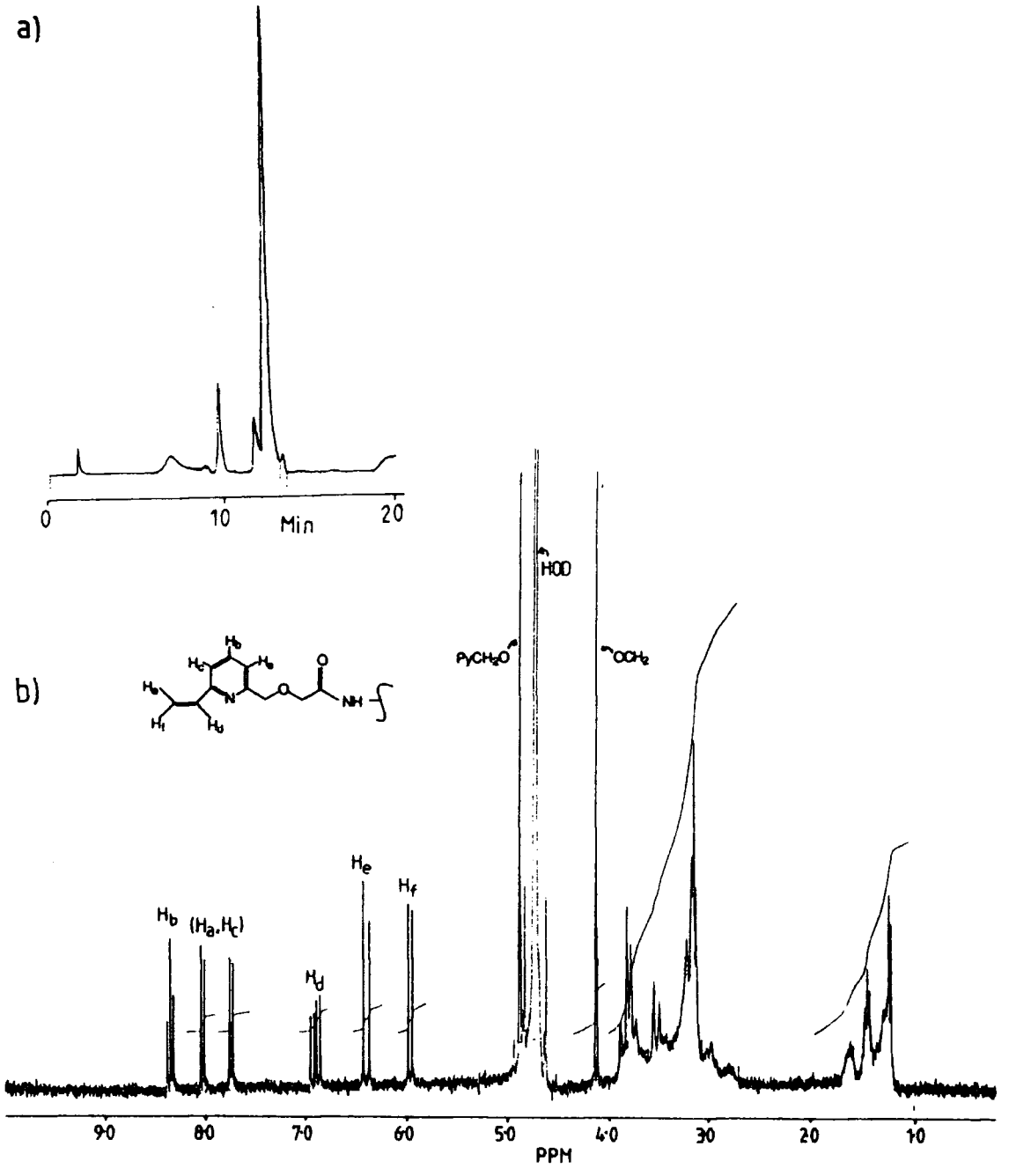

Fig. 3.8. a) Reverse phase HPLC trace and b) the ^{1}H nmr of (72).

which is reactive selectively towards thiols. Maleimides tend to hydrolyse readily in aqueous solution, at high pH ($\geq$ 7.5) to maleamic acid [Fig. 3.9]. More recently, new maleimide cross linker reagents which are less susceptible to hydrolysis than the original MBS system, have become commercially available. One such maleimide ester,

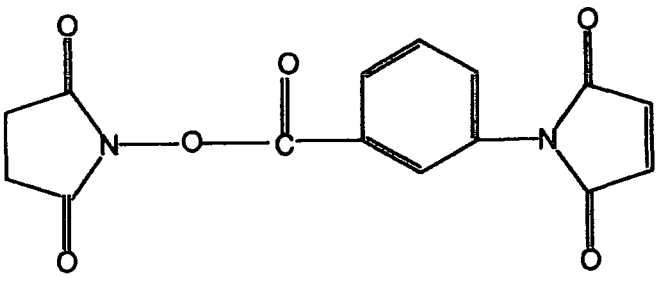

(73) MBS

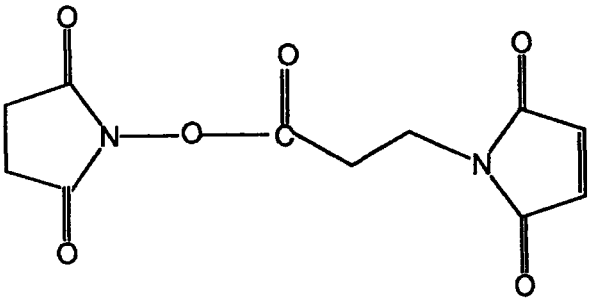

(74)

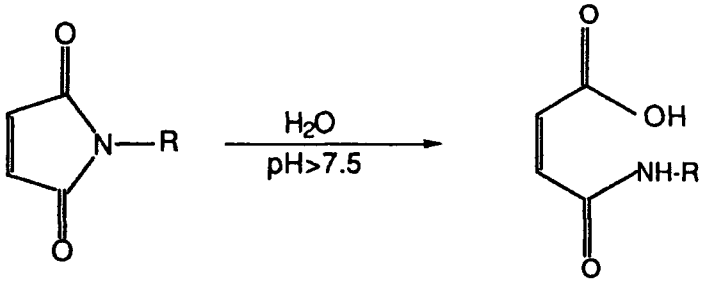

Fig. 3.9. Hydrolysis of maleimides.

N-succinimidyl-3-maleimidopropionate (74) [Sigma] was selected for use in the studies described herein.

3.4.4. <u>Synthesis of macrocycle-maleimide linker conjugates</u>

The synthesis of the maleimide cross linker conjugates is reported here for the "mono" and "di-" N-functionalised macrocycles (68) and (70). However, the methods described lend themselves equally as well to the C-functionalised systems.

Two different methods were attempted for the synthesis of (75) and

(76) [Scheme 3.8]. The reaction was attempted using a water-dioxane system buffered at pH 6.8-7.0 ("pipes" buffer) as described for the vinylpyridine conjugate synthesis. However, this method failed to yield an appreciable amount of product (the main reaction component after 24 hours was the ester hydrolysis product (77)). A more successful

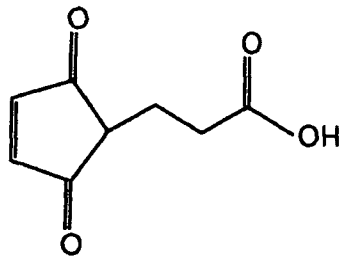

(77)

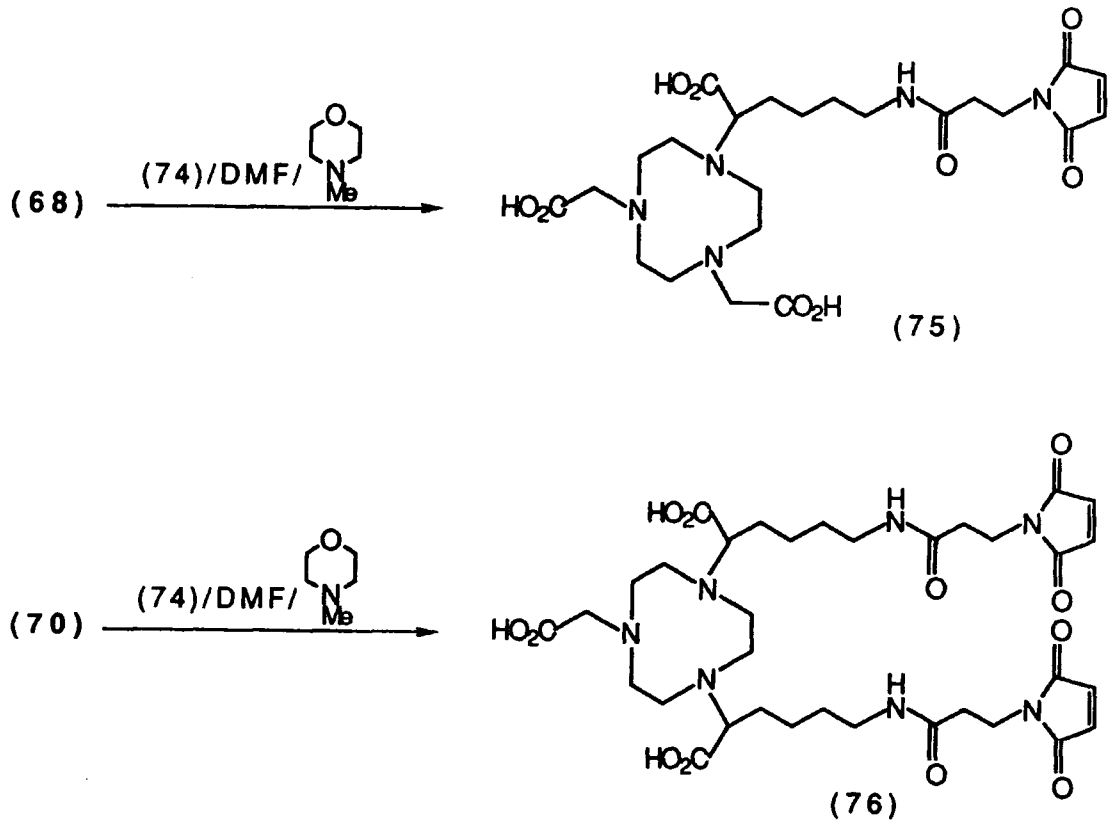

Scheme 3.8. Synthesis of "mono" and "di" N-functionalised macrocycle-maleimide conjugates.

synthesis was effected using DMF as the solvent. The maleimide ester (1.2 eq) in DMF was added to the deprotected amine (68) followed by the addition of N-methylmorpholine (5 eq). Immediate precipitation of the deprotonated macrocycle resulted, hence a minimum amount of water (8-10% vol) was added in order to redissolve the material. The majority of the starting material had been consumed after 5 hours, though the reaction was stopped after 12 hours to ensure completion of reaction. Similar reaction conditions were employed for the "di" functionalised system (70), except that 7 equivalents of base were required in order to deprotonate the amine and aid nucleophilic attack at the ester site. In both cases reaction was followed by reverse phase HPLC (at λ = 282 nm) eluting with H_2O (0.1% TFA)/MeCN (0.1% TFA) from 95:5 to 5:95 over 20 minutes. Retention times included; 10.5 min. for the "di" N-linked maleimide conjugate (76); 9.3 min. for the maleimide ester starting material (73); 8.7 min. for the "mono" N-linked maleimide conjugate (75) and 6.6 min. for the maleimide ester hydrolysis product (77). Purification was thus achieved by reverse phase HPLC. In subsequent reactions it was found that mixtures of "mono" and "di" functionalised starting material could be condensed with the maleimide ester in the same reaction mixture, requiring purification at the final stage i.e. as the maleimide macrocycle conjugates. This provided a relatively quick and convenient route to the required products (75) and (76). In the ^1H nmr spectra of the maleimide macrocycle conjugates, two triplets centred at 2.49 and 3.79 ppm, attributable to the 'N-CH_2CH_2CO' group and the single olefinic resonance at 6.9 ppm, were particularly diagnostic. Typical ^1H nmr spectra and HPLC traces are presented in Fig. 3.10. The HPLC trace of the "di-" maleimide product (76) revealed the presence of a small amount (ca. 10%) of the maleimide ester hydrolysis product (77).

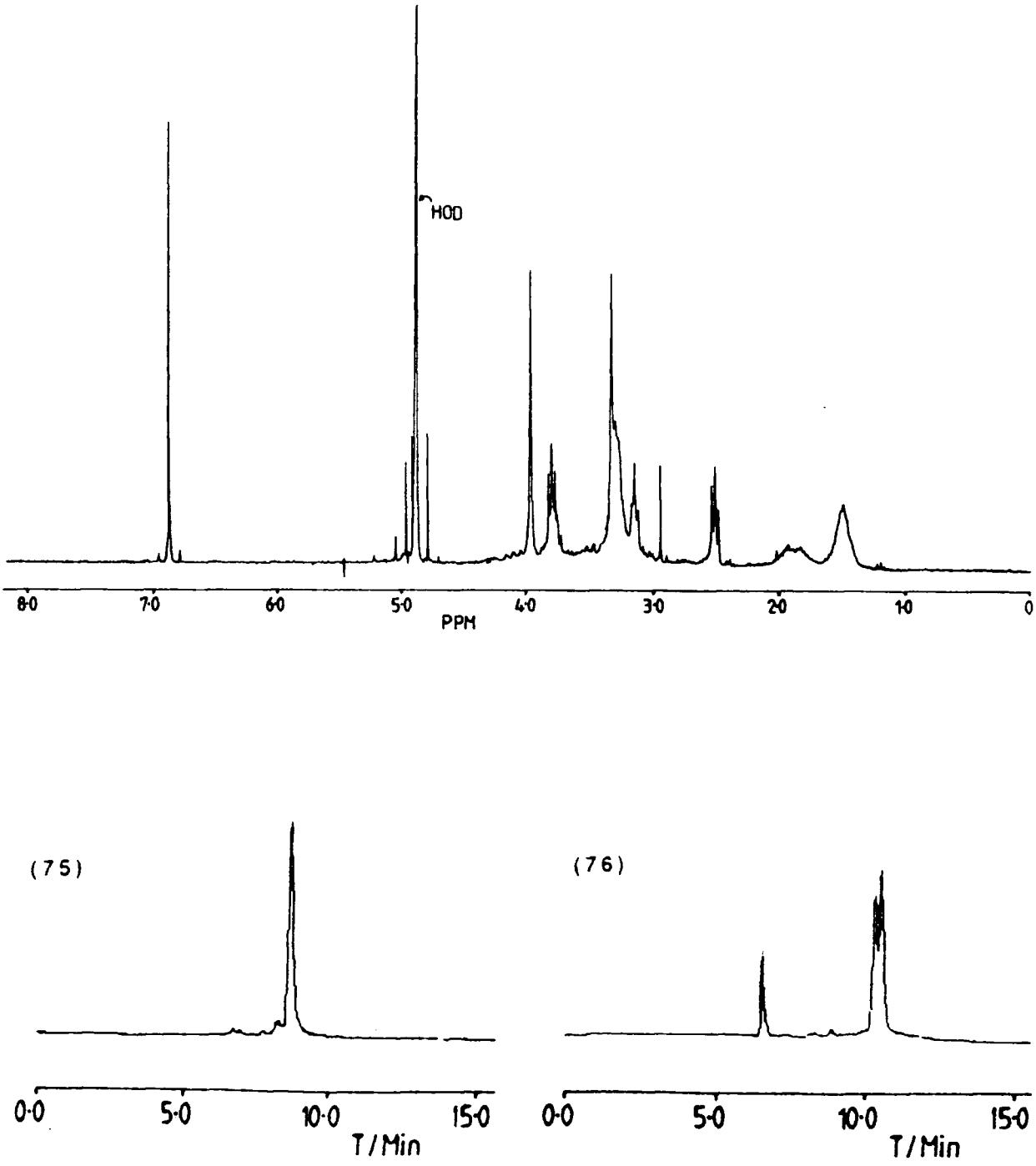

Fig. 3.10. ^{1}H nmr of (75) and HPLC traces of (75) and (76).

Further purification was considered unnecessary (as this would have resulted in the loss of valuable milligrams of product) since it was recognised that the impurity could be removed in the purification step (gel filtration) of the antibody conjugation reaction (section 3.5.).

The product (76) appears as a doublet in the HPLC trace, possibly attributable to the existence of a mixture of RS and RR/SS diastereomers. In contrast to the C-functionalised systems, the synthetic route to the N-functionalised systems involved alkylation with a racemic α-bromoester (63), so that racemates were produced.

The maleimide conjugates of C-functionalised [9]N_3-triacid and C-functionalised DTPA (Fig. 3.11) have been prepared using similar methods.

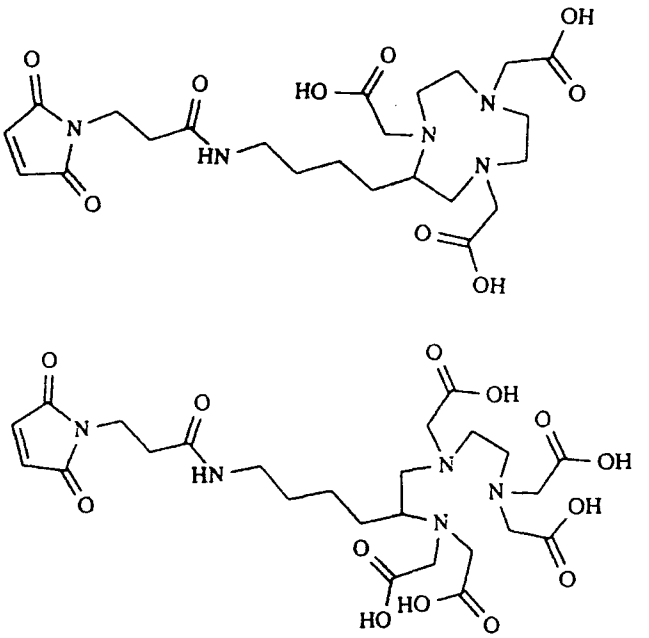

Fig. 3.11. C-functionalised, [9]N_3-triacid and DTPA, maleimide conjugates.

3.5. Antibody Conjugation

3.5.1. The use of "Traut's reagent"

The monoclonal antibody used in the work discussed here is "B72.3" which binds to a tumour associated glycoprotein found in human breast and colorectal cancers. B72.3 production and synthesis of antibody-macrocycle conjugates was carried out at Celltech Ltd.

The generation of free thiols on the antibody was required for

their reaction with either maleimide groups or vinylpyridine groups. Reaction of the antibody (Lysine residue) with 2-iminothiolane [Fig. 3.12] was carried out in buffered solution (phosphate buffer, pH 7.4) at

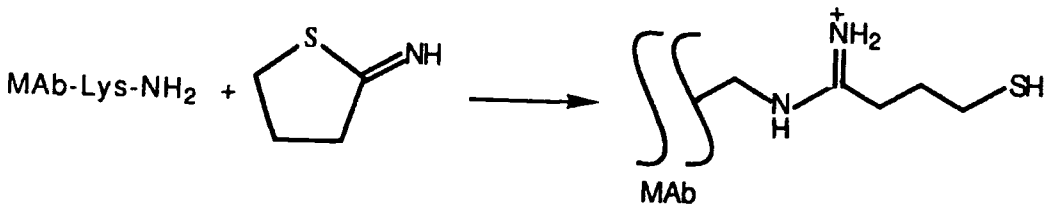

Fig. 3.12. Reaction of 2-iminothiolane with an antibody lysine residue.

4°C. The product was purified by gel filtration through Sephadex G-50. Incubation of the modified antibody (ca. 2-3 thiols per antibody) with the functionalised macrocycle (pH = 7, 4°C) yielded the antibody-macrocycle conjugate, which was purified by either gel filtration or HPLC. Reaction of the 2-vinylpyridine conjugates with the thiol residues on the antibody was found to be rather slow, hence the maleimide conjugates were selected as the preferred reagents for antibody conjugation.

3.5.2. <u>Alternative methods for macrocycle-antibody conjugation</u>

<u>Site Specific Attachment</u>

Using the method outlined above, the thiol groups and hence the macrocycles are introduced with a completely random distribution along the antibody structure. A preferable strategy would be to generate thiol groups specifically outside the immunologically important variable region of the antibody. The number of macrocycles linked to the antibody could then be increased without impairing antigen recognition. The use of genetically engineered antibodies with thiol groups generated at the hinge region (i.e. between the 'Fab' and 'Fc' portions of the antibody - see section 1.2.1.) enabling "site specific" attachment of

macrocycles, is currently being investigated.

"DFM" Method

An alternative approach to macrocycle antibody conjugation currently being developed at Celltech Ltd., is referred to as the "Di-Fab-Maleimide" (DFM) method. The disulphide bonds that link the two halves of the antibody are cleaved to give the F(ab) fragments (see section 1.2.4.). A macrocycle-linker conjugate which possesses two maleimide groups may be inserted between the two fragments, by reaction with the free thiols, when the two halves are recombined [Fig. 3.13].

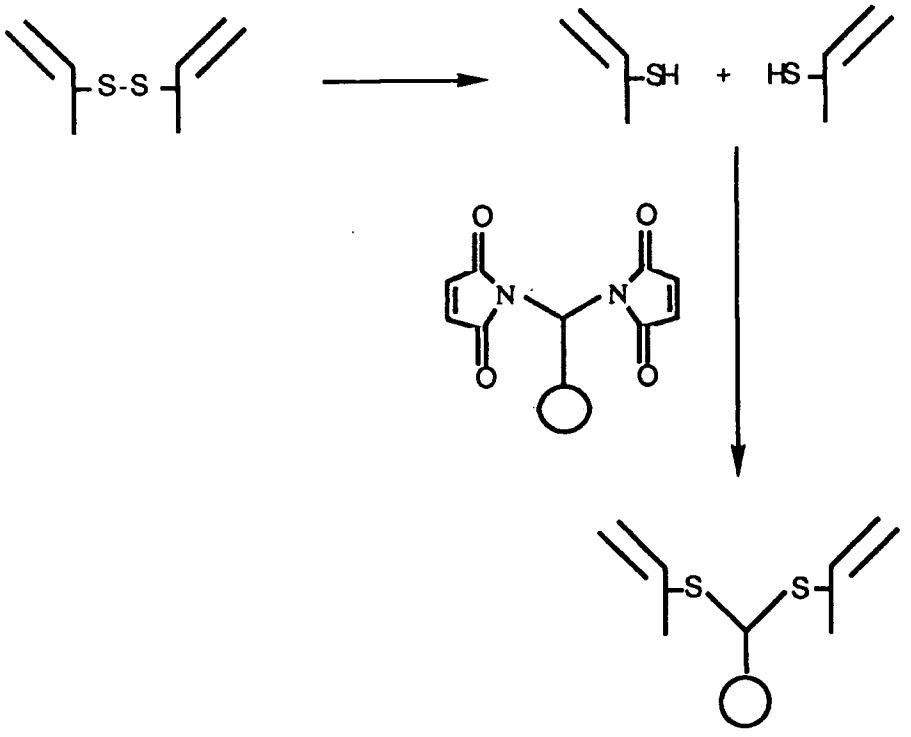

Fig. 3.13. "DFM" approach to macrocycle-antibody conjugation.

The major advantage is that antibody-macrocycle conjugation is restricted to the constant domain of the 'long chain' and is unlikely to

affect the variable region of the antibody. This is likely to minimise any adverse effects that macrocycle linkage may have on antigen recognition and immunogenic response of the antibody conjugate.

In order to attach the C-functionalised [9]N_3-triacid macrocycle (52) to the antibody, using this approach, it was necessary to synthesise a modified maleimide-macrocycle conjugate (79). Reaction of 'Bis-Z-lys-osu' (78) [Sigma, Z = $C_6H_5CH_2OCO$-] with the primary amine of the C-functionalised macrocycle (52), followed by removal of the benzoxycarbonyl ('Z') groups (TMSiI) generated two primary exocyclic amino groups, which were condensed with N-succinimidyl-3-maleimido-propionate (2.1 eq) to give the bis maleimide (79).

Alternatively the "di-" N-functionalised [9]N_3-triacid (70) requires no modification for antibody linkage using the 'DFM' approach, by virtue of the two maleimide groups already attached to the macrocycle. However, this particular method has not yet been attempted.

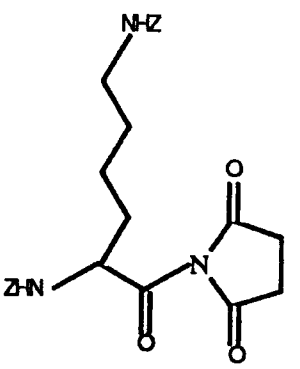

(78)

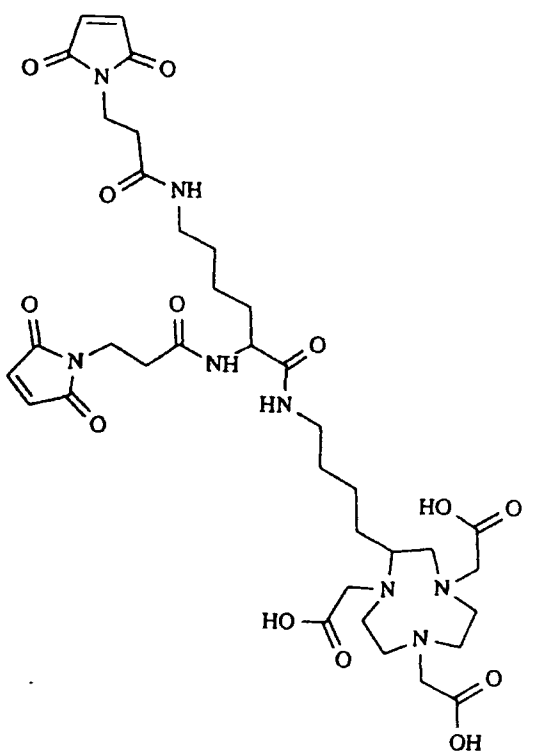

(79)

3.6. Tumour Imaging - Biodistribution Studies[21]

Initial biodistribution studies in tumour bearing mice have been carried out on the ^{111}In labelled C-functionalised $[9]N_3$-triacid-B72.3 conjugate. The antibody macrocycle conjugate was radiolabelled using $^{111}InCl_3$ in 0.1M sodium acetate buffer at pH 5 (> 80% efficiency at ~ 30 μM in macrocycle).

Athymic mice bearing the LS-174T human colon carcinoma Xenograft (implant) were injected intraveneously with the ^{111}In labelled macrocycle-B72.3 conjugate. Biodistribution data recorded at 24 and 96 hours (postinjection), expressed as percentage of injected dose per gram of tissue (% 1D/g) are presented in Table 3.1.

Table 3.1

Biodistribution data for ^{111}In labelled B72.3-$[9]N_3$-triacid conjugate expressed as % 1D/g (24 hr. and 96 hr.)

	% 1D/g			
	24 hr.		96 hr.	
Tissue	Mean	±SD	Mean	±SD
Blood	8.17	1.32	4.02	0.84
Liver	4.67	1.00	4.55	0.47
Kidney	5.92	1.53	3.83	0.80
Lung	3.65	0.56	2.42	0.65
Spleen	3.39	0.65	3.31	0.70
Colon	1.55	0.16	1.29	0.53
Muscle	1.17	0.38	0.77	0.32
Tumour	8.00	1.54	9.54	0.82
Bone	1.65	0.32	1.32	0.37

Localisation of the radiolabelled antibody at the tumour is apparent, with superior tumour to background ratios observed at 96 hours. However, these and subsequent studies have shown that significant background levels of radiation are observed in the liver and kidneys. A significant amount of activity in the majority of tissues is accounted for by the blood associated activity in these tissues. Hence, a useful form in which to express the results is as blood-to-tissue ratios, thereby minimising the effect of "blood pool" differences. Blood-to-tissue ratios in the liver, kidney and tumour are presented in Table 3.2 and are compared to the values obtained in analogous experiments using a DTPA-B72.3 conjugate ('CA-DTPA' - see section 3.1). At 24 and 96 hours the tumour-to-blood ratio for the macrocyclic conjugate is superior to that of the DTPA conjugate. The macrocyclic conjugate also shows lower accumulation of radioactivity in the kidneys, although accumulation in the liver is greater than for the DTPA conjugate.

Table 3.2

Blood-to-tissue ratios for B72.3-[9]N_3 and B72.3-DTPA conjugates at 24 and 96 hours

Conjugate	Time/hr.	Blood/tumour	Blood/kidney	Blood/liver
B72.3-[9]N_3	24	1.02	1.38	1.75
	96	0.42	1.05	0.88
B72.7-DTPA	24	1.28	1.42	2.28
	96	0.62	0.77	1.20

Similar biodistribution studies were carried out using conjugates with chimaeric ("humanised") B72.3 antibody (see section 1.2.4.). The biodistribution data for the ^{111}In labelled conjugate of $[9]N_3$ in mice bearing the LS-174T Xenograft at 24 and 72 hours are presented in Table 3.3.

Table 3.3

Biodistribution of ^{111}In labelled chimaeric B72.3-$[9]N_3$ conjugate expressed as % 1D/g after 24 and 72 hr.

	% 1D/g			
Tissue	24 hr.		72 hr.	
	Mean	± SD	Mean	± SD
Blood	13.33	1.24	9.72	1.20
Liver	4.40	0.73	4.09	1.23
Kidney	13.90	1.60	16.47	1.88
Lung	5.96	0.37	4.70	0.30
Spleen	3.30	0.35	3.37	0.43
Colon	1.63	0.29	1.22	0.12
Muscle	1.49	0.26	1.20	0.53
Bone	1.61	0.11	1.39	0.22
Tumour	14.48	0.55	19.74	0.31

The very high levels of radioactivity found in the kidneys in these studies were not observed with the analogous murine B72.3 studies and are most likely to be a feature of the modified antibody. A significant proportion of the conjugate did not remain intact after injection into the mice, resulting in relatively rapid excretion via the kidneys. This is possibly a consequence of the mouse partially rejecting the

"humanised" antibody in a similar response to that observed with murine antibodies in human patients. However, observation of the blood-to-liver and blood-to-tumour ratios determined between 24 and 144 hr. for both $[9]N_3$ and DTPA chimaeric B72.3 conjugates (Table 3.4) show an improvement over the previous set of results. The $[9]N_3$ conjugate shows significantly reduced accumulation in the liver compared to the DTPA conjugate, although only a slightly superior blood-to-tumour ratio was observed for the macrocyclic conjugate.

Table 3.4

Blood-to-tissue ratios for ^{111}In labelled $[9]N_3$ and CA-DTPA chimaeric B72.3 conjugates between 24 and 144 hrs.

Conjugate	Time/hr.	Blood/tumour	Blood/liver
$[9]-N_3$	24	0.92	3.03
	48	0.56	3.27
	72	0.49	2.38
	144	0.27	1.22
DTPA	24	0.87	1.88
	48	0.65	1.45
	72	0.53	1.24
	144	0.35	0.51

Clearly more studies are required in order to draw any further conclusions. Studies are in progress using conventional and 'DFM' antibody-macrocycle conjugates, which are to be compared with the C-functionalised DTPA ligand (60), the preparation of which was reported in section 3.2.4.

3.7. References

1. D.J. Hnatowich, W.W. Layne and R.L. Childs, Int. J. Radiat. Isot., 33, 327 (1982).

2. C.H. Paik, P.R. Murphy et al., J. Nucl. Med., 24, 1158 (1983).

3. M.W. Brechbiel and O.A. Gansow et al. (ref. 32 - chapter 1).

4. C.F. Meares and T.G. Wensel, Acc. Chem. Res., 17, 202 (1984).

5. C.F. Meares, Nucl. Med. Biol., 13(4), 311 (1986).

6. C.F. Meares, M.J. McCall, D.T. Rearden, D.A. Goodwin, C.I. Diananti and M. McTigue, Anal. Biochem., 142, 68 (1984).

7. W.C. Enkelman and C.H. Paik, Nucl. Med. Biol. Int. J. Radiat. Appl. Instrum. part B, 13(4), 335 (1986).

8. Y. Arano, A. Yokoyama, Y. Magata, K. Horiuchi, H. Saji and K. Torizuka, Appl. Radiat. Isot.; Int. J. Radiat. Appl. Instrum. Part A, 37(7), 587 (1986).

9. M.K. Moi, C.F. Meares, M.J. McCall, W.C. Cole and S.J. Denardo, Anal. Biochem., 148, 249 (1985).

10. B.K. Vriesema, J. Buter and R.M. Kellogg, J. Org. Chem., 49, 110 (1984).

11. This reaction was carried out by Dr. I.M. Helps (formerly Durham University).

12. D. Parker, I.M. Helps and K. Jankowski, unpublished results.

13. Synthesised by K. Jankowski and R.S. Matthews (Durham University).

14. J.C. Eck and C.S. Marvel, Org. Synth. Coll. vol. 2, 74 (1943).

15. W. Walz, K. Wieghardt, B. Nuber and J. Weiss, Inorg. Chem., 27, 2484 (1988).

16. T. Kitagawa and T. Aikawa, J. Biochem., 79, 233 (1976).

17. B. Yoshitake, Y. Yamada, E. Ishikawa and R. Masseyeff, Int. J. Biochem., 101, 395 (1979).

18. a) J.R. Morphy and D. Parker et al., J. Chem. Soc. Chem. Commun., 156 (1988).
b) J.R. Morphy, Ph.D. thesis 1988 (University of Durham).

19. J.F. Cavins and M. Friedman, Anal. Biochem., 35, 489 (1970).

20. a) A.J. Paterson and J. Schlom, Int. J. Cancer, 37, 659 (1986).
b) D. Colcher, P. Horan-Hand, M. Nati and J. Schlom, Proc. Nat. Acad. Sci. U.S.A., 78, 3199 (1981).

21. These experiments were carried out at Charing Cross Hospital.

CHAPTER FOUR

MACROCYCLIC COORDINATION CHEMISTRY OF SILVER(I)

4.1. Factors Affecting the Macrocyclic Coordination of Silver(I)

4.1.1. Introduction

The most common oxidation state for silver is unipositive. The Ag^+ ion in water probably exists as $Ag(H_2O)_2^+$, but the water is very labile and no hydrated salts are known. The silver(I) cation is a relatively large, polarisable d^{10} cation with an ionic radius of 1.15Å. As a d^{10} cation, it has no preference for any particular coordination geometry from ligand field considerations. In practice, silver(I) exhibits a preference for linear two coordination and tetrahedral four coordination. With polydentate macrocyclic ligands, five and six coordinate complexes are quite common, but six, seven and eight coordinate complexes have also been reported.[1]

4.1.2. Donor atoms

Being a "soft" cation (according to the classification of Pearson[2]) silver(I) has a strong preference for the "soft" sulphur and nitrogen donor atoms over the hard oxygen donor atom.[3,4] The interaction of silver(I) with nitrogen and sulphur donor atoms is more covalent in nature than the electrostatic ion-dipole interaction that occurs with oxygen donor atoms.

This preference is illustrated by the stability constants of the silver(I) complexes of the 1,10-diaza and 1,10-dithia derivatives of 18-crown-6, (81) and (82), compared to that for 18-crown-6 (1) itself (Table 4.1).[5,6] By replacing just two of the six oxygen donor atoms with nitrogen or sulphur donor atoms, there is a greater than 10^5 fold increase in complex stability. The estimated bond enthalpies for the three different donor atoms with silver(I) have been reported and are shown in Table 4.2.

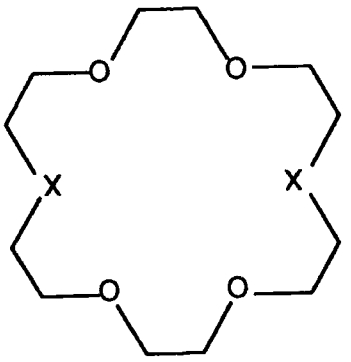

		Abbrev^{n}
(1)	X=O	[18-C-6]
(81)	X=N	[2.2]
(82)	X=S	[DT18C6]

Table 4.1

Ligand	log K[a]	-ΔH/kJ mol^{-1}	TΔS/kJ mol^{-1}
[18C6]	4.58	39.1	-13
[2.2]	10.02	44.9	12
[DT18C6]	10.33	64	-5.3

[a] log K values determined by potentiometric titration in MeOH at 25^{o}C.

Table 4.2

Donor Atom	Bond energy (kJ mol^{-1})
O	6
NH	22
S	25

Thus, from purely enthalpic considerations, the order of preference for silver(I) is

$$S > N >> O.$$

For ligand (81) it should be noted that the observed enthalpy of complexation is lower than that expected from the relative bond

energies, given in Table 4.2. This can be attributed to a conformational change of the diamine during complexation. It is known that bicyclic diamines (with bridgehead nitrogens) can exist in different conformational forms[7] (exo-exo, endo-exo and endo-endo) and it is likely that monocyclic aza-crowns can do the same, Fig. (4.1).[5]

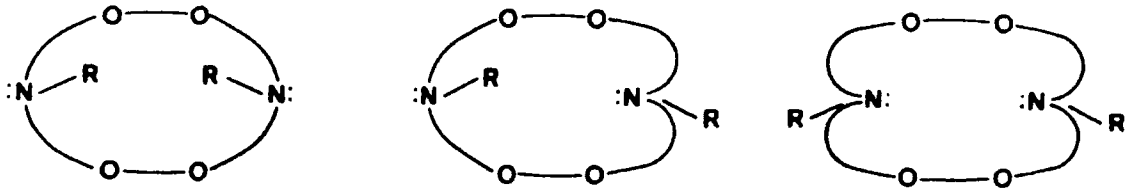

exo-exo exo-endo endo-endo

Fig. 4.1. Different conformations of diaza crowns.

In a polar medium (e.g. H_2O, MeOH) the lone pairs are usually directed outside the cavity (exo-exo) but during complexation the ligand must change to the endo-endo conformation. The difference in observed and calculated enthalpy of complexation for ligand (81) with silver(I) is similar to the energy of inversion of bicyclic diamines.

The solid state structure of the silver(I) complex of the mono-thia derivative of 18-crown-6 (83)[8] [Fig. 4.2] provides a good example of the affinity of the silver(I) cation for sulphur over oxygen.

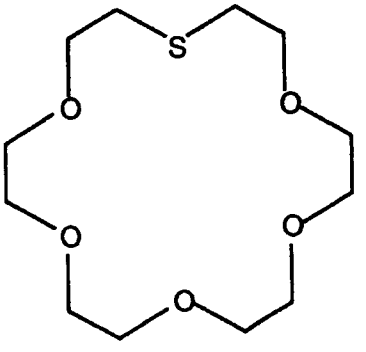

(83)

Two similar conformations exist, one being the near mirror image of the other. The silver binds to two sulphurs, one intramolecular

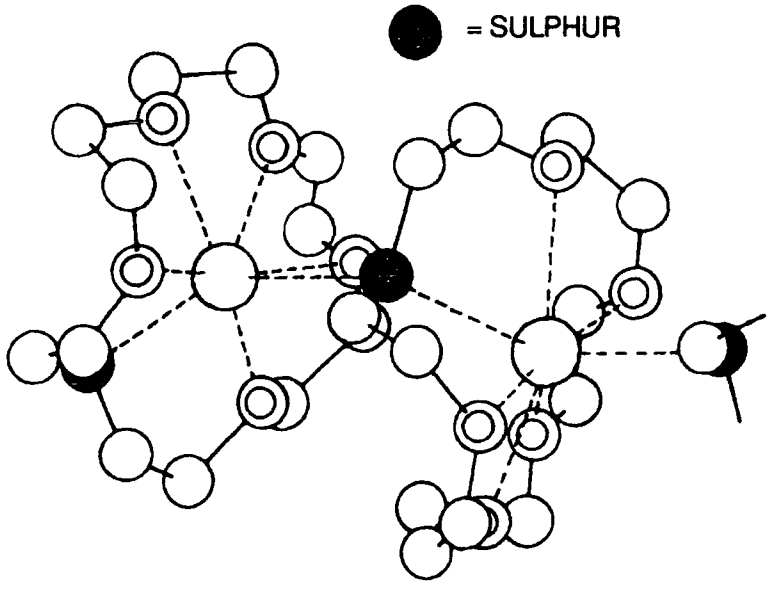

Fig. 4.2. X-ray structure of the silver(I) complex of (83).

interaction (Ag-S 2.58 and 2.60Å) and one intermolecular interaction (Ag-S 2.61 and 2.67Å) with a sulphur from an adjacent ligand. Only one of the five oxygen donor atoms forms a moderately strong bond (Ag-O 2.48Å) the remaining Ag-O distances (2.66-2.92Å) indicating just weak cation-dipole interaction.

4.1.3. **Cavity size**

A simple way to determine the most suitable macrocyclic cavity size for silver(I) is to look at the stability constants for a series of ligands of varying size, (Table 4.3).

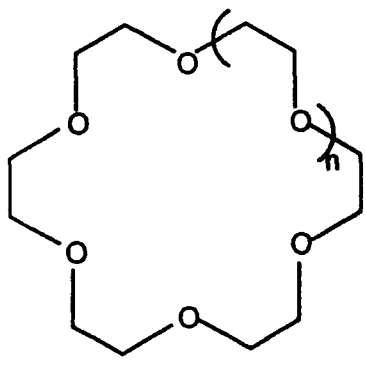

		Abbrev$^{n=}$
(84)	n=0	15C5
(1)	n=1	18C6
(85)	n=2	21C7

Table 4.3

Stability constants for the silver(I) complexes of 15C5, 18C6 and 21C7

Ligand	log K[a]	Cavity size[b]/Å
15C5	3.65	0.9
18C6	4.58	1.4
21C7	2.46	1.9

[a] log K measured in MeOH at 25°C.

[b] ref. 5.

The stability constants indicate that the 18C6 ligand (1) has the optimal cavity size. This is in good agreement with the calculated cavity size[9] of 1.40Å and the ionic radius of Ag^+ (1.15Å). In further agreement with this are the stability constants for the Ag^+ complexes of the dithia and diaza analogues of 15C5 and 18C6, (Table 4.4).

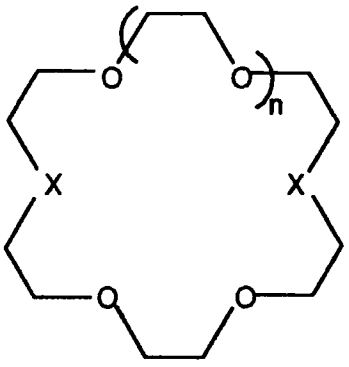

X=NH;		abbrev[n]
(86)	n=0	[2.1]
(81)	n=1	[2.2]
X=S;		
(87)	n=0	[DT15C5]
(82)	n=1	[DT18C6]

The smaller 15C5 analogues show reduced stability constants.

Lindoy, McPartlin and Tasker[10-15] have carried out extensive studies on dibenzo and tribenzo mixed donor macrocyclic ligands, of the type (88), (89) and (90), with systematic variation of ring size and donor atom sequence.

Table 4.4

Stability constants for the Ag^+ complexes of ligands (86), (81), (87) and (82)

Ligand	log K[a]
[2.1]	7.63
[2.2]	10.02
DT15C5	9.85
DT18C6	10.33

[a] measured in MeOH, 25°C.

The aromatic substituents reduce the flexibility of these ligands compared to their crown ether analogues. This may have an unfavourable effect, in restricting any conformational changes necessary

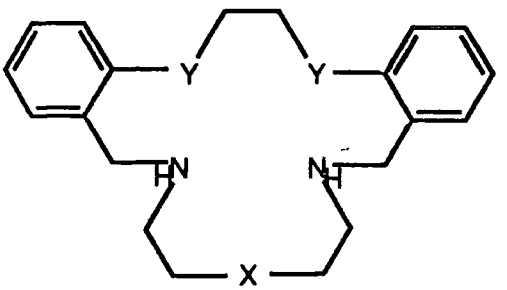

(88)

	Y	X		Y	X
a)	O	O	f)	S	NH
b)	O	S	g)	NH	O
c)	O	NH	h)	NH	S
d)	S	O	i)	NH	NH
e)	S	S			

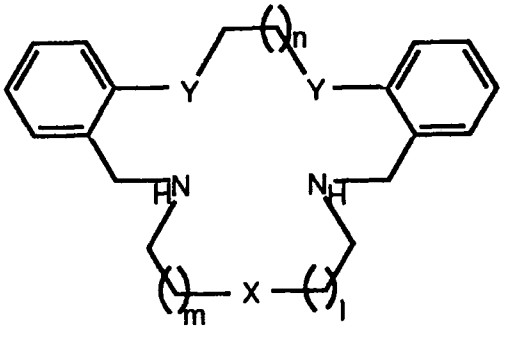

(89) X,Y = NH, O or S
l,m,n = 1 or 2

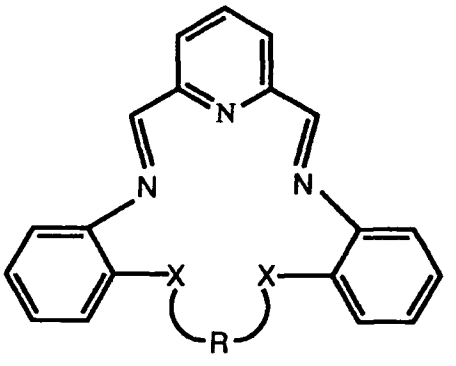

(90) X = NH, O or S
R = $(CH_2)_n$
n = 2, 3 or 4

for complexation, but, as with other more rigid systems (e.g. 'cryptates'), it leads to a greater dependence on matching cavity size with cation size.

Lindoy[16] has reported that, within this series, the most stable complex with silver(I) is formed with the 17 membered mixed sulphur and nitrogen donor ligand 88(e) [log K = 12.4 in MeOH, 25°C].

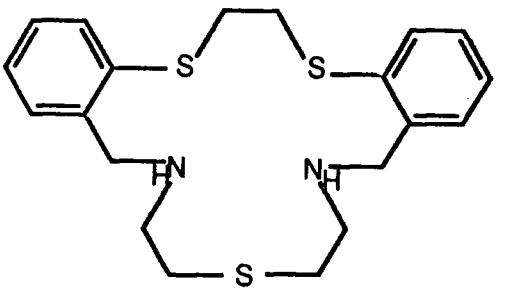

(88e) Dibenzo[17]-N_2S_3

The highest stability constant known for a Ag(I) complex, in methanol, is with the cryptand [2.2.1] (17b).[5] For the slightly smaller and slightly larger cryptates, [2.1.1] (17a) and [2.2.2] (17c) respectively, the stability constants are significantly lower, (Table 4.5).

Table 4.5

Stability constants for the silver(I) complexes of [2.1.1], [2.2.1] and [2.2.2] (298K, MeOH)

Cryptand	log K
[2.1.1]	10.46
[2.2.1]	14.44
[2.2.2]	12.22

4.1.4. **Macrocyclic effect**

Schwing-Weill[35] reported on the macrocyclic effect for a series of transition metal ions, with the mixed donor macrocycle (91) and its acyclic analogue (92).

Only a moderate macrocyclic effect was observed for silver(I) compared to larger effects for copper(II) and nickel(II), but also an absence of an effect for lead(II). The stability constants are given

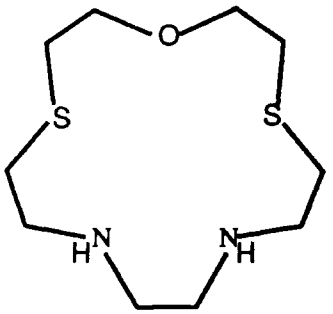

(91)

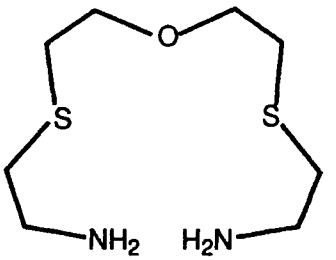

(92)

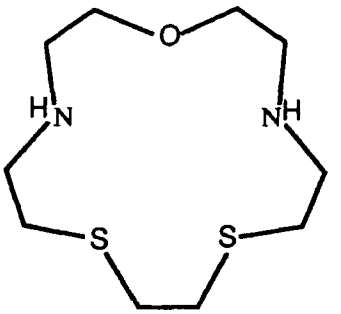

(93)

in Table 4.6.

Table 4.6

The stability constants for the Ag^{+}, Cu^{2+}, Ni^{2+} and Pb^{2+} complexes of ligands (91) and (92)

Cation	log K (91)	log K (92)	Δ log K
$Ag\text{-}L^{+}$	9.91±0.02	7.32±0.05	2.59
$Cu\text{-}L^{2+}$	13.26±0.08	9.15±0.04	4.11
$Ni\text{-}L^{2+}$	8.06±0.02	4.78±0.04	3.28
$Pb\text{-}L^{2+}$	6.78±0.02	7.49±0.04	-0.71

The nature of the cation clearly has a marked influence upon the macrocyclic effect, as does the nature of the ligand. The structurally isomeric ligand (93) forms a somewhat weaker silver(I) complex than ligand (91) [log K = 8.95].

The absence of a macrocyclic effect for the silver(I) complex of the diaza crown [2.2] (81) or, a cryptate effect for the bicyclic diamine [2.2.2] (17c) has been reported[17] and can be attributed to the conformational changes of the ligand during complexation (as discussed in section 4.1.2). In these examples, the unfavourable enthalpic contributions are partially compensated for by a favourable entropic contribution. This is a result of the liberation of solvent molecules from the ligand in its uncomplexed form (exo-exo) during the transition to the endo-endo conformation.

The macrocyclic effect has not been assessed for the mixed sulphur and nitrogen 18-crown-6 systems.

4.1.5. <u>Structure and conformations of thioether crowns</u>

From considerations of bond enthalpy alone, sulphur donor atoms are preferred over nitrogen donor atoms. However, recent work has highlighted the tendency of sulphur atoms in macrocycles to adopt exodentate conformations,[18,19] with the lone pairs directed away from the macrocyclic cavity. The thioether crowns 12-S-4 and 15-S-5 have only exodentate sulphurs and 18-S-6 has four exodentate and two endodentate sulphurs. Cooper has reported[19] that all three of these ligands adopt solid state structures which are composed of right angle "bracket" units (Fig. 4.3), with a sulphur atom at the corner; 12-S-4

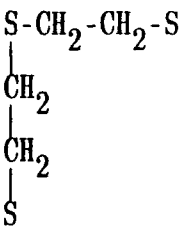

Fig. 4.3. "bracket" unit of thioether crowns.

contains two of these units fused at the terminal sulphurs; 15-S-5 consists of two units fused at one end by the terminal sulphurs and linked at the other by an ethylene bridge and 18S6 consists of two bracket units linked at both ends by ethylene bridges. This conformational preference, which is not observed for oxygen or nitrogen crowns, can be rationalised according to the preferred torsional angles of the C-S and C-C bonds. Sulphur atoms show a strong tendency for the gauche conformation [gauche = $\pm 60^{0}$ and anti = $\pm 180^{0}$] (Fig. 4.4) whereas

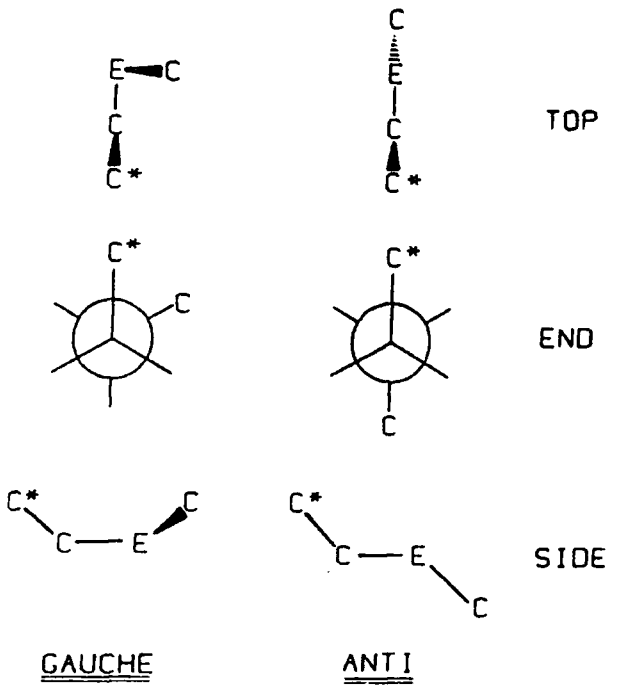

Fig. 4.4. Gauche and anti placements at C-C-E-C bonds.

oxygen prefers the anti arrangement. Two types of 1,4 interaction are proposed to account for this. A gauche C-C-O-C linkage (Fig. 4.5) suffers an unfavourable steric interaction between the two terminal hydrogens, whereas the equivalent sulphur linkage avoids this by virtue of the longer C-S bond. However, gauche placements at O-C-C-O linkages (Fig. 4.6) are favoured for oxygen crowns due to favourable O...O

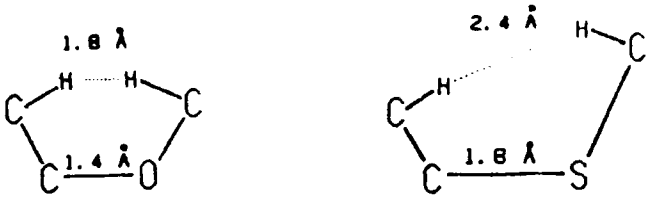

Fig. 4.5. 1,4 Interactions at gauche C-C-E-C linkages.

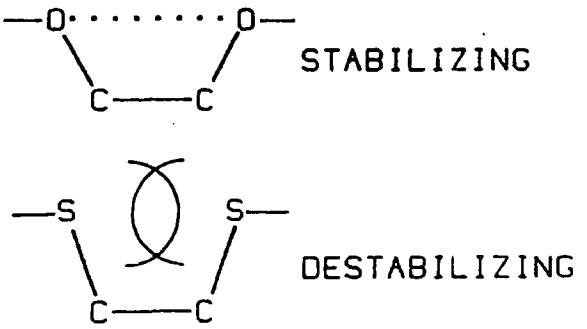

Fig. 4.6. 1,4 Interactions at gauche E-C-C-E linkages.

interactions (dispersion forces), whereas the equivalent sulphur linkages are disfavoured due to steric repulsion between the large sulphur atoms.

The unfavourable conformation associated with thioether linkages results in an unfavourable contribution to the entropy of complexation. This is illustrated by the thermodynamic parameters for the silver complexes of ligands [2.2] (81), [2s2o] and [2s2s] which have increasing numbers of S atoms, Table 4.7.

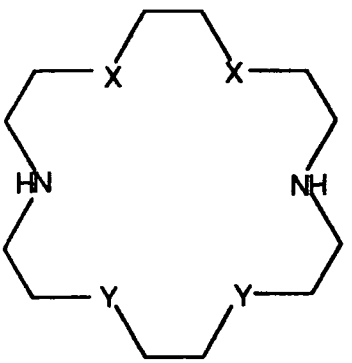

		abbrev
X=S	Y=O	[2s2o]
X=S	Y=S	[2s2s]

Table 4.7

Thermodynamic parameters for Ag(1) complexes of [2.2] (81), [2s2o] and [2s2s]

Ligand	log K[a]	-ΔH/kJ mol^{-1}	TΔS/kJ mol^{-1}
[2.2]	10.02	51.4	5.7
[2s2o]	11.5	67.7	-2.0
[2s2s]	13.7	83.2	-5.0

[a] log K in MeOH (25°C).

Of interest are the entropies of complexation, which start at a favourable +5.7 for ligand [2.2] and become more unfavourable for the dithia and tetrathia macrocycles [2s2o] and [2s2s].

This point is discussed again with some of our own thermodynamic results in Chapter 5.

4.2. Coordination Geometry

This section contains a brief review of some of the silver(I) macrocyclic structures reported to date, highlighting the different coordination geometries observed.

The X-ray structures of the Ag^+ complexes of the two 15-membered N_2S_2O macrocycles (91) and (93) were determined as their thiocyanate salts [Fig. 4.7 and Fig. 4.8].[20,21] Both complexes exhibit distorted square pyramidal coordination with the silver ion sitting inside the cavity of the macrocycle, binding to the two sulphurs and two nitrogens. The thiocyanate anion occupies the apical site, binding through the sulphur. With ligand (93) there is a weak silver-oxygen interaction (Ag-O 2.9Å), but not with ligand (91) (Ag-O 3.72Å).

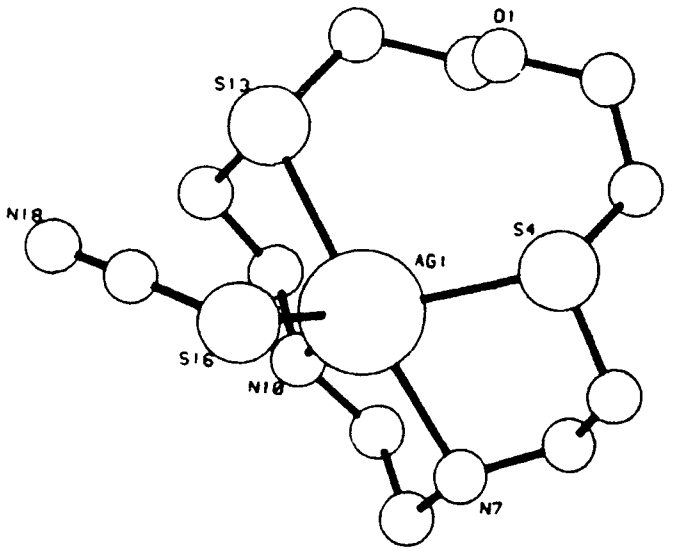

Fig. 4.7. X-ray structure of the Ag(1) (SCN) complex of (91) [15-N_2S_2O]

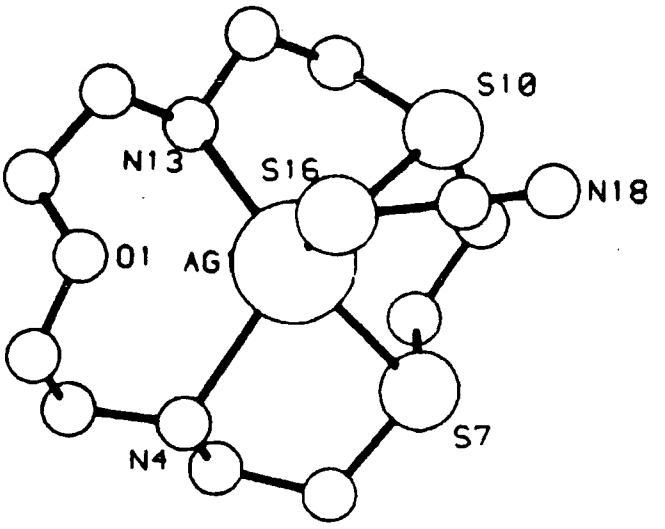

Fig. 4.8. X-ray structure of the Ag(1) (SCN) complex of (93) [15-S_2N_2O]

The silver(I) acetate complex of the 16-membered N_2S_2 macrocycle (94),[22] has an approximately square pyramidal coordination (Fig. 4.9) distorted towards trigonal bipyramidal, with axial nitrogen donors [N-Ag-N 179.3°, Ag-N 2.48 and 2.43Å] and equatorial aceto oxygen [Ag-O 2.69Å] and sulphur donors [Ag-S both 2.59Å]. All four of the six membered chelates form twist-boat conformations.

The 17-membered N_3S_2 macrocycle (95) provides an example of the silver coordinating to five macrocyclic donor atoms, in a distorted trigonal bipyramidal arrangement,[23] with the two sulphurs and the pyridine nitrogen equatorial [Fig. 4.10]. The major deviation from idealised geometry is due to the geometrical restrictions imposed by the pyridine-N_2 unit [N-$\hat{A}$g-N ca. 72°].

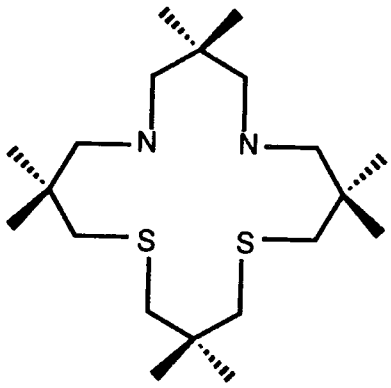

(94)

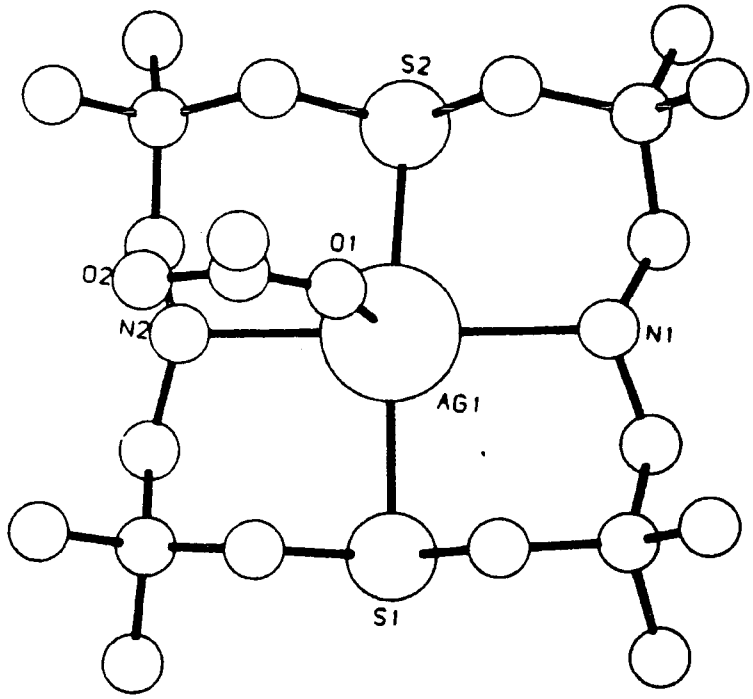

Fig. 4.9. X-ray crystal structure of the Ag(I) (OCOMe) complex of (94) [16-N_2S_2].

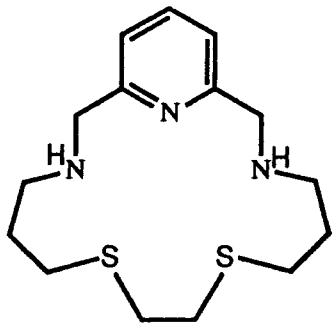

(95)

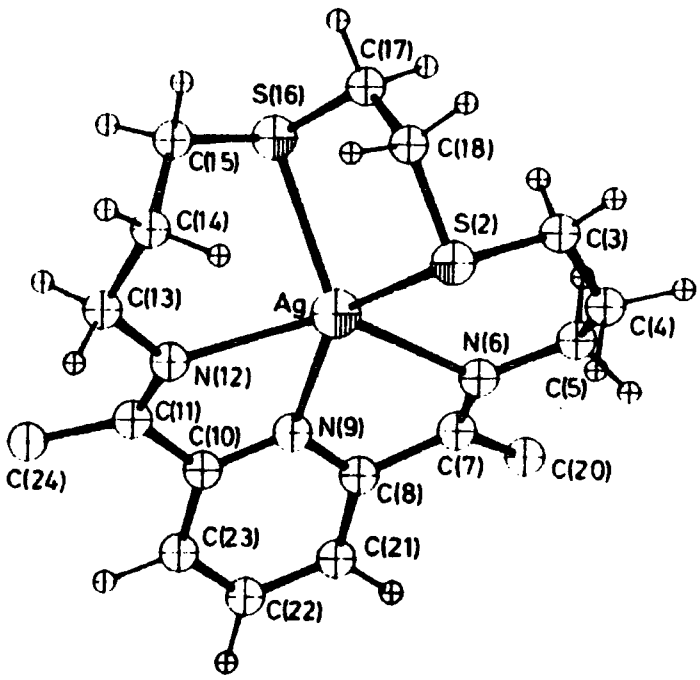

Fig. 4.10. X-ray crystal structure of the Ag(I) complex of (95) [17-N_3S_2].

A six coordinate macrocyclic complex has been observed with the trithia diimino pyridine ligand (96) [Fig. 4.11].[24] The coordination is irregular and strained, as a consequence of the geometrical restrictions

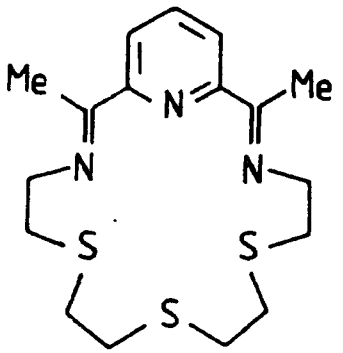

(96)

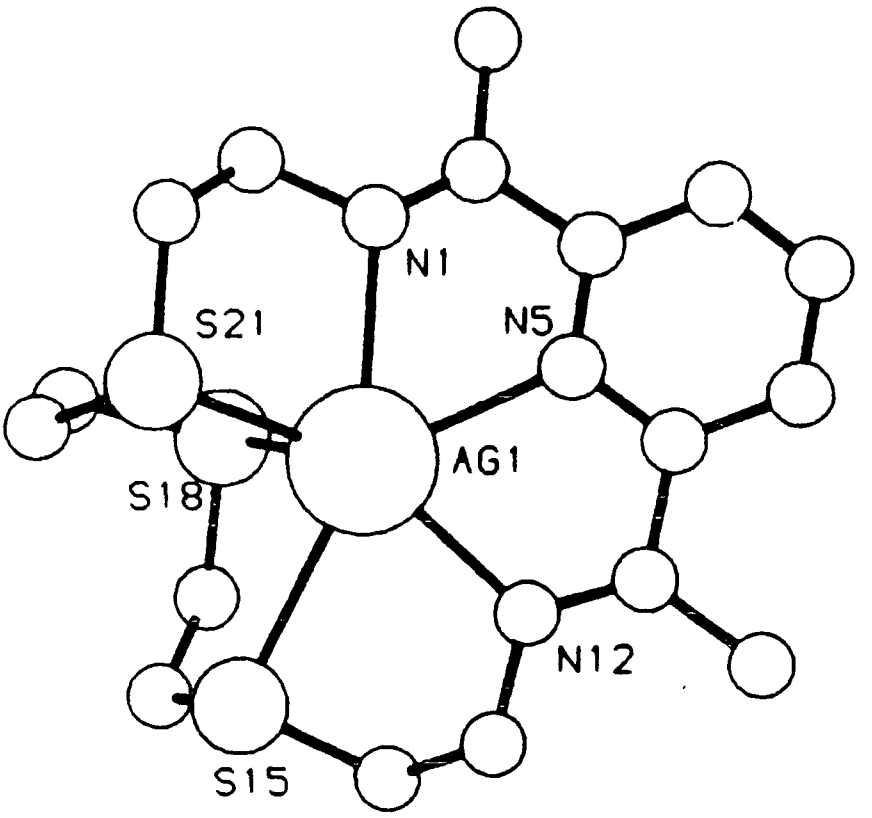

Fig. 4.11. X-ray crystal structure of the Ag(I) complex of (96) [18-N_3S_3].

imposed by the planar diiminopyridine unit. The three sulphur atoms deviate from the plane by 0.52, 2.32 and -1.05Å with bond lengths 2.95, 2.67 and 2.65Å respectively and the S-Ag-N angles vary from 87.1° to 122.0°.

More recently, a novel six coordinate structure has been reported with two nine membered S_3 rings (97)[25] coordinating facially to a silver cation sandwiched between the two (Fig. 4.12).

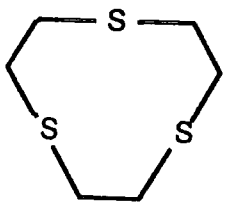

(97)

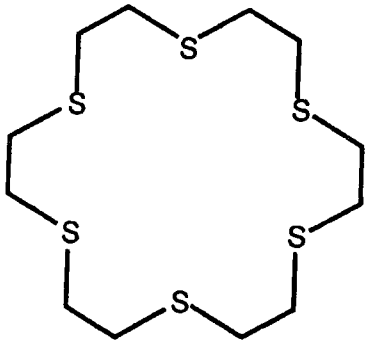

(98)

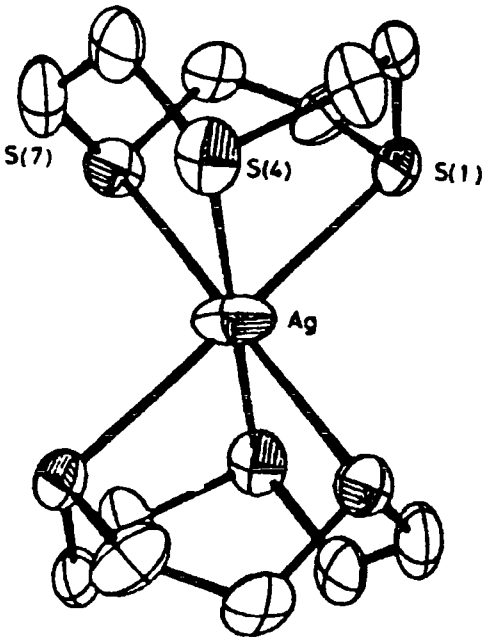

Fig. 4.12. X-ray crystal structure of the bis [9]-S_3-Ag(I) complex.

Trigonal elongation results in a distortion of the potentially octahedral coordination of the silver cation. Silver-sulphur bond lengths vary from 2.696 to 2.753Å. The elongation is illustrated by the silver-sulphur bond angles which are on average 80.0^{o} for S(1)-Ag-S(1) and 100^{o} for S(1)-Ag-S(2).

Weighardt[26] has reported a similar 2:1 silver complex of $[9]S_3$. He also isolated a crystalline solid which was found to be made up of two cations; the monomeric AgL_2^+ [as shown in Fig. 4.12] and a trimeric

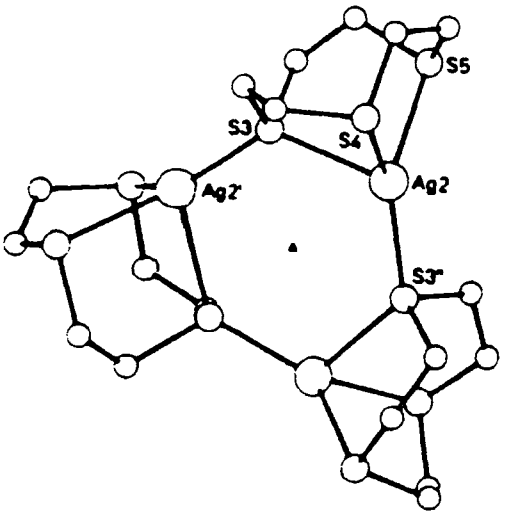

Fig. 4.13. X-ray crystal structure of $[Ag_3L_3]^{3+}$.

$[Ag_3L_3]^{3+}$ [Fig. 4.13]. In this case the silver adopts tetrahedral coordination with the apical site being occupied by a sulphur from an adjacent ligand. The six membered Ag_3S_3 ring is almost planar.

For the hexathia 18-crown-6 ligand (99) a simple 1:1 structure has not been observed, though recently a disilver picrate complex $[Ag_2(18S6)(pic)](pic)$[27] has been reported, Fig. 4.14.

Two distinct coordination geometries are observed for Ag(1) and Ag(2). The former has a distorted trigonal bipyramidal coordination, binding with three sulphurs from the ligand, one sulphur from an adjacent ligand and the picrate ion. Ag(2) has a distorted tetrahedral coordination with three sulphurs from the ligand (one of which is shared with an Ag(1) of an adjacent ligand) and one sulphur from an adjacent ligand resulting in polymeric chains of $[Ag_2(18S6)pic]^+$ cations. The

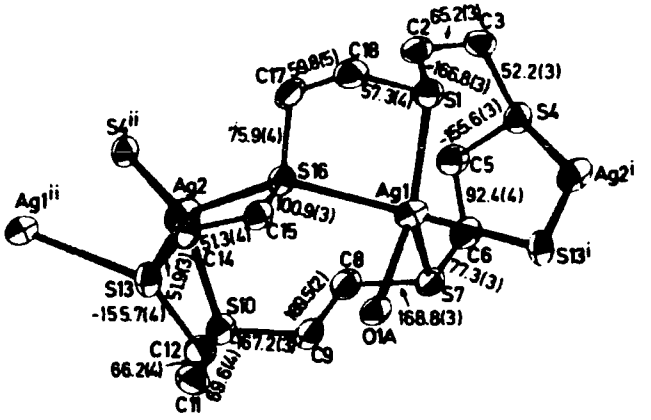

Fig. 4.14. X-ray crystal structure of $[Ag_2(18S6)(pic)](pic)$

18S6 ligand is obviously not well suited to the formation of a regular hexacoordinate complex with silver(I). The conformational effects of replacing oxygen donor atoms with sulphur donor atoms in crown ethers is discussed in section 4.1.5.

A bis 'sandwich' macrocyclic complex of silver(I) has been reported previously[28] with the crown ether 12-Crown-4, providing an example of an eight coordinated silver complex [Fig. 4.15].

In summary, a variety of coordination geometries have been reported for silver(I) macrocyclic complexes, but they are often irregular. For example, a regular octahedral coordination geometry has not been observed, the closest being in the bis $9[S]_3$ structure [Fig. 4.12].

4.3. Design of New Macrocycles to Bind Silver (I)

In designing new macrocyclic ligands to bind silver(I) our objectives were to obtain complexes of greater kinetic and thermodynamic stability. As the rate of complexation is an important feature with respect to applications for radioimmunotherapy, we initially considered relatively flexible monocyclic ligands.

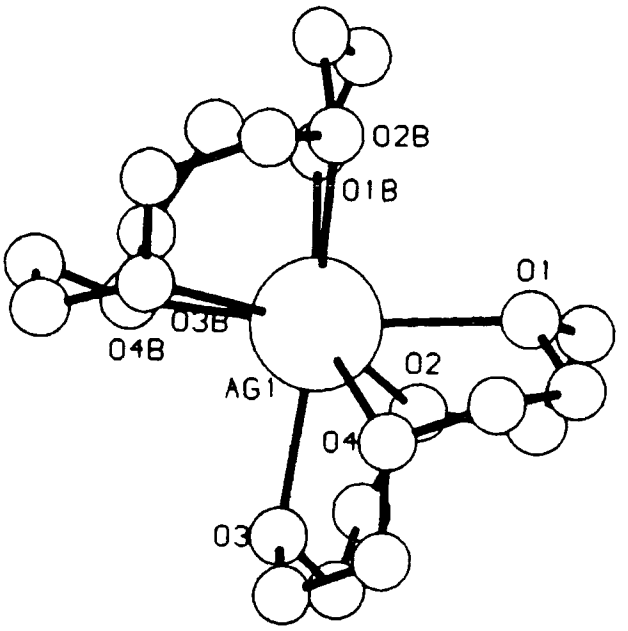

Fig. 4.15. X-ray structure of the Ag(I) complex of 12-Crown-4.

The main factors to consider were cavity size, the number and type of donor atoms and the likely coordination geometry that would result. Each of these factors have been discussed in previous sections and lead to the following conclusions;

(1) The 18-crown-6 cavity size is optimum for Ag(I).

(2) Six symmetrically placed donor atoms provide the best chance of obtaining a regular octahedrally coordinated complex.[29,30]

(3) Sulphur and nitrogen donor atoms are much preferred to oxygen donor atoms and mixed sulphur and nitrogen systems form the most stable complexes. Tertiary nitrogens are preferred over secondary nitrogens in terms of bond enthalpies i.e. NR > NH but intraannular steric interactions may also be important.

(4) In mixed sulphur and nitrogen 18-crown-6 systems a majority of sulphur atoms is more likely to lead to an unfavourable conformation of the free ligand than a majority of nitrogen atoms. The target molecules chosen for synthesis were the 18 membered N_4S_2

macrocycle 1,10-dithia-4,7,13,16-tetraazacyclooctadecane (100) and its N-methylated derivative, N,N',N",N"'-tetramethyl-1,10-dithia-4,7,13,16-tetraazacyclooctadecane (101).

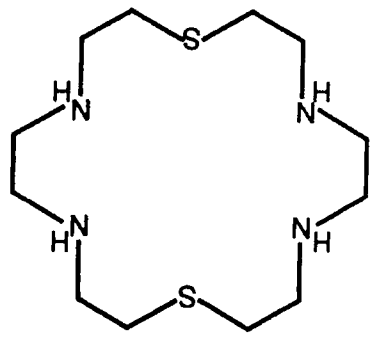

(100)

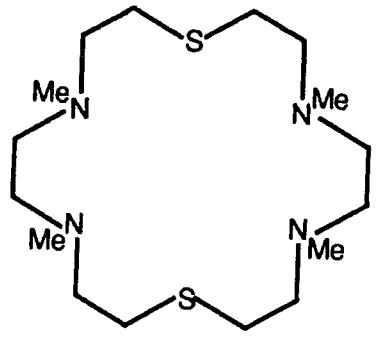

(101)

A third target molecule chosen for synthesis was the N,N'-ethylene bridged bis-(1,4-dithia-7-azacyclononane) ligand (102).

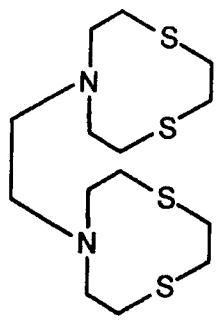

(102)

This ligand was designed as a means of providing an N_2S_4 donor set, in a potentially octahedral coordination, without encountering the unfavourable conformation effects that may be associated with the single ring analogue. The more rigid nine-membered rings are ideally set up for facial coordination to a metal centre. In addition, it was hypothesised that the flexibility about the N-N' linkage would facilitate rapid complexation. Similar N,N' bridged bis-macrocyclic

ligands have been reported, for example, the bis-[9]-N_3 ligand (103)[31,32] and the bis-[12]-NO_3 ligand (104).[33,34]

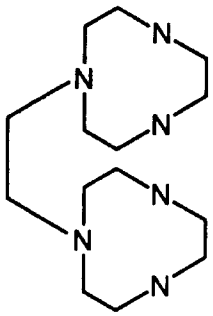

(103)

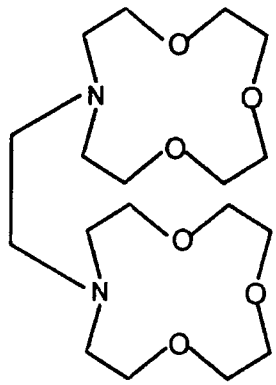

(104)

4.4. References

1. D. Parker and K.E. Matthes, Ch. 3 in "Stereochemical and Stereophysical Behaviour of Macrocycles", I. Bernal (ed.), Elsevier (1987).

2. a) R.G. Pearson, J. Am. Chem. Soc., 85, 3533 (1963).
   b) R.G. Pearson, J. Chem. Ed., 45, 581, 643 (1968).

3. H.K. Frensdorf, J. Am. Chem. Soc., 93, 600 (1971).

4. C.J. Pedersen, J. Org. Chem., 36, 254-7 (1971).

5. H.J. Buschmann, Inorg. Chim. Acta, 102, 95 (1985).

6. a) H.J. Buschmann, Chem. Ber., 118, 4297 (1985).
   b) H.J. Buschmann, Thermochim. Acta, 107, 219 (1986).

7. a) H.E. Simmons and C.H. Park, J. Am. Chem. Soc., 90, 2428 (1968).
   b) B. Dietrich, J.M. Lehn and J.P. Sauvage, Tetrahedron, 29, 1629 (1973).

8. M.L. Campbell and N.K. Dalley, Acta Cryst., B37, 1750 (1981).

9. C.J. Pedersen, R.M. Izatt and J.J. Christensen (eds.), "Synthetic Multidentate Macrocyclic Compounds", Academic Press, New York, 1978.

10. L.F. Lindoy, "Heavy Metal Chemistry of Mixed Donor Macrocyclic Ligands", Ch. 2 in Prog. Macrocyclic Chem., 53 (1987).

11. K.R. Adam, D. Baldwin, P.A. Duckworth, A.J. Leong, L.F. Lindoy, M. McPartlin and P.A. Tasker, J. Chem. Soc. Chem. Commun., 1124 (1987).

12. D.C. Liles, M. McPartlin and P.A. Tasker, J. Chem. Soc. Dalton Trans., 1631 (1987).

13. K.R. Adam, K.P. Dancey, B.A. Harrison, A.J. Leong, L.F. Lindoy, M. McPartlin and P.A. Tasker, J. Chem. Soc. Chem. Commun., 1351 (1983).

14. K.R. Adam, A.J. Leong, L.F. Lindoy, H.C. Lip, B.W. Skelton and A.H. White, J. Am. Chem. Soc., 105, 4645 (1983).

15. K.R. Adam, L.G. Brigden, K. Henrick, L.F. Lindoy, M. McPartlin, B. Minnagh and P.A. Tasker, J. Chem. Soc. Chem. Commun., 710 (1985).

16. L.F. Lindoy, results reported at the 13th Int. Symp. on Macrocyclic Chemistry, Hamburg (1988).

17. H.J. Buschmann, Ch. 2 in "Stereochemical and Stereophysical Behaviour of Macrocycles", I. Bernal (ed.), Elsevier (1987).

18. R.E. Wolf, J.R. Hartman, J.M.E. Storey, B.M. Foxman and S.R. Cooper, J. Am. Chem. Soc., 109, 4328 (1987).

19. R.E. DeSimone and M.D. Glick, J. Am. Chem. Soc., 97, 942 (1975); idem ibid., 98, 762 (1976).

20. R. Louis, D. Pelissard and R. Weiss, Acta Cryst. B32, 1480 (1976).

21. R. Louis, Y. Agnus and R. Weiss, Acta Cryst., B33, 1418 (1977).

22. G. Ferguson, R. McCrindle and M. Parvez, Acta Cryst., C40, 354 (1984).

23. M.G.B. Drew, C. Cairns, S.G. McFall and S.M. Nelson, J. Chem. Soc. Dalton Trans., 2020 (1980).

24. M.G.B. Drew, D.A. Rice, S.B. Silong, Acta Cryst., C40, 2014 (1984).

25. J. Clarkson, R. Yagbasan, P.J. Blower, S.C. Raule and S.R. Cooper, J. Chem. Soc. Chem. Commun., 950 (1987).

26. H-J. Kupper, K. Wieghardt, Y-H. Tsay, C. Kruger, B. Nuber and J. Weiss, Angew. Chem. Int. Ed. Eng., 26(16), 575 (1987).

27. N. Galesic, M. Herceg and D. Sevdic, Acta Cryst., C44, 1405 (1988).

28. P.G. Jones, T. Gries, H. Grutzmacher, H.W. Roesky, J. Schimkowiak and G.M. Sheldrick, Angew. Chem. Int. Ed. Eng., 23(5), 376 (1984).

29. L. Lindoy and D.H. Busch, J. Am. Chem. Soc., 91, 4690 (1969).

30. D.St.C. Black and I.A. McLean, J. Chem. Soc. Chem. Commun., 1004 (1968).

31. N. Tamaka, Y. Kobayashi and S. Takamoto, Chem. Lett., 107 (1977).

32. K. Wieghardt, I. Tolksdorf and W. Herrman, Inorg. Chem., 24, 1230 (1985).

33. J.E. Bulkowski, P.C. Burk, M-F. Ludman and J.A. Osborn, J. Chem. Soc. Chem. Commun., 498 (1977).

34. a) M.J. Calverly and J. Dale, J. Chem. Soc. Chem. Commun., 684 (1981); idem. ibid., 1084 (1981).
b) T. Alfheim, J. Dale, P. Groth and K.D. Krautwurst, J. Chem. Soc. Chem. Commun., 1502 (1984).

35. F. Arnaud-Neu, M.J. Schwing-Weill, R. Louis and R. Weiss, Inorg. Chem., 18, 2956 (1979).

CHAPTER FIVE

SYNTHESIS AND PROPERTIES OF SILVER(I) MACROCYCLIC COMPLEXES

5.1. Synthesis of Macrocycles to Bind Silver(I)

5.1.1. 1,10-dithia-4,7,13,16-tetraazacyclooctadecane (100)

Several attempts to synthesise the [18]-N_4S_2 macrocycle (100) were made before a successful route was developed. Initially, a short synthetic route to the basic cycle (R = H, (100)) was sought, such that the silver(I) complexation chemistry of the ligand could be investigated. However, a stepwise synthesis of the ligand which would

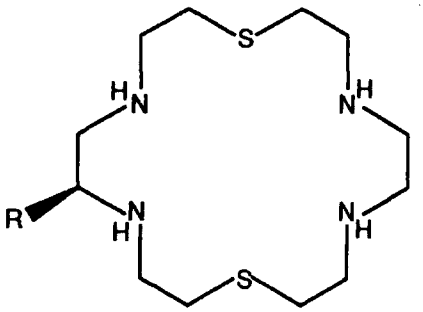

R = H (100)

R = $-(CH_2)_nNH_2$ (105)

R = p-$CH_2C_6H_4(CH_2)_nNH_2$ (106)

enable the C-functionalisation of the ligand (e.g. R = $(CH_2)_nNH_2$ or p-$CH_2C_6H_4(CH_2)_nNH_2$) at a later stage was also required.

Many mixed polyoxapolyaza and polythiapolyaza macrocycles have been synthesised by the so-called "high dilution" technique (high dilution encourages intramolecular reaction over intermolecular reaction). In particular, the "high dilution" condensation of acid dichlorides with diamines to yield macrocyclic and macrobicyclic ligands has been used extensively by Lehn and co-workers.[1-8] For example, the 12-membered N_2S_2 macrocycle and the 15-membered N_2S_2O and N_2S_3 macrocycles were synthesised by this method [Fig. 5.1]. The macrocyclic amides thus produced were reduced to the corresponding amines using BH_3.THF. The 18-membered N_2S_4 macrocycle (107) was also synthesised by this method, though a previous preparation of the ligand, reported by Black and McClean,[10] involved the high dilution reaction of ethane-1,2-diol and di(2-bromoethyl)amine (8% yield) [Fig. 5.2].

Initially, the synthesis of the [18]-N_4S_2 macrocycle (100) was

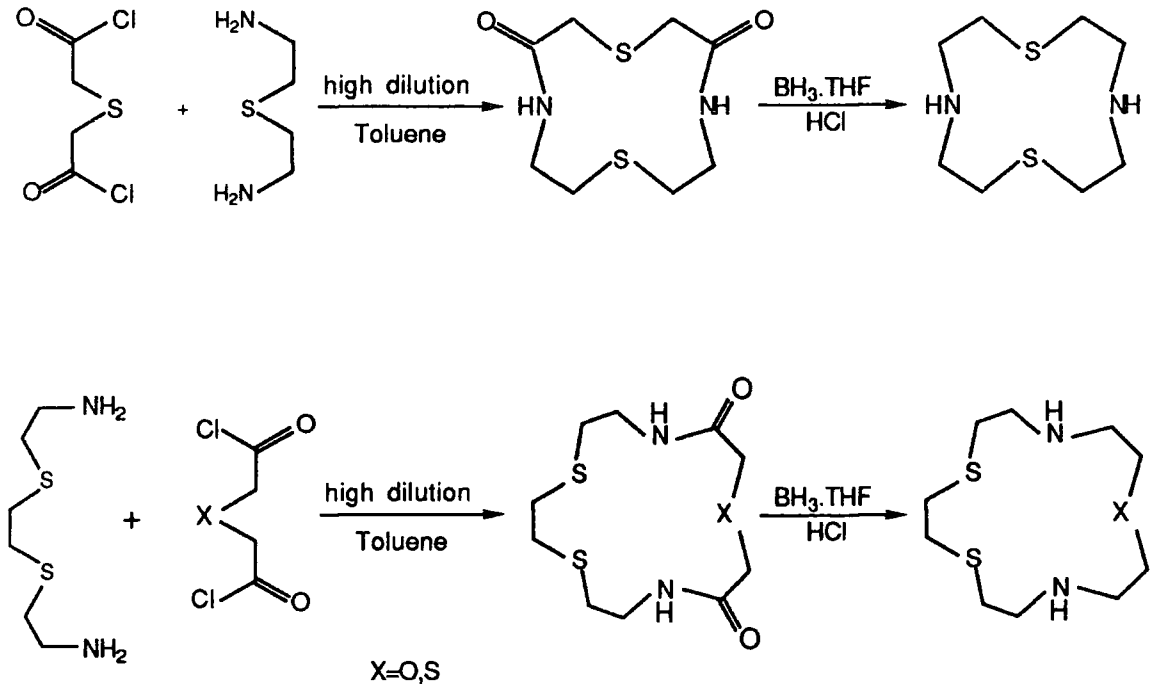

Fig. 5.1. Synthesis of macrocyclic ligands using the "high-dilution" reaction of acid-dichlorides and diamines.

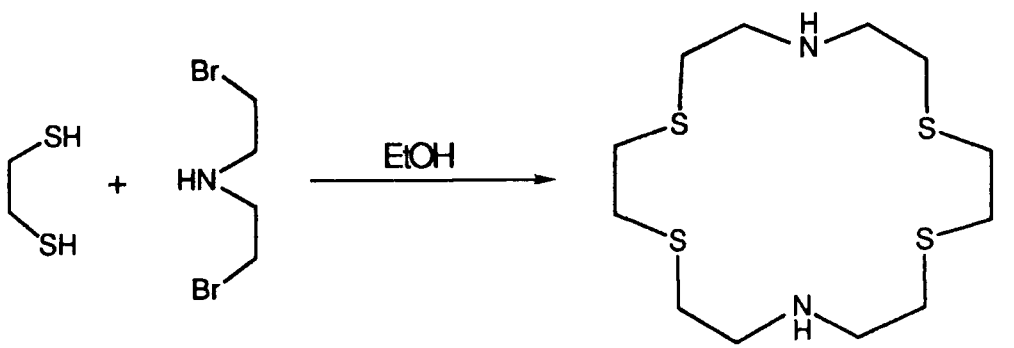

(107)

Fig. 5.2. Synthesis of [18]-N_2S_4 (107).

attempted using two 'short' routes, involving 'one-pot' co-cyclisation reactions (in which two molecules of each starting reagent were required to form the [18]-ring). The first of these involved the reaction of the diethyl ester of thiodiglycollic acid (108) with ethylenediamine, under

high dilution conditions, in ethanol [Scheme 5.1].

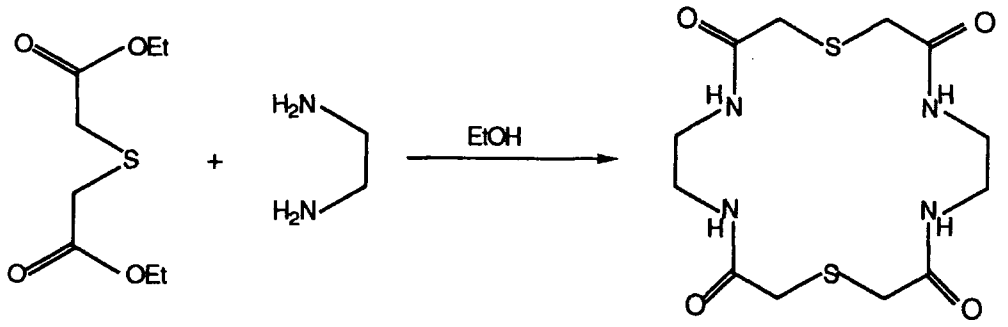

(108) (109)

Scheme 5.1

The diester (108), synthesised from thiodiglycollic acid ($EtOH/H_2SO_4$/reflux 3 hr.), was used as an alternative reagent to the highly toxic mustard gas derivative, $S(CH_2COCl)_2$. The reaction failed to afford an appreciable yield of the cyclic tetraamide (109), giving predominantly a mixture of oligomeric products.

An alternative "one-pot" reaction was attempted using the tosylamide ring closure method of Richman and Atkins[11] [Scheme 5.2]. Ethylenediamine ditosylamide (110) and thiodiethanol ditosylate (111) were prepared using standard tosylation techniques (pyridine/TsCl/0^oC). Treatment of (110) with sodium in ethanol gave the disodium salt (112),

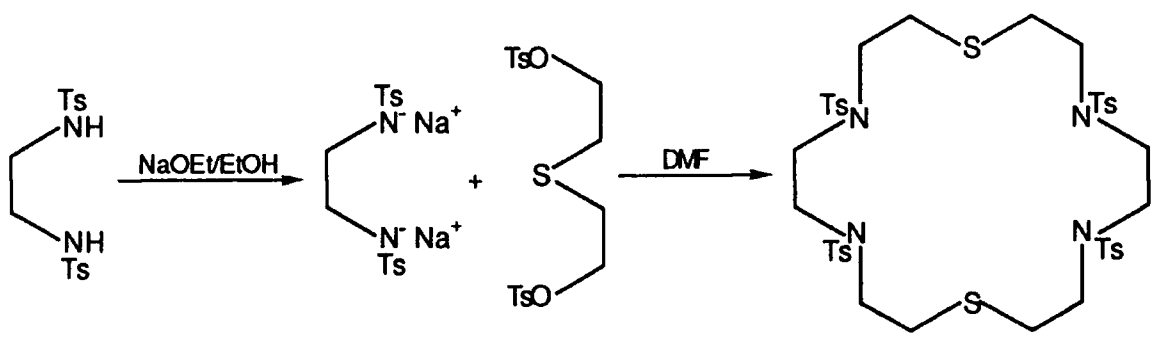

(110) (112) (111) (113)

Scheme 5.2

which was reacted with an equimolar quantity of the 1,5-ditosylate (111) ($110^{o}C$, 24 hr.). Again a mixture of oligomers was obtained, with no evidence (^{1}H nmr, mass spectrometry) of any cyclised product (either [18]- or [9]-membered rings).

The [18]-N_4S_2 macrocycle (100) was eventually prepared by a seven step synthetic route, Scheme 5.3. Thiodiglycollic anhydride (114) was prepared by treatment of thiodiglycollic acid with acetylchloride (heated under reflux for 18 hours) and purified by recrystallisation from chloroform. The di-carboxylic acid (115) was prepared by dropwise addition of ethylenediamine to a solution of the anhydride (114) (2 equivalents) in dichloromethane. The exothermic reaction resulted in the immediate precipitation of a resinous white solid. The crude diacid (115) was collected by filtration and washed with dichloromethane. Conversion to the diester (116) was effected by heating under reflux in ethanol with 1% sulphuric acid. A large volume of solvent was required, with heating under reflux for 48-60 hours, in order to consume the insoluble starting material. The cooled reaction mixture yielded the diethyl ester of thiodiglycollic acid (the product of a competitive amide cleavage reaction) as a white crystalline solid (ca. 50% yield). The required diester (116) was obtained in overall 27% yield (2 steps) after extraction into chloroform from basic aqueous solution, followed by recrystallisation from toluene. Although the yield of (116) was rather poor due to the competitive amide cleavage, sufficient quantities (20 g) of the required product were obtained to continue with the synthetic route.

Reaction of the diester (116) with ethylenediamine in ethanol, heated under reflux (120 hr.) failed to give the cyclic tetraamide (109). The major component, by thin layer chromatography, was the

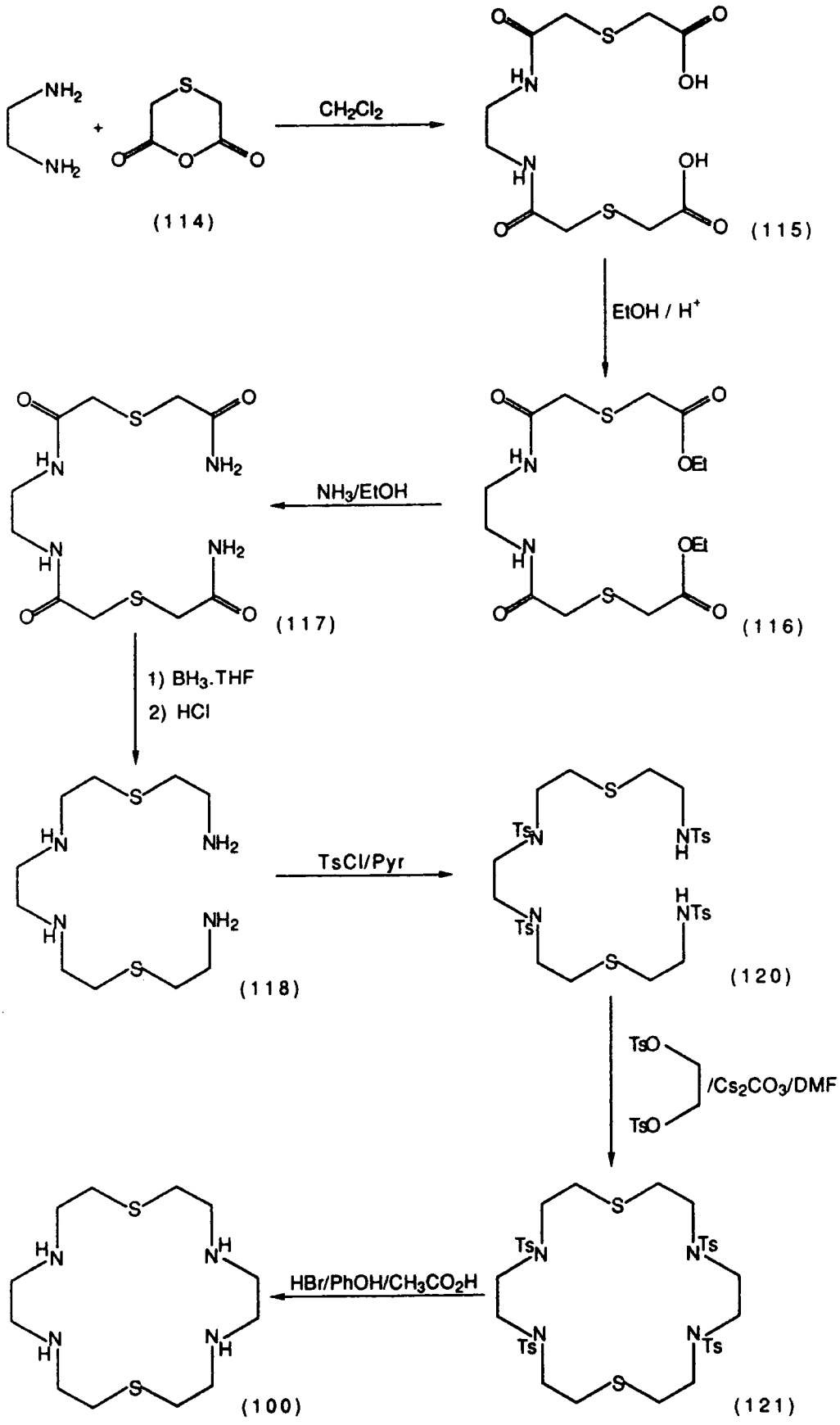

Scheme 5.3. Synthesis of [18]-N_4S_2 (100).

unreacted starting material (116).

The diester was converted to the corresponding tetraamide (117) by treatment with ethanol, saturated with ammonia (60 hr.), in a tightly stoppered vessel. The product was collected by filtration as a white solid (75%). Reduction of the tetraamide to the tetraamine (118) was effected using an excess (4 eq. per amide group) of borane.THF complex (1.0M) in THF, with heating under reflux for 60 hours. Treatment of the resulting amino-borane compound with hydrochloric acid (6 Molar/110^{o}C/3 hr.) followed by extraction into chloroform from basic aqueous solution, gave the tetraamine as a clear oil (71%). Thin film IR revealed that all four amide groups had been reduced and ^{1}H and ^{13}C nmr (Fig. 5.3) confirmed that the product did not require further purification. The synthesis of the [19]-membered N_4S_2 macrocycle (119) (Scheme 5.4) was

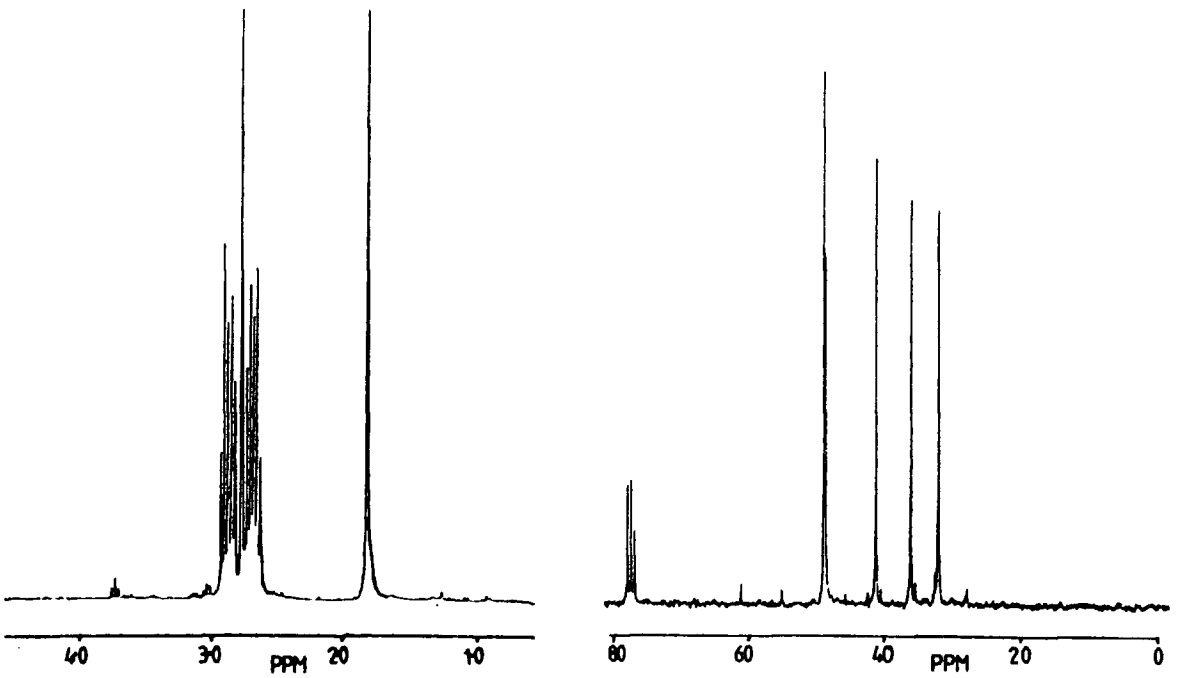

Fig. 5.3. ^{1}H and ^{13}C nmr of the tetraamine (118).

attempted by reaction of the tetraamine (118) with diethylmalonate in ethanol (120 hr.), according to the method reported by Tabushi et al.[12] for the synthesis of cyclam (the use of substituted diethylmalonates

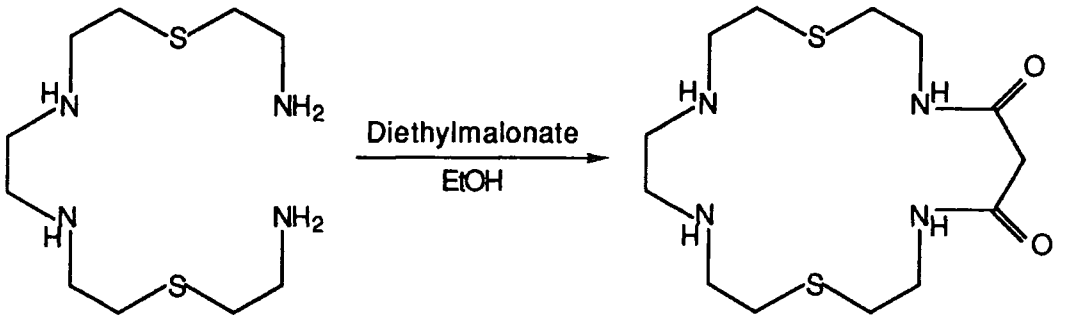

(118) (119)

Scheme 5.4

provided a convenient synthesis of C-functionalised cyclams). The failure to obtain any of the required product in this reaction was a further indication of the reluctance of the N_4S_2 system to undergo intramolecular cyclisation.

The tetraamine (118) was converted to the tetratosylamide (120) by reaction with tosyl chloride in pyridine, at 0^oC, under anhydrous conditions. The product was purified by recrystallisation from MeOH-$CHCl_3$ to give a pale brown solid (56%). Cyclisation was affected by the reaction of the tetratosylamide (120) with ethylene glycol ditosylate in DMF in the presence of caesium carbonate. The use of caesium carbonate as the preferred base for the promotion of ring closure reactions, in particular for long chain ditosylamides, has been reported by Kellogg et al.[13,14] The cyclic tetratosylamide (121) was isolated as a fine cream coloured solid from hot toluene (62%).

Detosylation was effected by two different methods. Treatment of the tetratosylamide with HBr/Phenol/acetic acid (80^oC, 10 days) gave the [18]-N_4S_2 macrocycle in 32% yield. The product was isolated from the cooled reaction mixture as the HBr salt, and obtained as the free amine after basification in aqueous solution (NaOH) followed by extraction

into the chloroform. The product was recrystallised from toluene to give a white solid. Detosylation of (121) using $Li/NH_3/THF/EtOH$ led to an improved yield of the amine (64%) after recrystallisation from toluene. In the ^1H nmr ($CDCl_3$) of the macrocyclic tetraamine (100) [Fig. 5.4] the N-CH_2CH_2-N protons gave a singlet at 2.76 ppm and the remaining CH_2S and CH_2N protons resonated as an A_2B_2M system centred at 2.81 ppm. [In D_2O the CH_2S and CH_2N protons resonated as triplets at 3.01 and 2.84 ppm with the N-CH_2CH_2-N singlet at 2.91 ppm.]

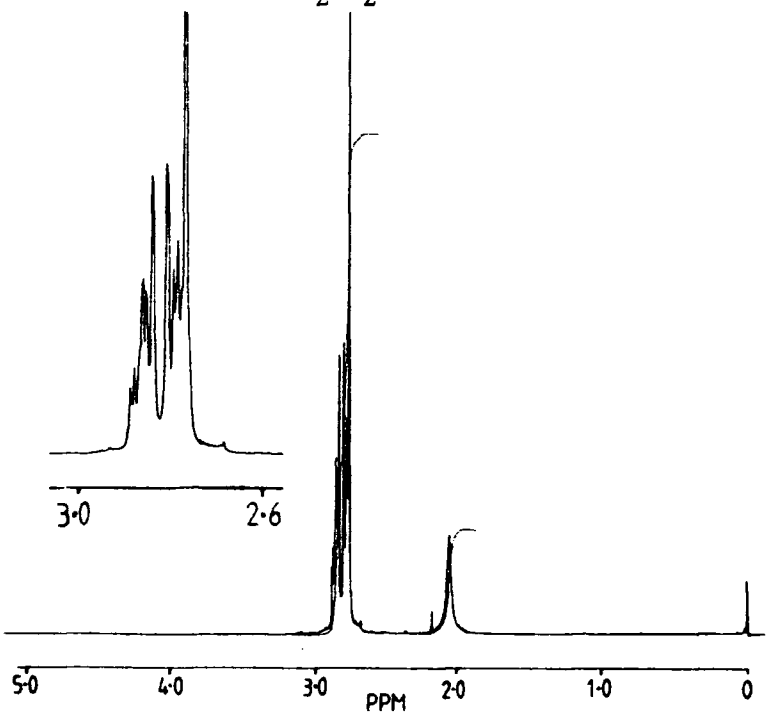

Fig. 5.4. ^1H nmr ($CDCl_3$) of the macrocycle (100).

5.1.2. N,N',N",N"'-tetramethyl-1,10-dithia-4,7,13,16-tetraazacyclooctadecane (101)

The [18]-N_4S_2 macrocycle was converted to its tetramethyl derivative (122) [Scheme 5.5] using the Eschweiler-Clarke methylation procedure. The tetraamine (100) was treated with an equimolar ratio of formaldehyde (37%) and formic acid (95°C, 20 hr.). Recrystallisation from hexane gave the macrocycle (101) as a white solid (55%). The ^1H

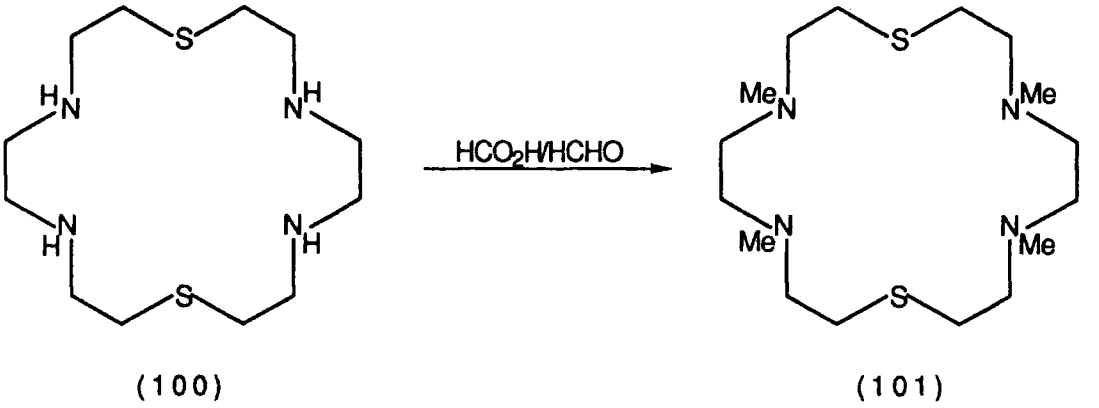

(100) (101)

Scheme 5.5. Synthesis of [18]-$N_4S_2Me_4$ (101).

and ^{13}C nmr were simple (Fig. 5.5), consistent with time averaged C_{2v} symmetry of the ligand. In contrast to the non-methylated cycle (100), the constitutionally heterotopic 'N-CH_2CH_2-S' protons were accidentally isochronous giving a singlet at 2.64 ppm in the ^1H nmr spectrum ($CDCl_3$).

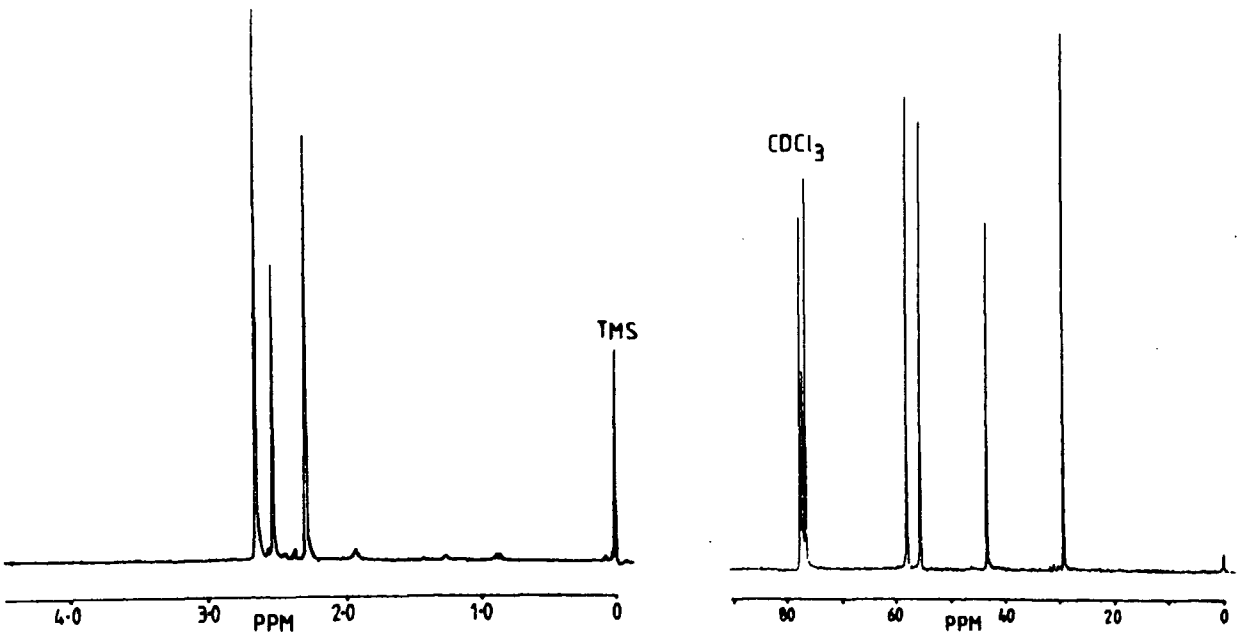

Fig. 5.5. ^1H and ^{13}C nmr ($CDCl_3$) of (101).

5.1.3. 1,2-Bis(1-aza-4,7-dithia-1-cyclononyl)ethane (102)

The N,N'-ethylene bridged [9]-NS_2 ligand (102) was synthesised by a

five step synthetic route starting from diethanolamine [Scheme 5.6]. The synthesis of the [9]-NS_2 macrocycle (126) (precursor to the N,N' linked system) has not previously been reported and completes the [9]-X_3 series (X = O, N, S).[15]

Treatment of diethanolamine with tosylchloride (pyridine/0^{o}C) afforded the tosylated product (123) which was purified by recrystallisation from ethanol-toluene (yield, 84%). The dithiol (124) was prepared using a method similar to that reported by Rosen and Busch[16] for the synthesis of 1,10-dithiols, as precursors to tetrathia macrocycles. The ditosylate (123) was treated with thiourea in ethanol to generate the isothiouronium salt, which was hydrolysed by heating

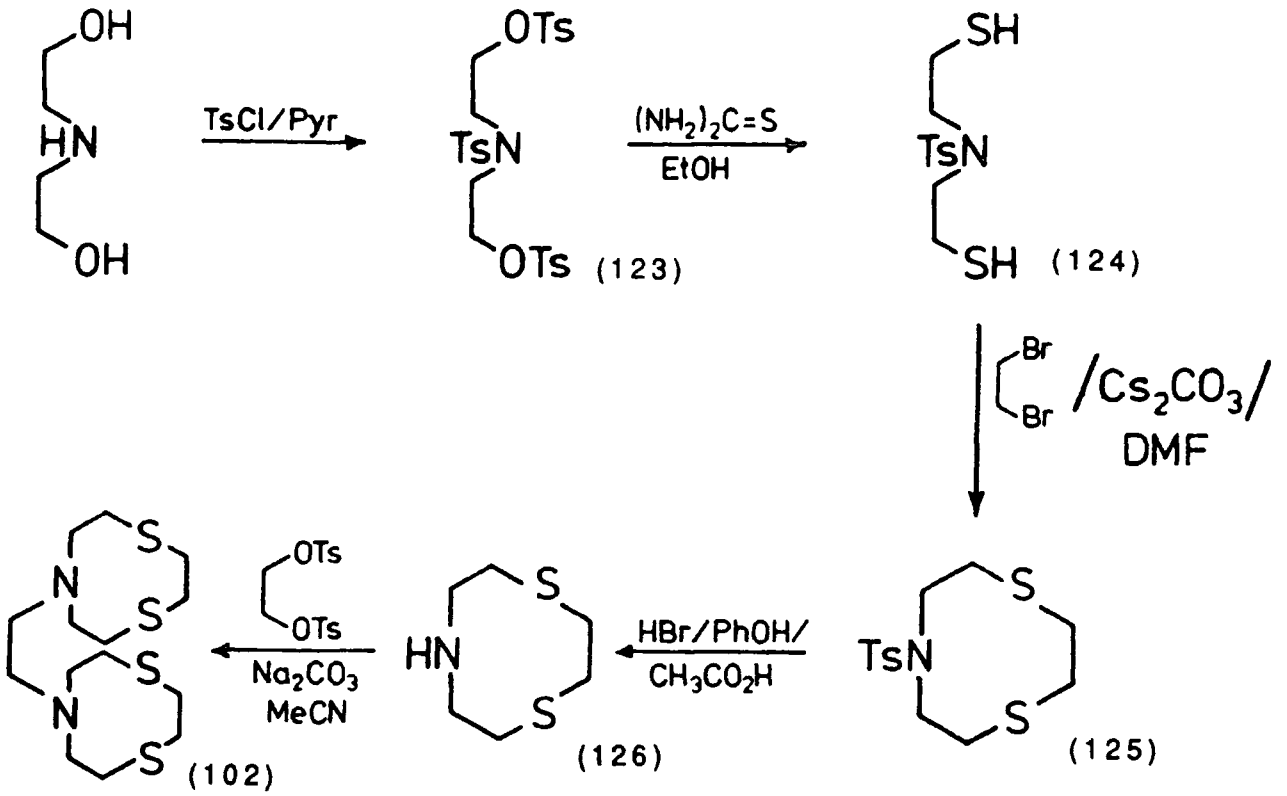

Scheme 5.6. Synthesis of N,N'-bridged [9]-NS_2 (102).

under reflux in saturated $NaHCO_3$ solution. Extraction from neutral aqueous solution gave a clear oil which was found to be a mixture of the required dithiol (124) and some monothiolated product (ca. 10% by ^1H nmr). The dithiol was obtained as a white solid (83%) after purification by "flash" silica chromatography. Ring closure to give the cyclic ditosylamide (125) was effected by the slow dropwise addition (12 hours) of solutions of the dithiol (124) and 1,2-dibromoethane in DMF to a well stirred suspension of caesium carbonate in DMF at 55°C. The preparation of cyclic thioethers by reaction of dithiols with dibromides has been well documented.[16,17] Kellogg[18] reported that the reaction was particularly efficient with the use of caesium carbonate in DMF. He originally postulated that the poor solvation of the large Cs^+ ion led to the formation of tight ion pairs ($RS^- Cs^+$) which encouraged intramolecular S_N2 reaction (Fig. 5.6). However, later studies,[14] using

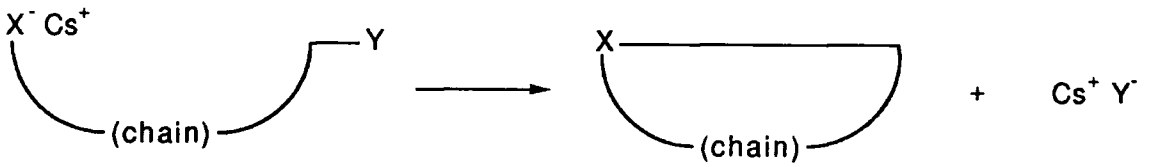

Fig. 5.6. Intramolecular S_N2 cyclisation reaction.

^{133}Cs nmr, revealed that the caesium salts (e.g. thiolates, carboxylates and amides) did not exist as tight ion pairs in DMF and in fact their greater solubility compared to other group I salts (Cs > Rb > K > Na) was contributing towards the enhancement of the intramolecular S_N2 reaction.

The reaction of the dithiol (124) with 1,2-dibromoethane was found to yield both the nine-membered ring (43%) and the eighteeen-membered

ring (128) (10%) [Scheme 5.7]. The two products were isolated as white crystalline solids by fractional crystallisation from toluene-hexane, the larger ring being the least soluble. Treatment of (125) with $HBr/PhOH/CH_3CO_2H$ (80^oC, 48 hr.) gave the detosylated product, 1,4-dithia-7-azacyclononane (126) in good yield (73%) after recrystallisation from toluene-hexane. Detosylation of the 18-membered ditosylamide (128) was effected in a similar manner, to give the [18]-N_2S_4 macrocycle (107) in 30% yield, after recrystallisation from

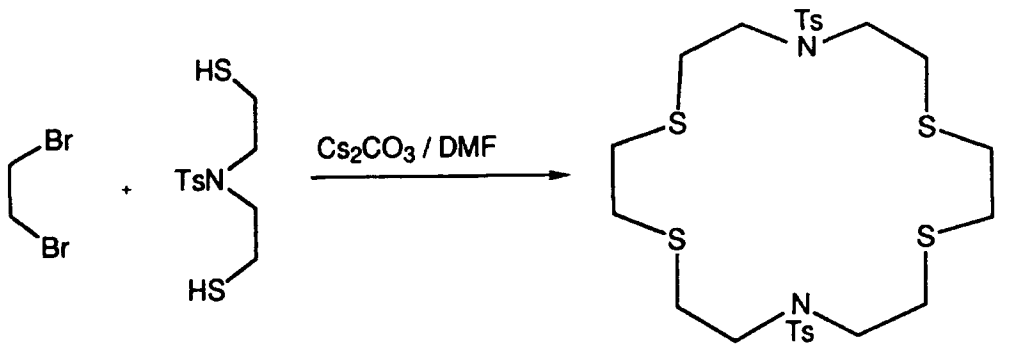

Scheme 5.7. Synthesis of the 18-membered ring (128).

chloroform-hexane. This provides a useful alternative synthesis of the [18]-N_2S_4 macrocycle which avoids the use of the highly toxic acid-dichlorides, as reported by Lehn et al.[7] The N,N'-bridged bis [9]-NS_2 ligand (102) was prepared by the reaction of 2 equivalents of the macrocyclic amine (126) with ethyleneglycol ditosylate (Na_2CO_3/MeCN) followed by recrystallisation from toluene (yield, 53%). In the ^1H nmr of the ligand (102) the N-CH_2CH_2-N and S-CH_2CH_2-S protons resonated as singlets (2.62 and 3.09 ppm respectively) and the remaining methylene ring protons resonated as a second order multiplet centred at 2.80 ppm. Two 'CH_2N' signals (58.7 and 55.6 ppm) and two 'CH_2S' signals (34.8, 33.1) were observed in the ^{13}C nmr (Fig. 5.7) consistent with the time averaged C_2-symmetry of the ligand.

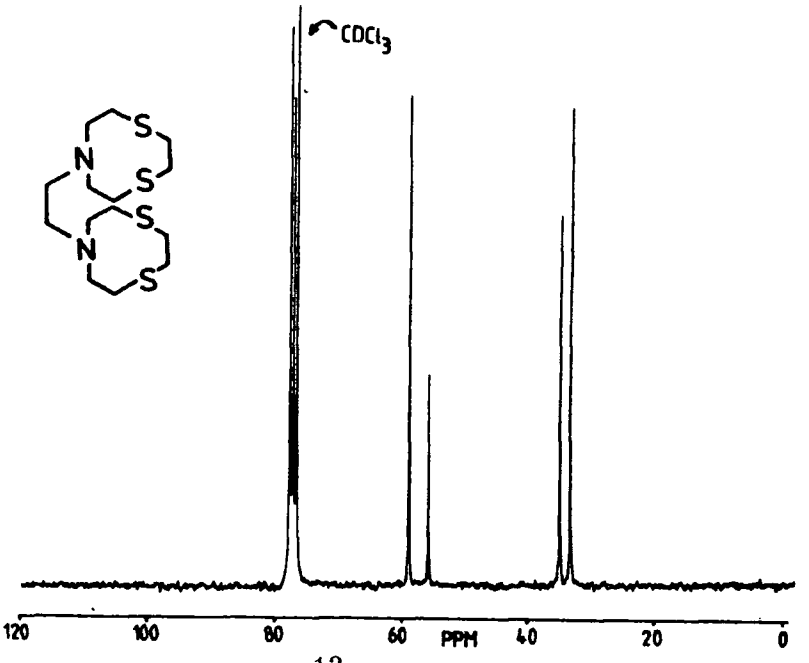

Fig. 5.7. ^{13}C nmr of ligand (127).

5.1.4. <u>1,10-dioxa-4,7,13,16-tetraazacyclooctadecane (131) and its tetramethyl derivative (132)</u>

In order to complete thermodynamic studies on the silver(I) complexes of mixed donor eighteen-membered macrocyclic ligands, the [18]-N_4O_2 macrocycle (131)[19] and its tetramethyl derivative (132) were synthesised [Scheme 5.8]. Reaction of ethylenediamine ditosylamide with 3-oxa-1,5-bis(p-toluensulphonato)pentane (Cs_2CO_3/DMF) gave a mixture of the nine and eighteen-membered ring products (41% and 20% respectively). Earlier experiments, which had been carried out at higher dilution, favoured the formation of the nine-membered ring (130). Detosylation was effected using HBr/PhOH/CH_3CO_2H followed by recrystallisation from chloroform-hexane, to give the [18]-N_4O_2 cycle as a colourless crystalline solid (yield, 25%). The tetramethyl derivative (132) was prepared using the Eschweiler-Clarke process, as for the [18]-N_4S_2 ligand.

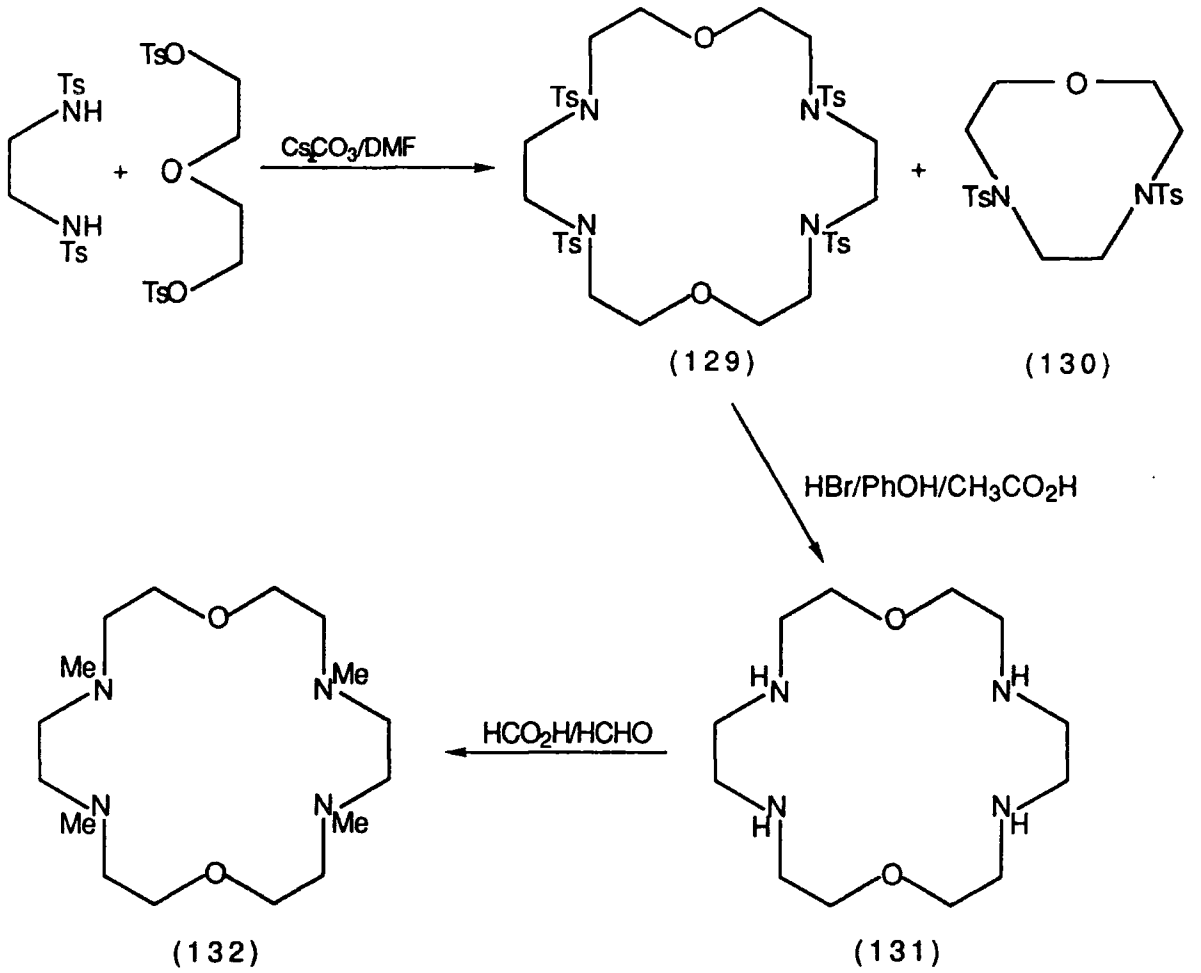

Scheme 5.8. Synthesis of the 18-membered N_4O_2 ligands (131) and (132).

5.2. Silver(I) Complexes

5.2.1. Silver(I) complex of [18]-N_4S_2 (100)

The 1:1 silver(I) complex of ligand (100) was prepared by the addition of one equivalent of silver nitrate, in acetonitrile, to a solution of the ligand in dichloromethane, at room temperature. Attempts to isolate a crystalline product from this reaction mixture were not successful. A solution of the crude complex in methanol was treated with a solution of ammonium hexafluorophosphate (1 eq.) in

methanol, in order to exchange the nitrate anion for the hexafluorophosphate counter ion. Colourless crystals of [Ag-L][PF_6] (134) were obtained after the solution was left to stand in the dark, at -20^{o}C, for 36 hours. The complex was initially characterised by Fast Atom Bombardment (FAB) mass spectrometry and ^{1}H nmr. Molecular ions (M^{+}) of approximately equal intensity were observed at m/e 399 and 401, consistent with complexes of the two isotopes of silver ($^{107}Ag^{+}$-L and $^{109}Ag^{+}$-L). Molecular ions corresponding to silver-ligand complexes of other stoichiometry (1:2 or 2:1) were not observed. The ^{1}H nmr (CD_3OD) gave a simple spectrum consistent with local C_2 symmetry for the complex, with all 6 donor atoms binding the silver. The N-CH_2CH_2-N protons gave a sharp singlet at 2.79 ppm and the adjacent CH_2S and CH_2N protons were accidentally isochronous, giving a singlet at 2.99 ppm. A similar spectrum was observed in D_2O.

By slow recrystallisation of the complex (over 72 hr.) in methanol, in the dark (dust free conditions) crystals suitable for X-ray diffraction studies were obtained. The molecular structure is illustrated in Fig. 5.8 with salient bond lengths and bond angles given in Table 5.1. The cationic silver complex (and the PF_6^- anion) possess

Table 5.1.

Selected bond lengths (Å) and bond angles (deg) for [Ag-L][PF_6], L = [18]-N_4S_2

Ag(1)-S(1)	2.658(5)	Ag(1)-N(1)	2.589(10)
Ag(1)-N(2)	2.553(11)		
S(1)-Ag(1)-N(1)	75.9(3)	S(1)-Ag(1)-N(2)	113.2(3)
N(1)-Ag(1)-N(2)	70.6(4)	S(1)-Ag(1)-S(1')	124.5(2)
S(1)-Ag(1)-N(1')	144.7	N(1)-Ag(1)-N(1')	104.3(4)
S(1)-Ag(1)-N(2')	74.6	N(1)-Ag(1)-N(2')	99.5(4)
N(2)-Ag(1)-N(2')	164.3		

Ag-L , L=

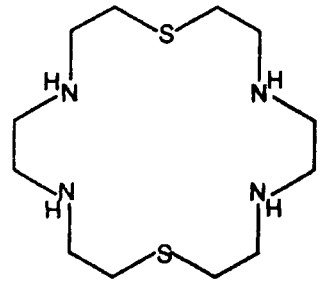

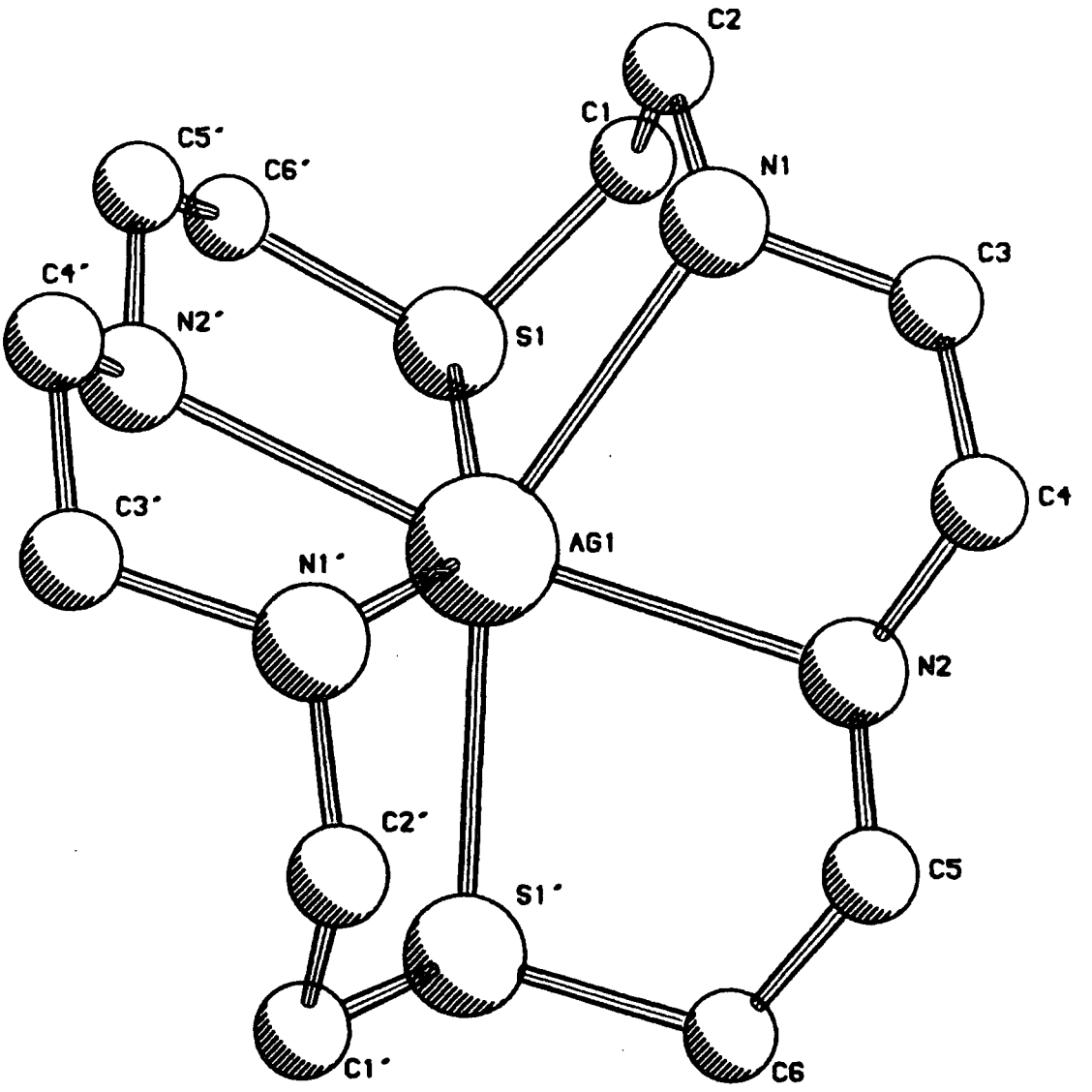

Fig. 5.8. X-ray crystal structure of the silver(I) complex of [18]-N_4S_2 (100).

crystallographically imposed C_2-symmetry. Only the central atom actually lies on the symmetry axis. The silver(I) ion is six coordinated by the full S_2N_4 donor set of the macrocycle. However, the geometry is far from octahedral with the most nearly 'trans' pair of

ligands being the symmetry-related secondary amine nitrogen atoms, N(2) and N(2') (N(2)-Ag-N(2'), 164.3°). If these donor atoms are considered as occupying the axial sites, S(1) and N(1') are displaced below the equatorial plane by 0.684 and 0.823Å respectively, with their C_2 symmetry related counterparts equally displaced above the plane.

Alternatively, the macrocycle can be viewed as providing two meridional, tridentate fragments comprising N(1), N(2) and S(1') (r.m.s. deviation of $AgSN_2$ plane, 0.060Å) which is inclined at 70° to its symmetry related equivalent, comprising atoms N(1'), N(2') and S(1). The silver-sulphur bond length [2.658(5)Å] compares favourably to those found for other silver(I)-macrocycle complexes. For example, bond lengths range from; 2.70-2.75Å in the bis-$9S_3$-Ag(1) complex reported by Cooper et al;[20] from 2.67-3.00Å in the [15]N_2S_2O-Ag(1) and [15]S_2N_2O-Ag(1) complexes[21] and from 2.65-2.95Å in the irregular [18]-PyN_2S_3-Ag(1) complex[22] [see section 4.2. for descriptions of these structures].

Both independent Ag-N distances are similar (2.553(11) and 2.589(10), those for the 'trans' pair are just 0.03Å shorter) and are within the range observed for the mixed sulphur nitrogen donor macrocyclic complexes just mentioned [2.40-2.61Å]. Surprisingly none of the secondary amines participate in any hydrogen bonding. Although the complex does not possess an octahedral coordination geometry as originally hypothesised, the silver ion is well encapsulated within the macrocyclic cavity forming relatively strong interactions with all six donor atoms, giving a complex with overall C_2 symmetry.

The rate of complexation of the [18]-N_4S_2 macrocycle with silver(I) was monitored by ^1H nmr in D_2O buffered at pD = 5 ($CD_3CO_2^-Na^+/CD_3CO_2D$) at 23°C. One equivalent of silver nitrate was added to the solution of the ligand [10^{-2} molar] and the proton nmr recorded immediately. The characteristic spectrum of the 1:1 silver complex (two singlets 2.79 and

2.99 ppm) was observed, with no sign of any free ligand. It was concluded that complexation was complete (≥ 95%) within the three minutes required to obtain the nmr spectrum.

5.2.2. Silver(I) complex of [18]-$N_4S_2Me_4$ (101)

The silver(I) complex of the ligand (101) was prepared, as the hexafluorophosphate salt [Ag-L][PF_6] (135), as described for the parent [18]-N_4S_2 ligand.

Initially, brown coloured crystals were obtained but subsequent recrystallisations from methanol yielded colourless crystals. However, crystals suitable for X-ray diffraction studies were not obtained. The complex was characterised by ^1H nmr (CD_3OD) [Fig. 5.9 - ^1H nmr of the silver complex is compared to that of the free ligand] and FAB mass spectrometry (molecular ions (M^+) at m/e 455 and 457). The ^1H nmr spectrum revealed that the 'CH_2S' protons, which resonated as a singlet (2.76 ppm) in the free ligand (CH_2N and CH_2S accidentally isochronous)

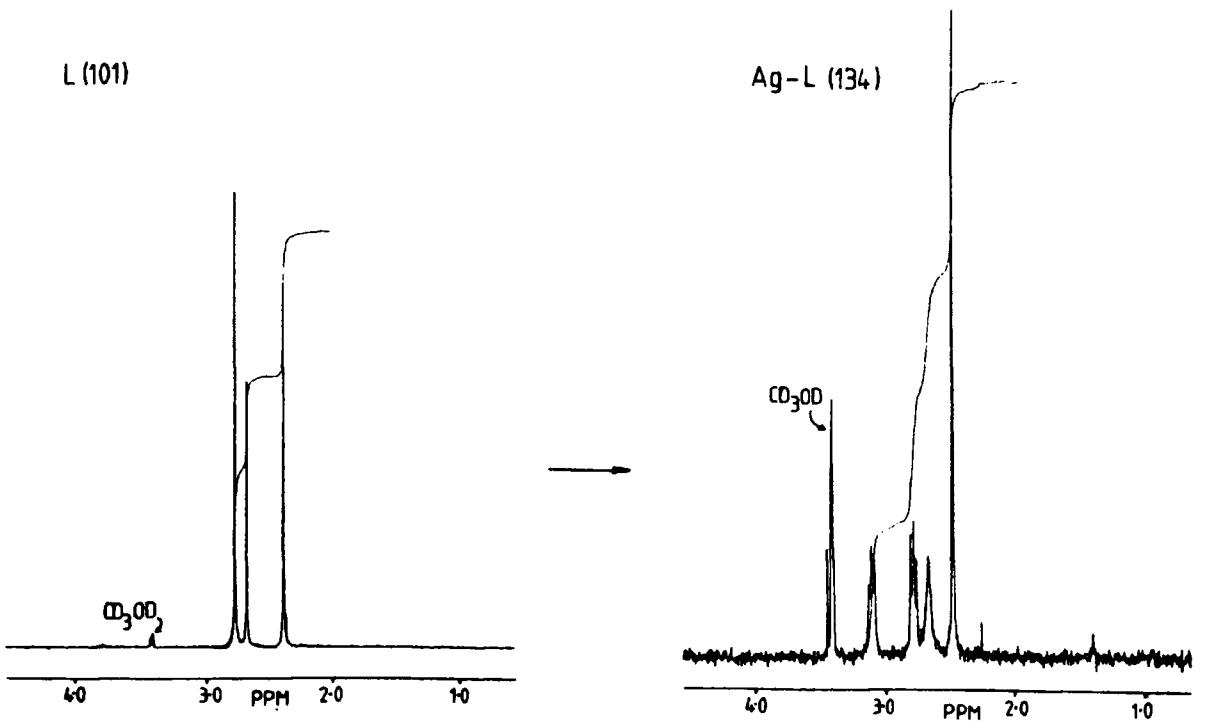

Fig. 5.9. ^1H nmr spectra (CD_3OD) of ligand (101) and its silver(I) complex (134).

were shifted to higher frequency (3.05 ppm, triplet) in the complex.

The rate of complexation was observed by ^1H nmr in D_2O at pD 5.5 (CD_3CO_2D/CD_3CO_2Na) at 23°C ($10^{-2}M$ in ligand). As noted for the [18]-N_4S_2 ligand, complexation was observed to be complete ($\geq$ 95%) within three minutes.

5.2.3. Silver(I) complex of bis N,N'-bridged [9]-NS_2 (102)

Reaction of equimolar quantities of silver nitrate and ligand (102) in dichloromethane-acetonitrile (1:1) led to the formation of the silver complex, which was isolated as the hexafluorophosphate salt [Ag-L][PF_6] (136). The ^1H nmr of the complex gave a broad multiplet between 2.6 and 2.9 ppm in both CD_3OD and D_2O. Molecular ions (M^+) at m/e 461 and 459 (^{109}Ag-L and ^{107}Ag-L respectively) were observed in the FAB mass spectrum. Slow recrystallisation of the complex from methanol-acetonitrile (10:1) in the dark, in a dust free vessel, yielded small crystals (0.1-0.2 mm diameter) suitable for X-ray diffraction studies. The crystal structure of the $[Ag\text{-}L]^+$ ion is presented in Fig. 5.10 and selected bond lengths and angles given in Table 5.2. The silver ion is bound by all six nitrogen and sulphur donor atoms, in a distorted octahedral coordination. Both the cation $[Ag\text{-}L]^+$ (and the PF_6^- anion) have 2-fold crystallographic symmetry. The nine-membered rings adopt the expected [3.3.3] conformation allowing facial coordination to the silver, with one short silver sulphur bond (Ag-S(7) = 2.611(2)Å), one long silver-sulphur bond (Ag-S(4) = 2.802(2)Å) and a relatively short silver-nitrogen bond (Ag-N(1) = 2.586(3)Å). The planes through the S(4), S(7) and N(1) atoms in the two rings are not parallel, but are inclined at an angle of 17°, indicating that the bridging ethylene group is a little too short to allow the rings to adopt the optimum binding position. The resultant coordination of silver is distorted octahedral, in which the trigonal donor sets N(1), S(4) and S(7) and N(1'), S(4')

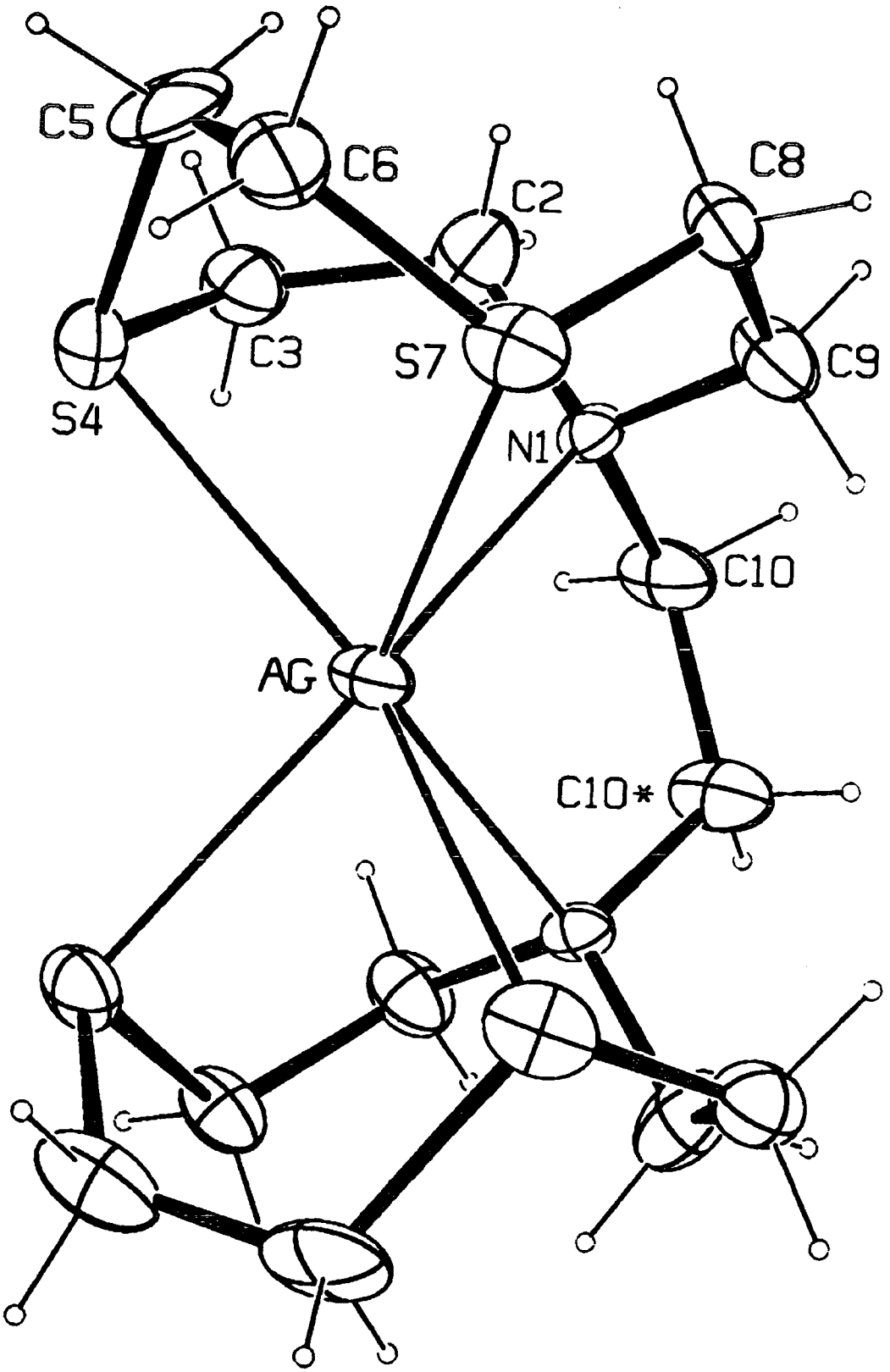

Fig. 5.10. X-ray crystal structure of the silver(I) complex of (102).

Table 5.2

Selected bond lengths (Å) and bond angles (deg) for [Ag-L][PF_6]
L = Bis [9]-NS_2 (101)

Ag-S(4)	2.802(2)	Ag-N(1)	2.586(5)
Ag-S(7)	2.611(2)		
S(4)-Ag-S(4')	156.83(7)	N(1)-Ag-N(1')	73.7(1)
S(4)-Ag-S(7)	80.90(7)	S(7)-Ag-S(7')	149.62(6)
S(4)-Ag-S(7')	93.04(6)	S(7)-Ag-N(1)	77.0(6)
S(4)-Ag-N(1)	74.0(1)	S(7)-Ag-N(1')	130.1(1)
S(4)-Ag-N(1')	126.6(1)		

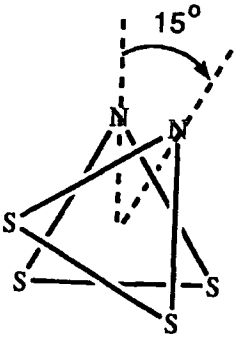

Fig. 5.11. Relative disposition of the two NS_2 donor sets in the $[Ag\text{-}L]^+$ complex (135).

and S(7') are twisted by 15^0 relative to one another [Fig. 5.11]. The rate of complexation was observed by ^1H nmr in D_2O (10^{-2}M in ligand, 23^oC). The pD was reduced to 4 ($CD_3CO_2D/CD_3CO_2^-Na^+$ buffer) in order to completely dissolve the ligand. As with the eighteen-membered macrocycles, complexation was complete ($\geq$ 95%) within three minutes.

5.2.4. Silver(I) complex of [9]-NS_2(126)

In order to synthesise a bis [9]-NS_2 silver complex, analogous to the [9]-S_3 system reported by Cooper et al.,[20] the ligand (126) was reacted with silver nitrate (0.5 eq.) in dichloromethane-acetonitrile (1:1). A small amount of complex was isolated as the PF_6^- salt from methanol solution, as a colourless crystalline solid. The ^1H nmr [Fig. 5.12] in CD_3OD gave a spectrum in which the ethylene 'S-CH_2CH_2-S' group

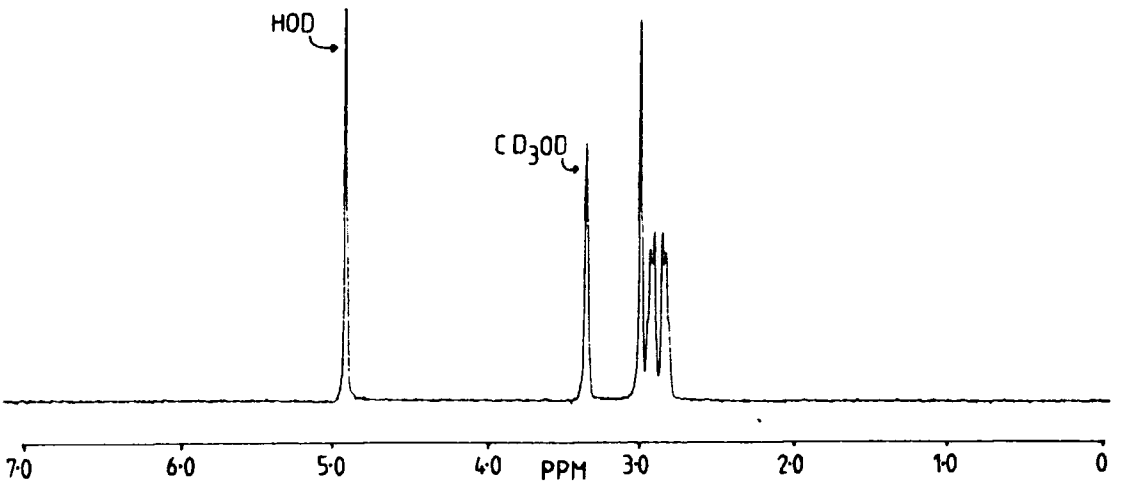

Fig. 5.12. ^1H nmr of the silver complex of [9]NS_2.

gave a singlet at 2.93 ppm, while the remaining methylene ring protons (CH_2N and CH_2S) resonated as an A_2B_2 system centred at 2.89 ppm [cf. two singlets 2.85 and 2.81 ppm for the free ligand in CD_3OD]. FAB mass spectrometry revealed molecular ions (M^+) at m/e 433 and 435 consistent with the bis-[9]-NS_2 cations $[^{107}Ag\text{-}L_2]^+$ and $[^{109}A\text{-}L_2]^-$. Unfortunately, due to loss of sample and failure to obtain the complex as a crystalline solid in subsequent syntheses, the molecular composition was not confirmed by elemental analysis or by X-ray diffraction studies.

5.2.5. Other silver(I) complexes

Attempts were made to prepare the 1:1 silver complexes of the macrocyclic ligands (137)-(140) using the same general procedure as

described previously. FAB mass spectrometry revealed molecular ions consistent with the formation of 1:1 complexes for all four ligands, but only ligand (140) yielded crystals $[Ag\text{-}L][PF_6]$ of sufficient quality for X-ray diffraction studies. The crystal structure revealed that the

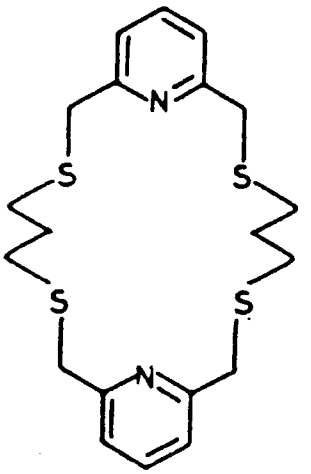

(137)

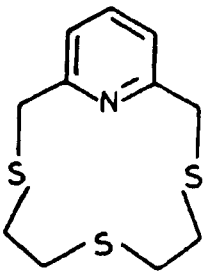

(138)

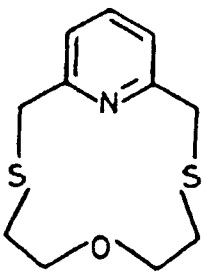

(139)

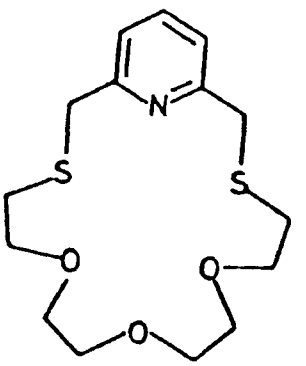

(140)

complex was dimeric $[Ag\text{-}L]_2[PF_6]_2$ in the solid state, with two five coordinate silver ions adopting approximately square pyramidal geometry, but in two distinctly different coordination environments [Fig. 5.13]. One silver ion is coordinated by an NSO_3 donor set with strong Ag-N [2.370(6)Å] and Ag-S [2.502(3)Å] bonds and three Ag-O bonds [2.398(6), 2.461(5) and 2.605(8)Å] from the same macrocycle. The second silver ion, which is coordinated by an NS_3O donor set, is bound by the pyridine nitrogen [although more weakly than the first, Ag(2)-N(1B) = 2.529(8)Å]

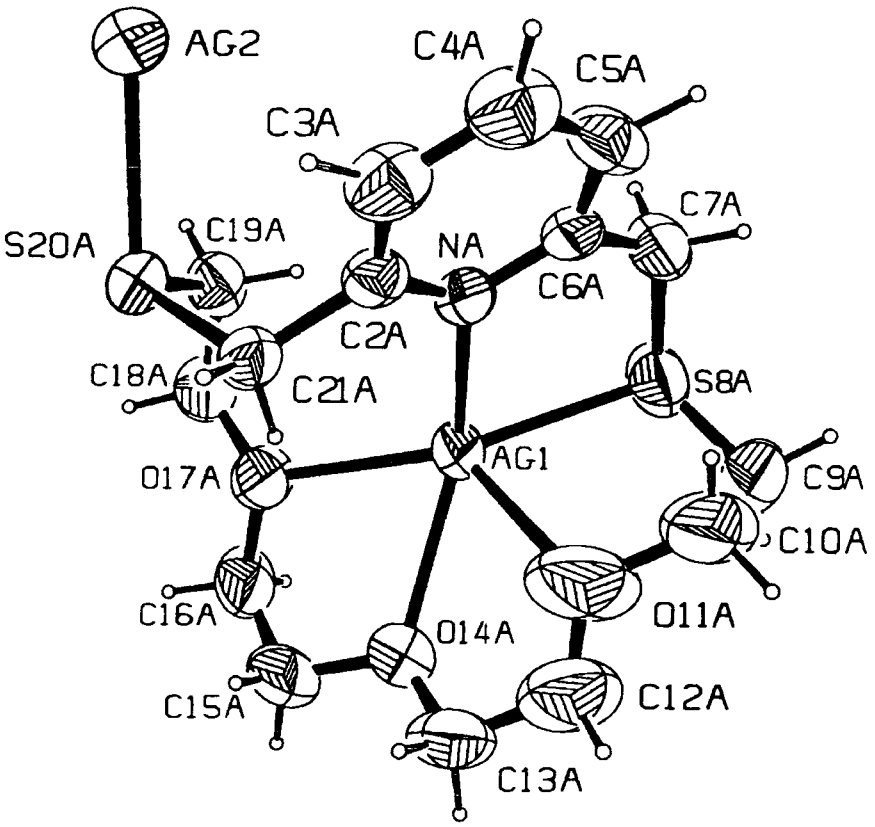

a)

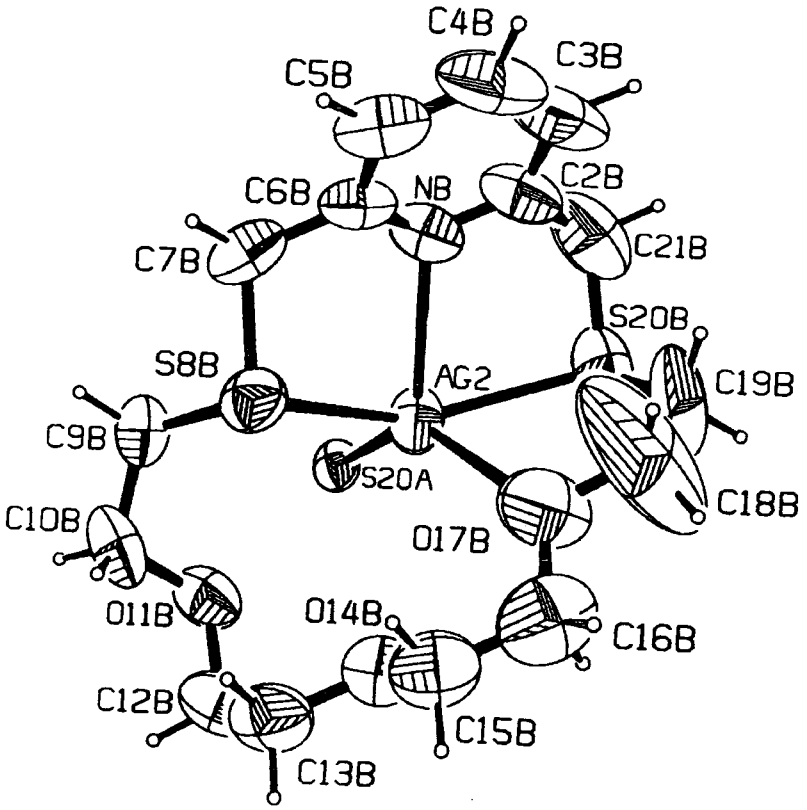

b)

Fig. 5.13. X-ray crystal structure of the silver(I) dimeric complex of ligand (137). The ORTEP diagrams showing the coordination spheres of silver atoms a) Ag(1) and b) Ag(2).

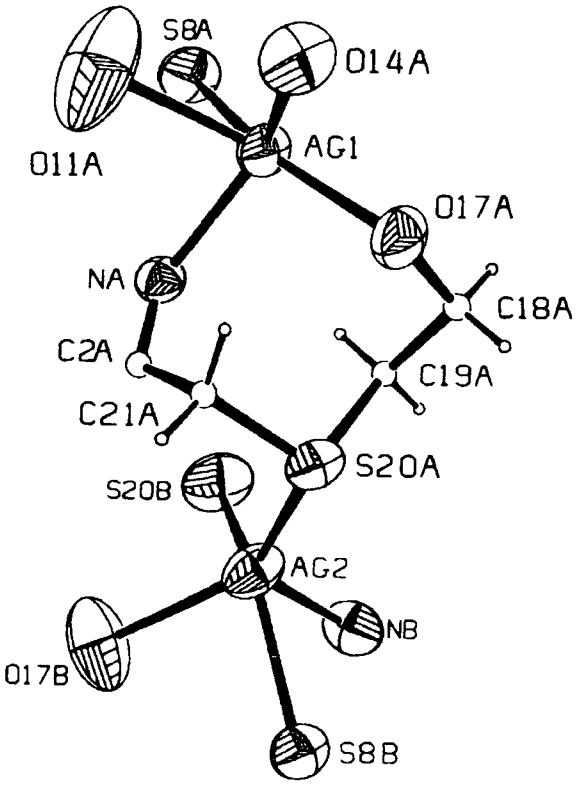

Fig. 5.14. The ORTEP diagram showing the link between the two silver monomeric units.

Table 5.3

Selected bond lengths (Å) and bond angles (deg) for $[Ag\text{-}L]_2[PF_6]_2$, L = (137)

Ag(1)-N(1A)	2.370(6)	Ag(2)-N(1B)	2.529(8)
Ag(1)-S(8A)	2.502(3)	Ag(2)-S(8B)	2.611(3)
Ag(1)-O(11H)	2.605(8)	Ag(2)-S(20B)	2.609(3)
Ag(1)-O(14A)	2.461(5)	Ag(2)-S(20A)	2.545(2)
Ag(1)-O(17A)	2.398(6)	Ag(2)-O(17B)	2.879(7)
N(1A)-Ag(1)-S(8A)	81.3(2)	S(20A)-Ag(2)-N(1B)	123.3(2)
N(1A)-Ag(1)-O(11A)	83.4(3)	S(20A)-Ag(2)-S(8B)	100.57(8)
N(1A)-Ag(1)-O(14A)	129.7(2)	S(20A)-Ag(2)-S(20B)	115.66(8)
N(1A)-Ag(1)-O(17A)	104.3(2)	N(1B)-Ag(2)-S(8B)	74.7(2)
S(8A)-Ag(1)-O(11A)	77.4(2)	N(1B)-Ag(2)-S(20B)	75.5(2)
S(8A)-Ag(1)-O(17A)	158.5(2)	S(8B)-Ag(2)-S(20B)	141.80(9)

by both sulphur atoms of the second macrocycle [2.611(3), 2.609(3)Å] and by one sulphur from the first macrocycle [Ag(2)-S(20A) = 2.545(2)Å], thereby constituting the bridge in the dimeric structure [Fig. 5.14]. A weak cation-dipole interaction with one oxygen [Ag(2)-O(17B) = 2.879(7)Å] completes the approximately square pyramidal geometry around the silver ion.

The structure reveals that the 2,6-di(thiomethyl) pyridine sub-unit is not ideally suited to binding the silver ion, as evidenced by the rather obtuse S(8B)-Ag(2)-S(20B) bond angle of 141.80(9)^{o} [cf. 169.8^{o} and 165.1^{o} in the five coordinate rhodium carbonyl[23] and copper(II) chloride[24] complexes of ligand (137)] and the long Ag(2)-N(1B) bond length. Also, torsional strain in the polyether chain of the macrocycle in this conformation is evidenced by the deviation of the torsional angles from the idealised strain free values of 180^{o} (trans) for C-O-C-C and ±60^{o} (gauche) for O-C-C-O[25] [e.g. C(10B)-O(11B)-C(12B)-C(13B) = -78.3^{o}].

In the ^{1}H nmr spectrum of the complex ($(CD_3)_2CO$), the benzylic methylene protons resonated as a singlet which broadened ($\omega_{\frac{1}{2}}$ 60 Hz, 203K) at lower temperature as did the eight methylene protons of the polyether chain ($OCH_2CH_2OCH_2CH_2O$). The ^{13}C nmr spectrum also indicated that the complex had the same symmetry (on the nmr time scale) as the free ligand. This behaviour suggests that either the pyridine nitrogen and both sulphurs do not bind the silver simultaneously in the solution state structure, or that the polyether chain is sufficiently mobile to permit rapid inversion of the sulphur centres (thereby rendering the geminal methylene benzylic protons isochronous).

5.3. Some Thermodynamic Aspects of Silver(I) Macrocycle Complexation

5.3.1. Potentiometric titrations

The stability constants (log K_s, MeOH) for the silver(I) complexes of ligands [18]-N_4S_2 (100), [18]-$N_4S_2Me_4$ (101), [18]-N_4O_2 (131) and [18]-$N_4O_2Me_4$ (132) were determined by potentiometry with a silver ion selective electrode,[26-29] using a technique originally developed by Frensdorff.[30] This work was carried out by H-J. Buschmann (Universität-GH Siegen, FRG) and H. Schneider (Max-Planck-Institut für Biophysikalische Chemie, FRG).

A solution of silver nitrate (1.0 mM, 20 ml) in methanol was titrated with a solution of the ligand in methanol (0.02M). The ionic strength was kept constant at I = 0.05M by addition of tetramethylammonium perchlorate. The concentration of free silver ion was measured using a silver ion selective electrode (Metrohm EA 282) with a second silver electrode as a reference electrode. The emf observed could be used directly to determine the free silver ion concentration, according to the Nernst equation, which simplifies to;

$$E = E_o + A \ln[Ag^+]$$

where $[Ag^+]$ is the concentration of free silver ion and 'A' is a constant which may be determined using appropriate calibration solutions.

The stability constant K_s which refers to the reaction;

$$Ag^+ + L \rightleftharpoons AgL^+$$

is defined as;

$$K_s = \frac{[AgL^+]}{[Ag^+][L]}$$

K_s is the concentration stability constant, assuming that the activity coefficients of the three species are equal to unity.

Using the assumption that only 1:1 complex formation was occurring it was noted that;

$$C^{o}_{Ag} = [Ag^{+}] + [AgL^{+}]$$

and

$$C^{o}_{L} = [L] + [AgL^{+}]$$

where C^{o}_{Ag} was the initial concentration of silver ion and C^{o}_{L} was the overall concentration of ligand in solution (free or complexed) thus;

$$K_S = \frac{C^{o}_{Ag} - [Ag^{+}]}{[Ag^{+}](C^{o}_{L} - [AgL^{+}])} = \frac{C^{o}_{Ag} - [Ag^{+}]}{[Ag^{+}](C^{o}_{L} - C^{o}_{Ag} + [Ag^{+}])}$$

Varying the initial silver ion concentration from $5x10^{-4}$M up to $5x10^{-3}$M did not effect the calculated K_S values. The enthalpies of complexation (ΔH) were measured by calorimetric methods thereby permitting the calculation of the entropies of complexation. The thermodynamic parameters (stability constant, enthalpy and entropy of complexation) are listed in Table 5.4 along with those reported for

Table 5.4

log K_S, ΔH and $T\Delta S$ values for the silver(I) complexes of 18-membered macrocyclic ligands

Macrocycle	log K_S (mol^{-1})[a]	$-\Delta H$ (kJ mol^{-1})	$T\Delta S$ (kJ mol^{-1})
N_4S_2	14.1	77.0	+3.3
$N_4S_2Me_4$	14.6	102.1	-18.7
N_4O_2	11.2	-	-
$N_4O_2Me_4$	13.4	84.3	-7.84
N_2O_4[b]	10.0	51.4	+5.7
S_2O_4[b]	10.3	64.0	-5.3
N_2S_4[b]	13.7	83.2	-5.0
O_6[c]	4.6	38.3	-12.1

a) errors in log K are typically ±0.1 or less and for ΔH ± 0.3 kJ mol^{-1} or less.
b) ref. 31.
c) ref. 32.

comparable eighteen-membered macrocyclic ligands. It may be noted that the silver binding constant for the [18]-$N_4S_2Me_4$ ligand (102) (log K_s = 14.6) is the highest recorded for a monocyclic ligand. Certain trends are apparent from the parameters listed in Table 5.4. The reaction enthalpies (ΔH) indicate that the sulphur atoms bind the silver ion slightly more strongly than secondary amine atoms (e.g. N_2S_4 ΔH = 83.2, N_4S_2 ΔH = 77.0 kJ mol^{-1}). However, more sulphur atoms in the macrocycle results in a less favourable entropy of complexation. Hence the N_4S_2 macrocycle has a slightly higher log K_s value than the N_2S_4 macrocycle. This is consistent with the observation that sulphur atoms in the macrocycles tend to adopt exodentate conformations, with the lone pairs directed away from the macrocyclic cavity, hence an unfavourable conformation change is associated with complexation,[26] (see section 4.1.5.). The high enthalpies of complexation for the N-methylated ligands indicate that a tertiary amine is a better donor atom for silver than either sulphur or secondary amines. However, this is not reflected in the metal binding constants, as large negative entropies of complexation are observed in complexes of these ligands. In particular, the entropy change ($T\Delta S$ = -18.7 kJ mol^{-1}) for the $N_4S_2Me_4$ silver(I) complexation is unusually large and contrasts to the favourable entropy change observed for the parent N_4S_2 macrocycle ($T\Delta S$ = +3.3 kJ mol^{-1}). This is likely to be due to unfavourable steric interactions associated with the N-Me groups in the complexed form of the macrocycle, which result in an unfavourable conformation change associated with complexation. This view is supported by the solid state structure of the silver(I) complex of (100) [section 5.2.1]. This reveals that the macrocycle is 'wrapped' around the metal ion in a conformation that may be envisaged to cause a considerable degree of steric crowding, if the

N-H groups were replaced by N-Me groups.

This is not wholly unexpected, as considerable evidence exists to suggest that N-methylation of macrocyclic polyamines has a significant effect upon their complexation properties. For example, Lehn has reported[33] that the dinuclear rhodium carbonyl complex of a 24-membered N_6O_2 macrocycle formed a cryptate-like structure, with a triply bridged $[Rh(CO)_3Rh]^{2+}$ unit held inside the macrocyclic cavity. However, the permethyl derivative of the ligand formed a dinuclear complex which contained only terminally bound carbonyls, indicating that methyl substitution of the ligand had introduced sufficient transannular steric effects to hinder bridging. Also, the relative instability (in both solution and solid state) of the ruthenium(VI) dioxo complex of the tetramethyl derivative of cyclam compared to that of cyclam itself, has been attributed to the destabilising interaction between the N-Me groups and the oxygen lone pairs.[34,35] Furthermore, the Cu(II) complex of [18]-$N_2S_4Me_2$ has been reported[36,37] to have a significantly different redox potential (Cu(II)|Cu(I), MeCN) to that of the Cu(II)-N_2S_4 complex. It was suggested that a substantial stereochemical change at the Cu(II) centre had resulted on going from the N_2S_4 complex to the dimethylated complex.

5.3.2. **pH-Metric titrations**

The acid dissociation constants for the macrocyclic ligands, [18]-N_4S_2 (100), [18]-$N_4S_2Me_4$ (101) and N,N'-bridged bis [9]-NS_2 (102) have been determined by pH-metric titration.[38] By analysis of the pH-metric titration curves of these ligands in the presence of one equivalent of silver ion (Ag^+), it was possible to determine the stability constants (log K_s, H_2O) of the silver(I) complexes.

Titrations were performed using the apparatus illustrated in Fig.

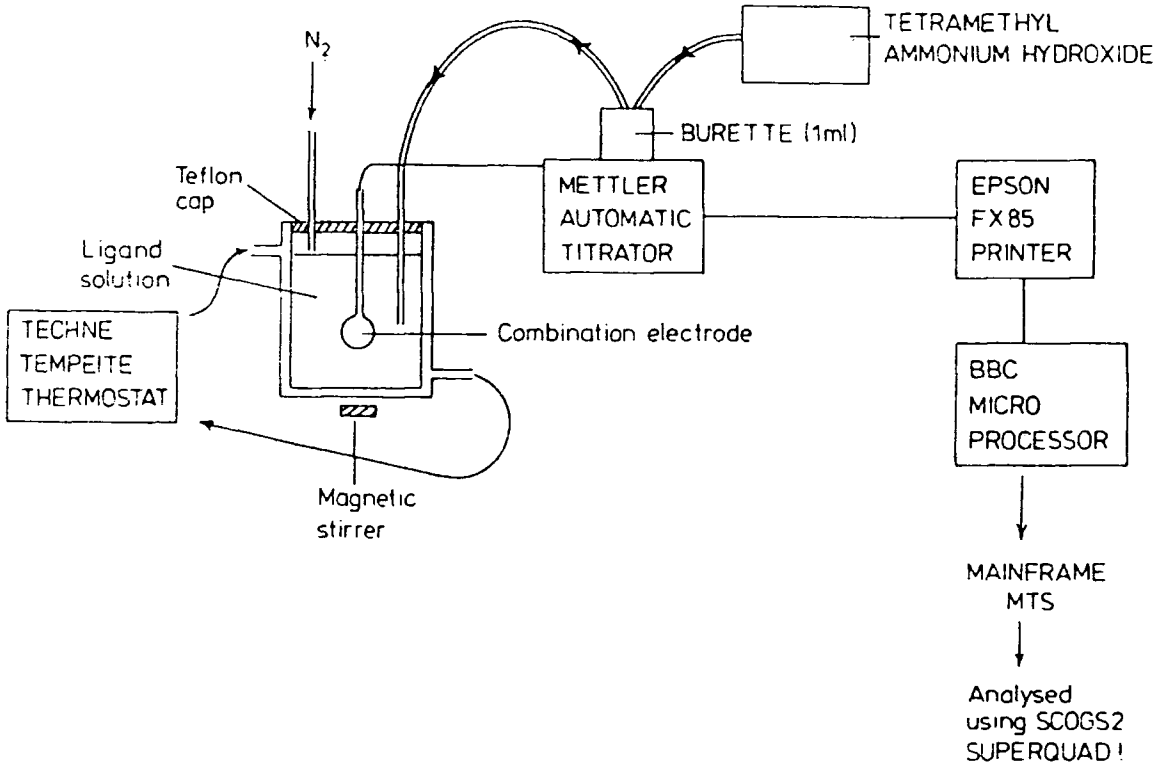

Fig. 5.15. Apparatus for pH-metric titrations.

5.15. Stock solutions of the ligand (0.002 mol dm^{-3}) in milli-Q water (25 ml), with nitric acid (1 equivalent per amine nitrogen of the ligand) and tetramethyl ammonium nitrate (to ensure constant ionic strength I = 0.1 mol dm^{-3}) were prepared. For each titration, 3.5 ml of the stock solution was placed in the titration cell which was thermostatted at 25°C and kept under an atmosphere of nitrogen. Titration with tetramethylammonium hydroxide solution (0.109 mol dm^{-3})

was performed using a Mettler DL20 automatic titrator, controlled by Basic software[39] on a BBC microprocessor. The pH was measured using a Corning 001854 combination microelectrode. The data was stored on the BBC microprocessor and transferred to the MTS mainframe (using KERMIT) and subsequently analysed by two non-linear least squares programs SCOGS2 and SUPERQUAD. Two titrations were performed on each ligand in the pH range 3-12. The results were analysed by Dr. R. Kataky.

The pK_a values for the ligands (100) to (102) are presented in Table 5.5, where for;

$$LH_n^{n+} \overset{K_{an}}{\rightleftharpoons} LH_{n-1}^{(n-1)+} + H^+$$

for example;

$$LH^+ \overset{K_{a1}}{\rightleftharpoons} L + H^+$$

Then;

$$K_{a1} = \frac{[L][H^+]}{[LH^+]} \text{ and } pK_{a1} = -\log K_{a1}$$

Table 5.5

Acid dissociation constants for ligands (100), (101) and (102)

Ligand	pK_{a1}	pK_{a2}	pK_{a3}	pK_{a4}	ψ^2 a	σ a
(100)	9.26	8.45	5.81	4.88	10.89	2.03
	9.41	8.47	6.06	4.94	11.69	1.58
(101)	8.82	8.35	4.13	3.71	3.79	1.87
	8.76	8.32	4.10	3.71	5.71	1.37
(102)†	6.53	6.00	-	-	-	-
	6.36	6.00	-	-	-	-

a) Deviations $\sigma \leq 3$ and ψ^2 (superquad) ≤ 12.6 for $\geq 95\%$ accuracy.

† There is some doubt as to the accuracy of the results for ligand (102) as the titration solutions became cloudy at pH > 7.15 due to the insolubility of the fully deprotonated ligand in water.

The pK_a values observed for the eighteen-membered rings are comparable to those reported for the [18]-N_4O_2 macrocycle (pK_{a1} 9.67, pK_{a2} 8.85, pK_{a3} 6.61 and pK_{a4} 3.21).[40] At pH $\geq$ 9.5 all four of the amine groups of ligands (100) and (101) are protonated. The N-methylated ligand is less basic than its parent N_4S_2 ligand, in accord with the fact that tertiary amino groups are less basic than secondary amino groups in aqueous solution.[41]

Determination of Stability Constants

The stability constants (log K_s, H_2O) for the 1:1 silver complexes of ligands (100)-(102) were determined by analysis of the pH-metric titration curves of the ligands, in the presence of one equivalent of silver ion. Stock solutions were prepared as for the acid dissociation measurements, with the addition of 1 equivalent of silver nitrate and titrations were performed as described previously.

The method for determining metal binding constants is based upon the change in pK of the amine groups of the ligand, upon complexation. The acidity of the LH_n^{n+} species will be increased due to competition for the ligand from the metal ion. The titration curves are thus strongly dependent on the cation complexation and their analysis may, in principle, yield all the equilibrium constants for protonation and complexation.

The silver binding constants and acid protonation constants (in brackets) are presented in Table 5.6. Species distribution plots of the 18-membered macrocycle complexes as a function of pH are given in Fig. 5.16. These may be used to determine which species are present at a given pH. Furthermore, at the point where two species alone ($AgLH_n$ and $AgLH_{n-1}$) are present in equal concentration, then pH = pK_{an}.

The binding constants for the silver(I) complexes in H_2O are

Table 5.6

Binding constants (and protonation constants) for the silver complexes of ligands (100), (101) and (102)

Macrocycle	log K_{AgL}	log K_{AgLH}	log K_{AgLH_2}	log K_{AgLH_3}
(100)	10.4	9.05	6.00	4.13
	(7.91)	(5.40)	(3.94)	
(101)	9.47	8.06	4.31	-
	(7.41)	(4.60)		
(102)	7.03	4.97	-	-
	(4.50)			

errors in log K values are typically ±0.1 mol^{-1}.

typically 3 orders of magnitude lower than those measured in methanol, due to the greater solvation of the silver ion in the former solvent. Of interest, is the binding constant for the [18]-$N_4S_2Me_4$ macrocycle (101), which is lower than that for the parent [18]-N_4S_2 macrocycle. Although this is a reversal of the relative values as determined in methanol, it is consistent with the idea that an unfavourable conformational change is associated with complexation for the N-methylated macrocycle. In water, the negative entropy of complexation appears to be even more significant than in methanol, resulting in a greater reduction of the log K_s value. The metal binding constants of the silver complexes of the monoprotonated 18-membered macrocycles are relatively high, indicating that the loss of one metal binding site does not greatly impair silver complexation. This is in contrast to the more significant loss of binding observed with the polyaza cryptands reported by Lehn.[38] Ligand (100) is particularly unusual in that the

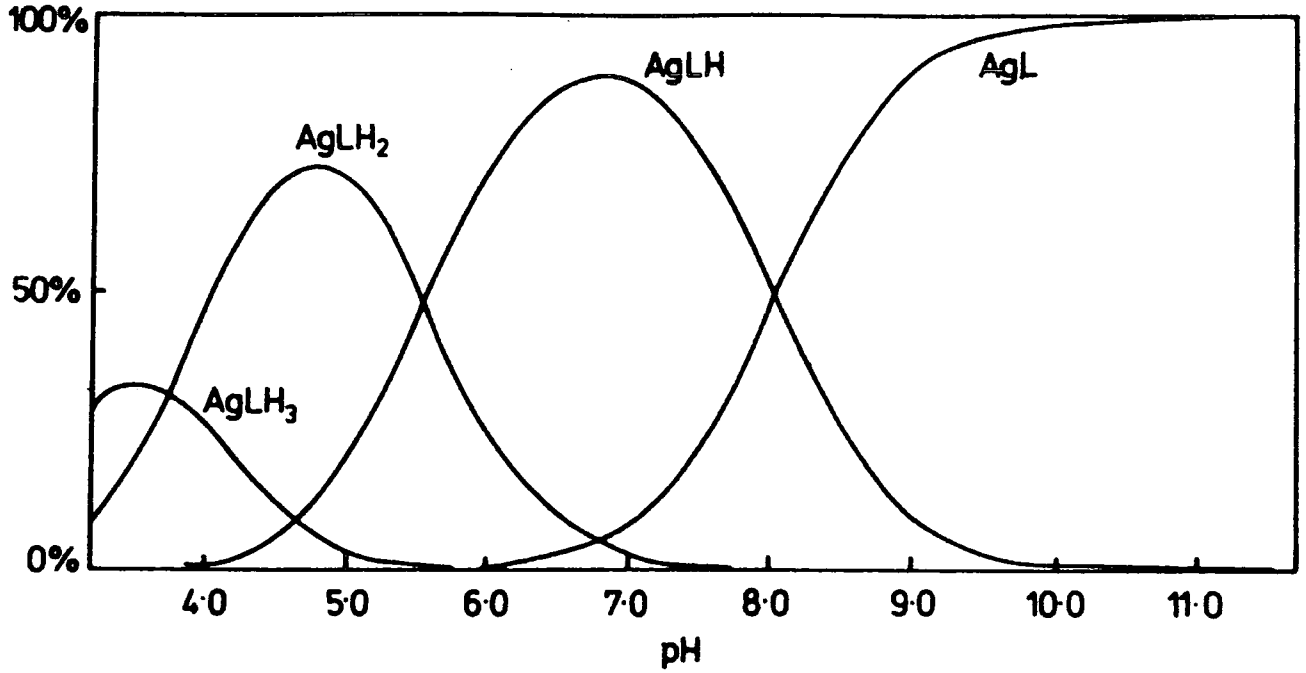

SPECIES DISTRIBUTION FOR [18]-N_4S_2 SILVER COMPLEXES

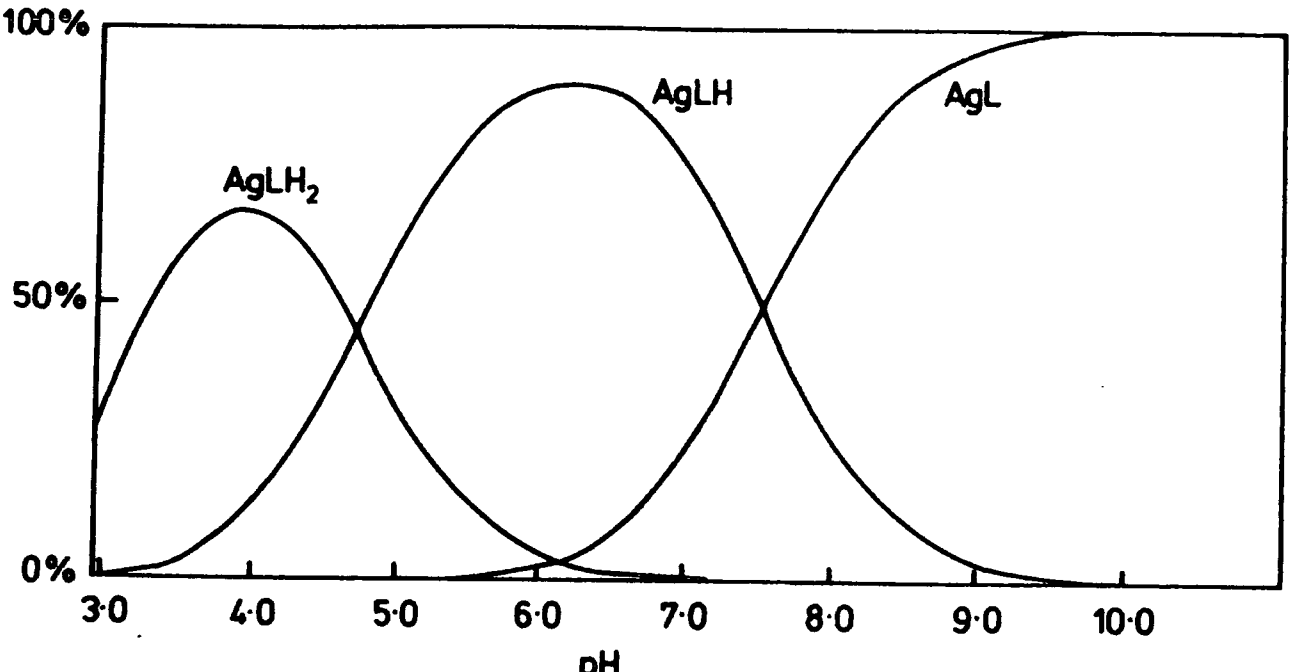

SPECIES DISTRIBUTION FOR [18]-$N_4S_2Me_4$ SILVER COMPLEXES

Fig. 5.16.

triprotonated silver complex was sufficiently stable to be observed (3.2 < pH < 5.0).

The metal binding constant for the silver complex of (102) was disappointingly low, although there is some doubt as to the accuracy of this measurement, due to the limited solubility of the fully deprotonated species in aqueous solution. A possible clue to the origin of this low value, is in the solid state structure (section 5.2.3.). This revealed that the bridging ethylene group was rather too short to allow the nine-membered rings to adopt ideal binding positions. The silver binding constant as determined in methanol and the calorimetric measurements for this complex will be of interest.

5.4. Conclusions

The metal binding constant for the silver complex of [18]-$N_4S_2Me_4$ is the highest recorded for a monocyclic ligand. However, between pH 3 and 7 the mono- and di-protonated complexes are the major species in solution for both this and the [18]-N_4S_2 silver complex. Although the protonated silver complexes show significantly enhanced thermodynamic stability over comparable polyaza cryptates,[36] it is doubtful whether these complexes will remain kinetically stable over the full physiological pH range (pH 2-9), as required for radiopharmaceutical application. However, *in vivo* studies have yet to be carried out. Additional studies which are necessary, include the investigation of the rate of complexation at low concentration (10-100 μM), under ambient conditions (e.g. pH 5, 20^{o}C).

If there were encouraging ^{111}Ag *in vivo* biodistribution results, then the synthesis of functionalised [18]-membered macrocycles could be undertaken in the future, using either substituted ethylenediamine (141)

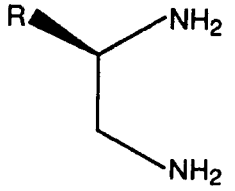

(141)

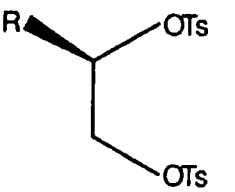

(142)

or ethyleneglycol ditosylate (142). Macrocycle antibody conjugation would then be possible using similar methods to those described for the functionalised [9]-N_3-triacid macrocycles (Chapter 3).

5.5. References

1. J.M. Lehn, Pure Appl. Chem., 52, 2441 (1980).
2. J.M. Lehn, S.H. Pine, E. Watanabe and A. Willard, J. Am. Chem. Soc., 99, 6766 (1977).
3. A.H. Alberts, R. Annuntziata and J.M. Lehn, J. Am. Chem. Soc., 99, 8502 (1977).
4. J.P. Gisselbrecht, M. Gross, A.H. Alberts and J.M. Lehn, Inorg. Chem., 19, 1386 (1980).
5. O. Khan, I. Morgenstern-Budarau, J.P. Audiere, J.M. Lehn and S.A. Sullivan, J. Am. Chem. Soc., 102, 5935 (1980).
6. J.M. Lehn, D. Parker and J. Rimmer, J. Chem. Soc. Dalton Trans., 1517 (1985).
7. B. Dietrich, J.M. Lehn and J.P. Sauvage, Chem. Commun., 1055 (1970).
8. B. Dietrich, J.M. Lehn, J.P. Sauvage and J. Blanzat, Tetrahedron, 29, 1629 (1973).
9. D. Pelissard and R. Louis, Tetrahedron Lett., 45, 4589 (1972).
10. D.St.C. Black and I.A. McClean, Chem. Commun., 1004 (1968).
11. J.E. Richman and T.J. Atkins, J. Am. Chem. Soc., 96, 2268 (1974).
12. I. Tabushi, Y. Taniguchi and H. Kato, Tet. Lett., 12, 1049 (1977).
13. B.K. Vriesema, J. Buter and R.M. Kellogg, J. Org. Chem., 49, 110 (1984).
14. G. Dijkstra, W.H. Kruizinga and R.M. Kellogg, J. Org. Chem., 52, 4230 (1987).
15. P. Chaudhuri and K. Weighardt, Prog. Inorg. Chem., 35, 329 (1987).
16. W. Rosen and D. Busch, J. Am. Chem. Soc., 91, 4694 (1969).
17. J.S. Bradshaw and J.Y.K. Hui, Reviews, 11, 649 (1974).
18. J. Buter and R.M. Kellogg, J. Org. Chem., 46(22), 4481 (1981).
19. J.F. Biernat and E. Luboch, Tetrahedron, 40(10), 1927 (1984).
20. J. Clarkson, R. Yagbasan, P.J. Blower, S.C. Rawle and S.R. Cooper, J. Chem. Soc. Chem. Commun., 950 (1987).
21. R. Louis, D. Pelissard and R. Weiss, Acta Cryst., B32, 1480 (1976).
22. R. Louis, Y. Agnus and R. Weiss, Acta. Cryst., B33, 1418 (1977).

23. G. Ferguson, K.E. Matthes and D. Parker, J. Chem. Soc. Chem. Commun., 1350 (1987).

24. K.E. Matthes, Ph.D. Thesis, University of Durham, (1987).

25. R.E. Wolf, J.R. Hartman, J.M.E. Storey, B.M. Foxman and S.R. Cooper, J. Am. Chem. Soc., 109, 4328 (1987).

26. H-J. Buschmann, Chem. Ber., 118, 2746 (1985).

27. H-J. Buschmann, Inorg. Chim. Acta, 102, 95 (1985).

28. H-J. Buschmann, Thermochimica Acta, 107, 219 (1986).

29. J. Guthnecht, H. Schneider and J. Stroka, Inorg. Chem., 17, 3326 (1978).

30. H.K. Frensdorff, J. Am. Chem. Soc., 93(3), 600 (1971).

31. H-J. Buschmann, Ch. 2 in "Stereochemical and Stereophysical Behaviour of Macrocycles", I. Bernal (ed.), Elsevier (1987).

32. R.M. Izatt, J.S. Bradshaw, S.A. Nielsen, J.D. Lamb and J.J. Christensen, Chem. Rev., 85, 271 (1985).

33. J-P. Lecomte, J.M. Lehn, D. Parker, J. Guillhem and C. Pascard, J. Chem. Soc. Chem. Commun., 296 (1983).

34. C.M. Ché, K.Y. Wong and C.W. Mak, J. Chem. Soc. Chem. Commun., 546 (1985); idem. ibid., 988 (1985).

35. K.E. Matthes and D. Parker, Ch. 3 in "Stereochemical and Stereophysical Behaviour of Macrocycles", I. Bernal (ed.), Elsevier, 1987.

36. A. Lavery and N. Atkinson, "Book of Abstracts" from the 13th Int. Symp. on Mac. Chem., 302 (1988).

37. N. Atkinson, A.J. Blake, M.G.B. Drew, G. Forsyth, A.J. Lavery, G. Reid and M. Schroder, J. Chem. Soc. Chem. Commun., 985 (1989).

38. J.M. Lehn and F. Montavon, Helv. Chim. Acta, 61, 67 (1978).

39. Software written by Dr. A. Royston (Durham University).

40. E. Luboch, A. Cygan and C.A. Biernat, Inorg. Chim. Acta, 68, 201 (1983).

41. C. Nave and M.R. Truter, J. Chem. Soc. Chem. Commun., 2351 (1974).

CHAPTER SIX

EXPERIMENTAL

6.1. Introduction

The synthetic procedures for the compounds used in this work are described in the proceeding section. Temperatures are reported in ^{o}C unless otherwise stated. R_F values refer to silica gel TLC (Merck. Art. 5735, Kieselgel 60 F_{254}) or alumina TLC (Merck. Art. 5550, Kieselgel 60 F_{254}) with the eluant system specified. Column chromatography employed "gravity" silica (Merck. Art. 7734, Kieselgel 60, 0.063-0.200 mm) or "flash" silica (Merck. Art. 9385, Kieselgel 60, 0.040-0.063 mm) or neutral alumina (Merck. Art. 1077, activity I, 0.063-0.200 mm). All HPLC analysis and purification was performed using a Varian Vista 5500/polychrom 9060 instrument, fitted with either a cation exchange ("Synchropak" CM300), anion exchange ("Synchropak" AX100) or reverse phase ("Spherisorb" 50DS2) column. The flow rates employed were 1.4 ml/min. for analytical columns (4.0 mm x 25.0 cm) and 4.0 ml/min. for semi-preparative columns (10.0 mm x 25.0 cm) using the solvent systems specified. Retention times 'R_t' are quoted in minutes. Infra-red spectra were recorded on a Perkin-Elmer 577 spectrometer either as a thin film or nujol mull on NaCl plates or as a KBr disc. ^{1}H and ^{13}C nmr spectra were recorded on a Bruker AC250 spectrometer, with spectral frequency 250.134 MHz and 62.896 MHz respectively. Chemical shifts are quoted in ppm to higher frequency of TMS at δ = 0 ppm and coupling constants (J) are given in Hz. Internal TMS reference was used for samples in $CDCl_3$, whereas samples in D_2O were referenced externally to TMS. ^{1}H nmr spectra recorded in CD_3OD were referenced to CD_2HOD at δ = 3.35 ppm. Mass spectra were recorded on a VG 7070E mass spectrometer operating in the EI, CI, DCI or FAB mode. Optical rotations were recorded on an "OPTICAL ACTIVITY" AA-10 automatic polarimeter.

Solvents were dried using the following reagents: Ethanol/Methanol

($Mg(OR)_2$); Dichloromethane (CaH_2); Chloroform (P_2O_5); Tetrahydrofuran (Na/benzophenone) and Toluene (Na). Anhydrous DMF (99+%) was purchased from Aldrich and water was pre-distilled. All other solvents were of reagent grade.

6.2. Synthetic Procedures

6.2.1. Macrocycles to bind indium(III) and gallium(III)

The ten and eleven-membered triaza macrocycles were synthesised by the tosylamide method using caesium carbonate.[1]

N,N',N''-tri(p-toluenesulphonyl)-1,4,7-triazacyclodecane [30]

Caesium carbonate (6.08 g, 18.5 mmol) was added to a solution of N,N-bis((N-p-toluenesulphonyl)-2-aminoethyl)p-toluenesulphonamide (5.0 g, 8.9 mmol) in anhydrous DMF (200 ml). A solution of 1,3-bis(p-toluenesulphonato)propane (3.4 g, 8.9 mmol) in anhydrous DMF (60 ml) was added dropwise over a period of 3 hours, with vigorous stirring. After stirring at room temperature (20^oC) for 12 hours the temperature was raised to 60^oC for 3 hours. Solvent was removed under reduced pressure and the residue taken up in dichloromethane (150 ml) and washed with distilled water (2 x 100 ml). The organic layer was dried over anhydrous magnesium sulphate, filtered and solvent removed under reduced pressure. The 'glassy' solid residue was recrystallised from ethanol-dichloromethane to give a white solid (4.2 g, 80%); m.p. 233-234^oC; [Lit:[2] 234-236^oC]; (Found: C, 54.8; H, 6.02; N, 6.34. $C_{28}H_{35}N_3S_3O_6.0.3H_2O$ requires C, 55.0; H, 5.83; N, 6.88); m/e (DCI, NH_3) 606 (M^++1) 605 (M^+) 450, 296; δ_H ($CDCl_3$) 7.73 (2H, d, J 8.1 Hz, aromatic H) 7.69 (4H, d, J 8.2 Hz, aromatic H) 7.34 (2H, d, J 8.2 Hz, aromatic H) 7.32 (4H, d, J 8.2 Hz, aromatic H) 3.37 (8H, s, N-CH_2CH_2-N) 3.20 (4H, t, N-$C\underline{H}_2$) 2.43 (12H, s, CH_3) 2.20 (2H, m, C-$C\underline{H}_2$).

1,4,7-triazacyclodecane [33]

The detosylation was effected using concentrated sulphuric acid, as reported by Zuberbühler et al.,[2] with slight modification.

Concentrated sulphuric acid (15 ml) was added to the tritosylamide [30] (4.0 g, 6.6 x 10^{-3} moles) and the solution heated at 120°C for 48 hours. The cooled reaction mixture (ice/water bath) was basified with aqueous sodium hydroxide solution (40%), filtered and extracted with chloroform (4 x 50 ml). The combined organic extracts were dried over anhydrous magnesium sulphate, filtered and solvent removed to give a pale brown oil (0.6 g, 60%); (Found: $(M^+ + 1)$ 144.1457. $C_7H_{15}N_3$ requires 144.1500); m/e (DCI, NH_3) 144 $(M^+ + 1)$ 143 (M^+); δ_H ($CDCl_3$, 60 MHz) 2.75 (12H, m, CH_2N) 1.75 (3H, s, NH) 1.60 (2H, m, CH_2C).

1,4,7-triazacyclodecane-N,N',N''-triacetate [25]; was synthesised using the chloroacetic acid method of Takahashi and Takamoto;[3]

Chloroacetic acid (1.16 g, 12.2 mmol) was added to a solution of 1,4,7-triazacyclodecane (0.50 g, 3.5 mmol) in distilled water (10 ml) and adjusted to pH 10 with lithium hydroxide. The mixture was heated to 45°C and the solution maintained at pH 10 for 8 hours with periodic addition of lithium hydroxide. The mixture was refluxed for 3 hours and the cooled solution adjusted to pH 2 with concentrated hydrochloric acid. The mixture was evaporated almost to dryness, ethanol (5 ml) added and the mixture stirred vigorously to give a white viscous material. The remaining solution was decanted off and the white residue redissolved in the minimum volume of water (0.5 ml). Ethanol (3.0 ml) was carefully pipetted on top of the aqueous layer and allowed to diffuse in slowly. After 12 hours a crystalline solid was collected by filtration (0.55 g, 50%); [Lit:[3] yield 35%]; (Found: C, 48.9; H,

7.60; N, 13.1. $C_{13}H_{21}N_3O_6$ requires C, 49.2; H, 7.25; N, 13.2); m/e (FAB, H_2O/Glycerol) 318 (M^++1); δ_H (D_2O) 3.83 (4H, s, N-CH_2CO_2) 3.80 (2H, s, N-CH_2-CO_2) 3.49 (12H, br s, CH_2N) 2.23 (2H, br s, C-CH_2-C).

N,N',N''-tri(p-toluenesulphonyl)-1,4,8-triazacycloundecane [31]

Caesium carbonate (3.46 g, 10.6 mmol) was added to a solution of N,N-bis((N-p-toluenesulphonyl)-3-aminopropyl)p-toluenesulphonamide (3.00 g, 5.06 mmol) in anhydrous DMF (200 ml). A solution of ethylene glycol ditosylate (1.87 g, 5.06 mmol) in anhydrous DMF (60 ml) was added dropwise over a period of 3 hours with stirring continued for 12 hours. After heating the mixture to 60°C for 3 hours the solvent was removed under reduced pressure and the residue taken up in dichloromethane (150 ml) and filtered. Solvent was removed from the filtrate to give a pale yellow residue. The tritosylate product was separated by 'gravity' silica gel chromatography with gradient elution, dichloromethane-methanol [(99:1) to (98:2)], to give a white solid (1.8 g, 57%); [Lit:[2] yield 53%]; m.p. 215-217°C; [Lit:[2] 217°C]; R_F 0.3 [silica gel: CH_2Cl_2-MeOH (99:1)]; m/e (CI, NH_3) 620 (M^++1) 464, 310; δ_H ($CDCl_3$) 7.69 (2H, d, J 8.0 Hz, aromatic H) 7.60 (4H, d, J 8.1 Hz, aromatic H) 7.33 (4H, d, J 8.0 Hz, aromatic H) 7.30 (2H, d, J 8.1 Hz, aromatic H) 3.43 (4H, t, J 6.7 Hz, CH_2-N) 3.28 (4H, s, N-CH_2CH_2-N) 2.99 (4H, t, J 5.3 Hz, CH_2N) 2.43 (12H, s, Me) 1.91 (4H, m, CH_2-C).

1,4,8-triazacycloundecane [34]

The detosylation of the tritosylate [31](2.1 g, 3.4 mmol) was effected using the concentrated sulphuric acid method as described for the synthesis of 1,4,7-triazacyclodecane [33]; a pale yellow oil was obtained (0.38 g, 73%); (Found: (M^++1) 158.2580. $C_8H_{20}N_3$ requires

158.2488); m/e (DCI, NH_3) 158 (M^++1) 157 (M^+); δ_H ($CDCl_3$, 60 MHz) 2.80 (12H, m, CH_2N) 2.50 (3H, s, NH) 1.55 (4H, m, CH_2-C).

1,4,8-triazacycloundecane-N,N',N''-triacetate [26] was synthesised using the chloroacetic acid method as described for the synthesis of 1,4,7-triazacyclodecane-N,N',N''-triacetate: reaction of the triamine (0.167 g, 1.06 mmol) with chloroacetic acid (0.349 g, 3.7 mmol) gave a colourless crystalline solid (132 mg, 39%); Decomp: 220-240°C; (Found: C, 49.1; H, 7.57; N, 12.1. $C_{14}H_{25}N_3O_6.0.5H_2O$ requires C, 49.4; H, 7.65; N, 12.3); m/e (FAB, Glycerol-water); m/e 332 (M^++1); δ_H (D_2O) 3.89 (2H, s, N-$C\underline{H}_2CO_2$) 3.72 (4H, s, N-$C\underline{H}_2CO_2$) 3.50-3.40 (12H, m, N-CH_2) 2.21 (4H, br s, C-CH_2).

1,4,7-triazacyclononane-N,N',N''-triacetate was synthesised by two methods; the first gave the product as the dihydrochloride salt and the second gave the product, chloride free, as the free amine.

1,4,7-triazacyclonane-N',N',N''-triacetate-dihydrochloride [24a]

1,4,7-triazacyclononane (0.198 g, 1.53 mmol) was trialkylated using the chloroacetic acid method as described for the synthesis of 1,4,8-triazacyclodecane N,N',N''-triacetate. The dihydrochloride salt of the product was obtained (0.324 g, 70%); m.p. 230-232; (Found: C, 38.3; H, 6.37; N, 10.9. $C_{12}H_{23}N_3O_6Cl_2$ requires C, 38.3; H, 6.12; N, 11.2); m/e (FAB, glycerol-H_2O) 304 (M^++1); δ_H (D_2O) 3.96 (6H, s, CH_2-CO_2) 3.42 (12H, s, CH_2N).

1,4,7-triazacyclonane-N,N',N''-triacetate (TCTA) [24b]

Bromoacetic acid (0.776 g, 5.58 mmol) was added to a solution of 1,4,7-triazacyclonane [Aldrich, 99%] (0.200 g, 1.55 mmol) in distilled

water (10 ml) and the solution adjusted to pH 10 with the addition of lithium hydroxide. The reaction mixture was heated to 45°C and the pH maintained at 10 over a period of 10 hours by regular addition of lithium hydroxide. The reaction mixture was stirred at 45°C for a further 24 hours after which the solution was adjusted to pH 2 with concentrated nitric acid. The mixture was evaporated almost to dryness after which ethanol (5 ml) was added with vigorous shaking. The remaining solution was decanted from a white viscous residue which was redissolved in a minimum volume of water (0.3 ml). Ethanol was added until a slight turbidity remained and the solution allowed to stand for 12 hours. A colourless crystalline solid was collected by filtration. Second and third crops of product were obtained when the volume was reduced and the above procedure repeated (0.25 g, 53%); Decomp: 210°C; (Found: C, 46.4; H, 6.90; N, 13.5. $C_{12}H_{21}N_3O_6.0.4H_2O$ requires C, 46.4; H, 7.02; N, 13.5); ^1H nmr and FAB mass spec. as for [24a].

6.2.2. **Indium(III) and Gallium(III) Complexes**

Indium (III) complex of 1,4,7-triazacyclononane N,N',N''-triacetate [24b], (In-L).$4H_2O$ [36]

A solution of indium nitrate (0.175 g, 0.582 mmol) in aqueous nitric acid (0.04 mol dm^{-3}, 1.0 ml) was added to a solution of the ligand (0.176 g, 0.582 mmol) in aqueous nitric acid (0.04 mol dm^{-3}, 1.0 ml) and the mixture allowed to stand at room temperature for 12 hours. Acetone (4.0 ml) was added to the aqueous solution until a slight turbidity remained. After several hours a fine white solid was collected by filtration. Recrystallisation from water-acetone (1:4) gave a fine white crystalline solid (0.164 g, 68%); (Found: C, 29.2; H, 4.61; N, 8.54. $C_{12}H_{18}N_3O_6In.4H_2O$ requires C, 29.6; H, 5.13; N, 8.62); m/e (DCI, NH_3) 416 (M^++1); δ_H (D_2O) 3.70 (6H, s, CH_2-CO_2) 3.24

(6H, m, CH_2N) 3.07 (6H, m, CH_2N).

The hydrated chloroindium complex (In-L).HCl.H_2O [37] was also prepared:

A solution of indium trichloride (18 mg, 80 mmol) in aqueous hydrochloric acid (0.04M, 1.0 ml) was added to a solution of the [9]-N_3-triacid dihydrochloride [24b] (30 mg, 80 mmol) in aqueous hydrochloric acid (0.04M, 1.0 ml). Slow evaporation of solvent over several days yielded colourless crystals (16 mg, 50%). Crystals suitable for X-ray diffraction were obtained; (Found: C, 29.6; H, 4.21; N, 8.49. $C_{12}H_{19}N_3O_6ClIn.2H_2O$ requires C, 29.5; H, 4.51; N, 8.61); FAB mass spectrometry and ^1H nmr characterisation as for [36]. For X-ray crystal structure cell data - see appendix.

Indium(III) complex of 1,4,8-triazacyclodecane-N,N',N''-triacetate [25], [In-L]

Synthesis as for [36]. White crystalline solid (12 mg, 58%); (Found: C, 36.7; H, 4.93; N, 9.78. $C_{13}H_{20}H_3O_6In$ requires C, 36.4; H, 4.66; N, 9.79); m/e (DCI, NH_3) 430 (M^++1); δ_H (D_2O) 3.90-2.60 (18H, br m's, CH_2CO_2, CH_2N) 2.24 (1H, br m, C-CH_2-C) 1.92 (1H, br m, C-CH_2-C).

Gallium(III) complex of 1,4,7-triazacyclononane [24], [*Ga-L*]

Synthesis as for [36], using gallium(III) nitrate. Colourless crystals (25 mg, 54%); (Found: C, 38.9; H, 4.99; N, 11.2. $C_{12}H_{18}N_3O_6Ga$ requires C, 38.9; H, 4.87; N, 11.4); m/e (FAB, p-NBA) 371, 369 (M^+) [^{71}Ga-L and ^{69}Ga-L]; δ_H (D_2O) 3.87 (6H, s, CH_2CO_2) 3.50 (6H, m, CH_2N) 3.20 (6H, m, CH_2N); X-ray crystal data - see appendix.

Gallium(III) complex of 1,4,8-triazacyclodecane-N,N',N''-triacetate [25], [*Ga-L*]

Synthesis as for [36]. White crystalline solid (16 mg, 45%); (Found: C, 40.4; H, 5.15; N, 10.8. $C_{13}H_{20}N_3O_6Ga$ requires C, 40.6; H, 5.21; N, 10.9); m/e (FAB, p-NBA) 385, 383 (M^+) [^{71}Ga-L and ^{69}Ga-L]; δ_H (D_2O) 3.81 (6H, m, CH_2CO_2) 3.67-3.45 (8H, m, CH_2N) 3.16 (4H, m, C-CH_2-N) 2.34 (1H, br m, C-C<u>H</u>H-C) 1.87 (1H, br m, C-CH<u>H</u>-C).

6.2.3. <u>C-functionalised [9]-N_3-triacid</u>

<u>Route A</u>

The starting material for the synthesis of a functionalised 1,4,7-triazacyclononane N,N',N''-triacetate system was (2S)-Lysine monohydrochloride (Fluka).

(2S)-Lysine methyl ester [43]

Acetyl chloride (25.0 ml) was added carefully to a solution of (2S)-Lysine monohydrochloride (15.0 g, 85.0 mmol) in methanol (250 ml) and the solution was heated under reflux for 14 hours. The volume of the solution was reduced (80 ml) under reduced pressure, and a white solid was filtered off, washed with cold methanol and dried in vacuo (16.1 g, 81%); m.p. 212-213°C; (Lit: 214-215°C); (Found: C, 35.2; H, 7.71; N, 11.5. $C_7H_{16}O_2N_2.2HCl.0.3H_2O$ requires C, 35.2; H, 7.80; N, 11.7).

2,6-diaminohexamide (*Lysine amide*) [44]

Ammonia (250 ml) was condensed into a reaction vessel containing (2S)-Lysine ester [43] (5.5 g, 0.024 moles) at -77°C (solid CO_2-acetone bath) and the mixture stirred for 3 hours. The ammonia was allowed to evaporate to give a cream coloured residue which was taken up in methanol (15.0 ml). A white solid was filtered off and solvent removed

from the filtrate, under reduced pressure, to give a cream coloured solid residue (estimated 90% pure from ^{13}C and ^{1}H nmr:- lactam impurity). This product was used without further purification; (Found: $(M^{+}+1)$ 146.1427. $C_6H_{16}N_3O$ requires 146.1293); IR (Nujol mull) 3400 cm^{-1} (br) (NH str) 1650 cm^{-1} (Amide I) 1440 cm^{-1}; m/e (DCI, NH_3) 146 $(M^{+}+1)$, 84; δ_H (D_2O) 3.93 (1H, t, J 6.5 Hz, CHN) 3.01 (2H, t, J 7.6 Hz, CH_2-N) 1.88 (2H, m, CH_2-C) 1.72 (2H, m, CH_2-C) 1.47 (2H, m, CH_2-C); δ_C (D_2O) 172.6 (C=O) 52.7, 39.0 (C-NH_2) 30.5, 26.1, 21.2 (CH_2-C).

1,2,6-triaminohexane [46]

To the Lysine amide [44] (5.0 g, 0.0229 moles) was added dry THF (250 ml) and Borane.DMS (10.0 M, 35.0 ml) and the mixture heated under reflux, under a nitrogen atmosphere, for 14 days. The reaction was quenched by adding methanol (100 ml). Solvent was removed under reduced pressure and methanol (2 x 100 ml) added and removed under reduced pressure. The oily residue was heated under reflux in hydrochloric acid (6 mol dm^{-3}, 200 ml) for 4 hours. Solvent was removed under reduced pressure and the residue taken up in methanol (2 x 75 ml) and solvent removed again to give a clear oil. The residue was taken up in KOH solution (100 ml, 6 mol dm^{-3}) and extracted with dichloromethane (4 x 100 ml). The combined organic extracts were dried over anhydrous potassium carbonate, filtered and solvent removed under reduced pressure to give a clear oil (3.0 g, 100%). The product was used without further purification. (Found: $(M^{+}+1)$ 132.1490. $C_6H_{18}N_3$ requires 132.1500); IR (thin film) 3400 cm^{-1} (br) (NH str) 1570 cm^{-1}, 1470 cm^{-1}; m/e (DCI, NH_3) 132 $(M^{+}+1)$; δ_H ($CDCl_3$) 3.53 (1H, m, C<u>H</u>N) 2.72-2.38 (4H, m, CH_2N) 1.72-1.21 (12H, m, CH_2-C, NH's); δ_C ($CDCl_3$) 56.2, 48.6, 42.1 (CH_2N, CHN) 35.5, 33.8, 23.5 (CH_2-C).

6-N-benzoyl-1,2,6-triaminohexane [47]

Copper(II) carbonate [$CuCO_3.Cu(OH)_2$, Aldrich] (2.95 g, 0.013 moles) was added to a solution of the triamine [46] (3.0 g, 0.023 moles) in distilled water and the solution stirred at room temperature for 30 minutes. The temperature was raised to 75°C for 90 minutes giving a very deep blue coloured solution. Benzoyl chloride (4.88 g, 0.035 moles) was added to the cooled solution (-1°C, ice-salt-water bath) with vigorous stirring over a period of 1 hour, with simultaneous addition of KOH (1.96 g, 0.035 moles) to maintain the pH $\geq$ 9. After stirring for a further 45 minutes the solution was decanted from a viscous oily residue and treated with hydrogen sulphide gas (10 min.). A brown precipitate formed which turned black on standing at room temperature for 20 minutes and was filtered,leaving a yellow/green solution. The volume of the aqueous layer was reduced (approx. 40 ml) under reduced pressure and the solution adjusted to pH 13 with KOH. After exhaustive extraction with dichloromethane the combined organic extracts were dried over anhydrous potassium carbonate, filtered and solvent removed under reduced pressure to give a clear oil (2.98 g, 49%). This material was used without further purification; (Found: $(M^+ + 1)$ 236.2074. $C_{13}H_{22}N_3O$ requires 236.1763); IR (thin film) 3300 cm^{-1} (br) (NH str) 1650 cm^{-1} (Amide I) 1540 cm^{-1} (Amide II); δ_H ($CDCl_3$) 7.70 (2H, d, J 8.5 Hz, aromatic H) 7.33 (3H, m, Aromatic H) 7.13 (1H, br s, NHCO) 3.32 (2H, m, CH_2NHCO) 2.64-2.30 (3H, m, CH_2N and CHN) 1.77 (4H, br s, NH_2) 1.60-1.10 (6H, br m, C-CH_2).

1,2-di(N-p-toluenesulphonyl)6-N-benzoyl-1,2,6-triaminohexane [48]

A solution of the 5,6-diaminobenzamide [47] (2.3 g, 9.8 mmol) in dichloromethane (40 ml) was added dropwise over a period of one hour to

a solution of p-toluenesulphonyl chloride (4.48 g, 2.35 x 10^{-2} moles) and triethylamine (2.37 g, 23.5 mmol) in dichloromethane (75 ml) with stirring. After stirring at room temperature for 18 hours the mixture was heated to 45°C for 20 minutes. The volume of the solvent was reduced (40 ml) under reduced pressure and a white precipitate filtered off. Solvent was removed under reduced pressure to give a brown oil from which the ditosylated product was separated by 'flash' silica gel chromatography; gradient elution dichloromethane-methanol (199:1 to 99:1) to give a 'glassy' solid (2.29 g, 43%); t.l.c.: R_F 0.2 [silica gel: CH_2Cl_2-MeOH (95:5)]; (Found: C, 60.2; H, 6.46; N, 7.23. $C_{27}H_{33}N_3O_5S_2$ requires C, 59.7; H, 6.08; N, 7.73); m/e (DCI, NH_3) 546 (M^++2) 545 (M^++1) 544 (M^+) 390, 359; δ_H ($CDCl_3$) 7.82 (2H, d, J 6.9 Hz, aromatic H) 7.66 (4H, m, aromatic H) 7.42 (3H, m, aromatic H) 7.22 (4H, m, aromatic H) 6.75 (1H, t, J 5.8 Hz, NHCO) 5.87 (2H, m, NH-SO_2) 3.29 (3H, m, CH_2N and CHN) 2.88 (2H, t, CH_2NHCO) 2.40 (3H, s, CH_3) 2.37 (3H, s, CH_3) 1.42 (4H, br m, CH_2-C) 1.10 (2H, br m, CH_2-C); δ_C ($CDCl_3$) 167.9 (NHCO) 143.4, 137.2, 136.7, 131.5, 129.6, 128.5, 127.1, 127.0, (aromatic C) 53.2, 46.6, 38.7 (CH_2-N, CH-N) 31.3, 29.0, 21.8 (CH_2-C) 21.5 (CH_3).

2-((N-benzoyl)-4-aminobutyl)-N,N',N''-tris(p-toluenesulphonyl)-1,4,7-triazacyclononane [49]

A solution of N,N-bis[2-(p-toluenesulphonato)ethyl]p-toluenesulphonamide (1.67 g, 2.95 mmol) in dry DMF (40 ml) was added dropwise over a period of 4 hours to a suspension of caesium carbonate (2.02 g, 6.20 mmol) in a solution of the ditosylamide [48] (1.60 g, 2.95 mmol) in dry DMF (200 ml) with vigorous stirring under an atmosphere of nitrogen. After stirring at room temperature for 18 hours the mixture was heated to 60°C for 3 hours. Caesium carbonate (0.5 g, 1.5 mmol) was added to

the reaction mixture which was stirred at 60°C for a further 24 hours. Solvent was removed under reduced pressure and the residue dried in vacuo (10^{-2} mm Hg, 50°C). The residue was taken up in dichloromethane (150 ml) and washed with distilled water (3 x 150 ml). The organic layer was dried over anhydrous potassium carbonate, filtered and solvent removed under reduced pressure to give a pale brown oil. The cyclised product was separated from the mixture by 'flash' silica gel chromatography with gradient elution, dichloromethane-methanol 399:1 to 199:1 to 99:1) (0.79 g, 35%); t.l.c.: R_F 0.7 [silica gel: CH_2Cl_2-MeOH (95:5)]; m.p. 105-108°C; (Found: C, 59.5; H, 6.25; N, 7.09. $C_{38}H_{46}N_4O_7S_3$ requires C, 59.5; H, 6.00; N, 7.31); m/e (DCI, NH_3) 769 (M^++3) 768 (M^++2) 767 (M^++1) 611, 570, 457, 395, 373, 301; δ_H ($CDCl_3$) 7.85-7.62 (8H, m, aromatic H) 7.49-7.28 (9H, m, aromatic H) 6.46 (1H, brs, NHCO) 3.77-2.98 (13H, m, CH_2N, CHN) 2.46 (3H, s, CH_3) 2.44 (3H, s, CH_3) 2.42 (3H, s, CH_3) 1.64-1.20 (6H, br m, CH_2-C); δ_C ($CDCl_3$) 167.5 (NHCO) 144.1, 143.8, 136.9, 134.5, 134.3, 134.2, 131.3, 129.9, 128.5, 127.6, 127.5, 127.3, 126.9 (aromatic C) 59.5, 53.7, 52.6, 50.8, 46.0, 39.0 (CH_2N, CHN) 29.3, 28.9, 23.8 (CH_2-C) 21.5 (CH_3); $[\alpha]_D^{20}$ + 9.2 (CH_2Cl_2).

2-((N-benzoyl)-4-aminobutyl)-1,4,7-triazacyclononane [50]

The tritosylate [49] (0.91 g, 1.19 mmol) was treated with concentrated sulphuric acid (10 ml) at 115°C with stirring for 36 hours. To the cooled solution (0°C, ice bath) was added NaOH solution (30%, 5 ml). The sodium sulphate precipitate was filtered off and washed with distilled water (3 ml). The combined filtrate and washings were extracted with dichloromethane (5 x 10 ml) and the organic layer dried over anhydrous potassium carbonate, filtered and solvent removed under

reduced pressure to give a pale brown oil (146 mg, 41%); HPLC: R_t 13.7 min. observed at λ = 254 nm (CM 300 "Synchropak") gradient elution A = H_2O B = 1.0 M NH_4OAc pH 5.6, C = CH_3CN from 70% A, 10% B, 20% C to 0% A, 80% B, 20% C over 20 min; (Found: $(M^+ + 1)$ 305.2564. $C_{17}H_{28}N_4O$ requires 305.2341); m/e (DCI, NH_3) 306 $(M^+ + 2)$ 305 $(M^+ + 1)$ 279, 262, 201, 188; δ_H ($CDCl_3$) 7.82 (2H, m, aromatic H) 7.42 (3H, m, aromatic H) 7.00 (1H, br s, NHCO) 3.45 (2H, m, CH_2NHCO) 3.07 (3H, br s, NH) 2.76 (11H, m, CH_2N, CHN) 1.63 (2H, br m, CH_2-C) 1.40 (4H, br m, CH_2-C); $[\alpha]_D^{20}$ + 4.1 (CH_2Cl_2).

2-((N-benzoyl)-4-aminobutyl)-1,4,7-triazacyclononane-N,N',N''-triacetate [51]

Bromoacetic acid (0.392 g, 2.82 mmol) was added to a solution of the triamine [50] (0.0855 g, 0.28 mmol) in water (5.0 ml) with stirring at 60°C. Lithium hydroxide (0.118 g, 2.82 mmol) was added in portions, to maintain a pH $\geq$ 10. More bromoacetic acid (0.784 g, 5.64 mmol) was added (in two portions after 23 hours and 39 hours) and again lithium hydroxide (0.236 g, 5.64 mmol) added to the reaction mixture to maintain the pH $\geq$ 10. After 46 hours the reaction mixture was allowed to cool and solvent was removed under reduced pressure to give a yellow brown residue which was taken up in HPLC grade water (500 ml). The triacetate product was separated by ion exchange chromatography (sepharose DEAE) with gradient elution from aqueous NH_4OAc (0.25 mMolar, pH 5.6) - CH_3CN (9:1) to aqueous NH_4OAc (0.25 Molar, pH 5.6) - CH_3CN (9:1). De-salting was achieved by reverse phase chromatography eluting with water (0.1% trifluoroacetic acid, 50 ml) followed by acetonitrile (0.1% trifluoroacetic acid, 50 ml). Solvent was removed from the eluates under reduced pressure to give a clear oil (0.106 g, 79%); HPLC: R_t =

6.5 min. observed λ = 254 nm ("Synchropak" A101) elution A = H_2O, B = 1.0 M NH_4OAc, pH 5.6, C = CH_3CN from 70% A, 10% B, 20% C to 0% A, 80% B, 20% C over 20 min; R_t = 12.0 min. observed λ = 254 nm ("Spherisorb" S5ODS) elution A = H_2O (0.1% TFA), B = CH_3CN (0.1% TFA) from 95% A, 5% B to 5% A, 95% B over 20 min; m/e (FAB, p-NBA) 479 (M+1); δ_H (D_2O) 7.81 (2H, d, J 7.1 Hz, aromatic H) 7.62 (3H, m, aromatic H) 4.05-3.60 (6H, m, CH_2CO_2) 3.55-2.90 (13H, m, CH_2N) 1.71 (3H, m, CH_2-C) 1.42 (3H, m, CH_2-C); $[\alpha]_D^{20}$ + 7.5 (H_2O).

Route B

2,6-diamino-N(2-aminoethyl)hexanamide [53]; was synthesised by Dr. Ian Helps (Durham University); (2S)-Lysine methyl ester (9.0 g, 39 mmol) was added in several portions to ethylenediamine (100 ml) with stirring over a period of 2 hours. The reaction mixture was heated under reflux for 16 hours after which the ethylenediamine was removed by distillation under reduced pressure (10^{-2} mm Hg). The residue was dissolved in water (40 ml) and basified with NaOH and the volume reduced (~ 15 ml) under reduced pressure. Sodium chloride was removed by filtration, washed with methanol and the combined filtrate and washings evaporated to dryness under reduced pressure. The residue was taken up in methanol (30 ml), filtered and filtrate evaporated to dryness and then redissolved in dichloromethane (100 ml). After filtration the organic layer was dried over anhydrous potassium carbonate and solvent removed to give a clear oil (6.3 g, 87%); (Found: (M^+) 188.1639. $C_8H_2N_4O$ requires 188.1637); IR (thin film) 3350 (br) 3280 (br) [NH str] 1650 (Amide I) 1550 (Amide II); m/e (DCI, NH_3) 189 (M^++1) 188 (M^+) 171, 156, 129; δ_H ($CDCl_3$) 7.56 (1H, br s, N<u>H</u>CO) 3.38 (1H, t, J 3.8 Hz, C<u>H</u>CONH) 3.33 (2H, t, J 5.7 Hz, C<u>H</u>$_2$NHCO) 2.83 (2H, t, J 6.0 Hz, CH_2N) 2.71 (2H, t, J 6.5 Hz, CH_2N) 1.87 (2H, m, CH_2-C) 1.46 (11H, m, CH_2-C,

NH_2).

1-N-(2-aminoethyl)-1,2,6-triaminohexane [54]

Borane.Tetrahydrofuran complex (1.0 Molar in THF, 300 ml) was added to a solution of the amide [53] (6.3 g, 40 mmol) and the mixture heated under reflux for 21 hours. The cooled solution (ice-water bath) was quenched carefully with methanol (100 ml) and after stirring for 1 hour solvent was removed under reduced pressure. The residue was treated with methanol (2 x 100 ml) and solvent removed under reduced pressure. The clear oil was taken up in hydrochloric acid (6.0 mol dm^{-3}, 150 ml) and heated under reflux for 3 hours. Solvent was removed under reduced pressure and the residue treated with methanol as before. The white solid was taken up in KOH solution (3 mol dm^{-3}, 50 ml) and extracted exhaustively with dichloromethane. The combined organic extracts were dried over anhydrous potassium carbonate, filtered and solvent removed under reduced pressure to give a pale yellow oil (5.2 g, 75%); (Found: (M^++1) 175.1730. $C_8H_{23}N_4$ requires 175.1537); m/e (DCI, NH_3) 175 (M^++1), 133; δ_H (HCl salt, D_2O) 2.96 (5H, m, CHN) 2.82 (3H, m, CHN) 2.60 (1H, m, CHN) 1.68 (2H, br m, CH_2-C) 1.47 (4H, m, CH_2-C); δ_C (HCl salt, D_2O) 53.0, 49.6, 48.0, (C-NH_2) 39.2, 36.9 (C-NH) 32.6, 27.1, 21.8 ($\underline{C}H_2$-C).

1-N-(2-aminomethyl)-6-N-benzoyl-1,2,6-triaminohexane [55]

Copper(II) carbonate [$CuCO_3.Cu(OH)_2$, Aldrich] (1.47 g, 6.65 mmol) was added to a solution of the tetraamine [54] (2.1 g, 12.1 mmol) in water (35 ml) and the mixture stirred at 50°C for 30 min. to give an intense deep blue solution. Benzoyl chloride (1.04 g, 1.70 g) was added in small portions over 90 minutes, to the cooled solution (0°C, ice

bath) with simultaneous addition of KOH to maintain a pH 9-10. The reaction mixture was stirred at room temperature for 1 hour followed by filtration, to remove a small amount of precipitate. The filtrate was treated with H_2S (10 min.), allowed to stand at room temperature for 20 minutes and copper sulphide removed by filtration. The yellow green filtrate was reduced in volume (~ 25 ml), adjusted to pH 14 with KOH and exhaustively extracted with dichloromethane. The combined organic extracts were dried over anhydrous potassium carbonate, filtered and solvent removed under reduced pressure to give a pale yellow oil (1.94 g, 58%); (Found: $(M^+ + 1)$ 279.2027. $C_{15}H_{27}N_4O$ requires 279.2010); IR (thin film) 1640 (NHCO) 1600 (aromatic H) 1580, 1540 (C-NH_2); m/e (DCI, NH_3) 280 $(M^+ + 2)$ 279 $(M^+ + 1)$; δ_H ($CDCl_3$) 7.78 (2H, d, J 7.0 Hz, aromatic H) 7.40 (3H, m, aromatic H) 6.70 (1H, br s, NHCO) 3.43 (2H, m, $C\underline{H}_2NHCO$) 2.76-2.30 (7H, m, CHN and CH_2N) 1.65 (5H, br s, NH and NH_2) 1.45-1.15 (6H, m, CH_2-C); δ_C ($CDCl_3$) 167.2 (CONH) 135.0, 131.2, 128.5, 126.8, (aromatic C's) 56.5, 52.5, 50.9, 41.7, 39.8 (CH_2N and CHN) 35.7, 29.7, 23.4 (CH_2-C).

1-N-((N-p-toluenesulphonyl)-2-aminoethyl)-1,2-di(N-p-toluene-sulphonyl)-6-N-benzoyl-1,2,6-triamine [56]

A solution of the triamine [55] (1.82 g, 6.55 mmol) in dichloromethane (35 ml) was added dropwise to a solution of p-toluenesulphonyl chloride (4.48 g, 23.6 mmol) and triethylamine (2.38 g, 23.6 mmol) in dichloromethane (50 ml) with stirring over a period of 1 hour. After stirring at room temperature for 12 hours the reaction mixture was washed with distilled water (25 ml), dried over potassium carbonate, filtered and solvent removed under reduced pressure. The brown residue was redissolved in dichloromethane (12 ml) and after

several minutes a white precipitate resulted. The solid was collected by filtration, washed with dichloromethane (15 ml) and dried in vacuo (10^{-2} mm Hg) (3.3 g, 68%); R_F 0.4 [silica gel; CH_2Cl_2-MeOH (95:5)]; m.p. 149-151°C; (Found: C, 58.1; H, 5.98; N, 7.25. $C_{36}H_{44}N_4O_7S_3$ requires C, 58.4; H, 5.94; N, 7.56); m/e (DCI, NH_3) 741 (M^++1) 740 (M^+), 373; δ_H ($CDCl_3$) 7.83 (2H, d, J 7.1 Hz,aromatic H) 7.72 (4H, d, J 7.9 Hz, part of AA'XX' system, aromatic H) 7.61 (2H, d, J 8.1 Hz, part of AA'XX' system aromatic H) 7.44 (3H, m, aromatic H) 7.31 (4H, d, J 8.0 Hz, part of AA'XX' system, aromatic H) 7.18 (2H, d, J 8.1 Hz part of AA'XX' system, aromatic H) 6.49 (1H, br t, NHCO) 5.30 (2H, m, N<u>H</u>-Ts) 3.40 (2H, br m, C<u>H</u>$_2$NHCO) 3.30 (2H, br m, CH_2N) 3.17 (5H, m, CH_2N and CHN) 2.44 (6H, s, CH_3) 2.32 (3H, s, CH_3) 1.44 (2H, m, CH_2-C) 1.25 (2H, m, CH_2-C) 1.06 (2H, m, CH_2-C).

2-((N-benzoyl)-4-aminobutyl)-N,N',N''-tri(p-toluenesulphonyl)-1,4,7-triazacyclononane [49]

Caesium carbonate (3.26 g, 10 mmol) was added to a solution of the tritosylamide [56] (3.70 g, 5.0 mmol) in anhydrous DMF (200 ml) under dry nitrogen. A solution of ethylene-glycol ditosylate (1.85 g, 5.0 mmol) in anhydrous DMF (50 ml) was added slowly over a period of 4 hours, with efficient stirring. After stirring for 12 hours (20°C) the temperature was raised to 65°C for 3 hours. Solvent was removed under reduced pressure and the residue dissolved in chloroform (200 ml) and washed with water (3 x 50 ml). The organic layer was dried over anhydrous potassium carbonate, filtered and solvent removed under reduced pressure. The pale brown residue was dissolved in the minimum volume of dichloromethane (15 ml) and ethanol added until a turbidity remained. After cooling to -20°C for 12 hours a colourless "glassy"

solid separated (2.7 g, 71%); m.p. 106-108°C; (Found: C, 59.8; H, 5.88; N, 7.02. $C_{38}H_{46}N_4O_7S_3$ requires C, 59.5, H, 6.00; N, 7.31) - fully characterised previously.

6.2.4. **C-functionalised DTPA**

1-N-(N,N-(bisaceto)-2-aminoethyl)-1-N-aceto-2-N,N-(bisaceto)6-N-benzoyl-1,2,6-triaminohexane [*59*]

A solution of potassium hydroxide (0.734 g, 13.1 mmol) in distilled water (3.0 ml) was added to a solution of bromoacetic acid (0.688 g, 4.81 mmol) in toluene (1.5 ml) at 0°C (ice salt bath). A solution of the triamine [55] (0.243 g, 0.874 mmol) in distilled water (0.5 ml) was added and the heterogeneous system stirred vigorously. More bromoacetic acid (0.688 g, 4.81 mmol) in toluene (0.75 ml) and potassium hydroxide (0.734 g, 13.1 mmol) in water (1.0 ml) were added after 24 hours and again after 48 hours. After 72 hours the aqueous solution was adjusted to pH 1.5 with concentrated hydrobromic acid and washed with diethyl ether (3 x 10 ml). The aqueous layer was evaporated to dryness, under reduced pressure to give a yellow solid residue. The product was separated from salts and hydrolysis products by ion exchange chromatography (Dowex-50W, H^+ form, dry mesh 100-200, cation exchange). The residue was loaded onto the column as a dry solid and eluted with distilled water (200 ml) followed by aqueous ammonia (0.2 M, 250 ml). The latter fractions from the column were combined and solvent removed to give a colourless 'gummy' solid (0.26 g, 52%). HPLC; R_t 17.7 min. observed at λ = 254 nm ("Synchropak" A100 anion exchange column) with gradient elution A = H_2O, B = 1.0 M NH_4OAc, pH 5.6, C = CH_3CN from 70% A, 10% B, 20% C to 0% A, 80% B, 20% C over 20 min.; (Found: $(M^+ + 1)$ 639.3752. $C_{25}H_{37}N_4O_{11}$ requires 639.3241); m/e (DCI, NH_3, methyl ester); m/e 640 $(M^+ + 2)$ 639 $(M^+ + 1)$ 626, 625, 611; δ_H (D_2O) 7.75 (2H, d,

J 7.1 Hz, aromatic H) 7.56 (3H, m, aromatic H) 3.90 (4H, s, $C\underline{H}_2CO_2$) 3.95-3.90 (6H, m, $C\underline{H}_2CO_2$) 3.50-2.84 (15H, m, CH_2N) 1.87-1.48 (6H, m, CH_2-C); δ_c (D_2O) 177.3 (NHCO) 170.4, 170.0, 169.9, 169.8 (CO_2) 133.3, 131.6, 128.4, 126.6 (aromatic C) 61.1, 59.4, 57.1, 56.7, 54.9, 53.3, 53.0, 48.2 (C-O, C-N, C-CO) 27.8, 24.9, 22.5 (CH_2-C).

6.2.5. **N- and N,N'-functionalised [9]-N_3-triacid**

2-bromo-N-benzoyl-6-aminohexylethanoate [63]

Synthesis was carried out by K. Jankowski and R. Matthews (Durham University) in two steps starting from N-benzoyl-6-aminohexanoic acid. The bromination step was effected with red phosphorous and bromine according to the literature method.[4] Esterification was achieved by standard methods using ethanol and acetyl chloride and the product purified by 'flash' silica chromatography eluting with ethylacetate-hexane (1:1).

1-N-(2'-(N-benzoyl-4-aminobutyl)ethoxycarbonylmethyl)-1,4,7-triaza-cyclonane [65]

Potassium carbonate (0.214 g, 1.54 mmol) was added to a solution of 1,4,7-triazacyclononane (0.380 g, 2.95 mmol) in anhydrous DMF (5 ml) under a nitrogen atmosphere and the mixture heated to 60°C. A solution of the α-bromo ester [63] (0.503 g, 1.48 mmol) in anhydrous DMF (5 ml) was added dropwise over a period of 5 hours and the mixture stirred for a further 15 hours at 60°C. The cooled reaction mixture was filtered and solvent removed under reduced pressure to give a pale brown oil. A small amount of product (50 mg) was separated by 'prep' HPLC ("Synchropak" CM300 cation exchange), but the remaining product was used without further purification.

Purified material: HPLC: R_t 7.8 min. observed at λ = 282 nm

("Synchropak" CM300 cation exchange) with gradient elution, 1.4 ml/min.; A = H_2O, B = 1.0 M NH_4OAc, C = CH_3CN from t = 0 min.; 80% A, 0% B, 20% C; to t = 5 min. 60% A, 20% B, 20% C; to t = 10 min., 0% A, 80% B, 20% C; IR (thin film) 3500-3300 (NH) 1720 (C=O ester) 1635 (NHCO); m/e (DCI, NH_3) 392 (M^++2) 391 (M^++1) 303, 264; δ_H ($CDCl_3$) 8.63 (1H, br t, NHCO) 8.01 (2H, d, J 7.8 Hz) 7.41 (3H, m, aromatic H) 4.14 (2H, q, J 7.3 Hz, O-CH_2) 3.63-3.29 (3H, m, $C\underline{H}_2NCO$ and CHN) 2.85-2.67 (10H, m, CH_2N) 2.45 (2H, m, CH_2N) 1.76-1.45 (6H, m, CH_2-C) 1.26 (3H, t, J 7.1 Hz, $CH_2C\underline{H}_3$); δ_C ($CDCl_3$) 173.4 (-CO_2-) 167.5 (NHCO) 134.7, 131.1, 128.2, 127.1 (aromatic C's) 64.2, 60.2, 57.8 ($\underline{C}H_2O$, $\underline{C}H_2CO$) 48.5, 46.9, 45.6, 45.3, 39.8 (CH_2N) 29.0, 23.5, 18.4 (CH_2-C) 14.3 (CH_3).

N-(2-(N-benzoyl-4-aminobutyl)ethoxycarbonylmethyl)-N',N''-bis-(ethoxycarbonylmethyl)-1,4,7-triazacyclononane [67]

Caesium carbonate (1.20 g, 3.68 mmol) and ethylbromoacetate (0.615 g, 3.68 mmol) were added to a solution of the crude monoalkylated triamine [65] [approx. 0.57 g, 1.5 mmol] in dry ethanol (6 ml) and the mixture stirred at 60°C for 20 hours. Solvent was removed under reduced pressure and the residue taken up in dichloromethane (6 ml) and a fine white precipitate removed by centrifuge. The organic layer was evaporated to dryness and the residue chromatographed on neutral alumina; gradient elution dichloromethane-methanol from (100:0) to (199:1) to (99:1) (0.1 g, 12%). R_f 0.4 [alumina: CH_2Cl_2-MeOH (98:2)]; HPLC: R_t 5.3 min. observed at λ = 254 nm ("Synchropak" CM300 cation exchange) gradient elution - as for previous expt. (Found: (M^++1) 563.3335. $C_{29}H_{47}N_4O_7$ requires 563.3227); IR (thin film) 3400, 3240 (br) (NH) 1725 (C=O ester) 1645 (NHCO); δ_H ($CDCl_3$) 7.81 (2H, d, J 6.8 Hz, aromatic H) 7.43 (3H, m, aromatic H) 4.13 (6H, q, J 6.9 Hz, O-CH_2)

3.46 (7H, m, CH_2-CO_2, CH-CO_2 and CH_2-NCO) 3.02-2.76 (12H, m, CH_2N) 1.50-1.28 (6H, m, CH_2-C) 1.25 (9H, t, J 7.1 Hz, $CH_2C\underline{H}_3$); δ_c ($CDCl_3$) 173.5, 171.7 (-CO_2-) 167.4 (CONH) 134.4, 131.1, 128.3, 126.7 (aromatic C's) 66.3, 60.3, 60.2, 58.4, 55.4, 54.8, 52.9, (C-N, C-O and C-CO) 39.7, 29.6, 29.0, 23.7, 14.2 (C-CH_2, C-CH_3).

N,N'-bis(2-(N-benzoyl-4-aminobutyl)ethoxycarbonylmethyl)-1,4,7-triazacyclononane [66]

Potassium carbonate (0.117 g, 0.85 mmol) was added to a solution of 1,4,7-triazacyclononane (0.104 g, 0.81 mmol) in anhydrous DMF under a nitrogen atmosphere and the mixture heated to 55°C. A solution of the α-bromo ester [63] (0.276 g, 8.1 mmol) in anhydrous DMF (4 ml) was added and the mixture stirred at 55°C for 48 hours. The cooled mixture was filtered and solvent removed under reduced pressure to give a pale yellow oil. The di-alkylated product was separated by 'prep' HPLC ("Synchropak" CM300 cation exchange 25 cm x 10 mm) gradient elution, 4.0 ml/min. A = H_2O, B = 1.0 M NH_4OAc pH 5.6, C = CH_3CN; t = 0 min., 80% A, 0% B, 20% C; to t = 5 min. 60% A, 20% B, 20% C; to t = 10 min. 0% A, 80% B, 20% C held for a further 5 min. The collected fractions were combined and solvent removed under reduced pressure, followed by sublimation to remove the ammonium acetate, to give a pale brown oil (0.11 g, 21%); HPLC: R_t = 5.7 min. observed at λ = 254 nm - conditions as above. IR (thin film) 3500-3300 (NH) 1720 (C=O ester) 1640 (NHCO); m/e (DCI, NH_3) 653 (M^++2) 652 (M^++1); δ_H ($CDCl_3$) 8.00-7.74 (4H, m, aromatic H) 7.45-7.42 (6H, m, aromatic H) 4.15 (4H, m, O-CH_2) 3.47-2.55 (18H, m, CH_2N and CHN) 1.59 (12H, m, CH_2-C) 1.24 (6H, m, $CH_2C\underline{H}_3$); δ_c ($CDCl_3$) 172.4 (C=O ester) 167.6 (CONH) 139.2, 131.1, 128.3, 127.3, 126.4, (aromatic C's) 65.3, 64.6, 60.6 (CH_2O, CH_2CO) 47.1, 46.6, 44.6, 43.2, 39.9 (CH_2N) 30.2, 28.9, 24.5 (CH_2-C) 14.4 (CH_3).

N,N'-bis(2-(N-benzoyl-4-aminobutyl)ethoxycarbonylmethyl)-N''-ethoxycarbonylmethyl-1,4,7-triazacyclononane [69]

Caesium carbonate (46.3 mg, 0.142 mmol) and ethylbromoacetate (24.0 mg, 0.142 mmol) were added to a solution of the dialkylated triamine [66] (88.0 mg, 0.135 mmol) in anhydrous DMF. The mixture was stirred at 60°C for 20 hours after which solvent was removed under reduced pressure. The residue was taken up in dichloromethane and a fine white precipitate removed by centrifuge. Solvent was removed under reduced pressure and the product purified by 'prep' HPLC ("Synchropak" CM300 cation exchange 25 cm x 10 mm) - conditions same as previous experiment. The collected fractions were combined, solvent removed under reduced pressure and the residue sublimed to remove ammonium acetate leaving a pale brown 'gummy' solid (54 mg, 54%); R_t = 6 min. observed at λ = 254 nm - conditions as above; IR (thin film) 3500-3300 (NH) 1720 (C=O ester) 1640 (NHCO); m/e (DCI, NH_3) 738 (M^++1) 621, 420; δ_H ($CDCl_3$) 7.79 (4H, d, J 7.0 Hz, aromatic H) 7.42 (6H, m, aromatic H) 6.66 (2H, br s, NHCO) 4.11 (6H, m, OCH_2) 3.46-3.17 (8H, m, CH_2CO, CHCO and CH_2NCO) 3.09-2.63 (12H, m, CH_2N) 1.68 (12H, m, CH_2-C) 1.24 (9H, t, J 7.1 Hz, $CH_2\underline{CH}_3$); δ_C ($CDCl_3$) 173.8, 172.4 (CO_2) 167.6 (NHCO) 134.8, 131.2, 128.4, 127.6, 127.0 (aromatic C's) 66.8, 60.2, 60.1, 56.0, 55.9, 53.4 (C-O, C-CO, C-N) 39.9, 30.1, 29.3, 23.9, (C-CH_2) 14.7 (CH_3).

6.2.6. **Maleimide linkage**

N-(2-(N-(3-maleimidopropanoyl)-4-aminobutyl)carboxymethyl)-N',N''-bis(carboxymethyl)-1,4,7-triazacyclononane [75]

The triester [67] (25 mg, 0.044 mmol) was dissolved in hydrochloric acid (6 mol dm^{-3}, 2.0 ml) and heated under reflux for 16 hours. Solvent was removed under reduced pressure and the residue dried in vacuo (40°C, 10^{-2} mm Hg). Hydrolysis of the ester and amide groups was seen to be

complete by ^{1}H nmr (D_2O) and FAB (p-NBA matrix) mass spectrometry (m/e 375 [M^++1]). The residue was dissolved in anhydrous DMF (200 μl) and a solution of N-succinimidyl-3-maleimidopropionate [14.1 mg, 0.053 mmol] in anhydrous DMF (60 μl) was added. N-methyl morpholine (26.9 mg, 0.222 mmol) was added to the mixture, resulting in an immediate precipitation. Milli-Q purified water (25 μl) was added until the precipitate redissolved and the mixture allowed to stand at room temperature for 24 hours. The product was separated by 'prep' HPLC ("Spherisorb" S5ODS2 reverse phase). R_t = 8.5 min. observed at λ = 282 nm gradient elution 1.4 ml/min. A = H_2O (0.1% TFA) B = CH_3CN (0.1% TFA) from 95% A, 5% B to 5% A, 95% B in 20 min.; m/e (FAB, p-NBA matrix) 526 (M^++1), 453, 391, 307; δ_H (D_2O) 6.85 (2H, s, CH=CH) 3.95 (5H, m, CH_2CO_2) 3.79 (4H, m, CH_2NHCO and CH_2NCO) 3.00-3.50 (12H, m, CH_2N) 2.49 (2H, t, J 6.2 Hz, CH_2CONH) 1.69 (3H, m, CH_2-C) 1.46 (3H, m, CH_2-C).

N,N'-bis(2-(N-(3-maleimidopropanoyl)-4-aminobutyl)carboxymethyl)-N''-carboxymethyl-1,4,7-triazacyclononane [76]

The triester [69] (38 mg, 0.051 mmol) was dissolved in hydrochloric acid (6 mol dm^{-3}, 3.0 ml) and heated under reflux for 16 hours. Solvent was removed under reduced pressure and the residue dried in vacuo (40^{o}C, 10^{-2} mm Hg). Hydrolysis was seen to be complete by ^{1}H nmr (D_2O) and FAB mass spectrometry (p-NBA matrix) [m/e 444 (M^++1)].

The procedure of the previous experiment was followed for the maleimide linkage step, (2.5 equivalents of N-succinimidyl-3-maleimidopropionate and 7 eq. of N-methyl morpholine required in this case); Yield (10 mg, 26%); R_t 10.4 min. ("Spherisorb" S5ODS2 reverse phase) conditions as for previous experiment; m/e (FAB, p-NBA matrix) 748 (M^++1) 596; δ_H (D_2O) 6.85 (4H, s, CH=CH) 3.96 (4H, m, CH_2CO_2) 3.79

(8H, m, $C\underline{H}_2NCO$ and $C\underline{H}_2NHCO$) 3.10-3.25 (12H, m, CH_2N) 2.49 (4H, t, J 6.3 Hz, CH_2CONH) 1.82 (3H, m, CH_2-C) 1.46 (3H, m, CH_2-C).

6.2.7. Macrocycles to bind silver(I)

3,13-dithia-6,9-diazatetradecyl-5,10-dione-1,14-diethanoate [116]

1,2-diaminoethane (6.14 g, 0.123 moles) in dichloromethane (90 ml) was added dropwise to a solution of thiodiglycollic anhydride (25.0 g, 0.189 mmoles) in dichloromethane (250 ml) with vigorous stirring to give a white resinous solid. After heating under reflux for two hours, the solid was collected by filtration and dried in vacuo (10^{-2} mm Hg). The crude di-acid [115] was heated under reflux in a solution of ethanol (1.5 litres) and concentrated sulphuric acid (15 ml) for 60 hours to give a clear solution. The volume of the reaction mixture was reduced to approximately 60 ml and a white solid removed by filtration. The filtrate was evaporated to dryness under reduced pressure and the residue dissolved in distilled water (50 ml) and basified with saturated sodium carbonate solution. The aqueous layer was extracted with chloroform (4 x 100 ml) dried over magnesium sulphate, filtered and solvent evaporated under reduced pressure to give a brown solid. Recrystallisation from toluene gave a white crystalline solid (9.6 g, 27%); m.p. 93-94°C; (Found; C, 41.7; H, 5.92; N, 6.39. $C_{14}H_{24}N_2O_6S_2.H_2O$ requires C, 42.2; H, 6.53; N, 7.03); IR (Nujol) 3295 cm^{-1} (NH) 1715 cm^{-1} (C=O ester) 1640 cm^{-1} (Amide I) 1535 cm^{-1} (Amide II); m/e (CI-NH_3) 381 (M^++1) 367, 363, 335; δ_H ($CDCl_3$) 7.36 (2H, brs, $N\underline{H}CO$) 4.19 (4H, q, J 7.2 Hz, CH_2-O) 3.46 (4H, m, CH_2-N) 3.34 (8H, s, CH_2-S) 1.29 (6H, t, J 9.3 Hz, CH_3); δ_C ($CDCl_3$) 14.1 (CH_3) 34.6, 36.4 (CH_2-S) 39.8 (CH_2N) 62.0 (CH_2-O) 170.2 (C=O, Amide) 174.4 (C=O, ester).

4,13-dithia-1,7,10,16-tetraaza-2,6,11,15-tetraonehexadecane [117]

The diester [116] (8.92 g, 23.5 mmol) was dissolved in ethanol (350 ml) saturated with ammonia and allowed to stand at room temperature in a tightly stoppered vessel for 60 hours. The solution was re-saturated with ammonia by bubbling ammonia gas through it every 12 hours. The white solid was collected by filtration and dried in vacuo (10^{-2} mm Hg) (5.67 g, 75%); m.p. 185-187^{o}C; (Found: C, 36.0; H, 5.28; N, 16.6. $C_{10}H_{18}N_4O_2S_2.0.5H_2O$ requires C, 36.2; H, 5.74; N, 16.9); m/e (CI, NH_3) 279 (M^+-$CONH_2$); IR (Nujol) 3360, 3295, 3180 (NH str) 1640 (Amide I) 1540 (Amide II); δ_H (D_2O) 3.36 (8H, s, CH_2S) 3.32 (4H, s, CH_2N); δ_C (D_2O) 34.8, 35.3 (CH_2S) 38.7 (CH_2N) 170.8 (CONH) 174.3 ($CONH_2$).

4,13-dithia-1,7,10,16-tetraazahexadecane [118]

A solution of BH_3.THF (250 ml, 0.250 moles) was added by syringe to the tetraamide [117] (4.73 g, 14.6 moles) under nitrogen and the mixture heated under reflux for 60 hours. After cooling, the reaction mixture was quenched cautiously with methanol (20 ml) and solvent evaporated under reduced pressure.

The residue was dissolved in methanol (3 x 40 ml) and solvent removed under reduced pressure. After reflux in hydrochloric acid solution (6 mol dm^{-3}, 100 ml) for 3 hours the solvent was evaporated under reduced pressure and the residue dissolved in potassium hydroxide solution (50 ml, 6 mol dm^{-3}). The aqueous layer was extracted with chloroform (4 x 50 ml) dried over magnesium sulphate, filtered and solvent evaporated under reduced pressure to give a pale brown oil (2.76 g, 71%); (Found: (M^++1), 267.1295; $C_{10}H_{27}N_4S_2$ requires 267.1295); IR (thin film) 3350 cm^{-1} br (NH str) 1575 cm^{-1} (NH bend) 1120 cm^{-1} (C-N str); m/e (DCI, NH_3) (M^++2) 268 (M^++1) 267; δ_H ($CDCl_3$) 2.78 (16H, d of

pentets, J 6.4 Hz, N-CH_2CH_2-S) 2.74 (4H, s, N-CH_2CH_2-N) 1.80 (6H, s, NH); δ_C ($CDCl_3$) 31.7, 35.6 (CH_2S); 41.0, 48.5, 48.71 (CH_2N).

4,13-dithia-N,N',N'',N'''-tetrakis(p-toluenesulphonyl)-1,7,10,16-tetraazahexadecane [120]

A solution of p-toluenesulphonyl chloride (9.31 g, 48.9 mmol) in pyridine (40 ml) was added to a solution of 4,13-dithia-1,7,10,16-tetraazahexadecane in pyridine (100 ml) under nitrogen over a period of 30 minutes. After heating at 60°C for two hours the cooled reaction mixture was poured onto ice (200 g) with stirring, using a glass rod, until the ice melted. After stirring at room temperature for one hour the aqueous layer was extracted with dichloromethane (3 x 200 ml) and washed with hydrochloric acid (2 x 300 ml, 1.0 mol dm^{-3}) and then with distilled water (2 x 300 ml). The organic layer was dried over magnesium sulphate, filtered and solvent removed under reduced pressure to give a brown oil. Two recrystallisations from chloroform/methanol (60 ml, 1:10) with cooling to -5°C gave a pale brown solid (4.82 g, 56%). R_F 0.8 [Silica Gel; CH_2Cl_2-MeOH (9:1)]; m.p. 131-133°C; (Found; C, 51.0; H, 5.71; N, 6.03; $C_{38}H_{50}N_4O_8S_6 0.5H_2O$ requires C, 51.2; H, 5.72; N, 6.28%); m/e (DCI, NH_3) 901 (M^++17) 884 (M^++2) 883 (M^++1) 730; δ_H ($CDCl_3$) 7.73 (4H, d, J 8.3 Hz, half of AA'XX' system, aromatic H) 7.68 (4H, d, J 8.1 Hz, half of AA'XX' system, aromatic H) 7.35 (4H, d, J 8.1 Hz, half of AA'XX' system, aromatic H) 7.27 (4H, d, J 8.1 Hz, half of AA'XX' system, aromatic H) 5.24 (2H, t, J 6.0 Hz, NH) 3.32 (4H, s, N-CH_2CH_2-N) 3.28 (4H, t, J 8.3 Hz, TsN-CH_2) 3.18 (4H, m, CH_2NHTs) 2.67 (8H, m, CH_2S) 2.45 (6H, s, CH_3) 2.40 (6H, s, CH_3); δ_C ($CDCl_3$) 21.3 (CH_3), 30.5, 32.0 (CH_2S), 42.4 (CH_2N), 49.5, 50.2 (CH_2NTs), 126.7, 127.0, 129.5, 129.6, 134.9, 136.7, 143.7 (tosyl aromatic).

N,N',N'',N'''-tetrakis(p-toluenesulphonyl)-1,10-dithia-4,7,13,16-tetraazacyclooctadecane [121]

Caesium carbonate (3.13 g, 9.62 mmol) and the tetratosylamide [120] (4.04 g, 4.58 mmol) were stirred vigorously in dry DMF (300 ml) under nitrogen. A solution of ethane 1,2-diol ditosylate (1.69 g, 4.58 mmol) in DMF (120 ml) was added dropwise over a period of three hours using a pressure equalised addition funnel. The mixture was stirred at room temperature for 18 hours then heated to 60°C for 4 hours. Solvent was removed under reduced pressure and the brown residue dried in vacuo (10^{-2} mm Hg, 60°C). Dichloromethane (50 ml) was added to the residue and the resulting suspension was filtered. After washing with distilled water (3 x 20 ml) the collected solid was dried in vacuo (10^{-2} mm Hg, 40°C). After treatment with hot toluene (50 ml) the resulting suspension was filtered and the collected pale brown solid dried in vacuo (10^{-2} mm Hg) (2.59 g, 62%); R_F 0.7 [silica gel: CH_2Cl_2:MeOH (97:3)]; m.p. 254-256°C; (Found: C, 52.0; H, 5.90; N, 6.21. $C_{40}H_{52}N_4O_8S_6.0.5H_2O$, requires C, 52.3; H, 5.78; N, 6.11); m/e (DCI, NH_3) 909 (M^++1) 753 (M^+-Ts); δ_H ($CDCl_3$) 7.68 (8H, d, J 8.1 Hz, part of AA'XX' system, aromatic H) 7.33 (8H, d, J 8.1 Hz, part of AA'XX' system, aromatic H) 3.34 (8H, s, N-CH_2CH_2-N) 3.29 (8H, t, J 11.4 Hz, CH_2N) 2.80 (8H, t, J 7.4 Hz, CH_2S) 2.43 (12H, s, CH_3).

1,10-dithia-4,7,13,16-tetraazacyclooctadecane [100]

The tetratosylamide [121] (1.80 g, 1.98 mmol) was dissolved in dry THF (50.0 ml) and dry ethanol (5.0 ml) and stirred vigorously in a reaction vessel fitted with an ammonia condenser with an anhydrous calcium carbonate guard tube. After cooling to -77°C (Solid CO_2/Acetone bath) ammonia (250 ml) was condensed into the reaction mixture and

lithium (0.75 g, 108 mmol) was added in several portions with vigorous stirring. A deep blue coloured solution resulted, lasting 5-6 minutes before changing to a yellow colour. After stirring at -77°C for 2 hours the solution was allowed to return to room temperature and the ammonia evaporated. Distilled water (20 ml) was added to the remaining solution and solvent removed under reduced pressure to give a white residue which was dissolved in hydrochloric acid (40 ml, 6 mol dm^{-3}) and washed with diethyl ether (2 x 40 ml). The aqueous layer was evaporated to dryness and the residue dissolved in KOH solution (40 ml, 6 mol dm^{-3}) and extracted with dichloromethane (5 x 50 ml). The organic layer was dried over anhydrous magnesium sulphate, filtered and solvent removed under reduced pressure to give a pale brown oil which solidified over five minutes. The crude product was recrystallised twice from toluene (20 ml) to give a white solid (0.37 g, 64%); m.p. 88-89°C; (Found: C, 49.5; H, 10.0; N, 18.8. $C_{12}H_{28}N_4S_2$ requires C, 49.3; H, 10.0; N, 19.1); m/e (DCl, NH_3) 293 (M^++1) 294 (M^++2) 295 (M^++3), 190, 116; δ_H ($CDCl_3$) 2.85 (8H, m, CH_2N, CH_2S) 2.78 (8H, m, CH_2N, CH_2S) 2.76 (8H, s, N-CH_2CH_2-N) 2.05 (4H, br s, NH); δ_c ($CDCl_3$) 32.93 (CH_2S) 48.0 (CH_2N) 48.3 (CH_2N).

4,7,13,16-tetramethyl-1,10-dithia-4,7,13,16-tetraazacyclooctadecane [101]

1,10-dithia-4,7,13,16-tetraazacyclooctadecane (80.0 mg, 0.274 mmol) was heated at 95°C with formaldehyde (0.24 ml, 37% solution) and formic acid (0.32 ml) for 20 hours. To the cooled solution was added hydrochloric acid (1.0 mol dm^{-3}, 5.0 ml) and the solution evaporated under reduced pressure to give a pale brown residue. After dissolving in water (3.0 ml) the pH was adjusted to 14 with KOH solution and the

solution extracted with dichloromethane (5 x 5 ml), dried over anhydrous potassium carbonate and solvent removed under reduced pressure to give a colourless residue. Recrystallisation from hexane gave a white solid (52.0 mg, 55%); m.p. 43-44^{o}C; (Found: C, 54.8; H, 10.8; N, 15.5; $C_{16}H_{36}N_4S_2.0.2H_2O$ requires C, 54.6; H, 10.4; N, 15.9); m/e (DCI, NH_3) 350 (M^++2) 351 (M^++3) 335, 323, 262, 161; δ_H ($CDCl_3$) 2.64 (16H, s, CH_2N, CH_2S) 2.51 (8H, s, CH_2N) 2.27 (12H, s, CH_3); δ_c ($CDCl_3$) 29.2 (CH_3) 43.1 (CH_2S) 55.2, 57.7 (CH_2N).

N-(p-toluenesulphonyl)-3-aza-1,5-bis(p-toluenesulphonato)pentane [123]

To a solution of p-toluenesulphonyl chloride (107.8 g, 0.565 moles) in pyridine (100 ml) was added a solution of diethanolamine (16.5 g, 0.157 moles) in pyridine (90 ml) dropwise over a period of 30 minutes, under nitrogen. The mixture was left at -18^{o}C for 48 hours. After pouring onto ice (400 g), with stirring until the ice melted, the mixture was left at room temperature for 2 hours to give a yellow/brown solid which was collected by filtration and twice recrystallised from ethanol/toluene (5:1) to give a yellow solid (75.0 g, 84%); m.p. 96-97^{o}C; (Found: C, 52.5; H, 4.92; N, 1.81. $C_{25}H_{29}NO_8S_3$ requires C, 52.9; H, 5.11; N, 2.11); m/e (DCI, NH_3) 585 (M^++18), 568 (M^++1); δ_H ($CDCl_3$) 7.75 (4H, d, J 8.1 Hz,part of AA'XX' system, aromatic H) 7.35 (4H, d, J 8.1 Hz,part of aromatic AA'XX' system, aromatic H) 7.60 (4H, d, J 8.1 Hz, part of AA'XX' system, aromatic H) 7.28 (4H, d, J 8.1 Hz, part of AA'XX' system, aromatic H) 4.11 (4H, t, J 5.9 Hz, CH_2O) 3.37 (4H, t, J 5.9 Hz, CH_2N) 2.43 (3H, s, CH_3) 2.35 (6H, s, CH_3).

N-(p-toluensulphonyl)-3-azapentane-1,5-dithiol [124]

Thiourea (22.8 g, 0.299 moles) was added to a solution of the

1,5-ditosylate [123] (75.0 g, 0.136 moles) in dry ethanol (500 ml) and the solution was heated under reflux, under a nitrogen atmosphere for 30 hours. Solvent was evaporated under reduced pressure and the residue taken up in saturated sodium bicarbonate solution (250 ml) and heated under reflux for 3 hours. The cooled solution was adjusted to pH 7 with hydrochloric acid (6 mol dm^{-3}). The aqueous layer was extracted with dichloromethane (3 x 250 ml) dried over anhydrous magnesium sulphate, filtered and solvent removed under reduced pressure. The colourless residue was chromatographed on 'flash' silica gel eluting with dichloromethane-methanol [199:1]. Evaporation of the eluates gave a clear oil which crystallised over a period of 24 hours (32.7 g, 83%); R_F 0.5 [silica gel:CH_2Cl_2-MeOH (99:1)]; (Found: (M^++1) 292.0460 $C_{11}H_{17}NO_2S_3$ requires 292.0496); m/e (DCI, NH_3) 292 (M^++1); δ_H ($CDCl_3$) 7.70 (2H, d, J 8.0 Hz, part of AA'XX' system, aromatic H) 7.33 (2H, d, J 8.1 Hz, part of AA'XX' system, aromatic H) 3.28 (4H, t, J 7.5 Hz, N-CH_2) 2.74 (4H, m, S-CH_2) 2.43 (3H, s, CH_3) 1.44 (2H, t, J 8.5 Hz, SH); δ_C ($CDCl_3$) 21.4 (CH_3) 23.8 (CH_2S) 52.6 (CH_2N) 126.7, 126.9, 129.7, 135.9, 143.6 (aromatic C).

N-(p-toluenesulphonyl)-1,4-dithia-7-azacyclononane [125] *(and N,N'-(p-toluenesulphonyl)-1,4,10,13-tetrathia-7,16-diazacyclooctadecane)* [128]

Caesium carbonate (3.60 g, 11.0 mmol) was added to dry DMF (500 ml) under a nitrogen atmosphere in a reaction vessel fitted with two pressure equalised addition funnels and the suspension heated to 55°C. A solution of N-(p-toluenesulphonyl)4-azapentane-1,5-dithiol (2.91 g, 10.0 mmol) in DMF (200 ml) and a solution of 1,2-dibromoethane (1.88 g, 10.0 mmol) in DMF (200 ml) were added synchronously over a period of 12

hours with vigorous stirring. After stirring for a further 6 hours at 55°C the solvent was removed under reduced pressure and the residue dried in vacuo (10^{-2} mm Hg, 50°C). The residue was taken up in dichloromethane (100 ml) and washed with distilled water (2 x 100 ml). The organic layer was dried over anhydrous magnesium sulphate, filtered and solvent removed under reduced pressure to give a pale brown oil. Two products were isolated as white crystalline solids by fractional crystallisation from toluene-hexane; [(4:1), 25 ml] gave the 18-membered ring product (0.31 g, 10%); [(2:1), 10 ml] gave the 9-membered ring product (1.38 g, 43%).

[128]; R_F = 0.4 [silica gel: Methanol-dichloromethane (1:99)]; m.p. 206°C; (Found: C, 49.2; H, 5.97; N, 4.20. $C_{26}H_{38}N_2O_4S_6$ requires C, 49.1; H, 5.83; N, 4.27); m/e (DCI, NH_3) 636 (M^++2) 576, 480; δ_H ($CDCl_3$) 7.72 (4H, d, J 8.2 Hz, part of AA'XX' system, aromatic H) 7.32 (4H, d, J 8.2 Hz, part of AA'XX' system, aromatic H) 3.32 (8H, t, J 7.2 Hz, CH_2N) 2.86 (8H, t, J 7.2 Hz, CH_2S) 2.79 (8H, s, S-CH_2CH_2-S) 2.42 (6H, s, CH_3).

[125]; R_F = 0.5 [silica gel: MeOH-CH_2Cl_2 (1:99)]; m.p. 122-124°C; (Found: C, 49.2; H, 5.99; N, 4.42. $C_{13}H_{19}NO_2S_3$ requires C, 49.1; H, 5.83; N, 4.27); m/e 318 (M^++1) 244 162; δ_H ($CDCl_3$) 7.70 (2H, d, J 8.1 Hz,part of AA'XX' system, aromatic H) 7.34 (2H, d, J 8.1 Hz,part of AA'XX' system, aromatic H) 3.40 (4H, m, CH_2N) 3.15 (4H, s, S-CH_2CH_2-S) 3.14 (4H, m, CH_2S) 2.43 (3H, s, CH_3); δ_c ($CDCl_3$) 21.3 (CH_3) 32.2, 34.0 (CH_2S) 53.3, (CH_2N) 127.3, 129.6, 134.0, 143.6 (Aromatic C).

1,4-dithia-7-azacyclononane [126]

A solution of hydrogen bromide in acetic acid (45%, 15.0 ml) and phenol (1.40 g, 14.9 mmol) were added to N-(p-toluenesulphonyl)-1,4-

dithia-7-azacyclononane (1.17 g, 3.69 mmol) and the solution was stirred at 80°C for 48 hours. (A further addition of hydrogen bromide in acetic acid (45%, 5.0 ml) was made after 12 hours.) Toluene was added to the cooled reaction mixture and solvent removed under reduced pressure [azeotrope: 72% toluene, 28% acetic acid]. The residue was taken up in dichloromethane (15 ml) and water (15 ml) and the aqueous layer separated and washed with dichloromethane (3 x 15 ml). The solution was adjusted to pH 14 with sodium hydroxide solution (5 mol dm^{-3}) and extracted with chloroform (4 x 20 ml). The combined organic extracts were dried over anhydrous magnesium sulphate and solvent removed under reduced pressure to give a pale brown solid. Recrystallisation from toluene-hexane gave a pale yellow solid (0.43 g, 73%); m.p. 71-72°C; (Found: C, 43.2; H, 7.83; N, 7.61. $C_6H_{13}NS_2.0.2H_2O$ requires C, 43.2; H, 8.04; N, 8.40); m/e (DCI, MeOH) 164 (M^++1) 116, 89; δ_H ($CDCl_3$) 3.00 (4H, s, S-CH_2CH_2-S) 2.95 (8H, d of m, CH_2N, CH_2S) 2.36 (1H, br s, NH); δ_C ($CDCl_3$) 33.1, 33.2 (CH_2S) 48.1 (CH_2N).

1,2-Bis(1-aza-4,7-dithia-1-cyclononyl)ethane [102]

A mixture of 1,4-dithia-7-azacyclononane (0.200 g, 1.23 mmol), ethane 1,2 diol ditosylate (0.227 g, 6.15 x 10^{-4} moles) and sodium carbonate (0.130 g, 1.23 mmol) in acetonitrile (30 ml) was heated under reflux for 36 hours. The cooled reaction mixture was filtered and solvent evaporated under reduced pressure. The brown coloured residue was dissolved in hydrochloric acid (0.3 mol dm^{-3}, 15 ml) and washed with dichloromethane (3 x 15 ml). The aqueous layer was adjusted to pH 14 with KOH solution (6.0 mol dm^{-3}) and extracted with dichloromethane (4 x 20 ml). The organic layer was dried over anhydrous magnesium sulphate, filtered and solvent removed under reduced pressure to give a pale brown

solid. Recrystallisation from toluene gave a pale yellow solid (0.114 g, 53%); R_F 0.9 [silica gel: MeOH-CH_2Cl_2 (1:99)]; m.p. 104-106°C; (Found: C, 47.3; H, 7.75; N, 7.31. $C_{14}H_{28}N_2S_4.0.3H_2O$ requires C, 47.2; H, 8.04; N, 7.87); m/e (DCI, NH_3) 353 (M^++1) 259, 232, 176; δ_H ($CDCl_3$) 3.09 (8H, s, S-CH_2CH_2-S) 2.87, 2.72 (4H, d of m, CH_2N, CH_2S) 2.62 (4H, m, N-CH_2CH_2-N); δ_C ($CDCl_3$) 58.7, 55.6 (CH_2N) 34.8, 33.1 (CH_2S).

N,N',N'',N'''-tetrakis(p-toluenesulphonyl)-1,10-dioxa-4,7,13,16-tetra-azacyclooctadecane [129]; *and*

N,N'-bis(p-toluenesulphonyl)-1-oxa-4,7-diazacyclononane [130]

Caesium carbonate (8.26 g, 25.4 mmol) was added to a solution of 3-oxa-1,5-bis(p-toluenesulphonato)pentane (5.00 g, 12.1 mmol) in anhydrous DMF (50 ml) under a nitrogen atmosphere. A solution of N,N'-bis(p-toluenesulphonyl)-1,2-diaminoethane (4.44 g, 12.1 mmol) in anhydrous DMF (50 ml) was added dropwise over a period of 4 hours with vigorous stirring. The reaction mixture was stirred at room temperature for 12 hours and heated to 60°C for 4 hours. The solvent was removed under reduced pressure and the residue taken up in dichloromethane (100 ml) and washed with distilled water (2 x 100 ml). The organic layer was dried over anhydrous magnesium sulphate, filtered and solvent removed under reduced pressure to give a pale yellow solid. The mixture was taken up in hot toluene (40 ml) and the 18 membered ring tetratosylamide was collected as a white solid by filtration (warmed filtration apparatus) (1.06 g, 20%). The nine membered ring ditosylamide was obtained from the cooled filtrate as a crystalline solid and collected by filtration and dried in vacuo (10^{-2} mm Hg) (2.17 g, 41%).

Ditosylamide [130]; m.p. 160-161°C [Lit.:[5] 160°C]; (Found: C,

54.8; H, 6.02; N, 6.34. $C_{20}H_{26}N_2O_5S_2$ requires C, 54.8; H, 5.94; N, 6.39); m/e (CI, NH_3) 440 (M^++2) 439 (M^++1) 283; δ_H ($CDCl_3$) 7.70 (4H, d, J 8.1 Hz, part of AA'XX' system, aromatic H) 7.32 (4H, d, J 8.2 Hz, part of AA'XX' system, aromatic H) 3.90 (4H, t, J 4.3 Hz, CH_2O) 3.47 (4H, s, N-CH_2CH_2-N) 3.26 (4H, t, J 4.3 Hz, CH_2N) 2.43 (6H, s, CH_3).

Tetratosylamide [129]; m.p. 242-244°C [Lit.:[6] 245°C]; (Found: C, 55.0; H, 6.13; N, 6.12. $C_{40}H_{52}N_4O_{10}S_4$ requires C, 54.8; H, 5.94; N, 6.39); m/e (CI, NH_3) 880 (M^++2) 879 (M^++1) 722, 440; δ_H ($CDCl_3$) 7.71 (8H, d, J 8.2 Hz, part of AA'XX' system, aromatic H) 7.32 (8H, d, J 8.1 Hz, part of AA'XX' system, aromatic H) 3.54 (8H, t, J 4.9 Hz, CH_2O) 3.32 (8H, s, N-CH_2CH_2-N) 3.22 (8H, t, J 4.8 Hz, CH_2N) 2.44 (12H, s, CH_3).

1,10-dioxa-4,7,13,16-tetraazacyclooctadecane [131]

A solution of hydrogen bromide in acetic acid (45%, 100 ml) and phenol (5.0 g, 53 mmol) were added to the tetratosylamide [129] (1.25 g, 1.43 mmol) and the solution heated under reflux for 6 days. Diethyl ether (40 ml) was added to the cooled reaction mixture and a fine white precipitate collected by filtration. This was taken up in distilled water (40 ml) basified with aqueous KOH (30%) and extracted with dichloromethane (4 x 40 ml). The organic layer was dried over anhydrous potassium carbonate, filtered and solvent removed under reduced pressure. The residue was recrystallised from dichloromethane-hexane to give a colourless crystalline solid (90 mg, 25%); m.p. 58-60°C [Lit.:[6] 58-60°C]; m/e (DCI, NH_3) 262 (M^++2) 261 (M^++1) 204, 131; δ_H ($CDCl_3$) 3.59 (8H, t, J 4.7 Hz, CH_2O) 2.80 (8H, t, J 4.9 Hz, CH_2N) 2.78 (8H, s, N-CH_2CH_2-N) 2.07 (4H, br s, NH); δ_C ($CDCl_3$) 70.0 (CH_2S) 49.2 (CH_2N).

4,7,13,16-tetramethyl-1,10-dioxa-4,7,13,16-tetraazacyclooctadecane [132]

1,10-dioxa-4,7,13,16-tetraazacyclooctadecane (60 mg, 23 mmol) was heated at 95°C with formaldehyde (37%, 0.20 ml) and formic acid (0.27 ml) for 20 hours. Hydrochloric acid (1.0 mol dm^{-3}, 5.0 ml) was added to the cooled solution and solvent removed under reduced pressure. The residue was redissolved in water (3.0 ml) and adjusted to pH 14 with potassium hydroxide. After extraction with dichloromethane (5 x 5 ml) the organic layer was dried over anhydrous potassium carbonate, filtered and solvent removed under reduced pressure. The residue was treated with hexane (3 x 5 ml), the extracts combined and solvent removed under reduced pressure to give a clear oil which crystallised on cooling (5°C) (59 mg, 80%); m.p. = 23-25°C; δ_H ($CDCl_3$) 3.55 (8H, t, J 5.5 Hz, CH_2O) 2.63 (8H, t, J 5.5 Hz, CH_2N) 2.59 (8H, s, NCH_2CH_2N) 2.28 (12H, s, CH_3).

6.2.8. Silver(I) complexes

Silver(I) complex of 1,10-dithia-4,7,13,16-tetraazacyclooctadecane [100], $[AgL][PF_6]$ (134)

Silver nitrate (8.4 mg, 4.9 x 10^{-5} moles) in dry acetonitrile (1.0 ml) was added to 1,10-dithia-4,7,13,16-tetraazacyclooctadecane (14.4 mg, 4.9 x 10^{-5} moles) in dry dichloromethane (1.0 ml). The solution was filtered to remove a small amount of dark coloured precipitate. Solvent was removed from the filtrate under reduced pressure and the residue dissolved in dry methanol (1 ml). To this was added ammonium hexafluorophosphate (8.0 mg, 4.9 x 10^{-5} mol) in methanol (1.0 ml). After rapid filtration the solution was left at -20°C in the dark for 3 hours. Colourless crystals were collected by filtration, washed with cold methanol (2 x 0.5 ml) and dried in vacuo (10^{-2} mm Hg) (19.5 mg, 73%); (Found: C, 25.3; H, 4.96; N, 9.84. $C_{12}H_{28}N_4S_2PF_6Ag.H_2O$

requires C, 25.6; H, 5.33; N, 9.95); m/e (FAB, glycerol) 401, 399 (M^+) [$^{109}Ag^+$-L and $^{107}Ag^+$-L]; δ_H (CD_3OD) 2.99 (16H, s, CH_2N, CH_2S) 2.79 (8H, s, CH_2N). X-ray crystal structure data - see appendix.

Silver(I) Complex of 4,7,13,16-tetramethyl-1,10-dithia-4,7,13,16-tetraazacyclooctadecane [101], *[Ag-L][PF_6]* (135)

Silver nitrate (13.2 mg, 7.76 x 10^{-5} moles) in acetonitrile (1.0 ml) was added to the ligand [101] (27.0 mg, 7.76 x 10^{-5} moles) in dichloromethane (1.0 ml). After standing for 30 min. the solution was filtered and the solvent evaporated from the filtrate under reduced pressure. The brown residue was dissolved in methanol (1.0 ml) and to this was added ammonium hexafluorophosphate (12.5 mg, 7.7 x 10^{-5} moles). After filtration the volume of solvent was reduced to 0.75 ml and the solution left in the dark at -20°C for 24 hours. Brown crystals were isolated and redissolved in hot methanol (0.5 ml) and left at -20°C for 12 hours. Colourless crystals were collected by filtration, washed with cold methanol (2 x 0.5 cm^3) and dried in vacuo (10^{-2} mm Hg) (28.4 mg, 61%); (Found: C, 31.4; H, 5.91; N, 8.89. $C_{16}H_{36}N_4S_2PF_6Ag$ requires C, 31.9; H, 5.99; N, 9.31); m/e (FAB, glycerol) 457, 455 (M^+) [$^{109}Ag^+$-L and $^{107}Ag^+$-L]; δ_H (CD_3OD) 3.05 (8H, t, J 5.8 Hz, CH_2S) 2.72 (8H, t, J 5.6 Hz, CH_2N) 2.60 (8H, br s, N-CH_2CH_2-N) 2.41 (12H, s, CH_3); δ_C (CD_3OD) 59.0 (CH_2N) 55.8 (CH_2N) 44.3 (CH_3-N) 33.4 (CH_2-S).

Silver(I) complex of 1,2-bis(1-aza-4,7-dithia-1-cyclononyl)ethane [102], *[Ag-L][PF_6]* (136)

Silver nitrate (9.4 mg, 5.5 x 10^{-5} moles) in acetonitrile (1.0 ml) was added to the ligand [102] (19.4 mg, 5.5 x 10^{-5} moles) in dichloromethane (1.0 ml) and the mixture filtered and solvent evaporated

from the filtrate under reduced pressure. The colourless residue was dissolved in methanol (1.0 ml) and to this was added ammonium hexafluorophosphate (9.0 mg, 5.5 x 10^{-5} moles) in methanol (1.0 ml) and the solution filtered. The volume of the filtrate was reduced to 0.5 ml and the solution left at -20°C for 36 hours. Needle shaped colourless crystals were collected by filtration and washed with cold methanol (2 x 0.5 ml) and dried in vacuo (10^{-2} mm Hg) (17 mg, 55%). Crystals suitable for X-ray diffraction studies were grown from a solution of the complex in MeOH:MeCN (10:1); (Found: C, 27.6; H, 4.61; N, 4.39. $C_{14}H_{28}N_2S_4PF_6Ag$ requires C, 27.8; H, 4.62; N, 4.62); m/e (FAB, glycerol) 461, 459 (M^+) [$^{109}Ag^+$-L and $^{107}Ag^+$-L]; δ_H (D_2O) 2.6-2.9 (28H, m). X-ray crystal structure data - see appendix.

Silver(I) complex of 1,4-dithia-7-azacyclononane [126], *[Ag-(L)$_2$][PF$_6$]*

Synthesis as for [134] using a 2:1 ratio of ligand to silver nitrate. Colourless crystals were obtained after recrystallisation from methanol (10 mg, 28%); m/e (FAB, Glycerol) 435, 433 [^{109}Ag-$(L)_2^+$ and ^{107}Ag-$(L)_2^+$]; δ_H (D_2O) 2.93 (8H, s, S-CH_2CH_2-S) 2.86 (8H, m, CH_2S) 2.78 (8H, m, CH_2N).

Silver(I) complex of 25,26-diaza-3,7,15,19-tetrathiatricyclo-[19.3.1.1.1]hexacosa 1(25)9(26),10,12,21,23-hexane [137], *[Ag-L][PF$_6$]*

Synthesis as for [134]; Yield (5 mg, 25%); m/e (FAB, Glycerol-MeOH) 531, 529 ($^{109}Ag^+$-L and $^{107}Ag^+$-L); δ_H (D_2O) 7.49 (2H, t, 7.7 Hz, Pyr H) 7.52 (4H, d, J 7.7 Hz, Pyr H) 4.29 (8H, s, Pyr-CH_2-S) 2.74 (8H, t, 7.5 Hz, S-CH_2-C) 1.75 (4H, p, J 7.5 Hz, C-CH_2-C).

Silver(I) complex of 15-diaza-3,6,9-trithiabicyclo[9.3.1]pentadecyl-1(15),11,13-triene-12-carboxylate ethyl ester [138], [*AgL*] [PF_6]

Synthesis as for [134]. Recrystallisation from acetonitrile gave yellow crystals (10 mg, 19%); m/e (FAB, Glycerol-H_2O) 438, 436 ($^{109}Ag^+$-L, $^{107}Ag^+$-L); δ_H (CD_3CN) 8.02 (1H, d, J 8.0, Pyr H) 7.19 (1H, d, J 7.8 Hz, Pyr H) 4.24 (2H, s, Pyr-CH_2-S) 4.14 (2H, q, J 7.1 Hz, $C\underline{H}_2CH_3$) 3.91 (2H, s, Ar-CH_2-S) 2.55 (4H, m, CH_2S) 2.29 (4H, m, CH_2S) 1.15 (3H, t, J 7.0 Hz, CH_3).

Silver(I) complex of 15-aza-3,9-dithia-6-oxabicyclo[9.3.1]pentadecyl-1(15),11,13-triene [139], [*Ag-L*] [NO_3]

Silver nitrate (17.0 mg, 0.099 mmol) was added to the ligand (24 mg, 0.099 mmol) in CH_2Cl_2-CH_3CN [(1:1), 1.0 ml]. A fine white precipitate was collected by filtration and recrystallised from water (0.4 ml) (9 mg, 22%); m/e [FAB, glycerol-H_2O] 350, 348 (Ag^+-L, $^{107}Ag^+$-L).

Silver(I) complex of 21-aza-3,15-dithia-6,9,12-trioxabicyclo-[15.3.1]Heneicosa-1(21),17,19-triene [140], [*Ag-L*]$_2$[PF_6]$_2$

Synthesis as for (134), colourless crystals (20 mg, 52%); m/e (FAB-Glycerol-MeOH) 438, 436 ($^{109}Ag^+$-L, $^{107}Ag^+$-L); δ_H ($(CD_3)_2CO$) 7.87 (1H, t, J 7.6 Hz, Pyr H) 7.47 (2H, d, J 7.6 Hz, Pyr H) 4.19 (4H, s, Pyr-CH_2-S) 3.79 (4H, t, J 5.2 Hz, S-$CH_2C\underline{H}_2$-O) 3.75 (8H, s, O-CH_2CH_2-O) 3.10 (4H, t, J 5.2 Hz, S-$C\underline{H}_2CH_2$-O). X-ray crystal structure cell data - see appendix.

6.3. pH-Metric Titrations

6.3.1. Apparatus

The titration cell was a double walled glass vessel (capacity 5 ml) which was maintained at 25^{o}C, using a Techne Tempette Junior TE-8J. Titration solutions were stirred using a magnetic stirrer and kept under an atmosphere of nitrogen. Titrations were performed using an automatic titrator (Mettler DL20, 1 ml capacity) and burette functions (volume increments and equilibration time) were controlled by a BBC microprocessor. The pH was measured using a Corning 001854 combination microelectrode which was calibrated using buffer solutions at pH 4.008 ($CO_2H.C_6H_4CO_2K$, 0.05M) and pH 6.865 (KH_2PO_4, 0.025M/Na_2HPO_4, 0.025M). Data was stored on the BBC microprocessor and transferred to the MTS mainframe using KERMIT and subsequently analysed by two non-linear least squares programs SCOG2 and SUPERQUAD.

6.3.2. Acid dissociation constants

Stock solutions of the ligand (0.002M) in milli-Q water (25.0 ml) with nitric acid (1 eq. per amine nitrogen of the ligand) and tetramethylammonium nitrate (I = 0.10 mol dm^{-3}) were prepared. In each titration 3.5 ml of the stock ligand solution was titrated with tetramethylammonium hydroxide (0.109M), the exact molarity of which was determined by titration against hydrochloric acid, 0.100M.

6.3.3. Metal binding constants

Stock solutions were prepared as above with the addition of one equivalent of silver nitrate. Titrations were performed as before.

6.4. NMR Experiments

6.4.1. ^{13}C nmr experiments

^{13}C nmr spectra of the ^{13}C-acetocarbonyl enriched (99%)

[9]-N_3-triacid and its indium(III) complex were recorded on a Bruker AC250 spectrometer (62.896 MHz). Solutions of the complex ($1.0x10^{-2}$M) in D_2O (2.0 ml) were acidified with concentrated nitric acid (15.6M). Typically 75-100 scans were required to obtain spectra which could be integrated (a line broadening factor of 6.0 Hz was employed). The shifts were quoted relative to an internal Dioxane reference at 66.296 ppm.

6.4.2. ^{71}Ga nmr experiments

^{71}Ga nmr were recorded on a Bruker AC250 spectrometer with spectral frequency 76.282 MHz. Chemical shifts are quoted in ppm, referenced to $Ga(D_2O)_6^{3+}$ at δ = 0 ppm and $Ga(OD)_4^-$ at 222.6 ppm. Solutions of the gallium [9]-N_3-triacid complex ($1.5x10^{-2}$M) in D_2O (0.6 ml) were acidified with concentrated nitric acid (15.6M).

6.5. X-ray Crystal Structure Determinations

The X-ray crystal structures of the $[Ag\text{-}pyS_2O_3]_2[PF_6]_2$, $[Ag\text{-}N,N'\text{-}bis[9]NS_2][PF_6]$ and $[In\text{-}[9]N_3\text{-}triacid]HCl.H_2O$ complexes were determined by Professor George Ferguson (Department of Chemistry, University of Guelph, Ontario, Canada). The X-ray crystal structures of the $[Ag\text{-}[18]N_4S_2][PF_6]$, $[Ga\text{-}[9]N_3\text{-}triacid]$ and $[In\text{-}[9]N_3\text{-}triacid]HCl.H_2O$ complexes were determined by Dr. Harry Adams and Dr. Neil Bailey (University of Sheffield, U.K.). Cell data, experimental details, positional and thermal parameters and molecular dimensions for each structure are given in the Appendix.

6.6. References

1. B.K. Vriesema, J. Buter and R.M. Kellogg, J. Org. Chem., 49, 110 (1984).

2. M. Briellmann, S. Kaderli, C.J. Meyer and A.D. Zuberbuhler, Helv. Chim. Acta, 70, 680 (1987).

3. M. Takahashi and S. Takamoto, Bull. Chem. Soc. Japan, 50(12), 3413 (1977).

4. J.C. Eck and C.S. Marvel, Org. Synth. Coll. vol. 2, 74 (1943).

5. W. Rasshofer, W. Wehner and F. Vögtle, Liebigs. Ann. Chem., 916 (1976).

6. J.F. Biernat and E. Luboch, Tetrahedron, 40(10), 1927 (1984).

PUBLICATIONS, COLLOQUIA AND CONFERENCES

PUBLICATIONS

1. Towards Tumour Imaging with Indium-III Labelled Macrocycle Antibody Conjugates, Andrew S. Craig, Ian M. Helps, Karl J. Jankowski, David Parker, Nigel R.A. Beeley, Byron A. Boyce, Michael A.W. Eaton, Andrew T. Millican, Kenneth Millar, Alison Phipps, Stephen K. Rhind, Alice Harrison and Carole Walker, J. Chem. Soc. Chem. Commun., 794 (1989).

2. The Solution and Solid State Structure of a Macrocyclic Silver(I) Complex with 6,9,12-trioxa-3,5-dithia-21-azabicyclo[15.3.1]-henicosa-1(21),17,19-triene, Andrew S. Craig, George Ferguson, Karen E. Matthes and David Parker, Acta Cryst., C45, 741 (1989).

3. Stable Macrocyclic Complexes of Silver(I), Andrew S. Craig, David Parker and Hans-Jürgen Buschmann, 13th International Symposium on Macrocyclic Chemistry - Book of Abstracts, 276-277 (1988).

4. Crystal and Molecular Structure of a Seven Coordinate Chloro-Indium(III) Complex of Triazacyclononanetriacetic Acid, Andrew S. Craig, Ian M. Helps, David Parker, Harry Adams, Neil A. Bailey, Mark G. Williams, John M.A. Smith and George Ferguson, Polyhedron (in press, 1989).

5. Gallium-71 NMR and Crystal Structure of the Gallium(III) Complex of 1,4,7-triazacyclononanetriacetic Acid:- An Emerging Radiopharmaceutical, Harry Adams, Neil A. Bailey, Andrew S. Craig and David Parker, J. Chem. Soc. Chem. Commun. (submitted, 1989).

6. A. Silver Sandwich Complex of an Aza-Thia Macrocycle, Andrew S. Craig, George Ferguson, Alan J. Lough and David Parker, Angew. Chem. Int. Ed. Eng. (submitted, 1989).

7. Synthesis, Solution Stability and Crystal Structure of Aza-Thia Macrocyclic Complexes of Silver(I), Andrew S. Craig, Ritu Kataky, David Parker, Harry Adams, Neil A. Bailey and Hermann Schneider, J. Chem. Soc. Perkin Commun. (submitted, 1989).

8. The Structure of a Conformationally Strained Macrocyclic Copper(II) Complex with N,N'-carboxymethyl-1,4-diaza-7-thiacyclononane, Andrew S. Craig, George Ferguson and David Parker, Acta Cryst. Sect. B (in press, 1989).

RESEARCH CONFERENCES ATTENDED

1. R.S.C. Graduate Symposium, University of Durham, 27th March (1987).

2. Molecular Recognition, University of Sheffield, 14th December, 1987.

3. R.S.C. Perkin Division, North East Regional Meeting, University of Newcastle upon Tyne, 21st September, 1987.

4. R.S.C. Graduate Symposium, University of Durham, 19th April, 1988.

5. 13th International Symposium on Macrocyclic Chemistry, Hamburg, F.R.G., 4-8th September, 1988.
   Poster presented: Stable Macrocyclic Complexes of Silver(I).

6. R.S.C. Perkin Division, North East Regional Meeting, University of York, 16th December, 1988.

7. U.K. Macrocycle Group, Annual Meeting, University of Durham, 6th January, 1989.

8. R.S.C. Graduate Symposium, University of Durham, 12th April, 1989.

RESEARCH COLLOQUIA, LECTURES AND SEMINARS

A list of all the research colloquia, seminars and lectures arranged by the Department of Chemistry during the period of the author's residence as a postgraduate student is presented; "*" indicating the author's attendance.

1st August 1986 to 31st July 1987

*16.10.86 Prof. N.N. Greenwood (University of Leeds)
Glorious Gaffes in Chemistry

*23.10.86 Prof. H.W. Kroto (University of Sussex)
Chemistry in Stars, between Stars and in the Laboratory

29.10.86 Prof. E.H. Wong (University of New Hampshire, U.S.A.)
Coordination Chemistry of P-O-P Ligands

*5.11.86 Prof. D. Döpp (University of Duisburg)
Cyclo-additions and Cyclo-reversions Involving Captodative Alkenes

*6.11.86 Dr. R.M. Scrowston (University of Hull)
From Myth and Magic to Modern Medicine

*13.11.86 Prof. Sir G. Allen (Unilever Research)
Biotechnology and the Future of the Chemical Industry

20.11.86 Dr. A. Milne/Mr. S. Christie (International Paints)
Chemical Serendipity - A Real Life Case Study

26.11.86 Dr. N.D.S. Canning (University of Durham)
Surface Adsorption Studies of Relevance to Heterogeneous Ammonia Synthesis

*3.12.86 Dr. J. Miller (Dupont Central Research, U.S.A.)
Molecular Ferromagnets: Chemistry and Physical Properties

8.12.86 Prof. T. Dorfmüller (University of Bielefeld)
Rotational Dynamics in Liquids and Polymers

22.1.87 Prof. R.H. Ottewill (University of Bristol)
Colloid Science a Challenging Subject

28.1.87 Dr. W. Clegg (University of Newcastle-upon-Tyne)
Carboxylate Complexes of Zinc; Charting a Structural Jungle

4.2.87 Prof. A. Thomson (University of East Anglia)
Metalloproteins and Magnetooptics

*5.2.87 Dr. P. Hubberstey (University of Nottingham)
Demonstration Lecture on Various Aspects of Alkali Metal Chemistry

11.2.87 Dr. T. Shepherd (University of Durham)
Pteridine Natural Products; Synthesis and Use in Chemotherapy

12.2.87 Dr. P.J. Rodgers (I.C.I. Billingham)
Industrial Polymers from Bacteria

*17.2.87 Prof. E.H. Wong (University of New Hampshire, U.S.A.)
Symmetrical Shapes from Molecules to Art and Nature

*19.2.87 Dr. M. Jarman (Institute of Cancer Research)
The Design of Anti Cancer Drugs

4.3.87 Dr. R. Newman (University of Oxford)
Change and Decay: A Carbon-13 CP/MAS NMR Study of Humification and Coalification Processes

*5.3.87 Prof. S.V. Ley (Imperial College)
Fact and Fantasy in Organic Synthesis

*9.3.87 Prof. F.G. Bordwell (Northeastern University, U.S.A.)
Carbon Anions, Radicals, Radical Anions and Radical Cations

11.3.87 Dr. R.D. Cannon (University of East Anglia)
Electron Transfer in Polynuclear Complexes

*12.3.87 Dr. E.M. Goodger (Cranfield Institute of Technology)
Alternative Fuels for Transport

*18.3.87 Prof. R.F. Hudson (University of Kent)
Homolytic Rearrangements of Free Radical Stability

6.5.87 Dr. R. Bartsch (University of Sussex)
Low Co-ordinated Phosphorus Compounds

7.5.87 Dr. M. Harmer (I.C.I. Chemicals & Polymer Group)
The Role of Organometallics in Advanced Materials

11.5.87 Prof. S. Pasynkiewicz (Technical University, Warsaw)
Thermal Decomposition of Methyl Copper and its Reactions with Trialkylaluminium

17.5.87 Prof. R.F. Hudson (University of Kent)
Aspects of Organophosphorus Chemistry

27.5.87 Dr. M. Blackburn (University of Sheffield)
Phosphonates as Analogues of Biological Phosphate Esters

*24.6.87 Prof. S.M. Roberts (University of Exeter)
Synthesis of Novel Antiviral Agents

26.6.87 Dr. C. Krespan (E.I. Dupont de Nemours)
Nickel(0) and Iron(0) as Reagents in Organofluorine Chemistry

<u>1st August 1987 to 31st July 1988</u>

15.10.87 Dr. M.J. Winter (University of Sheffield)
Pyrotechnics (Demonstration Lecture)

*22.10.87 Prof. G.W. Gray (University of Hull)
Liquid Crystals and their Applications

*29.10.87 Mrs. S. van Rose (Geological Museum)
Chemistry of Volcanoes

4.11.87 Mrs. M. Mapletoft (Durham Chemistry Teachers' Centre)
Salters' Chemistry

*5.11.87 Dr. A.R. Butler (University of St. Andrews)
Chinese Alchemy

12.11.87 Dr. J. Davidson (Heriot-Watt University)
Metal Promoted Oligomerisation Reactions of Alkynes

*12.11.87 Prof. D. Seebach (E.T.H. Zurich)
From Synthetic Methods to Mechanistic Insight

*26.11.87 Dr. D.H. Williams (University of Cambridge)
Molecular Recognition

*27.11.87 Prof. R.L. Williams (Metropolitan Police Forensic Science)
Science and Crime

*3.12.87 Dr. J. Howard (I.C.I. Wilton)
Chemistry of Non-Equilibration Processes

*10.12.87 Dr. C.J. Ludman (Durham University)
Explosives

16.12.87 Mr. R.M. Swart (I.C.I.)
The Interaction of Chemicals with Lipid Bilayers

19.12.87 Prof. P.G. Sammes (Smith, Kline and French)
Chemical Aspects of Drug Development

*21.1.88 Dr. F. Palmer (University of Nottingham)
Luminescence (Demonstration Lecture)

*25.1.88 Dr. L. Harwood (Oxford University)
Synthetic Approaches to Phorbols Via Intramolecular Furan Diels-Alder Reactions: Chemistry Under Pressure

*28.1.88 Dr. A. Cairns-Smith (Glasgow University)
Clay Minerals and the Origin of Life

*11.2.88 Prof. J.J. Turner (University of Nottingham)
Catching Organometallic Intermediates

*18.2.88 Dr. K. Borer (University of Durham Industrial Research Labs.)
The Brighton Bomb - A Forensic Science View

*25.2.88 Prof. A. Underhill (University of Bangor)
Molecular Electronics

*3.3.88 Prof. W.A.G. Graham (University of Alberta, Canada)
Rhodium and Iridium Complexes in the Activation of Carbon-Hydrogen Bonds

16.3.88 L. Bossons (Durham Chemistry Teachers' Centre)
GCSE Practical Assessment

7.4.88 Prof. M.P. Hartshorn (University of Canterbury, New Zealand)
Aspects of Ipso-Nitration

13.4.88 Mrs. E. Roberts (SATRO Officer for Sunderland)
Durham Chemistry Teachers' Centre Talk: Links Between Industry and Schools

18.4.88 Prof. C.A. Nieto de Castro (University of Lisbon and Imperial College)
Transport Properties of Non-Polar Fluids

*19.4.88 Graduate Chemists (Northeast Polytechnics and Universities)
R.S.C. Graduate Symposium

25.4.88 Prof. D. Birchall (I.C.I. Advanced Materials)
Environmental Chemistry of Aluminium

27.4.88 Dr. R. Richardson (University of Bristol)
X-Ray Diffraction from Spread Monolayers

*27.4.88 Dr. J.A. Robinson (University of Southampton)
Aspects of Antibiotic Biosynthesis

*28.4.88 Prof. A. Pines (University of California, Berkeley, U.S.A.)
Some Magnetic Moments

*11.5.88 Dr. W.A. McDonald (I.C.I. Wilton)
Liquid Crystal Polymers

11.5.88 Dr. J. Sodeau (University of East Anglia)
Durham Chemistry Teachers' Centre Lecture: Spray Cans, Smog and Society

8.6.88 Prof. J.-P. Majoral (Université Paul Sabatier)
Stabilisation by Complexation of Short-Lived Phosphorus Species

*29.6.88 Prof. G.A. Olah (University of Southern California)
New Aspects of Hydrocarbon Chemistry

1st August 1988 to 31st July 1989

6.10.88 Prof. R. Schmutzler (Technische Universitat Braunschweig)
Fluorophosphines Revisited - New Contributions to an Old Theme

18.10.88 Mr. F. Bollen (Durham Chemistry Teachers' Centre)
Lecture about the use of SATIS in the classroom

*18.10.88 Dr. J. Dingwall (Ciba Geigy)
Phosphorus-containing Amino Acids: Biologically Active Natural and Unnatural Products

18.10.88 Dr. C.J. Ludman (Durham University)
The Energetics of Explosives

*21.10.88 Prof. P. Von Rague Schleyer (Universitat Erlangen Nurnberg)
The Fruitful Interplay Between Calculational and Experimental Chemistry

*27.10.88 Prof. C.W. Rees (Imperial College London)
Some Very Heterocyclic Compounds

*9.11.88 Dr. G. Singh (Teesside Polytechnic)
Towards Third Generation Anti-Leukaemics

*10.11.88 Prof. J.I.G. Cadogan (British Petroleum)
From Pure Science to Profit

16.11.88 Dr. K.A. McLauchlan (University of Oxford)
The Effect of Magnetic Fields on Chemical Reactions

24.11.88 Drs. R.R. Baldwin and R.W. Walker (Hull University)
Combustion: Some Burning Problems

1.12.88 Dr. R. Snaith (Cambridge University)
Egyptian Mummies: What, Where, Why and How?

7.12.88 Dr. G. Hardgrove (St. Olaf College, U.S.A.)
Polymers in the Physical Chemistry Laboratory

9.12.88 Dr. C. Jäger (Friedrich-Schiller University GDR)
NMR Investigations of Fast Ion Conductors of the NASICON Type

14.12.88 Dr. C. Mortimer (Durham Chemistry Teachers' Centre)
The Hindenberg Disaster - an Excuse for Some Experiments

*26.1.89 Prof. R.R. Jennings (Warwick University)
Chemistry of the Masses

1.2.89 Mr. D. Waters and T. Cressey (Durham Chemistry Teachers' Centre)
GCSE Chemistry 1988: A Coroner's Report

*2.2.89 Prof. L.D. Hall (Addenbrooke's Hospital, Cambridge)
NMR - A Window to the Human Body

*9.2.89 Prof. J.E. Baldwin (Oxford University)
Recent Advances in the Bioorganic Chemistry of Penicillin Biosynthesis

*13.2.89 Prof. R.R. Schrock (M.I.T.)
Recent Advances in Living Metathesis

*15.2.89 Dr. A.R. Butler (St. Andrews University)
Cancer in Linxiam: The Chemical Dimension

*16.2.89 Prof. B.J. Aylett (Queen Mary College, London)
Silicon-Based Chips:- The Chemist's Contribution

22.2.89 Dr. G. MacDougall (Edinburgh University)
Vibrational Spectroscopy of Model Catalytic Systems

23.2.89 Dr. B.F.G. Johnson (Cambridge University)
The Binary Carbonyls

1.3.89 Dr. R.J. Errington (University of Newcastle-upon-Tyne)
Polymetalate Assembly in Organic Solvents

*9.3.89 Dr. I. Marko (Sheffield University)
Catalytic Asymmetric Osmylation of Olefins

14.3.89 Mr. P. Revell (Durham Chemistry Teachers' Centre)
Implementing Broad and Balanced Science 11-16

15.3.89 Dr. R. Aveyard (University of Hull)
Surfactants at your Surface

*20.4.89 Dr. M. Casey (University of Salford)
Sulphoxides in Stereoselective Synthesis

*27.4.89 Dr. D. Crich (University College London)
Some Novel Uses of Free Radicals in Organic Synthesis

3.5.89 Mr. A. Ashman (Durham Chemistry Teachers' Centre)
The Chemical Aspects of the National Curriculum

*3.5.89 Dr. P.C.B. Page (University of Liverpool)
Stereocontrol of Organic Reactions Using 1,3-dithiane-1-oxides

10.5.89 Prof. P.B. Wells (Hull University)
Catalyst Characterisation and Activity

11.5.89 Dr. J. Frey (Southampton University)
Spectroscopy of the Reaction Path: Photodissociation Raman Spectra of NOCl

16.5.89 Dr. R. Stibr (Czechoslovak Academy of Sciences)
Recent Developments in the Chemistry of Intermediate-Sited Carboranes

*17.5.89 Dr. C.J. Moody (Imperial College)
Reactive Intermediates in Heterocyclic Synthesis

23.5.89 Prof. P. Paetzold (Aachen)
Iminoboranes XB≡NR: Inorganic Acetylenes?

14.6.89 Dr. M.E. Jones (Durham Chemistry Teachers' Centre)
Discussion Session on the National Curriculum

15.6.89 Prof. J. Pola (Czechoslovak Academy of Sciences)
Carbon Dioxide Laser Induced Chemical Reactions - New Pathways in Gas-Phase Chemistry

28.6.89 Dr. M.E. Jones (Durham Chemistry Teachers' Centre)
GCSE and A Level Chemistry 1989

11.7.89 Dr. D. Nicholls (Durham Chemistry Teachers' Centre)
Demo.: Liquid Air

APPENDIX - CRYSTAL DATA

(1) [In-(9)-N_3-triacid].HCl.H_2O

Crystal data for [(L)InCl].0.46(H_2O), 0.18(H_2O); $C_{12}H_{19}ClInN_3O_6$.0.64(H_2O), M_r = 463.1. Crystal dimension 0.25 x 0.43 x 0.55 mm, Monoclinic a = 7.017(3), b, 17.701(5), c = 14.083(3) Å, β = 99.02(2)°. U = 1728(2) $Å^3$, D_c = 1.78 gcm^{-3}, Z = 4. Space group $P2_1/n$ Mo-K_α radiation (λ = 0.71073 Å), μ(Mo-K_α) = 15.3 cm^{-1}, $F(000)$ = 929.6.

Three dimensional data were collected using a CAD4 diffractometer in the range $4^\circ < 2\theta < 40^\circ$ by the $\omega/2\theta$ scan method. Collection of data in the range $40^\circ < 2\theta < 54^\circ$ was terminated because of rapid decay of the crystal soon after data collection for this shell started; there had been no significant decay during the initial data collection. Structure solution and refinement progressed with the 4-40° data set. The cell data were determined by a least-squares analysis of the setting angles of 25 reflections with $14 < 2\theta < 40^\circ$. 3259 reflections were collected of which 2564 were unique (R-factor on averaging 1.6%). The data were corrected for absorption (max. and min. transmission coefficients 0.734, 0.664) and during refinement for secondary extinction. The 1488 reflection with $I > 3\sigma(I)$ were labelled observed and used in structure solution and refinement. The structure was solved via the heavy atom method and refined by full-matrix least-squares calculations. Two sites corresponding to partially occupied water molecules were also located. No hydrogen of water molecules could be located form difference maps, but all hydrogens of the complex were clearly visible. The complex molecules are linked by an unusually short O-H-O hydrogen bond (2.487(6) Å) and a difference map showed a clear maximum midway between the two oxygen atoms. All other hydrogen atoms were positioned geometrically (C-H 0.95 Å) and included but not refined in the refinement process. Refinement converged with R = 0.039, R_w = 0.075 (largest shift/error ratio 0.05). Scattering factor and anomalous dispersion data were taken from International Tables for Crystallography and all calculations were done with SDP-Plus. In the refinement cycle, weights were derived from the counting statistics; a final difference map had no chemically significant maxima.

Table

Positional and thermal parameters and their e.s.d.'s

Atom	x	y	z	B(Å^2)
In	0.00307(6)	0.15377(2)	0.18844(3)	1.87(1)
CL	0.1644(3)	0.15215(8)	0.3518(1)	3.39(5)
O1	0.1160(5)	0.2749(2)	0.1920(3)	2.73(9)
O2	0.0896(6)	0.3854(2)	0.2636(3)	3.5(1)
O3	0.1028(6)	0.0225(2)	0.1918(3)	2.71(9)
O4	0.0882(6)	-0.0811(2)	0.2767(3)	3.6(1)
O5	0.1989(6)	0.1441(2)	0.0891(3)	2.5(1)
O6	0.2295(6)	0.1133(3)	-0.0587(3)	3.7(1)
O7	0.200(3)	0.336(1)	0.017(1)	11.0(6)
O8	0.210(7)	0.498(2)	0.003(3)	10(1)
N1	-0.2499(6)	0.2359(3)	0.2043(3)	2.3(1)
N2	-0.2407(7)	0.0760(3)	0.2281(3)	2.2(1)
N3	-0.2012(8)	0.1443(2)	0.0454(4)	2.4(1)
C1	-0.4095(8)	0.1984(3)	0.2439(4)	2.6(1)
C2	-0.3489(9)	0.1236(4)	0.2886(4)	2.5(1)
C3	-0.1557(9)	0.0109(4)	0.2791(5)	2.8(1)
C4	0.0228(9)	-0.0162(3)	0.2446(4)	2.6(1)
C5	-0.3638(9)	0.0517(4)	0.1373(5)	3.2(2)
C6	-0.2748(9)	0.0640(4)	0.0485(5)	3.0(1)
C7	-0.0795(10)	0.1537(3)	-0.0300(5)	3.2(2)
C8	0.1336(9)	0.1346(4)	0.0020(5)	2.6(1)
C9	-0.3604(9)	0.2001(4)	0.0374(4)	2.9(1)
C10	-0.3149(9)	0.2652(4)	0.1057(5)	2.9(1)
C11	-0.1632(8)	0.2986(3)	0.2642(4)	2.7(1)
C12	0.0287(9)	0.3200(3)	0.2378(5)	2.5(1)

Atoms O7 and O8 are from water molecules that have partial occupancies (0.46 and 0.18 respectively). Atom O8 was refined isotropically.

Anisotropically refined atoms are given in the form of the isotropic equivalent thermal parameter defined as:

$$4/3[a^2B_{11} + b^2B_{22} + c^2B_{33} + abcos\gamma B_{12} + accos\beta B_{13} + bccos\alpha B_{23}]$$

Table . Molecular dimensions

(a) Bond lengths (Å)

		(1)	(2)
In	CL	2.399(2)	2.406(4)
In	O1	2.284(4)	2.281(6)
In	O3	2.424(4)	2.413(6)
In	O5	2.116(5)	2.106(5)
In	N1	2.332(5)	2.338(6)
In	N2	2.331(5)	2.335(6)
In	N3	2.288(5)	2.281(6)
O1	C12	1.246(8)	1.262(9)
O2	C12	1.267(7)	1.254(8)
O3	C4	1.212(8)	1.219(9)
O4	C4	1.292(7)	1.287(8)
O5	C8	1.252(7)	1.275(8)
O6	C8	1.228(8)	1.214(9)
N1	C1	1.483(8)	1.490(9)
N1	C10	1.486(8)	1.479(9)
N1	C11	1.468(7)	1.459(8)
N2	C2	1.489(8)	1.490(9)
N2	C3	1.437(8)	1.473(9)
N2	C5	1.489(8)	1.485(9)
N3	C6	1.514(8)	1.492(9)
N3	C7	1.473(10)	1.468(10)
N3	C9	1.482(8)	1.486(9)
C1	C2	1.499(9)	1.513(10)
C3	C4	1.492(9)	1.489(11)
C5	C6	1.499(10)	1.516(11)
C7	C8	1.531(10)	1.493(12)
C9	C10	1.502(9)	1.515(10)
C11	C12	1.501(9)	1.507(10)

O1	O7	2.84(2)	2.84
O2	O4(I)	2.487(6)	2.497
O7	O8	2.87(5)	2.96
O8	O8(II)	2.94(7)	2.79

(b) Bond angles (°)

			(1)	(2)
CL	In	O1	83.1(1)	83.4(2)
CL	In	O3	83.0(1)	82.8(2)
CL	In	O5	112.0(1)	112.0(1)
CL	In	N1	99.6(1)	99.7(2)
CL	In	N2	91.0(1)	91.2(2)
CL	In	N3	168.3(2)	168.6(3)
O1	In	O3	143.2(1)	143.2(2)
O1	In	O5	80.3(1)	80.5(2)
O1	In	N1	71.3(2)	71.1(2)
O1	In	N2	144.5(2)	144.9(2)
O1	In	N3	104.8(2)	104.3(2)
O3	In	O5	73.8(1)	73.6(2)
O3	In	N1	144.8(2)	145.0(2)
O3	In	N2	69.5(2)	69.4(2)
O3	In	N3	94.9(1)	95.3(2)
O5	In	N1	134.2(2)	134.3(2)
O5	In	N2	133.5(2)	132.9(2)
O5	In	N3	78.1(2)	77.9(2)
N1	In	N2	75.3(2)	75.7(2)
N1	In	N3	75.4(2)	75.5(2)
N2	In	N3	77.6(2)	77.7(2)
In	O1	C12	114.6(4)	115.0(4)
In	O3	C4	113.3(4)	113.5(5)
In	O5	C8	118.9(4)	118.8(4)

In	N1	C1	112.8(3)	112.4(4)
In	N1	C10	104.8(4)	105.0(4)
In	N1	C11	105.9(3)	105.8(4)
C1	N1	C10	111.6(4)	111.9(5)
C1	N1	C11	113.0(5)	112.6(5)
C10	N1	C11	108.2(5)	108.8(5)
In	N2	C2	105.2(4)	104.9(4)
In	N2	C3	109.3(4)	109.2(4)
In	N2	C5	108.3(4)	109.0(4)
C2	N2	C3	112.1(5)	110.1(5)
C2	N2	C5	112.1(4)	112.2(5)
C3	N2	C5	109.7(5)	111.3(5)
In	N3	C6	102.3(3)	102.2(4)
In	N3	C7	105.8(4)	106.0(4)
In	N3	C9	112.2(4)	113.1(4)
C6	N3	C7	111.5(5)	110.7(6)
C6	N3	C9	111.8(5)	111.3(5)
C7	N3	C9	112.6(5)	113.1(5)
N1	C1	C2	111.8(5)	111.9(5)
N2	C2	C1	113.3(5)	113.1(6)
N2	C3	C4	113.6(5)	111.4(6)
O3	C4	O4	123.0(6)	123.8(7)
O3	C4	C3	120.7(5)	121.6(6)
O4	C4	C3	116.3(6)	114.5(6)

N2	C5	C6	114.4(5)	112.7(5)
N3	C6	C5	110.4(5)	112.2(6)
N3	C7	C8	114.4(6)	115.6(6)
O5	C8	O6	124.6(6)	123.7(6)
O5	C8	C7	116.7(6)	116.6(6)
O6	C8	C7	118.7(6)	119.7(6)
N3	C9	C10	112.4(5)	111.7(5)
N1	C10	C9	109.5(5)	110.3(5)
N1	C11	C12	110.8(5)	110.9(6)
O1	C12	O2	124.2(6)	124.3(7)
O1	C12	C11	120.0(5)	118.9(6)
O2	C12	C11	115.7(6)	116.7(6)
O1	O7	O8	117.(1)	116
O7	O8	O8(II)	90.(2)	86

The roman numerals refer to the following equivalent positions:

I. 0.5 - x, 0.5 + y, 0.5 - z

II. -x, 1 - y, - z.

Deposition data

General Temperature Factor Expressions - U's

Name	U(1,1)	U(2,2)	U(3,3)	U(1,2)	U(1,3)	U(2,3)
In	0.0158(3)	0.0272(4)	0.0282(4)	-0.0010(2)	0.0038(3)	-0.0030(2)
CL	0.037(1)	0.057(1)	0.032(1)	0.0013(7)	-0.0022(9)	-0.0034(7)
O1	0.025(2)	0.029(2)	0.053(2)	-0.007(2)	0.014(2)	-0.011(2)
O2	0.037(3)	0.033(3)	0.065(3)	-0.005(2)	0.009(2)	-0.010(2)
O3	0.029(2)	0.029(2)	0.046(2)	0.009(2)	0.012(2)	0.012(2)
O4	0.039(3)	0.031(3)	0.067(3)	0.013(2)	0.011(2)	0.016(2)
O5	0.021(2)	0.044(3)	0.028(2)	-0.005(2)	0.005(2)	-0.005(2)
O6	0.041(3)	0.057(3)	0.049(2)	-0.002(2)	0.023(2)	-0.011(2)
O7	0.09(1)	0.26(2)	0.067(9)	-0.03(1)	0.005(9)	0.060(9)
N1	0.013(2)	0.031(3)	0.043(3)	-0.004(2)	0.007(2)	-0.007(2)
N2	0.017(3)	0.031(3)	0.033(3)	-0.001(2)	-0.001(2)	-0.007(2)
N3	0.024(3)	0.035(3)	0.031(3)	-0.000(2)	0.002(2)	-0.013(2)
C1	0.017(3)	0.041(4)	0.041(3)	0.008(3)	0.008(3)	-0.003(3)
C2	0.020(3)	0.047(4)	0.031(3)	-0.000(4)	0.011(3)	0.003(3)
C3	0.031(4)	0.030(4)	0.047(4)	0.005(3)	0.008(3)	0.011(3)
C4	0.032(4)	0.037(4)	0.031(3)	-0.007(3)	0.006(3)	-0.010(3)
C5	0.027(3)	0.025(4)	0.073(4)	-0.006(3)	0.017(3)	-0.002(3)
C6	0.034(4)	0.028(3)	0.047(4)	-0.009(3)	-0.007(3)	-0.014(3)
C7	0.028(4)	0.062(5)	0.031(4)	-0.003(3)	0.001(3)	0.002(3)
C8	0.029(4)	0.033(3)	0.037(4)	-0.006(3)	0.009(3)	-0.004(3)
C9	0.026(3)	0.046(4)	0.035(3)	0.003(3)	-0.001(3)	0.006(3)
C10	0.025(3)	0.037(4)	0.050(4)	0.008(3)	0.005(3)	0.008(3)
C11	0.022(3)	0.033(4)	0.046(4)	-0.005(3)	0.003(3)	-0.011(3)
C12	0.038(4)	0.014(3)	0.044(4)	-0.006(3)	0.006(3)	0.008(3)

The form of the anisotropic thermal parameter is:

$$\exp[-2\pi^2(U_{11}h^2a^{*2}+U_{22}k^2b^{*2}+U_{33}l^2c^{*2}+2U_{12}hka^*b^*+2U_{13}hla^*c^*+2U_{23}klb^*c^*)]$$

Deposition data

Calculated hydrogen coordinates (C-H 0.95 Å, Biso 5 Å^2)

Atom	x	y	z
H(02-04)	0.2506	0.4021	0.2434
H1a	-0.4494	0.2302	0.2913
H1b	-0.5142	0.1907	0.1933
H2a	-0.4612	0.0969	0.2990
H2b	-0.2688	0.1324	0.3484
H3a	-0.1241	0.0235	0.3452
H3b	-0.2477	-0.0288	0.2715
H5a	-0.3900	-0.0006	0.1422
H5b	-0.4812	0.0793	0.1307
H6a	-0.3689	0.0550	-0.0065
H6b	-0.1702	0.0299	0.0485
H7a	-0.1282	0.1217	-0.0823
H7b	-0.0881	0.2048	-0.0506
H9a	-0.3831	0.2191	-0.0264
H9b	-0.4732	0.1755	0.0511
H10a	-0.4272	0.2952	0.1052
H10b	-0.2154	0.2950	0.0861
H11a	-0.2470	0.3410	0.2550
H11b	-0.1458	0.2837	0.3298

(2) Ga-[9]N_3-triacid

Crystal data for [{$(CH_2)_2$.N.CH_2.CO_2)$_3$Ga]; $C_{12}H_{18}GaN_3O_6$; M = 370.01. Crystallises from *solvent* as colourless needles; crystal dimensions 0.68 x 0.05 x 0.13 mm. Monoclinic, a = 8.927(10), b = 13.646(15), c = 12.086(10) Å, beta = 105.36(7) °, U = 1419.6(25) Å^3; D_c = 1.731 g cm^{-3}, Z = 4. Space group $P2_1/n$ (a non-standard setting of $P2_1/c$, C_{2h}^5, No. 14), Mo K_{alpha} radiation ($\overline{\lambda}$ = 0.71069A), μ(Mo K_{alpha}) = 19.62 cm^{-1}, F(000) = 759.78.

Three-dimensional, room temperature X-ray data were collected in the range 3.5 < 2θ < 50° on a Nicolet R3 4-circle diffractometer by the omega scan method. The 1491 independent reflections for which |F|/σ(|F|) > 3.0 were corrected for Lorentz and polarisation effects, and for absorption, by analysis of 10 azimuthal scans. The structure was solved by Patterson and Fourier techniques and refined by blocked cascade least squares methods. Hydrogen atoms were included in calculated positions with isotropic thermal parameters related to those of the supporting atom. Refinement converged at a final R 0.0627, with allowance for the thermal anisotropy of all non-hydrogen atoms. Complex scattering factors were taken from reference Z, and from the program package SHELXTL[Y] as implemented on the Data General Nova 3 computer. A weighting scheme w^{-1} = [$\sigma^2(F)+g(F)^2$], with g = 0.00025, was used in the final cycles of refinement. Table 1 lists atomic positional parameters with estimated standard deviations.

Reference Z International Tables for X-ray Crystallography, Vol. 4, Kynoch Press, Birmingham, 1974.

Reference Y G. M. Sheldrick, SHELXTL, An integrated system for solving, refining and displaying crystal structures from diffraction data (Revision 4), University of Gottingen, F.R.Germany.

Supplementary material

anisotropic thermal vibrational parameters with e.s.ds.
hydrogen atom position parameters
observed structure amplitudes and calculated structure factors.

TABLE 2. (a) Bond lengths (Å)

Ga(1)-O(1)	1.948(5)	Ga(1)-O(3)	1.933(6)
Ga(1)-O(5)	1.940(5)	Ga(1)-N(1)	2.104(6)
Ga(1)-N(2)	2.102(6)	Ga(1)-N(3)	2.110(6)
O(1)-C(4)	1.306(10)	O(2)-C(4)	1.215(9)
O(3)-C(8)	1.307(10)	O(4)-C(8)	1.228(11)
O(5)-C(12)	1.314(10)	O(6)-C(12)	1.224(9)
N(1)-C(1)	1.521(10)	N(1)-C(10)	1.484(10)
N(1)-C(11)	1.504(10)	N(2)-C(2)	1.490(10)
N(2)-C(3)	1.494(9)	N(2)-C(5)	1.516(9)
N(3)-C(6)	1.520(11)	N(3)-C(7)	1.480(11)
N(3)-C(9)	1.511(9)	C(1)-C(2)	1.522(11)
C(3)-C(4)	1.545(11)	C(5)-C(6)	1.538(12)
C(7)-C(8)	1.534(12)	C(9)-C(10)	1.529(12)
C(11)-C(12)	1.539(11)		

TABLE 2. (b) Bond angles (deg.)

O(1)-Ga(1)-O(3)	95.6(2)	O(1)-Ga(1)-O(5)	94.2(2)
O(3)-Ga(1)-O(5)	95.0(2)	O(1)-Ga(1)-N(1)	167.1(2)
O(3)-Ga(1)-N(1)	97.2(2)	O(5)-Ga(1)-N(1)	83.6(2)
O(1)-Ga(1)-N(2)	83.5(2)	O(3)-Ga(1)-N(2)	167.7(2)
O(5)-Ga(1)-N(2)	97.3(2)	N(1)-Ga(1)-N(2)	84.2(2)
O(1)-Ga(1)-N(3)	98.8(2)	O(3)-Ga(1)-N(3)	83.8(2)
O(5)-Ga(1)-N(3)	167.0(2)	N(1)-Ga(1)-N(3)	83.7(2)
N(2)-Ga(1)-N(3)	84.3(2)	Ga(1)-O(1)-C(4)	116.1(4)
Ga(1)-O(3)-C(8)	115.9(5)	Ga(1)-O(5)-C(12)	115.5(5)
Ga(1)-N(1)-C(1)	108.8(4)	Ga(1)-N(1)-C(10)	105.7(5)
C(1)-N(1)-C(10)	112.0(5)	Ga(1)-N(1)-C(11)	103.7(4)
C(1)-N(1)-C(11)	111.7(6)	C(10)-N(1)-C(11)	114.4(6)
Ga(1)-N(2)-C(2)	105.1(5)	Ga(1)-N(2)-C(3)	103.8(4)
C(2)-N(2)-C(3)	115.1(6)	Ga(1)-N(2)-C(5)	109.0(5)
C(2)-N(2)-C(5)	111.2(5)	C(3)-N(2)-C(5)	112.0(6)
Ga(1)-N(3)-C(6)	104.1(4)	Ga(1)-N(3)-C(7)	102.9(4)
C(6)-N(3)-C(7)	114.9(6)	Ga(1)-N(3)-C(9)	108.7(4)
C(6)-N(3)-C(9)	113.0(5)	C(7)-N(3)-C(9)	112.2(7)
N(1)-C(1)-C(2)	112.1(5)	N(2)-C(2)-C(1)	110.7(6)
N(2)-C(3)-C(4)	112.6(6)	O(1)-C(4)-O(2)	125.2(7)
O(1)-C(4)-C(3)	115.1(6)	O(2)-C(4)-C(3)	119.6(7)
N(2)-C(5)-C(6)	111.7(6)	N(3)-C(6)-C(5)	108.7(6)
N(3)-C(7)-C(8)	111.7(7)	O(3)-C(8)-O(4)	124.4(7)
O(3)-C(8)-C(7)	115.5(7)	O(4)-C(8)-C(7)	120.2(7)
N(3)-C(9)-C(10)	112.4(6)	N(1)-C(10)-C(9)	109.6(7)
N(1)-C(11)-C(12)	111.1(7)	O(5)-C(12)-O(6)	124.1(7)
O(5)-C(12)-C(11)	116.2(7)	O(6)-C(12)-C(11)	119.8(7)

TABLE 1. Atom coordinates ($\times 10^4$) and temperature factors ($\AA^2 \times 10^3$)

atom	x	y	z	U_{eq}
Ga(1)	1103(1)	2517(1)	3169(1)	27(1)*
O(1)	2924(6)	1670(4)	3532(4)	30(2)*
O(2)	5199(6)	1441(4)	3117(5)	47(2)*
O(3)	389(6)	2151(4)	4488(4)	34(2)*
O(4)	-889(6)	977(4)	5164(5)	49(2)*
O(5)	2235(6)	3666(4)	3886(4)	32(2)*
O(6)	1879(6)	5172(4)	4510(5)	46(2)*
N(1)	-658(6)	3541(4)	2475(5)	26(2)*
N(2)	1615(6)	2648(5)	1575(5)	30(2)*
N(3)	-563(7)	1487(4)	2308(5)	30(2)*
C(1)	-475(8)	3888(5)	1322(6)	30(3)*
C(2)	1131(9)	3661(6)	1176(7)	36(3)*
C(3)	3323(7)	2459(7)	1850(6)	38(3)*
C(4)	3902(9)	1791(6)	2909(6)	33(3)*
C(5)	689(9)	1890(6)	758(6)	36(3)*
C(6)	141(8)	1050(6)	1404(6)	35(3)*
C(7)	-671(10)	807(6)	3237(8)	42(4)*
C(8)	-405(9)	1336(6)	4393(7)	34(3)*
C(9)	-2077(9)	2015(6)	1798(7)	36(3)*
C(10)	-2145(9)	3013(6)	2357(7)	38(3)*
C(11)	-361(9)	4354(6)	3345(7)	35(3)*
C(12)	1378(9)	4432(6)	3967(6)	31(3)*

* Equivalent isotropic U defined as one third of the trace of the orthogonalised U_{ij} tensor

TABLE Anisotropic temperature factors ($Å^2 \times 10^3$)

atom	U_{11}	U_{22}	U_{33}	U_{23}	U_{13}	U_{12}
Ga(1)	26(1)	29(1)	25(1)	1(1)	8(1)	1(1)
O(1)	30(3)	40(3)	21(3)	3(2)	8(2)	1(3)
O(2)	28(3)	64(4)	48(4)	-0(3)	9(3)	14(3)
O(3)	41(3)	36(3)	27(3)	-3(2)	13(3)	-2(3)
O(4)	64(4)	44(4)	53(4)	10(3)	38(3)	5(3)
O(5)	30(3)	34(3)	32(3)	-5(3)	9(2)	-3(3)
O(6)	51(4)	37(3)	48(4)	-12(3)	10(3)	-15(3)
N(1)	23(3)	29(4)	26(4)	3(3)	7(3)	0(3)
N(2)	27(3)	31(4)	31(3)	3(3)	9(3)	6(3)
N(3)	33(4)	33(4)	29(3)	6(3)	17(3)	5(3)
C(1)	34(5)	20(4)	41(5)	6(4)	17(4)	12(4)
C(2)	36(5)	42(5)	31(5)	9(4)	9(4)	7(4)
C(3)	32(4)	46(4)	41(4)	3(6)	19(3)	-0(6)
C(4)	32(5)	35(5)	33(5)	1(4)	14(4)	-3(4)
C(5)	43(5)	41(5)	28(5)	-5(4)	16(4)	-6(4)
C(6)	24(4)	45(5)	33(5)	-7(4)	4(4)	3(4)
C(7)	44(6)	33(5)	53(6)	11(5)	18(5)	-2(5)
C(8)	33(5)	38(5)	35(5)	5(4)	14(4)	12(4)
C(9)	22(5)	41(5)	41(5)	5(5)	0(4)	-5(4)
C(10)	35(5)	41(5)	39(5)	-12(5)	9(4)	3(4)
C(11)	36(5)	38(5)	30(5)	2(4)	6(4)	7(4)
C(12)	38(5)	34(5)	26(4)	1(4)	13(4)	-4(4)

The anisotropic temperature factor exponent takes the form:

$$-2\pi^2(h^2a^{*2}U_{11}+k^2b^{*2}U_{22}+ \ldots +2hka^*b^*U_{12})$$

TABLE Hydrogen coordinates ($\times 10^4$) and temperature factors ($Å^2 \times 10^3$)

atom	x	y	z	U
H(1a)	-616	4586	1284	37
H(1b)	-1249	3584	713	37
H(2a)	1871	4119	1614	44
H(2b)	1103	3717	379	44
H(3a)	3555	2153	1199	49
H(3b)	3858	3074	2002	49
H(5a)	1336	1619	313	44
H(5b)	-200	2199	255	44
H(6a)	-622	664	872	40
H(6b)	1010	643	1767	40
H(7a)	-1681	509	3051	55
H(7b)	107	308	3305	55
H(9a)	-2205	2104	991	43
H(9b)	-2913	1621	1916	43
H(10a)	-2320	2930	3102	48
H(10b)	-2974	3394	1882	48
H(11a)	-698	4961	2956	43
H(11b)	-938	4233	3898	43

(3) $[Ag\text{-}(18)\text{-}N_4S_2][PF_6]$

Crystal data for $[(S.(CH_2)_2.NH.(CH_2)_2.NH.(CH_2)_2)_2Ag]^+$ $(PF_6)^-$; $C_{12}H_{28}AgF_6N_4PS_2$; M = 545.34. Crystallises from *solvent* as colourless, elongated blocks; crystal dimensions 0.45 x 0.25 x 0.225 mm. Orthorhombic, a = 10.859(22), b = 20.247(26), c = 9.742(10) Å, U = 2142(6) Å^3; D_c = 1.691 g cm^{-3}, Z = 4. Space group Pbcn (D_{2h}^{14}, No. 60), Mo K_{alpha} radiation (λ = 0.71069A), μ(Mo K_{alpha}) = 12.46 cm^{-1}, F(000) = 1103.84.

Three-dimensional, room temperature X-ray data were collected in the range 3.5 < 2θ < 50° on a Nicolet R3 4-circle diffractometer by the omega scan method. The 1205 independent reflections for which $|F|/\sigma(|F|) > 3.0$ were corrected for Lorentz and polarisation effects, and for absorption, by analysis of 7 azimuthal scans. The structure was solved by Patterson and Fourier techniques and refined by blocked cascade least squares methods. Hydrogen atoms were included in calculated positions with isotropic thermal parameters related to those of the supporting atom. Refinement converged at a final R 0.0718, with allowance for the thermal anisotropy of all non-hydrogen atoms. Complex scattering factors were taken from reference Z, and from the program package SHELXTL[Y] as implemented on the Data General Nova 3 computer. A weighting scheme $w^{-1} = [\sigma^2(F)+g(F)^2]$, with g = 0.0009, was used in the final cycles of refinement. Table 1 lists atomic positional parameters with estimated standard deviations.

Reference Z International Tables for X-ray Crystallography, Vol. 4, Kynoch Press, Birmingham, 1974.

Reference Y G. M. Sheldrick, SHELXTL, An integrated system for solving, refining and displaying crystal structures from diffraction data (Revision 4), University of Gottingen, F.R.Germany.

Supplementary material

anisotropic thermal vibrational parameters with e.s.ds.
hydrogen atom position parameters
observed structure amplitudes and calculated structure factors.

TABLE 2. (a) Bond lengths (Å)

Ag(1)-S(1)	2.658(5)	Ag(1)-N(1)	2.589(10)
Ag(1)-N(2)	2.553(11)	S(1)-C(1)	1.805(13)
S(1)-C(6a)	1.822(13)	N(1)-C(2)	1.438(18)
N(1)-C(3)	1.480(20)	N(2)-C(4)	1.472(18)
N(2)-C(5)	1.461(18)	C(1)-C(2)	1.540(18)
C(3)-C(4)	1.481(21)	C(5)-C(6)	1.459(21)
P(1)-F(1)	1.447(16)	P(1)-F(2)	1.513(13)
P(1)-F(3)	1.561(14)		

TABLE 2. (b) Bond angles (deg.)

S(1)-Ag(1)-N(1)	75.9(3)	S(1)-Ag(1)-N(2)	113.2(3)
N(1)-Ag(1)-N(2)	70.6(4)	S(1)-Ag(1)-S(1a)	124.5(2)
S(1)-Ag(1)-N(1a)	144.7(3)	N(1)-Ag(1)-N(1a)	104.3(4)
S(1)-Ag(1)-N(2a)	74.6(3)	N(1)-Ag(1)-N(2a)	99.5(4)
N(2)-Ag(1)-N(2a)	164.3(5)	Ag(1)-S(1)-C(1)	100.4(4)
Ag(1)-S(1)-C(6a)	101.1(5)	C(1)-S(1)-C(6a)	104.2(7)
Ag(1)-N(1)-C(2)	113.4(8)	Ag(1)-N(1)-C(3)	107.7(8)
C(2)-N(1)-C(3)	115.4(10)	Ag(1)-N(2)-C(4)	107.1(8)
Ag(1)-N(2)-C(5)	111.5(8)	C(4)-N(2)-C(5)	112.0(11)
S(1)-C(1)-C(2)	117.2(9)	N(1)-C(2)-C(1)	113.0(11)
N(1)-C(3)-C(4)	112.6(11)	N(2)-C(4)-C(3)	110.4(11)
N(2)-C(5)-C(6)	112.9(12)	C(5)-C(6)-S(1a)	119.0(9)
F(1)-P(1)-F(2)	91.1(10)	F(1)-P(1)-F(3)	166.6(8)
F(2)-P(1)-F(3)	87.7(8)	F(1)-P(1)-F(1a)	110.7(12)
F(1)-P(1)-F(2a)	91.1(10)	F(2)-P(1)-F(2a)	176.2(16)
F(1)-P(1)-F(3a)	82.7(8)	F(2)-P(1)-F(3a)	89.4(8)
F(3)-P(1)-F(3a)	84.0(10)		

TABLE 1. Atom coordinates ($\times 10^4$) and temperature factors (Å$^2 \times 10^3$)

atom	x	y	z	U_{eq}
Ag(1)	0	953(1)	2500	58(1)*
S(1)	-1502(3)	341(1)	760(4)	81(1)*
N(1)	-107(12)	1738(4)	405(10)	81(4)*
N(2)	2162(9)	1125(5)	1535(12)	88(4)*
C(1)	-1331(12)	859(6)	-736(13)	88(5)*
C(2)	-1128(13)	1602(7)	-492(14)	92(6)*
C(3)	1119(15)	1739(7)	-258(15)	100(6)*
C(4)	2141(13)	1746(7)	749(15)	99(6)*
C(5)	3087(13)	1136(8)	2624(15)	116(7)*
C(6)	3000(11)	569(7)	3544(16)	103(6)*
P(1)	5000	1395(2)	7500	86(2)*
F(1)	6068(15)	989(7)	7225(21)	321(12)*
F(2)	4687(11)	1420(10)	5988(13)	262(10)*
F(3)	4058(12)	1969(6)	7717(12)	201(7)*

* Equivalent isotropic U defined as one third of the trace of the orthogonalised U_{ij} tensor

TABLE Hydrogen coordinates (x10^4) and temperature factors ($Å^2$x10^3)

atom	x	y	z	U
H(N1)	-232	2167	797	97
H(N2)	2350	771	914	102
H(1a)	-2066	812	-1276	100
H(1b)	-638	697	-1248	100
H(2a)	-1856	1781	-74	98
H(2b)	-992	1813	-1362	98
H(3a)	1188	1349	-815	115
H(3b)	1190	2124	-829	115
H(4a)	2031	2107	1376	104
H(4b)	2908	1799	270	104
H(5a)	2983	1534	3146	126
H(5b)	3890	1133	2212	126
H(6a)	3309	192	3057	108
H(6b)	3527	663	4311	108

TABLE Anisotropic temperature factors ($Å^2$x10^3)

atom	U_{11}	U_{22}	U_{33}	U_{23}	U_{13}	U_{12}
Ag(1)	53(1)	63(1)	57(1)	0	-6(1)	0
S(1)	86(2)	52(1)	105(2)	-2(2)	-42(2)	-0(2)
N(1)	136(9)	44(4)	64(6)	-5(4)	19(8)	5(7)
N(2)	73(7)	94(8)	99(8)	-32(7)	11(6)	-17(6)
C(1)	103(10)	91(9)	70(8)	-16(7)	-20(8)	22(8)
C(2)	133(12)	75(9)	68(8)	25(7)	5(9)	26(9)
C(3)	157(14)	68(9)	76(10)	3(7)	44(11)	-23(9)
C(4)	113(11)	88(10)	96(11)	-12(9)	53(10)	-41(9)
C(5)	71(8)	155(14)	124(13)	-54(12)	19(10)	-27(9)
C(6)	65(8)	108(10)	134(13)	-37(10)	-35(8)	13(8)
P(1)	65(2)	72(3)	120(4)	0	-25(4)	0
F(1)	264(17)	267(16)	432(28)	-188(17)	-164(17)	204(13)
F(2)	147(10)	507(27)	131(9)	-149(15)	-27(8)	-37(13)
F(3)	222(12)	213(12)	169(11)	29(9)	4(10)	103(10)

The anisotropic temperature factor exponent takes the form:

$-2\pi^2(h^2a^{*2}U_{11}+k^2b^{*2}U_{22}+ \ldots +2hka^*b^*U_{12})$

(4) [Ag-N,N'-bis(9)NS_2][PF_6]

Table of Experimental Details

A. Crystal Data

C14 H28 Ag F6 N2 P S4

F.W. 605.48 F(000) = 1224

crystal dimensions: 0.07 x 0.18 x 0.20 mm

peak width at half-height = 0.30°

Mo Kα radiation (λ = 0.71073 A)

temperature = 21 ± 1°

tetragonal space group P41212

a = 10.128 (3) A c = 21.711 (4) A

V = 2227.0 Å^3

Z = 4 D_c = 1.81 g/cm^3

μ = 13.8 cm-1

Table of Experimental Details

B. Intensity Measurements

Instrument:	Enraf-Nonius CAD4 diffractometer
Monochromator:	Graphite crystal, incident beam
Attenuator:	Zr foil, factor 17.6
Take-off angle:	2.8°
Detector aperture:	2.0 to 2.5 mm horizontal
	4.0 mm vertical
Crystal-detector dist.:	21 cm
Scan type:	ω-2θ
Scan rate:	1 - 7 /min (in omega)
Scan width, deg:	0.6 + 0.350 tan θ
Maximum 2@:	50.0°
No. of refl. measured:	4341 total, 1946 unique
Corrections:	Lorentz-polarization
	Reflection averaging (agreement on I = 4.3%)
	Numerical absorption (from76.52 to91.96 on I)

C. Structure Solution and Refinement

Solution:	Patterson method
Minimization function:	$\Sigma w(\|Fo\|-\|Fc\|)$
Least-squares weights:	$4Fo^2 \eta^2 (Fc^2)$
Anomalous dispersion:	All non-hydrogen atoms
Reflections included:	1050 with $Fo^2 > 3.0\ (Fo^2)$
Parameters refined:	141
Unweighted agreement factor:	0.030
Weighted agreement factor:	0.035
Esd of obs. of unit weight:	1.05
Convergence, largest shift:	< 0.005
High peak in final diff. map:	0.52 (9) e/A^3
Computer hardware:	PDP-11
Computer software:	SDP-PLUS (Enraf-Nonius &
	B. A. Frenz & Associates, Inc.)

Table

Molecular dimensions

(a) Bond lengths (A)

Ag	S4	2.802(2)
Ag	S7	2.611(2)
Ag	N1	2.586(5)
S4	C3	1.804(9)
S4	C5	1.853(9)
S7	C6	1.783(9)
S7	C8	1.805(7)
N1	C10	1.431(8)
N1	C2	1.450(10)
N1	C9	1.517(10)
C10	C10(I)	1.465(9)
C2	C3	1.497(11)
C5	C6	1.475(13)
C8	C9	1.488(11)
P	F1	1.525(4)
P	F2	1.539(4)
P	F3	1.572(5)
P	F4	1.574(5)

The distances involving the minor components of the disordered atoms were constrained as follows;

N1	C2*	1.469
N1	C9*	1.469
C3	C2*	1.524
C6	C5*	1.524
C8	C9*	1.524
S4	C5*	1.817

(b) Bond angles ( )

S4	Ag	S4(I)	156.83(7)	C10	N1	C9	106.5(6)
S4	Ag	S7	80.90(7)	C2	N1	C9	111.8(5)
S4	Ag	S7(I)	93.04(6)	N1	C10	C10(I)	121.2(6)
S4	Ag	N1	74.0(1)	N1	C2	C3	115.3(7)
S4	Ag	N1(I)	126.6(1)	S4	C3	C2	116.1(6)
S7	Ag	S7(I)	149.62(6)	S4	C5	C6	115.7(6)
S7	Ag	N1	77.0(1)	S7	C6	C5	121.1(6)
S7	Ag	N1(I)	130.1(1)	S7	C8	C9	117.2(5)
N1	Ag	N1(I)	73.7(1)	N1	C9	C8	113.2(6)
Ag	S4	C3	95.6(3)	F1	P	F2	180.0
Ag	S4	C5	100.8(3)	F1	P	F3	90.0(2)
C3	S4	C5	99.5(4)	F1	P	F4	89.8(2)
Ag	S7	C6	101.3(3)	F2	P	F3	90.0(2)
Ag	S7	C8	100.2(2)	F2	P	F4	90.2(2)
C6	S7	C8	106.1(4)	F3	P	F4	68.1(3)
Ag	N1	C10	105.7(3)	F3	P	F4(I)	91.9(3)
Ag	N1	C2	115.5(4)	N1	C2*	C3	112.(3)
Ag	N1	C9	100.8(4)	S4	C5*	C6	116.(2)
C10	N1	C2	115.3(6)	N1	C9*	C8	114.(3)

The romal numeral (I) refers to equivalent position y, x, -z.

Table 1.

Positional and thermal parameters and their e.s.d.'s

Atom	x	y	z	B(A)
Ag	0.09287(5)	0.09287(5)	0.0	3.56(1)
S4	0.2831(2)	-0.0188(2)	-0.0779(1)	5.03(5)
S7	0.2638(2)	0.0174(2)	0.0828(1)	4.47(5)
N1	0.0564(4)	-0.1596(5)	0.0051(3)	2.8(1)
C10	-0.0805(7)	-0.1797(6)	-0.0082(5)	5.1(2)
C2	0.1472(8)	-0.2384(8)	-0.0312(4)	4.1(2)
C3	0.1979(9)	-0.1736(9)	-0.0884(3)	5.1(2)
C5	0.4093(8)	-0.0711(8)	-0.0211(5)	5.2(3)
C6	0.4099(9)	0.0023(10)	0.0376(4)	7.3(3)
C8	0.2070(7)	-0.1488(7)	0.0967(3)	4.0(2)
C9	0.0733(8)	-0.1841(8)	0.0736(4)	3.4(2)
P	0.5103(2)	0.5103(2)	0.0	4.14(4)
F1	0.4038(6)	0.4038(6)	0.0	12.5(2)
F2	0.6177(5)	0.6177(5)	0.0	11.6(2)
F3	0.4345(5)	0.5862(5)	0.0524(2)	7.8(1)
F4	0.5867(6)	0.4329(6)	0.0518(2)	9.8(2)
C2*	0.062(4)	-0.197(4)	-0.061(2)	3.3(9)
C5*	0.431(4)	-0.001(4)	-0.032(2)	2.8(9)
C9*	0.147(4)	-0.232(4)	0.045(2)	2.4(8)

C2/C2*, C5/C5*, and C9/C9* are disordered atom sites with relative occupancies 0.84/0.16.

The x and y coordinates of each of the atoms, Ag, P, F1, and F2 were constrained to be equal.

Anisotropically refined atoms are given in the form of the isotropic equivalent thermal parameter defined as:

$$4/3[a^2B_{11} + b^2B_{22} + c^2B_{33} + abcos\gamma B_{12} + accos\beta B_{13} + bccos\alpha B_{23}]$$

Deposition data

General Temperature Factor Expressions - U's

Name	U(1,1)	U(2,2)	U(3,3)	U(1,2)	U(1,3)	U(2,3)
AG	0.0307(2)	U(1,1)	0.0738(4)	-0.0007(4)	-0.0104(3)	-U(1,3)
S4	0.052(1)	0.071(1)	0.069(1)	-0.002(1)	0.013(1)	0.023(1)
S7	0.044(1)	0.049(1)	0.076(1)	-0.007(1)	-0.018(1)	0.001(1)
N1	0.026(3)	0.031(2)	0.051(3)	-0.000(2)	-0.000(3)	0.001(3)
C10	0.039(3)	0.033(3)	0.121(6)	-0.008(3)	-0.001(6)	0.017(5)
C2	0.056(5)	0.034(5)	0.066(6)	-0.003(4)	0.018(5)	-0.006(5)
C3	0.073(5)	0.065(5)	0.057(5)	0.006(4)	0.009(5)	-0.001(5)
C5	0.028(4)	0.052(5)	0.119(9)	0.009(5)	0.010(6)	0.013(5)
C6	0.032(4)	0.133(8)	0.114(7)	0.005(6)	-0.011(6)	0.045(6)
C8	0.049(5)	0.055(4)	0.048(4)	-0.004(4)	0.000(4)	0.018(4)
C9	0.035(5)	0.044(4)	0.052(5)	-0.006(4)	-0.009(4)	0.015(4)
P	0.0555(9)	U(1,1)	0.046(1)	0.018(1)	0.006(1)	-U(1,3)
F1	0.176(4)	U(1,1)	0.123(5)	-0.095(6)	0.062(5)	-U(1,3)
F2	0.159(4)	U(1,1)	0.123(6)	-0.095(5)	0.023(6)	-U(1,3)
F3	0.094(4)	0.128(4)	0.076(3)	0.043(3)	0.022(3)	-0.029(3)
F4	0.144(4)	0.153(5)	0.074(3)	0.087(3)	-0.008(3)	0.013(3)

The form of the anisotropic thermal parameter is:

$$\exp[-2\pi^2(U_{11}h^2a^{*2}+U_{22}k^2b^{*2}+U_{33}l^2c^{*2}+2U_{12}hka^*b^*+2U_{13}hla^*c^*+2U_{23}klb^*c^*)]$$

Deposition data

Calculated hydrogen coordinates (C-H 0.95 A, Biso 5.0 A)

Atom	x	y	z
H101	-0.0868	-0.1919	-0.0514
H102	-0.1054	-0.2589	0.0122
H21	0.1029	-0.3172	-0.0428
H22	0.2208	-0.2596	-0.0059
H31	0.1246	-0.1580	-0.1148
H32	0.2573	-0.2332	-0.1077
H51	0.4937	-0.0608	-0.0396
H52	0.3947	-0.1616	-0.0120
H61	0.4375	0.0896	0.0281
H62	0.4740	-0.0389	0.0630
H81	0.2072	-0.1625	0.1400
H82	0.2684	-0.2072	0.0779
H91	0.0098	-0.1327	0.0951
H92	0.0582	-0.2751	0.0815

Torsion angles (°)

S7	Ag	S4	C3	99.7
S7	Ag	S4	C5	-1.2
N1	Ag	S4	C3	20.7
N1	Ag	S4	C5	-80.2
N1(I)	Ag	S4	C3	-34.1
N1(I)	Ag	S4	C5	-135.0
S7(I)	Ag	S4	C3	-110.2
S7(I)	Ag	S4	C5	148.9
S4(I)	Ag	S4	C3	175.9
S4(I)	Ag	S4	C5	75.1
S4	Ag	S7	C6	20.5
S4	Ag	S7	C8	-88.3
N1	Ag	S7	C6	96.1
N1	Ag	S7	C8	-12.7
N1(I)	Ag	S7	C6	151.4
N1(I)	Ag	S7	C8	42.6
S7(I)	Ag	S7	C6	-59.9
S7(I)	Ag	S7	C8	-168.7
S4(I)	Ag	S7	C6	-137.0
S4(I)	Ag	S7	C8	114.2
S4	Ag	N1	C10	-127.3
S4	Ag	N1	C2	1.3
S4	Ag	N1	C9	121.9
S7	Ag	N1	C10	148.6
S7	Ag	N1	C2	-82.8
S7	Ag	N1	C9	37.9
N1(I)	Ag	N1	C10	9.5
N1(I)	Ag	N1	C2	138.2
N1(I)	Ag	N1	C9	-101.2
S7(I)	Ag	N1	C10	-47.0
S7(I)	Ag	N1	C2	81.6
S7(I)	Ag	N1	C9	-157.7
S4(I)	Ag	N1	C10	64.5
S4(I)	Ag	N1	C2	-166.9
S4(I)	Ag	N1	C9	-46.2
S4	Ag	N1(I)	C10(I)	64.5
S7	Ag	N1(I)	C10(I)	-47.0
N1	Ag	N1(I)	C10(I)	9.5
S7(I)	Ag	N1(I)	C10(I)	148.6
S4(I)	Ag	N1(I)	C10(I)	-127.3
Ag	S4	C3	C2	-47.5
C5	S4	C3	C2	54.5
Ag	S4	C5	C6	-24.8
C3	S4	C5	C6	-122.5
Ag	S7	C6	C5	-49.0
C8	S7	C6	C5	55.2
Ag	S7	C8	C9	-14.6
C6	S7	C8	C9	-119.6
Ag	N1	C10	C10(I)	-30.4
C2	N1	C10	C10(I)	-159.2
C9	N1	C10	C10(I)	76.2
Ag	N1	C2	C3	-30.6
C10	N1	C2	C3	93.2
C9	N1	C2	C3	-145.1
Ag	N1	C9	C8	-61.8
C10	N1	C9	C8	-171.9
C2	N1	C9	C8	61.4
N1	C10	C10(I)	N1(I)	46.5
N1	C2	C3	S4	57.8
S4	C5	C6	S7	54.0
S7	C8	C9	N1	55.7
C10	C10(I)	N1(I)	Ag	-30.4

(5) $[Ag\text{-}PyS_2O_3]_2[PF_6]_2$

Table of Experimental Details

A. Crystal Data

C15 H23 AG F6 N 03 P S2

F. W. 582. 32 F(000) = 2336

crystal dimensions: 0. 18 x 0. 25 x 0. 30 mm

peak width at half-height = 0. 25@

Mo K@ radiation (@ = 0. 71073 A)

temperature = 21 @ 1@

monoclinic space group P21/N

a = 23. 678 (3) A b = 18. 721 (4) A c = 9. 690 (3) A

@ = 96. 31 (1) @

V = 4269. 3 A@

Z = 8 @ = 1. 82 g/cm@

@ = 12. 7 cm-1

Table of Experimental Details

B. Intensity Measurements

Instrument:	Enraf-Nonius CAD4 diffractometer
Monochromator:	Graphite crystal, incident beam
Attenuator:	Zr foil, factor 17.0
Take-off angle:	2.8@
Detector aperture:	2.0 to 2.4 mm horizontal
	2.0 mm vertical
Crystal-detector dist.:	21 cm
Scan type:	w-@
Scan rate:	1 - 4@/min (in omega)
Scan width, deg:	0.6 + 0.350 tan @
Maximum 2@:	48.0@
No. of refl. measured:	7496 total, 6651 unique
Corrections:	Lorentz-polarization
	Reflection averaging (agreement on I = 2.1%)
	Numerical absorption (from74.58 to83.72 on I)

C. Structure Solution and Refinement

Solution:	Patterson method
Refinement:	Block-diagonal least-squares
Minimization function:	@w(|Fo|-|Fc|)@
Least-squares weights:	4Fo@/@@(Fo@)
Anomalous dispersion:	All non-hydrogen atoms
Reflections included:	3689 with Fo@>3.0@(Fo@)
Parameters refined:	523
Unweighted agreement factor:	0.046
Weighted agreement factor:	0.056
Esd of obs. of unit weight:	1.76
Convergence, largest shift:	0.07@
High peak in final diff. map:	0.88 (8) e/A@
Computer hardware:	PDP-11
Computer software:	SDP-PLUS (Enraf-Nonius &
	B. A. Frenz & Associates, Inc.)

Table

Molecular dimensions

(a) Bond lengths (Å)

Ag1	N1A	2.370(6)	C16A	O17A	1.408(10)
Ag1	S8A	2.502(3)	O17A	C18A	1.429(10)
Ag1	O11A	2.605(8)	C18A	C19A	1.488(11)
Ag1	O14A	2.461(5)	C19A	S20A	1.796(9)
Ag1	O17A	2.398(6)	S20A	C21A	1.818(8)
N1A	C2A	1.335(10)	S20A	Ag2	2.545(2)
N1A	C6A	1.331(10)	Ag2	N1B	2.529(8)
C2A	C3A	1.374(11)	Ag2	S8B	2.611(3)
C2A	C21A	1.516(11)	Ag2	S20B	2.609(3)
C3A	C4A	1.375(13)	N1B	C2B	1.319(13)
C4A	C5A	1.372(14)	N1B	C6B	1.314(12)
C5A	C6A	1.375(11)	C2B	C3B	1.398(14)
C6A	C7A	1.520(13)	C2B	C21B	1.489(20)
C7A	S8A	1.809(8)	C3B	C4B	1.318(18)
S8A	C9A	1.751(12)	C4B	C5B	1.375(16)
C9A	C10A	1.497(20)	C5B	C6B	1.381(13)
C10A	O11A	1.426(15)	C6B	C7B	1.493(14)
O11A	C12A	1.234(13)	C7B	S8B	1.823(10)
C12A	C13A	1.443(15)	S8B	C9B	1.790(9)
C13A	O14A	1.414(12)	C9B	C10B	1.505(14)
O14A	C15A	1.409(12)	C10B	O11B	1.434(12)
C15A	C16A	1.475(15)	O11B	C12B	1.427(12)

(continued...)

C12B	C13B	1.460(14)
C13B	O14B	1.432(13)
O14B	C15B	1.398(12)
C15B	C16B	1.445(17)
C16B	O17B	1.370(15)
O17B	C18B	1.320(18)
C18B	C19B	1.158(27)
C19B	S20B	1.814(14)
S20B	C21B	1.783(14)
P1	F11	1.538(7)
P1	F12	1.553(7)
P1	F13	1.527(7)
P1	F14	1.563(7)
P1	F15	1.476(9)
P1	F16	1.535(8)
P2	F21	1.566(9)
P2	F22	1.504(8)
P2	F23	1.467(10)
P2	F24	1.557(8)
P2	F25	1.552(10)
P2	F26	1.411(11)

(b) Bond angles (°)

N1A	Ag1	S8A	81.3(2)	C7A	S8A	C9A	103.1(5)
N1A	Ag1	O11A	83.4(3)	S8A	C9A	C10A	115.2(9)
N1A	Ag1	O14A	129.7(2)	C9A	C10A	O11A	118.(1)
N1A	Ag1	O17A	104.3(2)	Ag1	O11A	C10A	107.3(6)
S8A	Ag1	O11A	77.4(2)	Ag1	O11A	C12A	110.9(7)
S8A	Ag1	O14A	124.9(2)	C10A	O11A	C12A	121.(1)
S8A	Ag1	O17A	158.5(2)	O11A	C12A	C13A	119.(1)
O11A	Ag1	O14A	65.6(2)	C12A	C13A	O14A	110.8(8)
O11A	Ag1	O17A	123.5(3)	Ag1	O14A	C13A	116.8(5)
O14A	Ag1	O17A	67.6(2)	Ag1	O14A	C15A	115.2(5)
Ag1	N1A	C2A	124.1(5)	C13A	O14A	C15A	114.4(7)
Ag1	N1A	C6A	116.0(5)	O14A	C15A	C16A	109.5(7)
C2A	N1A	C6A	118.7(6)	C15A	C16A	O17A	108.8(8)
N1A	C2A	C3A	122.9(7)	Ag1	O17A	C16A	111.9(5)
N1A	C2A	C21A	116.8(6)	Ag1	O17A	C18A	118.9(5)
C3A	C2A	C21A	120.3(7)	C16A	O17A	C18A	116.4(7)
C2A	C3A	C4A	118.0(8)	O17A	C18A	C19A	107.7(7)
C3A	C4A	C5A	119.5(8)	C18A	C19A	S20A	115.0(6)
C4A	C5A	C6A	119.3(8)	C19A	S20A	C21A	105.1(4)
N1A	C6A	C5A	121.7(8)	C19A	S20A	Ag2	102.8(3)
N1A	C6A	C7A	119.8(7)	C21A	S20A	Ag2	105.1(2)
C5A	C6A	C7A	118.4(7)	C2A	C21A	S20A	114.8(5)
C6A	C7A	S8A	119.0(6)	S20A	Ag2	N1B	123.3(2)
Ag1	S8A	C7A	97.3(3)	S20A	Ag2	S8B	100.57(8)
Ag1	S8A	C9A	103.3(4)	S20A	Ag2	S20B	115.66(8)

(continued....)

N1B	Ag2	S8B	74.7(2)	O14B	C15B	C16B	111.8(9)
N1B	Ag2	S20B	75.5(2)	C15B	C16B	O17B	114.(1)
S8B	Ag2	S20B	141.80(9)	C16B	O17B	C18B	116.(1)
Ag2	N1B	C2B	114.0(6)	O17B	C18B	C19B	134.(2)
Ag2	N1B	C6B	113.2(6)	C18B	C19B	S20B	123.(1)
C2B	N1B	C6B	118.6(8)	Ag2	S20B	C19B	104.5(5)
N1B	C2B	C3B	121.(1)	Ag2	S20B	C21B	97.9(4)
N1B	C2B	C21B	116.4(8)	C19B	S20B	C21B	101.3(6)
C3B	C2B	C21B	123.(1)	C2B	C21B	S20B	114.9(8)
C2B	C3B	C4B	121.(1)	F11	P1	F12	91.6(4)
C3B	C4B	C5B	119.(1)	F11	P1	F13	177.9(5)
C4B	C5B	C6B	119.(1)	F11	P1	F14	89.0(4)
N1B	C6B	C5B	122.7(9)	F11	P1	F15	88.6(5)
N1B	C6B	C7B	115.8(8)	F11	P1	F16	90.4(5)
C5B	C6B	C7B	121.6(9)	F12	P1	F13	87.9(4)
C6B	C7B	S8B	109.0(7)	F12	P1	F14	178.5(4)
Ag2	S8B	C7B	97.4(4)	F12	P1	F15	90.6(5)
Ag2	S8B	C9B	108.1(3)	F12	P1	F16	89.9(4)
C7B	S8B	C9B	99.4(5)	F13	P1	F14	91.5(4)
S8B	C9B	C10B	109.8(6)	F13	P1	F15	93.5(5)
C9B	C10B	O11B	108.6(7)	F13	P1	F16	87.6(5)
C10B	O11B	C12B	114.9(7)	F14	P1	F15	90.8(5)
O11B	C12B	C13B	113.1(8)	F14	P1	F16	88.7(4)
C12B	C13B	O14B	110.6(7)	F15	P1	F16	178.8(6)
C13B	O14B	C15B	111.5(7)	F21	P2	F22	89.1(5)

(continued....)

Table

Positional Parameters and Their Estimated Standard Deviations

Atom	x	y	z	B(Å^2)
Ag1	−0.05753(3)	0.26287(4)	−0.13113(6)	4.37(1)
N1A	0.0163(3)	0.2976(3)	0.0408(6)	3.7(1)
C2A	0.0714(3)	0.2965(4)	0.0227(7)	3.6(2)
C3A	0.1125(4)	0.3285(5)	0.1133(9)	4.9(2)
C4A	0.0954(4)	0.3644(5)	0.2254(9)	5.7(2)
C5A	0.0387(4)	0.3670(4)	0.2431(8)	4.8(2)
C6A	0.0002(4)	0.3321(4)	0.1499(7)	3.9(2)
C7A	−0.0614(4)	0.3285(5)	0.1802(8)	5.0(2)
S8A	−0.1167(1)	0.3200(2)	0.0368(3)	5.94(6)
C9A	−0.1253(6)	0.4076(6)	−0.0250(11)	10.2(3)
C10A	−0.0760(7)	0.4372(6)	−0.0908(11)	11.2(5)
O11A	−0.0558(5)	0.3972(4)	−0.2005(7)	12.8(3)
C12A	−0.0759(6)	0.4057(6)	−0.3224(11)	9.7(4)
C13A	−0.0613(5)	0.3560(6)	−0.4267(9)	6.8(3)
O14A	−0.0680(3)	0.2847(3)	−0.3831(6)	5.8(2)
C15A	−0.0426(4)	0.2333(6)	−0.4626(9)	6.8(3)
C16A	−0.0433(4)	0.1631(5)	−0.3935(9)	6.5(3)
O17A	−0.0163(3)	0.1696(3)	−0.2571(6)	5.4(1)
C18A	0.0000(4)	0.1045(5)	−0.1869(9)	4.9(2)
C19A	0.0364(4)	0.1231(4)	−0.0569(8)	4.7(2)
S20A	0.10321(9)	0.1639(1)	−0.0816(2)	4.23(5)

Positional Parameters and Their Estimated Standard Deviations (cont.)

Atom	x	y	z	B(Å^2)
C21A	0.0875(3)	0.2585(4)	-0.1054(7)	3.8(2)
Ag2	0.15862(3)	0.15456(4)	0.15813(7)	5.56(2)
N1B	0.1692(3)	0.0394(4)	0.2951(8)	6.0(2)
C2B	0.1487(4)	0.0424(6)	0.4162(10)	6.9(3)
C3B	0.1780(5)	0.0114(6)	0.5343(11)	9.2(3)
C4B	0.2279(5)	-0.0190(6)	0.5284(11)	9.2(3)
C5B	0.2492(5)	-0.0228(5)	0.4022(11)	7.2(3)
C6B	0.2183(4)	0.0077(5)	0.2881(9)	5.7(2)
C7B	0.2388(4)	0.0062(5)	0.1480(11)	6.7(3)
S8B	0.2530(1)	0.0973(1)	0.0951(3)	5.24(6)
C9B	0.2471(4)	0.0850(5)	-0.0891(9)	5.4(2)
C10B	0.2679(4)	0.1507(6)	-0.1573(9)	6.7(3)
O11B	0.2317(3)	0.2095(3)	-0.1313(6)	6.2(2)
C12B	0.2589(4)	0.2777(6)	-0.1236(10)	6.7(3)
C13B	0.2930(4)	0.2902(6)	0.0091(11)	6.9(3)
O14B	0.2575(3)	0.2931(3)	0.1195(6)	6.0(2)
C15B	0.2897(5)	0.2963(6)	0.2492(11)	7.4(3)
C16B	0.2543(5)	0.2977(7)	0.3613(11)	8.9(3)
O17B	0.2225(4)	0.2372(4)	0.3720(7)	9.7(2)
C18B	0.1953(9)	0.2321(13)	0.4835(14)	26.8(8)
C19B	0.1509(7)	0.2113(9)	0.5031(11)	13.2(5)

Positional Parameters and Their Estimated Standard Deviations (cont.)

Atom	x	y	z	B(Å^2)
S20B	0.0999(1)	0.1754(2)	0.3672(3)	8.11(9)
C21B	0.0956(5)	0.0846(8)	0.4210(11)	9.5(4)
P1	0.1157(1)	0.4457(1)	0.6676(2)	5.00(6)
F11	0.1378(4)	0.4530(4)	0.5248(6)	11.8(2)
F12	0.0895(3)	0.3713(3)	0.6285(8)	11.1(2)
F13	0.0916(4)	0.4389(4)	0.8068(6)	14.1(3)
F14	0.1404(3)	0.5213(3)	0.7069(7)	11.6(2)
F15	0.1702(3)	0.4119(5)	0.7196(11)	17.2(3)
F16	0.0595(3)	0.4815(5)	0.6111(11)	16.1(3)
P2	0.4034(1)	0.4069(2)	0.6736(3)	6.72(7)
F21	0.4494(4)	0.3468(4)	0.6967(9)	14.5(3)
F22	0.4187(4)	0.4306(6)	0.8213(7)	19.2(3)
F23	0.3670(4)	0.4705(5)	0.6575(9)	19.6(3)
F24	0.3893(4)	0.3773(5)	0.5236(8)	15.7(3)
F25	0.4527(4)	0.4491(4)	0.6185(10)	16.5(3)
F26	0.3614(4)	0.3661(6)	0.7301(12)	27.1(4)

Anisotropically refined atoms are given in the form of the isotropic equivalent thermal parameter defined as:

$$4/3[a^2B_{11} + b^2B_{22} + c^2B_{33} + abcos\gamma B_{12} + accos\beta B_{13} + bccos\alpha B_{23}]$$

Deposition data

Torsion Angles

C6A	N1A	C2A	C3A	1.2
C6A	N1A	C2A	C21A	-178.1
C2A	N1A	C6A	C5A	0.5
C2A	N1A	C6A	C7A	-174.5
N1A	C2A	C3A	C4A	-1.5
C21A	C2A	C3A	C4A	177.8
N1A	C2A	C21A	S20A	-89.8
C3A	C2A	C21A	S20A	90.8
C2A	C3A	C4A	C5A	0.1
C3A	C4A	C5A	C6A	1.5
C4A	C5A	C6A	N1A	-1.9
C4A	C5A	C6A	C7A	173.2
N1A	C6A	C7A	S8A	-31.5
C5A	C6A	C7A	S8A	153.3
C6A	C7A	S8A	C9A	-80.5
C7A	S8A	C9A	C10A	67.7
S8A	C9A	C10A	O11A	54.0
C9A	C10A	O11A	C12A	88.2
C10A	O11A	C12A	C13A	-169.4
O11A	C12A	C13A	O14A	48.8
C12A	C13A	O14A	C15A	-166.1
C13A	O14A	C15A	C16A	169.9
O14A	C15A	C16A	O17A	-55.7
C15A	C16A	O17A	C18A	-164.4
C16A	O17A	C18A	C19A	170.0
O17A	C18A	C19A	S20A	-65.4
C18A	C19A	S20A	C21A	84.7
C19A	S20A	C21A	C2A	68.4

C6B	N1B	C2B	C3B	-1.2
C6B	N1B	C2B	C21B	174.6
C2B	N1B	C6B	C5B	0.2
C2B	N1B	C6B	C7B	179.9
N1B	C2B	C3B	C4B	2.7
C21B	C2B	C3B	C4B	-172.8
N1B	C2B	C21B	S20B	-56.8
C3B	C2B	C21B	S20B	118.9
C2B	C3B	C4B	C5B	-3.2
C3B	C4B	C5B	C6B	2.2
C4B	C5B	C6B	N1B	-0.7
C4B	C5B	C6B	C7B	179.6
N1B	C6B	C7B	S8B	65.1
C5B	C6B	C7B	S8B	-115.2
C6B	C7B	S8B	C9B	-157.1
C7B	S8B	C9B	C10B	-169.5
S8B	C9B	C10B	O11B	-63.3
C9B	C10B	O11B	C12B	149.5
C10B	O11B	C12B	C13B	-78.3
O11B	C12B	C13B	O14B	-65.1
C12B	C13B	O14B	C15B	172.8
C13B	O14B	C15B	C16B	-178.8
O14B	C15B	C16B	O17B	64.0
C15B	C16B	O17B	C18B	171.3
C16B	O17B	C18B	C19B	140.8
O17B	C18B	C19B	S20B	-0.1
C18B	C19B	S20B	C21B	114.8
C19B	S20B	C21B	C2B	-66.2